The role of the histone demethylase KDM5B, in the normal and malignant mammary gland

Okonjo, Fiona Akinyi

Awarding institution:
King's College London

The role of the histone demethylase KDM5B, in the normal and malignant mammary gland

Fiona Akinyi Okonjo

School of Cancer & Pharmaceutical Sciences

King's College London

A thesis submitted according to the requirements for the degree of Doctor of Philosophy

2018

Declaration

I declare that I carried out all the work presented in this thesis. Any work carried out by others has been fully acknowledged.

This PhD thesis was carried out under the direction and supervision of Professor Joy Burchell and Professor Joyce Taylor-Papadimitriou.

Acknowledgements

I am deeply grateful to my supervisors Professors Joy Burchell and Joyce Taylor-Papadimitriou for their guidance and encouragement throughout my PhD. Without their expert knowledge, constant support and feedback, this PhD would not have been achievable. Thank you for believing in me. You have equipped me with knowledge and tools required to become an independent researcher. I would also like to thank my second supervisor Dr Elinor Sawyer and my PhD committee members Dr Anita Grigoriadis, Dr Paul Lavender, Dr Claire Wells and Professor Eric So, for their scientific advice and suggestions.

I would like to thank the Biomedical Research Centre at Guy's Hospital for giving me the opportunity to undertake my PhD studies, by providing financial support as well as, biomedical research training.

I am thankful to members of the Breast Cancer Biology lab, both past and present (Franco, Richard, Ros, Steve, Virginia and Grace) for their scientific input, support and for providing an enjoyable and enriching lab environment, during the past 3.5 years. Franco, thank you for encouraging me to stay in Joy's lab. It was indeed a good decision.

I thank Dr Paul Lavender for his assistance with the microarray gene expression experiments. I am also grateful to Professor Eric Bennett, Dr Yang Zhang, Yen-Hsi and all the members in the Genome Editing Centre at the University of Copenhagen, for training me and for always providing technical assistance with the CRISPR technology.

To all my friends who have encouraged and supported me throughout this journey, I am so grateful. To Artemis, Daniela and Antonella, I say thank you my friends for making time to unwind and talk about anything else but science (well, we tried but didn't always succeed). To Jelmar, thank you for helping me with anything and everything bioinformatics. To Diane, Karen and Sidi, thank you for your encouragement, prayers and for lending a listening ear when I was overwhelmed. To the Wood Green small group, Daniel, Jill, Jonathan, Josh, Keriann, Nadina and many others, thank you also for your constant prayers. I wouldn't have made it without them. To Albert, Ursil, Marsha and Ali thank you for feeding us, particularly during the thesis writing period.

To my parents, siblings (Jack, Aileen and Flora) and in-laws (Mr and Mrs Okonjo, Veronica, Karanja, Emily, Joyner, Don, McKenzie, Gilbert, Brenda), thank you for your support, encouragement and prayers. To my husband Jeremmy, thank you for your constant support and for being a shoulder to lean on, listening to my complaints and celebrating my achievements, during these PhD years. For pushing me to write when I

felt like giving up, for your prayers and for believing in me. Above all I am grateful to God. Without Him completing this PhD wouldn't have been possible.

I dedicate this PhD to my parents Mr Josephat Kogera and Mrs Peninah Kogera for their unconditional love and encouraging me to always aim high and pursue my dreams.

Abstract

Histone demethylases are involved in transcriptional regulation and have recently been implicated in human diseases including cancer. KDM5B belongs to the KDM5 family of histone demethylases, which catalyse the removal of the methyl group from the active tri-methyl mark, H3K4me3, thereby regulating transcription. KDM5B was first identified in our lab as being downregulated when HER2 was inhibited by Trastuzumab (Herceptin). KDM5B is widely expressed in breast cancer and other cancers, where it may act by repressing genes such as Caveolin1 (CAV1). Recent studies have implicated KDM5 proteins in resistance to targeted therapies and so considerable effort is being employed to develop KDM5 small molecule inhibitors. A role for KDM5B in mammary gland development has also been demonstrated. In the mouse model lacking demethylase activity (ΔARID mouse), KDM5B has been shown to repress CAV1 in the mid-pregnant mammary gland. Thus, suggesting similar pathways operate in the normal and malignant mammary gland.

This PhD aimed to further understand the role of KDM5B in breast cancer and in the normal mammary gland. The first aim was to generate KDM5B knockout (KO) breast cancer cell line models using CRISPR-Cas9 technology and investigate the effect of this modulation on gene expression, proliferation and drug resistance. The second aim was to investigate the extent of CAV1 downregulation by KDM5B in breast cancer and, identify the cell types where this downregulation may occur in the developing mammary gland.

KDM5B KO cell lines were generated in two HER2+ breast cancer cell lines, BT-474 and SKBr3. KDM5B KO significantly reduced cell proliferation of SKBr3, but not BT-474 cells in cell viability assays. Treatment of KDM5B KO cells with Herceptin and Lapatinib, showed increased sensitivity to Herceptin in BT-474. There was no significant increase in sensitivity to Lapatinib in the KDM5B KO cells. Microarray gene expression analysis in the SKBr3 KDM5B KO was used to elucidate targets of KDM5B and revealed the early response gene EGR1, in addition to CAV1 and MYC, to be amongst the top upregulated genes. Surprisingly, CAV1 was not upregulated in BT-474 KO cells. Immunohistochemistry analysis showed co-localisation of CAV1 and KDM5B in the myoepithelial and stromal cells, in the mid-pregnant mouse mammary gland.

The data demonstrate a cell phenotype dependent role for the function of KDM5B and the importance of pre-clinical investigations for potential therapeutic targets. These cell line models can be used to identify novel mechanisms through which KDM5B promotes cancer progression and drug resistance in breast cancer. This will in turn enable interrogation of these mechanisms for the development of novel therapies.

Table of Contents

List of Figures

List of Tables

Abbreviations

2A	Peptide sequence 2A
α–SMA	α-smooth muscle actin

A

ABCC2	ATP binding cassette (ABC) transporter
ADCC	Antibody-dependent cellular cytotoxicity
AML	Acute myelogenous leukemia
ANXA1	Annexin A1
AOL	Amine oxidase-like domain
AR	Androgen receptor
ARID	AT-rich interactive

B

Bcl-2	B-cell lymphoma 2
BCL6	B-cell lymphoma 6
BH	Benjamini-Hochberg
BF-1	Brain factor -1
BMI	Body mass index
BMP7	Bone morphogenetic protein 7
Bp	Base pair
BRCA1	Breast cancer susceptibility gene 1
BRCA2	Breast cancer susceptibility gene 2
BRSM1	Breast cancer metastasis suppressor 1
BSA	Bovine serum albumin

C

CAF	Cancer-associated fibroblast
Cas	CRISPR associated
CAV1	Caveolin-1
Cba	Chicken beta actin
ccRCC	Clear cell renal carcinoma
CDK	Cyclin dependent kinase
cDNA	Complementary DNA
CGI	CpG Islands
CHD4	Chromodomain helicase DNA binding protein 4
ChIP	Chromatin immunoprecipitation
CN	Copy number
COC	Combined oral contraceptives
CRISPR	Clustered, regularly interspaced, short palindromic repeat
CRPC	Castration resistant prostate cancer
crRNA	CRISPR RNA
CSD	Caveolin scaffolding domain
Ct	Cycle threshold

CTSZ	Cathepsin Z

D

DCIS	Ductal carcinoma in situ
DMEM	Dulbecco's Modified Eagle's Medium
DMSO	Dimethyl sulfoxide
DNMT	DNA methyltransferase
DOTL	DOT1-like
Dri	Dead ringer
DSB	Double strand break

E

ECL	Enhanced chemiluminescence
EGF	Epidermal growth factor
EGFR	EGF receptor
EGR1	Early growth response gene 1
ER	Estrogen receptor
ESC	Embryonic stem cell
ET	Endocrine therapy

F

F	Forward
FACS	Fluorescence-activated cell sorting
FAD	Flavine adenine dinucleotide
FBS	Fetal Bovine Serum
FDR	False discovery rate
FI	Fluorescent intensity

G

GE	Gene expression
GFP	Green fluorescent protein
GO	Gene Ontology
gRNA	guide RNA

H

HAT	Histone acetyltransferase
HCC	Hepatocellular carcinoma
HCl	Hydrochloric acid
HDACi	Histone deacetylase inhibitor
HDAC	Histone deacetylase
HDR	Homology directed repair
HER2	Human epidermal growth factor receptor 2
HR	Homologous recombination
HRP	Horseradish peroxidase

I

ID2	Inhibitor of differentiation 2
IDAA	Indel detection by amplicon analysis
IGF-1R	Insulin like growth factor 1 receptor

J

JAK2	Janus kinase 2
JARID	Jumonji AT-rich interactive domain
JmjC	Jumonji C
JmjN	N-terminal Jumonji

K

KD	Knockdown
KDM	Lysine demethylase
KMT	Lysine methyltransferase
KO	Knockout

L

LB	Lysogeny broth
LCN2	Lipocalin 2
Lid	Little imaginal disk
LSD	Lysine specific demethylase
LumA	Luminal A
LumB	Luminal B

M

MAPK	Mitogen activated protein kinase
MBD	Methyl-CpG binding domain
MEC	Mammary epithelial cell
MEF2	Myocyte enhancer factor 2
mESC	Mouse embryonic stem cell
METABRIC	Molecular Taxonomy of Breast Cancer International Consortium
miRNA	MicroRNA
mRNA	Messenger RNA
mTOR	Mammalian target of rapamycin
MTT	Thiazolyl blue tetrazolium bromide

N

NaN_3	Sodium Azide
NaOAc	Sodium acetate
NaOH	Sodium hydroxide
NF-kB	Nuclear factor–kB
NHEJ	Non-homologous end joining
NHSBSP	National Health Service breast screening programme
NK	Natural killer

NMD	Nonsense-mediated decay
Nt	Nucleotide
NuRD	Nucleosome remodelling and deacetylase

O

OD	Optical density
OSCC	Oral squamous cell carcinoma

P

PAM	Protospacer adjacent motif
PAM50	Prediction analysis of microarray 50
PARP	Poly (ADP-ribose) polymerase
PAX-9	Paired box 9
PBS	Phosphate buffered saline
PD-1	Programmed cell death-1
PDL-1	Programmed death ligand 1
PHD	Plant homeodomain
pHER2	Phosphorylated HER2
PI3K	Phosphoinositide 3-kinase
PIK3CA	Phosphatidylinositol-4,5-bisphosphate 3-Kinase Catalytic Subunit Alpha
PLCγ1	Phospholipase C gamma 1
PMSF	Phenylmethylsulfonyl fluoride
PR	Progesterone receptor
pRb	Retinoblastoma binding protein
PRC2	Polycomb repressive complex 2
Prl	Prolactin
Prl-R	Prolactin receptor
PRMT	Protein arginine methyltransferase
pSTAT5	Phosphorylated STAT5
PTEN	Phosphatase and tensin homolog
PTM	Post-translational modification

Q

qRT-PCR	quantitative reverse transcriptase polymerase chain reaction

R

R	Reverse
RA	Retinoic acid
RIN	RNA integrity number
RNAi	RNA interference
RPMI	Roswell Park Memorial Institute 1640

S

SAM	S-adenosylmethionine

SDS-PAGE	Sodium dodecyl sulfate polyacrylamide gel electrophoresis
SERM	Selective estrogen modulator
SET	SU(VAR)3-9, Enhancer of zeste and Trithorax
sgRNA	Single guide RNA
shRNA	short hairpin RNA
SLC40A1	Solute carrier family 40 member 1
SNP	Single Nucleotide Polymorphism
SOC	Super optimal broth with catabolite repression
STAT	Signal transducers and activators of transcription
SWIRM	SWI3, RSC8 and Moira

T

T-DM1	Trastuzumab emtansine
TALEN	Transcription activator-like effector nucleases
TBS	Tris-buffered saline
TBST	Tris-buffered saline/Tween
TCGA	The Cancer Genome Atlas
TEB	Triton Extraction buffer
TET	Ten-eleven translocation
TFAP2C	Transcription factor AP-2 gamma
TGFβ	Transforming growth factor-beta
TN	Triple negative
TNBC	Triple negative breast cancer
TNC	Tenascin C

U

UK	United Kingdom
UNG	Uracil-DNA glycosylase
UPR	Unfolded protein response

W

WT	Wild-type

Z

ZFN	Zinc-finger nucleases

1 : Introduction

1.1 The normal mammary gland: steroid hormones in development and tumorigenesis

The adult breast is made up of branched, tree-like structures of ducts that are lined by two layers of epithelial cells and surrounded by fibroblasts and adipose tissue (reviewed by [1]). The lobules, also known as terminal ductal lobular unit (TDLU), are the milk-producing component of the breast. Maturation of lobules from alveolar buds into secretory sacs known as alveoli, occurs after menarche and becomes fully developed during pregnancy, when they expand in preparation for lactation. The lobules involute after lactation, resembling those in the non-pregnant gland, although the number of alveoli per lobule may increase over those seen before pregnancy. Alveoli consist of an inner layer of luminal epithelial and an outer basal, myoepithelial cell layer which contacts the basement membrane. Proliferation of epithelial cells occurs mainly in the luminal cells of the non-pregnant gland. Histopathologically, epithelial hyperplasia and carcinoma of the breast arise from the lobules.

During normal human mammary gland development, the ovarian steroids estrogen and progesterone, play a crucial role [2]. These hormones act through nuclear receptors found predominantly on female reproductive tissues, to exert their function. The estrogen receptor (ER) and progesterone receptor (PR) are found on luminal epithelial cells [3], where they regulate expression of specific genes when bound to their ligands. Discovery of a second ER gene [4], led to renaming the classic ER protein as ERα and the new receptor as ERβ. In the normal breast, ERα expression is restricted to luminal epithelial cells, whereas ERβ is more widely expressed, as it is also expressed in the myoepithelial, endothelial, stromal cells and lymphocytes [5]. PR also has two isoforms namely PRA and PRB [6]. Although both PRA and PRB are expressed at the same level and in the same cells [7], PRB appears to be the active PR [6].

In the premenopausal breast, steroid hormones promote proliferation of approximately 5% epithelial cells, which surprisingly do not express the gene encoding ER (*ESRA*)[8]. These cells are instead adjacent or in close proximity to cells that express ESRA, thus suggesting that proliferation of ERα-negative (ERα-) cells occurs through paracrine factors secreted by ERα-positive (ERα+) cells, in response to estrogen (reviewed by [1]). Indeed, several studies have reported that steroid receptor synthesis in the mammary epithelium is dissociated from cell proliferation [9–11]. This dissociation is however dysregulated in the early stages of breast tumorigenesis, as observed by increased proliferating ERα+ cells [12], which are dependent on estrogen for their growth [12].

Contrastingly, expression of ERβ decreases in the transition from normal to malignant cells and correlates with reduced proliferation and pathological grade [13]. ERβ expression

has been observed in approximately 70% of invasive breast cancers [14,15] and a subset of these tumours also express ERα [15]. ERβ is also expressed in a subset of ER- breast cancers [15], which are usually characterised by overexpression of genes encoding growth factor receptors such as human epidermal growth factor receptor 2 (*HER2*) [16]. The role of ERβ in ERα+ breast cancers however, has not yet been determined. ERβ exerts an anti-proliferative function in ERα+ breast cancer cells [17] and is believed to negatively regulate ERα signalling. The exact role of ERβ in breast cancer however, remains unclear. Currently, clinical decisions are based solely on expression of ERα, which is also the targeted receptor in breast cancer therapies.

Alterations in PRA and PRB during breast tumorigenesis have also been observed, where PRA is the predominantly expressed isoform in atypical ductal hyperplasia, ductal carcinoma in situ (DCIS) and invasive tumours [7]. PR expression is generally associated with good prognosis in invasive breast cancer [18].

1.2 Breast Cancer

1.2.1 Epidemiology

Breast cancer is the most common cancer and leading cause of cancer death in women worldwide, with an estimated 1.7 million cases and 521,900 deaths reported in 2012 [19,20]. In the United Kingdom (UK), breast cancer is the most common cancer and the second leading cause of cancer death in women, with 54,833 cases and 11,360 deaths reported in 2014 (**Fig 1.1 and 1.2**) [21]. Of the total breast cancer cases in UK (2014), 389 (around 1%) were reported in males. It is estimated that 1 in 8 women and 1 in 870 men, will be diagnosed with breast cancer in their lifetime. Although breast cancer incidence has increased since the early 1990s, mortality rates have decreased over time [22]. This is mainly attributed to advances in medicine which have led to early detection of the disease and better treatment strategies, as discussed below.

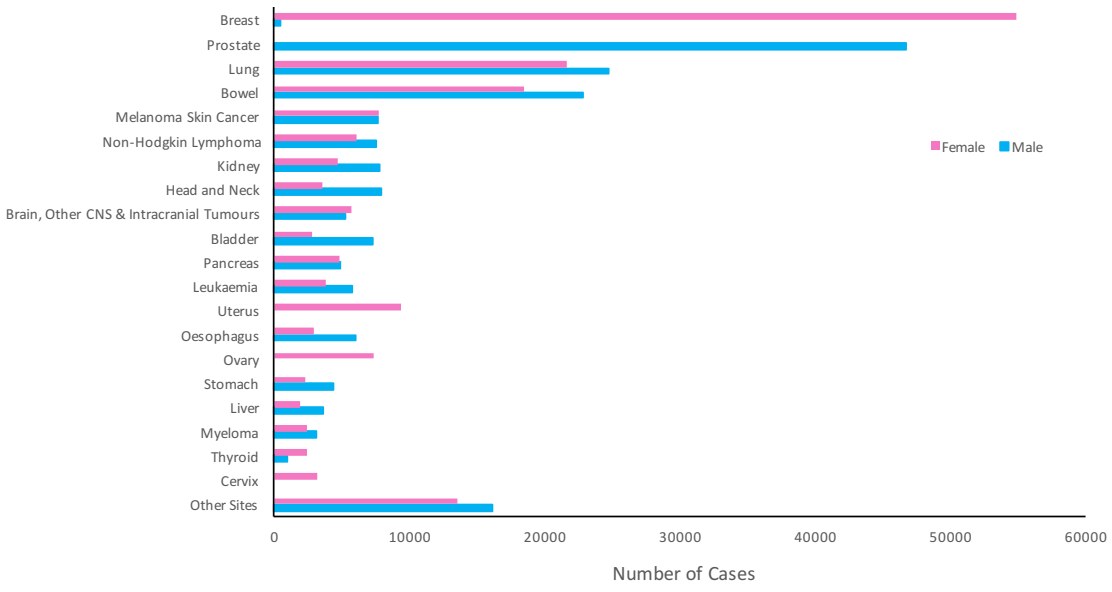

Figure 1.1: Twenty most common cancers, UK (2014). Breast cancer is the most common cancer in UK.

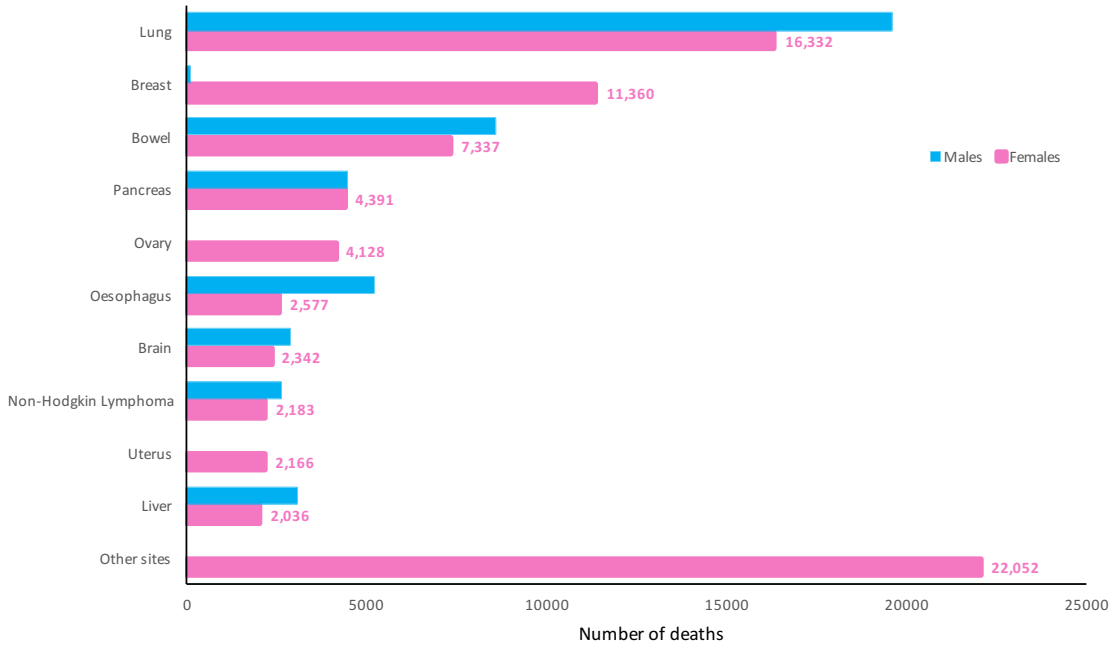

Figure 1.2: Ten most common causes of cancer death in females, UK (2014). Breast cancer is the second most common cause of cancer death in females.

1.2.2 Risk factors

Breast cancer is mostly diagnosed in older age groups, with 48% of diagnoses occurring in women aged 65 and over [21]. Less than 10% of breast cancers are attributed to an inherited genetic mutation, whilst the majority are attributed to reproductive, lifestyle and environmental factors. These risk factors are summarised in **Table 1.1** and show their associate relative risk [23]. Relative risk indicates the risk for an individual who is positive for a factor versus who is negative for that same factor. A relative risk of 1 denotes no increased risk, whereas a relative risk of 10 denotes a 10-fold increase in risk [23].

Table 1.1: Risk factors associated with Breast Cancer

Risk Factor	Category at risk	Comparison category	Relative Risk
Age [24]	Women aged 65 and over	Women aged less than 65	5.8
Reproductive Factors			
Age of menarche [25]	Menses before age 12	Menses after age 15	1.3
Age of menopause [25,26]	Menopause after 55 years	Menopause before 45 years	1.2-1.5
Age of first birth [27,28]	Nulliparous or first child after 30 years	First child after 20 years	1.7-1.9
Lifestyle and Environmental Factors			
Alcohol consumption [29]	2 drinks/day	Non-drinker	1.2
Body Mass Index [30]	80th percentile, age 55	20th percentile	1.2
Radiation exposure [31,32]	Receiving radiation therapy for Hodgkin's disease Having repeated fluoroscopy	No exposure No exposure	5.2 1.6
Genetic Factors			
Family history [33]	First degree relative at ≥50 years with postmenopausal breast cancer First degree relative with premenopausal breast cancer Second degree relative with breast cancer Two first degree relative with breast cancer	No first or second degree relative with breast cancer No first or second degree relative with breast cancer No first or second degree relative with breast cancer No first or second degree relative with breast cancer	1.8 3.3 1.5 3.6
Genetic mutations [34]	Women aged <40 years who are heterozygous for BRCA1 Women aged 60-69 who are heterozygous for BRCA1	Not heterozygous for BRCA1 at age <40 Not heterozygous for BRCA1 at age 60-69	200* 15*
Exogenous hormones			
Hormone replacement therapy with estrogen and progesterone [35]	Current user for at least 5 years	Never used	1.3
Past history of breast cancer [36,37]	Previous history of invasive breast carcinoma	No history of invasive breast carcinoma	6.8

*It has been suggested that these relative risks may overestimate the true risk associated with germline mutations in *BRCA* genes as they are subject to ascertainment bias[38].

1.2.3 Breast Cancer screening

Population based screening of breast cancer is carried out using mammography. Mammography involves taking two radiographs of each breast to detect changes in breast tissue [39]. In England, the National Health Service breast screening programme (NHSBSP) offers free breast screening for women aged 50-70, every three years [40]. Women at a higher risk of developing breast cancer are however screened at an earlier age. Approximately 1300 lives are saved per year, as a result of mammography screening [41].

1.2.4 Histological and Molecular classification of Breast Cancer

For many years, breast cancer was considered a single disease with diverse histopathological features and a range of clinical behaviours. It was later determined that breast cancer could be divided into two groups, according to expression of ER. Traditionally, treatment strategies were based on clinicopathological features that had prognostic value such as, histological type, histological grade, lymph node metastasis and expression of predictive markers (ER, PR and HER2) (reviewed by [42]). Advances in gene expression analysis using high throughput platforms, have demonstrated that breast cancer is a heterogeneous disease consisting of multiple subtypes with distinct histological patterns, biological features and clinical outcome [43,44].

Perou and colleagues were the first to demonstrate that breast cancer can be classified into distinct molecular subtypes[43]. The authors revealed that ER+ and ER- breast cancers are molecularly distinct tumours, based on their expression of an 'intrinsic gene subset'. Furthermore, clustering analysis identified four distinct molecular breast cancer subtypes namely luminal, HER2-positive (HER2+), basal-like and normal-like. Using a larger cohort, Sorlie and colleagues later confirmed this classification and found that the luminal subtype could be further divided into 2 groups namely luminal A and luminal B[44] (**Table 1.2**). The luminal subtype corresponds to ER+ tumours and their division into two subgroups is based on expression of proliferation-related genes. The HER2+ subtype consists of tumours that have HER2 amplification and generally express low levels of ER. HER2+ tumours that also express ER are classified under the luminal B subtype. Basal-like breast cancers are characterised by the absence or low levels of ER and ER related genes including PR, general lack of HER2 overexpression (i.e. triple negative), high expression of proliferation related genes and genes associated with basal epithelial cells (e.g. cytokeratin 5/6 and 17). The normal-like subtype was found to express high levels of genes associated with adipose tissue and normal breast tissue. Recent studies

have however demonstrated that tumours classified under the normal-like subtype, may be an artefact of having a high proportion of normal tissue in the tumour specimen [45].

These molecular subtypes have also been shown to be clinically relevant, as observed by better disease-free and overall survival of luminal A tumours in comparison to the other subtypes [44]. Luminal B tumours have an intermediate outcome, whereas basal-like and HER2+ subtypes displayed the shortest survival times (**Table 1.2**). To further evaluate the prognostic value of these 'intrinsic subtypes', a study by Parker and colleagues, developed a 50-gene prognostic model for node negative breast cancer, using the intrinsic subtypes and clinical information [45]. The assay was termed 'prediction analysis of microarray 50 (PAM 50)', and demonstrated that intrinsic subtypes can be used to predict efficacy to neoadjuvant chemotherapy. Further validation is however still required before this assay can be used in the clinic.

Table 1.2: Molecular subtypes of breast cancer.

Subtype	Immunohistochemistry Status	Outcome
Basal-like	ER-, PR-, HER2+/-	Poor
Luminal A	ER+, PR+/-, HER2-	Good
Luminal B	ER+, PR+/-, HER2+/-	Intermediate
HER2+	ER+/-, PR-, HER2+	Poor
Normal-like	ER+/-, PR+/-, HER2-	Intermediate

More recently, in an effort to further define breast cancer subtypes, an integrated analysis using genomic and transcriptomic data from 2000 breast tumours was used[46]. Through joint clustering of copy number and gene expression data, the authors identified 10 integrative clusters/subgroups labelled as 'IntClust 1-10'. These 10 subgroups were defined by their copy number profiles and showed distinct clinical outcomes. Surprisingly, a subgroup of ER+ tumours (IntClust 2) was found to be high risk, since they displayed poor clinical outcome. This work revealed novel subgroups and demonstrated the effect of copy number aberrations on gene expression, in breast cancer.

Gene expression profiling has also been used to develop breast cancer prognostic signatures. These prognostic signatures are used to predict clinical outcome of individual patients and to identify patients requiring adjuvant chemotherapy. A prognostic signature that is currently approved in the NHS, is Oncotype DX. Oncotype Dx is a quantitative reverse transcriptase polymerase chain reaction (qRT-PCR)-based assay, that measures expression of 21 genes associated with ER and HER2 signalling and cell

proliferation [47]. It is the most widely used assay for prognosis and prediction analysis, and has been suggested as a decision-making tool for adjuvant chemotherapy in ER positive, lymph node negative and HER2 negative early breast cancer [48].

1.2.5 Breast Cancer Treatment

The main standard treatments for breast cancer include, surgery, radiotherapy, chemotherapy, hormone/endocrine therapy and targeted therapy [49]. Currently, breast cancer patients are often given a combination of standard treatments, as well as optional complementary treatments that range from acupuncture to diet management. Surgery and radiotherapy are used mainly to remove the primary breast tumour and any surrounding cancerous tissue. Chemotherapy and targeted therapies on the other hand, reduce tumour burden and also prevent, control or treat cancer metastasis and/or resistance (reviewed by [50]). Hormone and targeted therapies are discussed in more detail below.

1.2.5.1 Endocrine/Hormone therapy

The majority of breast cancers (approximately 70%) are ER+ and so constitute the largest clinical group [43]. Since these cancers are driven by the hormone estrogen, ER+ breast cancers are normally treated with endocrine therapy (ET) which can be given in the neo-adjuvant, adjuvant and metastatic setting. ET include selective estrogen modulators (SERMs) and aromatase inhibitors. Tamoxifen was the first SERM to be approved for the adjuvant treatment of ER+ breast cancer, and has reduced breast cancer recurrence by approximately 40-50% in women with early breast cancer [51]. Overall, the use of Tamoxifen has reduced the yearly breast cancer mortality rate by one third [51]. Tamoxifen has also been approved for the prevention of breast cancer in high risk pre-and post-menopausal women [52]. Another SERM, Raloxifene has also been approved as a preventive treatment for post-menopausal women with osteoporosis or women at high risk of invasive breast cancer [53]. Although Raloxifene is not as effective as Tamoxifen in preventing invasive breast cancer, it has fewer side effects and so might be preferred by some patients. Aromatase inhibitors such as anastrozole, exemestane and letrozole, are used to treat postmenopausal women with early ER+ breast cancer [49].

1.2.5.2 Targeted therapies

1.2.5.2.1 PARP inhibitors

Breast cancers that lack overexpression of HER2, ER and PR are referred to as triple negative breast cancer (TNBC). Approximately 20% of breast cancers are of the TNBC subtype [54], of which around 75% are characteristic of the basal-like molecular subtype [55]. TNBC represents the most aggressive phenotype of breast cancer [44,55] and currently, specific targeted therapies to TNBC are unavailable. Standard treatment for TNBC patients is chemotherapy, particularly anthracycline and taxanes (reviewed by [56]).

Although genetic predisposition to TNBC has not been widely studied, the frequency of TNBC in BRCA1 and BRCA2 mutation carriers was found to be 57% and 23%, respectively [57]. Approximately 20% of TNBC cases harbour BRCA1 (15.6%) or BRCA2 mutations (3.9%) [58]. BRCA-related breast cancers are often characterised by genomic instability and an aberrant homologous recombination DNA repair pathway [59]. Targeting these aberrations using agents such as Poly (ADP-ribose) polymerase (PARP) inhibitors, are potential therapeutic strategies. PARP enzymes are involved in single strand break DNA repair. Inactivation of the BRCA1 and/or BRCA2 genes allows for DNA repair via PARP enzymes, and so presents a mechanism through which cancer cells can continue to grow [60]. Blocking PARP enzymes in BRCA1/2 mutated cells, blocks the only functioning DNA repair pathway and so results in tumour cell death, due to synthetic lethality [60]. PARP inhibitors for the treatment of BRCA1 mutation carriers are currently being investigated in clinical trials (NCT00516373) and indeed Olaparib has been approved by the FDA and NICE for the treatment of advanced Ovarian cancer patients with germline BRCA mutations [61].

1.2.5.2.2 Immunotherapy

Breast cancer was considered a non-immunogenic disease for many years. Recently however, the HER2 and TNBC subtypes have been shown to be characterised by an immune infiltrate. The aim of immunotherapy is to activate the immune response so it recognises tumours as foreign entities, eventually killing them. Expression of programmed death ligand 1 (PDL-1) has been observed in breast cancer clinical samples, particularly in TNBC tumours and cell lines [62,63]. PDL-1 is a ligand for the immune checkpoint receptor, programmed cell death-1 (PD-1) found on T cells, which negatively regulates their function, preventing autoimmunity and inflammatory response [64]. Thus, blocking PD-1 and PDL-1, should enhance antibody function in cancer patients. Currently, there are several clinical trials that are investigating the efficacy of inhibiting

the PD-1/PDL-1 axis with specific antibodies, for treatment of TNBC and HER2+ breast cancer (reviewed by [65,66]). Several other immunotherapy modalities are also currently being evaluated for their efficacy (reviewed by [66]).

1.2.5.2.3 HER2 targeted therapies

Amplification of HER2 is observed in approximately 20% of breast carcinomas and is associated with increased disease progression and poor prognosis[67]. HER2 is a transmembrane tyrosine kinase belonging to the EGF receptor (EGFR/HER) family (reviewed by [68]). This family constitutes of four members (EGFR/HER1, HER2, HER3 and HER4), which stimulate various signalling pathways (**Fig 1.3**). Of these four members, HER2 has a unique feature, in that it does not have a known ligand. HER2 is the favoured dimerization partner of the other EGFR/HER family members, with robust signalling activity observed between EGFR/HER2 and HER2/HER3 heterodimers. HER2 can also form homodimers, which become functional upon overexpression of HER2.

The first drug that was approved by the FDA for the treatment of HER2+ breast cancers was the monoclonal antibody, Trastuzumab (Herceptin)[69,70]. Although Herceptin treatment improved overall survival of HER2+ breast cancer patients with advanced disease, a subset of patients did not respond to treatment. Furthermore, most of the patients who initially responded, later acquired resistance [69,70]. This therefore led to development of additional approaches of targeting HER2 which have included: development of antibodies that bind to different sites of HER2 compared to Herceptin such as Pertuzumab [71]; HER2 tyrosine kinase inhibitors such as Lapatinib [72]; and antibody-drug conjugates such as Trastuzumab emtansine (T-DM1) [73]. Currently, five drugs have been approved for the treatment of HER2+ breast cancer: Trastuzumab (Herceptin), Pertuzumab, Trastuzumab emtansine (T-DM1), Lapatinib and Neratinib (**Fig 1.3**). These HER2 targeted therapies are discussed below.

1.2.5.2.3.1 Trastuzumab (Herceptin)

Herceptin is a monoclonal antibody that binds to the extracellular domain IV of HER2 [74]. Herceptin is currently administered in combination with chemotherapy in the adjuvant setting, to early stage HER2+ breast cancer patients, for one year [49]. This treatment regimen has proven to be beneficial, since it has resulted in 40% fewer cancer recurrences and 34% fewer deaths [75]. Herceptin is also administered in combination with Pertuzumab and the chemotherapeutic agent docetaxel, in the neoadjuvant setting, for patients with advanced or early stage HER2+ breast cancer [49,76].

Different modes of action have been suggested for Herceptin which include suppression of downstream mitogen activated protein kinase (MAPK) and phosphoinositide 3-kinase (PI3K)/AKT/mammalian target of rapamycin (mTOR) signalling pathways [77,78], blocking ligand-independent HER2/HER3 heterodimerization [78] and antibody-dependent cellular cytotoxicity (ADCC) through engaging natural killer (NK) cells [79,80].

1.2.5.2.3.2 Trastuzumab emtansine (T-DM1)

T-DM1 is an antibody-drug conjugate where Trastuzumab is linked with the microtubule toxin, emtansine. Upon binding to HER2, the conjugate is internalized and emtansine is released into the cell, leading to cell death [81]. T-DM1 is used for the treatment of advanced HER2+ breast cancer [82,83].

1.2.5.2.3.3 Pertuzumab

Pertuzumab is a monoclonal antibody that binds to the extracellular domain II of HER2, therefore inhibiting HER2 dimerization with other HER proteins, particularly HER3 [71]. Like Herceptin, Pertuzumab also activates ADCC with equivalent efficacy, resulting in cell death [84]. As aforementioned, Pertuzumab is administered in the neo-adjuvant setting, in combination with Herceptin and docetaxel in advanced and early stage HER2+ breast cancer [49,76].

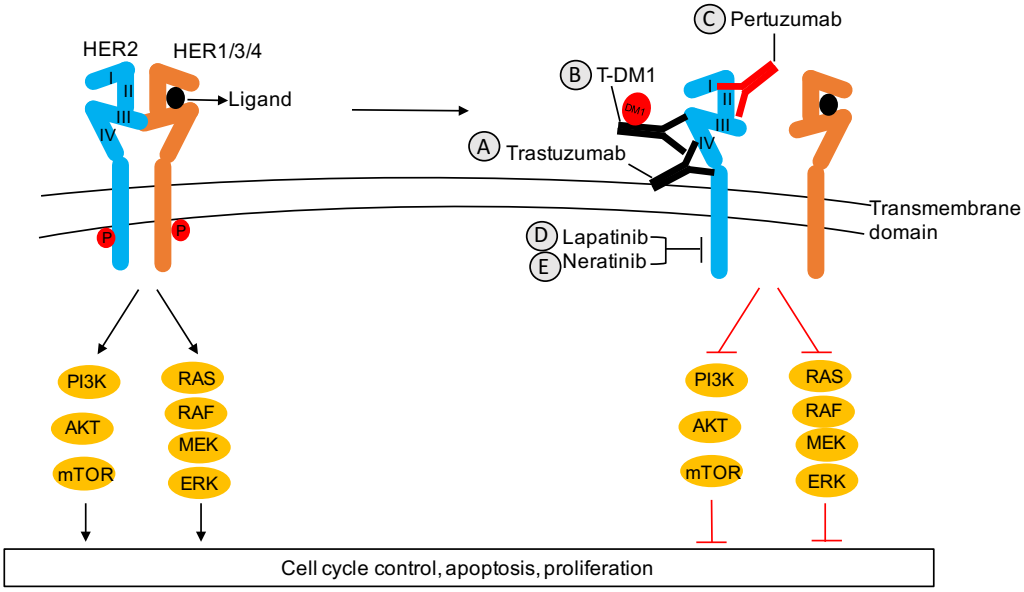

Figure 1.3: HER2 signalling pathway and targeted therapies. The human epidermal growth factor (EGF) receptor family (HER1, HER2, HER3, HER4), are receptor tyrosine kinases involved in signalling pathways that lead to biological processes such as cell cycle control and proliferation. The HER proteins are made up of an extracellular binding domain, a transmembrane domain and an intracellular tyrosine kinase domain (with the exception of HER3 which has no kinase activity). Upon binding of a ligand to the extracellular binding domain of a HER receptor, the receptor forms homodimers or heterodimers with other HER family members. HER2 is the only receptor that does not have a ligand and is the preferential dimerization partner of the other members of the HER family. Homo-and hetero-dimerization results in phosphorylation of the tyrosine kinase domain therefore activating downstream signalling pathways including the PI3K-AKT-mTOR and the MAPK (also known as RAS-RAF-MEK-ERK) pathways. These pathways are involved in cell cycle control, proliferation and apoptosis. Current HER2 targeted therapies for the treatment of HER2+ breast cancer includes: A) Trastuzumab, a monoclonal antibody that binds to extracellular domain IV of the HER2 receptor. Different modes of action of Trastuzumab have been suggested including inhibiting downstream signalling pathways such as PI3K/AKT pathway. B) T-DM1, an antibody-drug conjugate consisting of Trastuzumab and DM1(the highly potent antimitotic drug, emantansine), binds to the extracellular domain of HER2 and allowing for delivery of DM1 to the cell. C) Pertuzumab, a monoclonal antibody that binds to extracellular domain II of HER2 thereby inhibiting dimerization of HER2 with other HER family members, especially with HER3. D) Lapatinib is a dual tyrosine kinase inhibitor targeting HER1 and HER2 and has been shown to inhibit the PI3K/AKT pathway. E) Neratinib is a pan-HER tyrosine kinase inhibitor that inhibits downstream signalling.

1.2.5.2.3.4 Lapatinib

Lapatinib is a dual EGFR and HER2 tyrosine kinase inhibitor, used for the treatment of metastatic HER2+ breast cancer [49]. Lapatinib has been shown to inhibit the activation of MAPK, PI3K-AKT and phospholipase C gamma 1 (PLCγ1) pathways due to reduced phosphorylation of the targeted receptors [72], thus resulting in reduced cell proliferation, metastasis, migration and increased apoptosis. Lapatinib is usually given in combination with the chemotherapy agent capecitabine, to breast cancer patients who have previously been treated with Herceptin, anthracycline and taxane [85,86]. Furthermore, when combined with the aromatase inhibitor letrozole, Lapatinib is used for the treatment

of hormone receptor positive and HER2+ metastatic breast cancer [87]. Combination of Lapatinib and Herceptin has also been shown to be more beneficial than single agents, in the neoadjuvant setting [88].

1.2.5.2.3.5 Neratinib

Neratinib is a pan-tyrosine kinase inhibitor of the EGFR/HER family, that binds to their kinase domain therefore inhibiting downstream signalling [89]. In a phase III trial, HER2+ breast cancer patients that received Neratinib for 12 months following chemotherapy and Herceptin-based adjuvant therapy, showed improved 2-year invasive disease-free survival, compared to patients who did not receive Neratinib treatment [90]. The results of this study, have led to Neratinib being approved by the FDA for treatment of early stage HER2+ breast cancer, following Herceptin-based adjuvant therapy [91].

1.2.5.3 Mechanisms of resistance in HER2 targeted therapies

Studies in this project were based on the HER2+ breast cancer subtype. Therefore, the mechanisms of resistance to HER2 targeted therapy will be discussed below.

Although HER2 targeted therapies have improved patient survival, most patients acquire resistance or exhibit primary resistance to these therapies. Various mechanisms of resistance have been proposed which can be classified as factors associated with either HER2 receptor level or components of downstream signalling pathways. Recent studies have also shown a role for epigenetics in promoting resistance of HER2+ breast cancers.

1.2.5.3.1 HER2 receptor

Mutation of HER2 results in a truncated protein, p95HER2, that lacks the extracellular domain binds and so is unable to bind to Trastuzumab [92]. The p95HER2 protein arises through extracellular domain shedding by a metalloprotease e.g. ADAM10 or by alternative translation of HER2 mRNA [93]. Expression of p95HER2 protein has been associated with Trastuzumab resistance [94,95]. Since this protein still has constitutive kinase activity, HER2+ breast cancer cells expressing p95HER2 have been shown to be sensitive to the HER2 tyrosine kinase inhibitors Lapatinib [94].

A HER2 splice variant (HER2Δ16) has been reported in breast cancer cell lines [96] and breast tumours [97]. HER2Δ16 is characterised by a 16-amino acid exon that is deleted in the extracellular domain [96]. The deleted exon was found to contain two cysteine residues

that were critical for HER2 transformation activity [96]. HER2Δ16 expression is tumour specific and has been shown to confer Trastuzumab resistance in breast cancer cell lines [98]. These functions of HER2Δ16 were found to be mediated by Src kinase, since treatment with the tyrosine kinase inhibitor, dasatinib, inactivated Src, destabilised HER2Δ16 and inhibited tumorigenecity [98]. A phase II clinical trial of dasatinib in advanced HER2+ and/or hormone receptor breast cancer patients however, only found one out of 24 HER2+ patients previously treated with anti-HER2 therapies, showing a partial response [99].

Hsp90 is a chaperone protein that activates several oncoproteins including HER2 [100]. Inhibition of Hsp90 has been shown to reduce the anti-tumour activity of Trastuzumab resistant and Trastuzumab sensitive xenografts and could potentially be a novel therapeutic strategy for the treatment of HER2+ breast cancers [101,102].

Loss of HER2 amplification following neoadjuvant Herceptin-based therapy has also been observed in patients with residual disease [103] and so may contribute to resistance.

1.2.5.3.2 Downstream signalling pathways

Activation of the PI3K/AKT pathway due to decreased phosphatase and tensin homolog (PTEN) expression and oncogenic mutations in phosphatidylinositol-4,5-bisphosphate 3-Kinase Catalytic Subunit Alpha (PIK3CA), have been associated with Herceptin resistance in breast cancer cell lines and tumours [104]. Similarly, loss of PTEN and PIK3CA mutations also confer Lapatinib resistance in breast cancer cell lines and xenograft models [105]. A later study showed that inhibition of HER2 using Lapatinib conferred resistance in breast cancer xenograft models and patients, through upregulation of ER and the anti-apoptotic protein B-cell lymphoma 2 (Bcl-2) [106]. Interestingly, the authors showed that 18% of tumours treated with Lapatinib in the neoadjuvant setting converted from ER- to ER+, thus providing an ER-dependent mechanism for survival.

Crosstalk between HER2 and insulin like growth factor 1 receptor (IGF-1R), has also been shown to promote Herceptin resistance, since inhibition of IGF-1R kinase activity led to decreased HER2 phosphorylation in resistant cells and re-sensitised these cells to Herceptin [107]. Additionally, Herceptin resistant breast cancer cells overexpress HER activating ligands, which lead to increased expression of EGFR and HER3 receptors. These receptors in turn form heterodimers with HER2, which are not inhibited with Herceptin, and so provide a mechanism for resistance through EGFR or HER3 signalling

pathways [108]. This corresponds to a report showing that inhibition of HER2 reactivates HER3 in HER2+ breast cancer cell lines [109].

1.2.5.3.3 A role for Epigenetics in resistance to HER2 targeted therapies

Various epigenetic proteins have been implicated in resistance to HER2 targeted therapies. microRNAs (miRNAs) have been shown to confer resistance to HER2 targeted therapies through various mechanisms including targeting PTEN and triggering nuclear factor–kB (NF-kB) signalling that in turn activates PI3K pathway [110]. Hypermethylation of transforming-growth factor β1 (TGFβ1), B- cell lymphoma 6 (BCL6), p53-regulated DNA replication inhibitor (KILLIN) and cathepsin Z (CTSZ) genes, were shown to be predictive biomarkers of Herceptin resistance in HER2+ breast cancer cells, since treatment with a demethylating agent restored their expression to similar levels with Herceptin sensitive cells [111]. Histone deacetylases have also been implicated in resistance to HER2 targeted therapy. This is demonstrated by treatment of HER2+ breast cancer cells with histone deacetylase inhibitors (HDACi) increasing sensitivity to Herceptin and lapatinib [112,113], as well as, overcoming Herceptin resistance[112]. Overexpression of histone demethylases (e.g. KDM5 family of histone demethylases) have also recently been shown to promote resistance of HER2+ breast cancer cells to Herceptin [114] and Lapatinib [115]. These will be discussed in more detail in **Section 1.8.**

1.3 Epigenetics and gene expression

Transcription is a fundamentally important process involving transfer of genetic information from DNA to messenger RNA (mRNA). Although this genetic material is the same in all cells of an organism, different cell types differ in their gene expression patterns, owing to their specific functions. For this reason, transcription is tightly regulated to ensure maintenance of gene expression patterns during mitotic cell division. This maintenance of gene expression patterns over many cell divisions, occurs through inherited information that is not encoded in the DNA sequence, and is known as epigenetic information (reviewed by [116]).

Epigenetics therefore describes heritable gene expression changes that occur without alterations in the DNA sequence. An additional definition of epigenetics however does not include the requirement for heritability. For instance, the US National Institute of Health roadmap epigenomics project (http://www.roadmapepigenomics.org) states that 'epigenetics refers to both heritable changes in gene activity and expression (in the progeny of cells or of individuals) and also stable, long-term, alterations in the transcriptional potential of a cell that are not necessarily heritable'. Regardless of definition, epigenetic processes that alter gene expression patterns are DNA methylation, post-translational modification (PTM) of histone proteins, chromatin remodelling and RNA based mechanisms [116]. Collectively, epigenetic modifications are referred to as the 'epigenome'. Since the epigenome plays an important role during cellular processes such as development and differentiation, inadequate maintenance can lead to development of diseases including cancer. Therefore, understanding molecular mechanisms driving epigenetic changes in cancer is imperative for the development of novel cancer therapies. This PhD thesis is based on a histone protein modification enzyme, and so this epigenetic process will be the focus of the discussions below.

1.3.1 Histone proteins and regulation of gene expression

Transcription in eukaryotic cells takes place in chromatin. Chromatin is a complex made up of histone proteins and DNA. The basic unit of chromatin is the nucleosome which consists of 147 bp of DNA wrapped around an octamer of two copies of each of the four core histone proteins (H2A, H2B,H3 and H4) [117,118] (**Fig 1.4**). Nucleosomes are separated by a linker DNA of 10-60bp which associates with a linker histone, H1 [117,118]. The core histones H3 and H4 contain amino-terminal tails that protrude from the nucleosome core and undergo PTM at specific amino acid residues. These histone PTM include:

- Phosphorylation (at serine and threonine residues)

- Acetylation (at lysine side chains)
- Methylation (at lysine and arginine residues)
- Ubiquitination (at lysine residues)
- Sumoylation (at lysine residues)
- ADP ribosylation (at glutamic acid residues)

Of these histone PTMs, the best characterised are methylation, phosphorylation and acetylation [116]. Histone PTMs are carried out by specific enzymes known as 'writers' and are inherited through cell division (reviewed by [119]) (**Fig 1.4**). This epigenetic information encoded within histone tails can be read by proteins known as 'readers', which in turn use this information to alter chromatin structure, thereby regulating transcription (**Fig 1.4**). Additionally, there are enzymes that remove these modifications and are so known as 'erasers' (**Fig 1.4**). Aberrations in these histone modification factors (writers, readers and erases) can contribute to development of diseases such as cancer. This PhD thesis, investigates the role of a specific eraser protein (histone lysine demethylase 5B (KDM5B)) in breast cancer, and so this group of proteins will be discussed below.

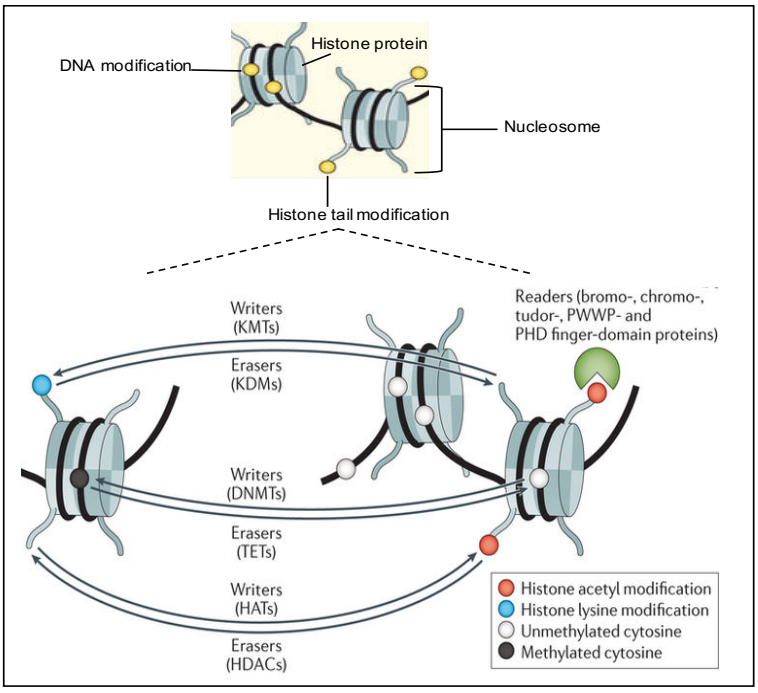

Figure 1.4: Epigenetic modifications in chromatin. The nucleosome, which is the basic unit of chromatin consists of a 147 bp of DNA sequence wrapped around an octamer of two copies of each of the four core histone proteins (H2A, H2B, H3 and H4). Epigenetic modifications (yellow circles) on DNA and histones regulate chromatin accessibility to transcription machinery. These epigenetic marks are established by 'writers' such as histone lysine methyltransferases (KMT), histone acetyltransferases (HATs) and DNA methyltransferases (DNMTs). The marks are in turn interpreted by 'readers'. Epigenetic modifications are reversible, a process mediated by a group of enzymes known as 'erasers' which include histone demethylases (KDMs), histone deacetylases (HDACs) and by the ten-eleven translocation (TET) family of 5-methylcytosine oxidases. Epigenetic proteins are important in regulating transcription and establishing and maintaining cellular identity. PHD, plant homeodomain. Modified image from[120].

1.3.2 Histone methylation

Histone methylation plays important roles in cellular processes such as transcription and genomic stability. Histones can become methylated on arginine or lysine residues by enzymes known as histone methyltransferases, which are responsible for catalysing this modification (reviewed by [121]). These proteins catalyse methylation by adding methyl groups to histones using the methyl donor S-adenosylmethionine (SAM). There are three families of histone methyltransferases namely protein arginine methyltransferases (PRMTs) [122–126] and histone lysine methyltransferases (KMTs) which are divided into two groups: SU(VAR)3-9, Enhancer of zeste and Trithorax (SET)-domain methyltransferases [127,128] and the non-SET domain proteins DOT1 and DOT1-like (DOT1L) [129,130].

Histones can become mono (me1)-, di (me2)- or tri (me3)- methylated on specific lysine residues in histone H3 and H4 proteins, whereas arginine residues can become monomethylated (me1), symmetrically dimethylated (me2s) or asymmetrically dimethylated (me2a) [131]. These modified histones have been shown to associate with different chromatin states thereby regulating transcription for example; H3K4me3, H3K36me3 and H3K79me3 are associated with active transcription, whereas H3K9me3 and H3K27me3 are associated with gene silencing [132,133].

1.3.3 Histone demethylases

Prior to the discovery of lysine specific demethylase 1 (LSD1) [134], histone methylation was considered an irreversible epigenetic modification, believed to only be erased upon histone exchange or DNA replication. Subsequent studies identified a second family of LSD demethylases containing a Jumonji C (JmjC) domain [135–137]. Consequently, demethylating enzymes of most methylated lysines have now been characterized [138], showing histone lysine methylation as a dynamic process regulating individual genes through recruitment of methyltransferases and demethylases.

1.3.3.1 The LSD family of histone demethylases

LSD1 belongs to the LSD family of histone demethylases which is composed of two members: LSD1 (also known as KDM1A, AOF2, BHC110 or KIAA0601) [134] and LSD2 (also known as KDM1B or AOF1) [139]. The LSD proteins contain an amine oxidase-like domain (AOL) of catalytic activity and a SWIRM (SWI3, RSC8 and Moira) domain, found only in chromatin associated proteins [119]. LSD enzymes can only catalyse the demethylation of me1 and me2 but not me3 on lysine residues, via an oxidation mechanism involving the flavine adenine dinucleotide (FAD) cofactor [140].

1.3.3.2 The JmjC domain containing histone demethylases

The JmjC family contains a catalytic Jumonji domain, present in 32 human proteins, 22 of which are histone demethylases (**Table 1.3**) [141]. Clustering of these proteins based on homology and structural similarities, divides them into seven subfamilies. The catalytic mechanism of these enzymes involves an oxidative reaction that requires two cofactors: Fe(II) and α-ketoglutarate. This reaction forms an oxoferryl (Fe(iv)=O) intermediate that hydrolyxylates the methyl group resulting in an unstable carbinolamine that breaks down, to form an unmethylated peptide and formaldehyde (**Fig 1.5**) [142]. This mechanism allows JmjC demethylases to demethylate all three methylation states (me1, me2 and me3) on histone lysines at H3K4, H3K9, H3K27 and H3K36 [135,137,143–146]. A prominent group among the JmjC histone demethylases, is the KDM5 (JARID1) protein family, whose members are involved in development, transcriptional regulation, genomic instability and have recently been implicated in progression and drug resistance of numerous cancers.

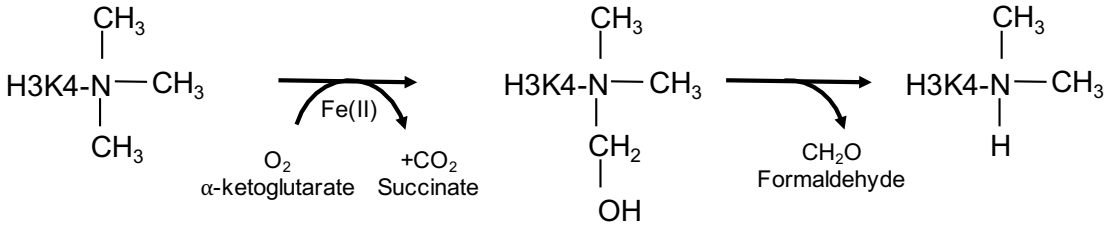

Figure 1.5: The catalytic mechanism of JmjC domain containing histone demethylases. This mechanism involves an oxidative reaction that is dependent on Fe(II) and α-ketoglutarate co-factors. The KDM5 family specifically demethylate H3K4me3/me2.

1.4 KDM5 histone demethylases

The KDM5 (also known as Jumonji AT-rich interactive domain (JARID1)) family of histone demethylases consist of four members: KDM5A (JARID1A/RBP2), KDM5B (JARID1B/PLU-1), KDM5C (JARID1C/SMCX) and KDM5D (JARID1D/SMCY). Single orthologues of the KDM5 family exist across species including *Drosophila melanogaster* (Little imaginal disks (Lid)) [147], *Caenorhabditis elegans* (RBR-2) and *Saccharomyces cerevisiae* (Jhd2p/Yjr119Cp) [148], where they have similar functions as transcriptional regulators and chromatin modifiers.

KDM5 proteins are capable of catalysing the demethylation of di- and tri-methyl states/marks on lysine 4 of histone H3 (H3K4me2/me3), thereby repressing transcription

of target genes [146,149–151]. KDM5A and KDM5B have also been shown to catalyse the demethylation of the mono-methylated mark at the same site (H3K4me1), *in vivo* [145,146].

Table 1.3: Protein domain and histone substrate of the JmjC histone demethylases

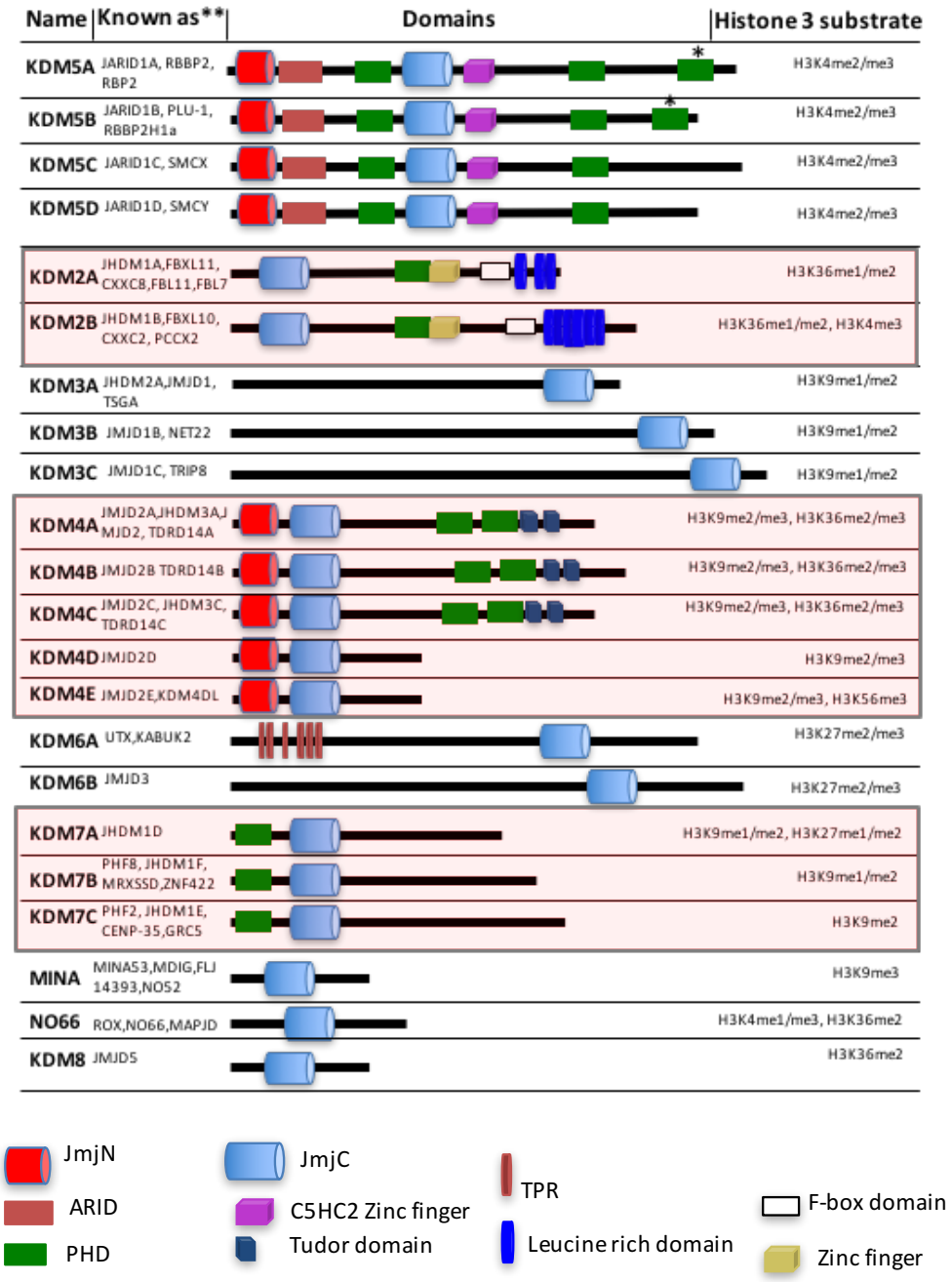

** This is not an exhaustive list of aliases. *The PHD3 of KDM5A and KDM5B bind to H3K4me3 substrate. Modified image from [152].

1.4.1 Structural organisation of KDM5 histone demethylases

KDM5 histone demethylases have a highly conserved multi-domain structure consisting of an N-terminal Jumonji (JmjN) domain, an AT-rich interactive (ARID) domain, a JmjC domain, a C_5HC_2 zinc-finger, and two to three plant homeodomain (PHD) fingers (**Fig**

1.6). Despite the conserved sequence homology, the KDM5 proteins have distinct structural features, in that KDM5A and KDM5B have two PHD fingers in their C-terminal region, whereas KDM5C and KDM5D only have one PHD finger in this region (**Fig 1.6**).

Among the Jumonji domain containing histone demethylases, the KDM5 family is unique in that, their catalytic domain is separated into two subunits (JmjN and JmjC) by insertion of the ARID and PHD1 domains (**Table 1.3**). However, Horton and colleagues have shown using a crystal structure, that the two Jumonji subunits (JmjN and JmjC) are linked through internal folding, and together with the C-terminal region of the C_5HC_2 zinc finger domain are required for enzymatic activity[153]. The ARID domain was first identified in the mouse B cell specific transcription factor, Bright [154] and the Dead ringer protein (Dri) of *Drosophila melanogaster* [155], as a domain that bound AT-rich sequences. In KDM5B, the ARID domain was also found to bind to a GCACA/C consensus sequence [156,157]. PHD1 and PHD3 fingers (numbering of PHD fingers starts from N terminal side of the protein) are required for histone tail recognition. PHD1 domain of KDM5A and KDM5B bind to unmethylated H3K4 histone tail (H3K4me0) [158,159]. In KDM5A, binding of PHD1 to H3K4me0 stimulates demethylation of the adjacent H3K4me3 mark, suggesting a model for spreading demethylation on chromatin through a positive feedback mechanism between the reader and catalytic domains [158]. PHD3 of KDM5A and KDM5B specifically binds to H3K4me3/me2 marks [159,160]. Conservation of structural domains is evident amongst the KDM5 homologs present in *Drosophila melanogaster* (Lid), *Caenorhabditis elegans* (RBR-2) and *Saccharomyces cerevisiae* (Jhd2p/Yjr119Cp) as observed by separated catalytic domains (**Fig 1.6**).

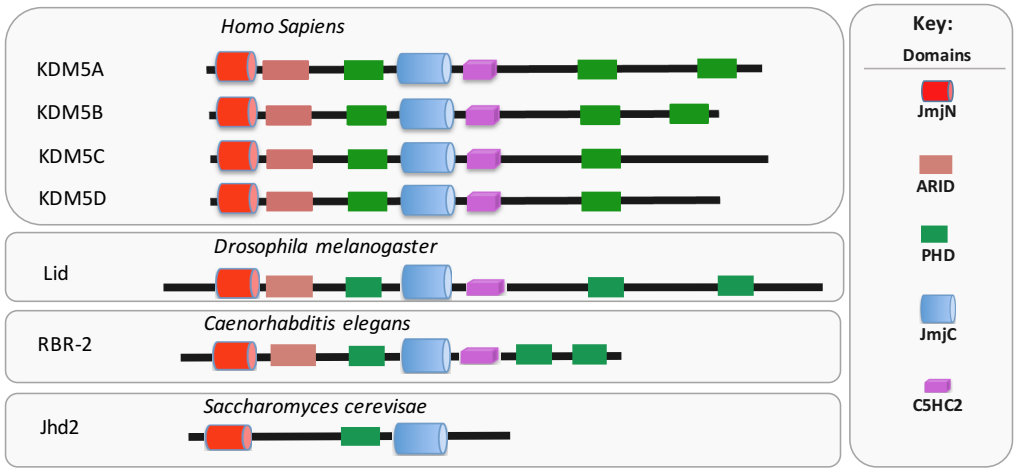

Figure 1.6: Domain structure of JARID1 histone demethylases. The domain structure of KDM5 proteins are conserved across species and consist of a JmjN, ARID, JmjC and C5HC2-zinc finger, and 2-3 PHD finger domains with the exception of the yeast, which only has one PHD finger and does not have a C_5HC_2 zinc-finger domain. JmjN: N-terminal Jumonji, ARID: AT-rich interactive, JmjC: C-terminal Jumonji, PHD: plant homeodomain finger.

1.4.2 KDM5 Histone Demethylase Function

The following section will discuss the function of KDM5A, KDM5C and KDM5D in normal development and cancer. The functions of KDM5B will be discussed separately in **section 1.5.**

1.4.2.1 KDM5 proteins in normal development

KDM5A, was first identified as a retinoblastoma binding protein (pRb) in a cDNA expression library [161]. A later report showed that KDM5A together with the transcription factor E2F4, enhanced Rb's transcriptional repression of target genes, during embryonic stem cell (ESC) differentiation [162]. Significantly, KDM5A$^{-/-}$ mice are viable and fertile but display behavioural abnormalities [145]. Surprisingly, deletion of KDM5A did not alter global H3K4me3 levels in mouse embryonic fibroblasts [145], probably due to redundancy of the other KDM5 proteins. During embryogenesis both KDM5A and KDM5B demethylate broad H3K4me3 domains found in mouse oocytes, which is required for normal activation of the zygotic genome and is important for early embryonic development [163].

KDM5C, encoded by the SMCX gene located on the X chromosome, was identified as an X-linked gene which during embryogenesis, is able to escape X-inactivation [164]. In human adult tissue, KDM5C shows strong expression in the brain, lung and skeletal muscle; and a moderate to low expression in the pancreas and heart [165]. Mutations, as well as loss of function of KDM5C are associated with X-linked mental retardation [165,166]. In mice, KDM5C null mutations were found to be embryonic lethal [167].

KDM5D, encoded by the SMCY gene is only expressed in males being located on the Y chromosome, and was reported to be a candidate for the male specific minor histocompatibility antigen H-Y [168]. KDM5D is moderately expressed in the brain, pancreas, skeletal muscle and lung [165] and in spermatogenesis. KDM5D is the least studied member of the KDM5 family.

1.4.2.2 KDM5 proteins in Cancer

KDM5A is overexpressed in gastric and cervical cancer cells, and its depletion leads to senescence and growth arrest, possibly due to increased expression of cyclin dependent kinase (CDK) inhibitors such as p21 [169]. Amplification of KDM5A has been reported in breast and head and neck cancers[170,171]. In breast cancer, *in vivo* studies have shown

that KDM5A promotes metastasis to the lungs, through positively regulating metastasis related genes such as tenascin C (TNC) [172]. Additionally, increased expression of KDM5A was found to promote cell proliferation of basal breast cancer cell lines, possibly through repressing CDK inhibitors and apoptosis related genes [170]. An oncogenic translocation between PHD3 of KDM5A and nucleoporin-98 (NUP98), has been shown to induce acute myelogenous leukemia (AML) in mice, thereby demonstrating a role of KDM5A in oncogenesis of AML [160].

KDM5C acts in a complex with the viral protein E2 to suppress the expression of viral oncoproteins E6 and E7 in human papilloma virus-associated cancers [173]. In clear cell renal carcinoma (ccRCC) 3% of tumours were found to harbour truncating KDM5C mutations [174], which can trigger genomic instability [175]. On the other hand, overexpression of KDM5C has been observed in hepatocellular carcinoma cells, where it promotes migration, invasion and metastasis by repressing the bone morphogenetic protein 7 (BMP7) [176]. KDM5C also promotes cell migration, metastasis and invasion in breast cancer by repressing the breast cancer metastasis suppressor 1 (BRSM1) [177]. In prostate cancer, KDM5C knockdown was found to inhibit proliferation of prostate cancer cells [178]. Furthermore, nuclear expression of KDM5C was associated with reduced prostate-specific antigen relapse free survival, and was proposed to be a prognostic marker [178].

KDM5D was initially reported by Perinchery and colleagues as a gene associated with prostate cancer, since it's deletion was observed in 52% of cases[179]. Recently, KDM5D was shown to be mutated or frequently deleted in metastatic prostate cancer, and that low levels were associated with poor prognosis[180]. Moreover, KDM5D suppresses invasion of prostate cancer cells both *in vivo* and *in vitro*, by repressing expression of invasion associated genes, through its enzymatic activity[180]. Another study has shown that KDM5D physically interacts with the androgen receptor (AR) in the nucleus, and regulates AR signalling by repressing AR target genes [181]. Similar to KDM5C, KDM5D has also been implicated in ccRCC as it was found to be downregulated due to loss of chromosome Y [182]. Further analysis showed that KDM5D reduced cell viability of renal cancer cells and thus its deletion may contribute to renal cancer progression [182].

1.5 KDM5B

KDM5B is a 176kDa protein encoded by a gene located on chromosome 1q32.1. KDM5B was first identified in a cDNA library screen as a gene whose expression was down-regulated upon inhibition of the tyrosine kinase, HER2, with Herceptin [183]. Following the identification of KDM5B, other splice variants have also been reported namely, RBP2-H1 [184] and RBP2-H1A [185]. RPB2-H1 was identified as a gene whose expression was frequently down-regulated in melanoma [184]. Although there is high homology between the cDNA sequences of these splice variants, RBP2-H1 contains an extra exon that encodes a region with strong homology to chromosomal ALU repeats [184]. Among the splice variants, PLU-1 (KDM5B) is the most widely studied and most abundant in a panel of breast cancer and melanoma cell lines examined [186].

1.5.1 KDM5B Expression

In normal human adult tissues, high KDM5B mRNA expression is restricted to testis, with moderate expression in the placenta and ovary [183]. Recently using an in-house antibody, we have shown expression of KDM5B on lymphoid cells within tonsil (Steven Catchpole personal communication). In the adult mouse, high KDM5b mRNA expression is restricted to testes with moderate expression in the ovary, prostate and eye [187]. Analysis of KDM5b mRNA expression during the different stages of mouse mammary gland differentiation, showed that KDM5b is expressed in the virgin (non-pregnant) gland, increased during pregnancy, decreased at lactation and re-expressed at involution [187–189]. In the mouse embryo, KDM5b is expressed in ESCs [190,191], neural progenitors [192] and embryonic mammary bud[187].

1.5.2 The Function of KDM5B

Consistent with the ability of KDM5 proteins to demethylate the active H3K4me3 mark, many studies have described them as transcriptional repressors, that act directly or in association with repressive complexes, to regulate gene expression. So far studies have demonstrated a role of KDM5B in biological processes such as, normal development, differentiation/cell fate, cell cycle, genome stability and mammary gland development.

1.5.2.1 Normal development and differentiation

KDM5B regulates H3K4 methylation marks close to promoters and enhancers of ESCs, thus affecting the balance between differentiation and self-renewal [193]. Indeed, Dey and

colleagues demonstrated that KDM5B bound on promoters of cell fate modulators early growth response gene 1 (Egr1), p27 and BMI1, repressing their expression through its demethylase activity [190], thus enhancing cell proliferation. Furthermore, during ESC-self-renewal KDM5B has been reported to catalyse the demethylation of H3K4me3 on intragenic regions, thus repressing cryptic transcription during expression of self-renewal genes [191].

The importance of KDM5b in regulating gene expression during early development is demonstrated by embryonic [188] and neonatal [194] lethality upon knockout of the gene, with the latter displaying neuronal defects such as disorganized cranial nerves, defective eye development and increased exencephaly [194]. Zou and colleagues however, successfully developed a KDM5b$^{-/-}$ mouse strain that remained viable beyond the embryonic and neonatal stages[195]. This mouse strain however, displayed phenotypic defects such as, delayed mammary gland development, reduced mammary epithelial cell proliferation and premature mortality [195]. The phenotype of the KOs from Zou and colleagues corresponded with those of a mouse strain with a deleted ΔARID domain (ΔARID mouse) that was developed in our laboratory [188]. The ΔARID mice were viable and fertile but also displayed developmental abnormalities in the mammary gland such as delayed development of the terminal end bud and side branching in early pregnancy and at puberty [188]. The differences observed in the KDM5b$^{-/-}$ mouse models may be related to colony maintenance, since different phenotypes were observed in mice with the same genetic background (C57BL/6).

1.5.2.2 Mammary gland development

KDM5B was found to be critical for the expression of mammary gland development regulators such as FOXA1, HER2, STAT5a and ESR1, since they were downregulated upon loss of KDM5B in mammary epithelial cells [195]. In the ΔARID mouse mammary gland, decreased phosphorylated STAT5 [196] and increased Caveolin-1 (CAV1) (Steven Catchpole personal communication), an inhibitor of phosphorylated STAT5 (pSTAT5), was observed at mid-pregnancy day 12.5. Thus, showing the requirement of KDM5B in regulating the janus kinase 2 (JAK2)/signal transducers and activators of transcription 5a (STAT5a) signalling pathway, during mammary gland development. Taken together with the observation that KDM5B interacts with ERα [188] and that loss of KDM5B reduces serum estrogen level [195], this demonstrates a role of KDM5B in luminal epithelial cell proliferation of the mammary gland. Thus, may explain the delayed side branching and terminal end bud in the mammary gland in KDM5b mouse models[195188].

1.5.2.3 Cell cycle progression

A role of KDM5B in positively regulating the cell cycle has been demonstrated. In ESCs, KDM5B was found to promote G_1-S progression through direct repression of the growth arrest-promoting proteins Egr1 and p27[190,197]. Consistently, KDM5B was also found to promote G_1-S progression in MCF-7 breast cancer cells, as demonstrated by accumulation of cells at G_1 phase and delay in cell cycle exit upon its knockdown [146]. Scibetta and colleagues further showed that in breast cancer cells, KDM5B positively regulated genes involved in control of spindle checkpoint, chromatin condensation and G_2/M checkpoint, therefore implicating it in cell cycle checkpoint regulation[156].

1.5.2.4 Genome stability

KDM5B has been described as a key regulator of genome stability, since its depletion promoted DNA damage and sensitised osteosarcoma and breast cancer cells to genotoxic insult[198]. KDM5B was shown to be essential for the recruitment of Ku70 and BRCA1, to sites of DNA damage and subsequent repair of DNA double strand break (DSB) via non-homologous end joining (NHEJ) and homologous recombination (HR) [198]. KDM5B demethylase activity was found to be important for its DSB repair function, since H3K4me3 demethylation by KDM5B triggered recruitment of BRCA1 to sites of DNA damage[198].

1.5.2.5 Interaction of KDM5B with other repressor proteins

KDM5B interacts with the developmental transcription factors brain factor -1 (BF1) and paired box 9 (PAX-9), via their conserved sequence motif (Ala-X-Ala-Ala-X-Val-Pro-X4-Val-Pro-X8-Pro) termed the VP motif in the transcription factors [199]. KDM5B was found to act as a transcriptional co-repressor of BF-1 and PAX9 as co-expression of KDM5B with either transcription factors enhanced their repression activity [199]. Since BF-1 is part of the Groucho repressive complex, the authors suggested that KDM5B may be involved in groucho-mediated transcriptional repression [199]. Furthermore, since PAX-9 mRNA was found to be elevated in breast cancer, it is possible that the KDM5B-BF-1-PAX9 interaction may be important in the development of breast cancer [186]. KDM5B also cooperates with the polycomb repressive complex 2 (PRC2) through the SUZ12 component of PRC2, where it acts as a co-activator of retinoic acid (RA) signalling [200].

An association between KDM5B and HDACs has been reported. KDM5B associates with HDAC4 by binding to the N-terminal half of HDAC4 which contains the myocyte enhancer

factor 2 (MEF2)-binding domain[189]. This interaction was found to be dependent on two PHD domains of KDM5B [189]. KDM5B and HDAC4 were found to be co-expressed in the pregnant mouse mammary gland, as well as, in breast cancer, thus suggesting an important of KDM5B in these processes [189]. Co-localisation of KDM5B with two catalytic subunits of the nucleosome remodelling and deacetylase (NuRD) complex: HDAC1 and chromodomain helicase DNA binding protein 4 (CHD4) has also been reported[159]. Since both subunits are important in regulating gene expression and chromatin remodelling, KDM5B may cooperate with HDAC1 and CHD4 in transcriptional repression. These interactions between KDM5B and different complexes/proteins may depend on the cell phenotype.

1.5.3 KDM5B in Cancer

Of the KDM5 proteins, the role of KDM5B in cancer progression is the most studied. Overexpression of KDM5B has been reported in various cancers including breast, melanoma, prostate and lung, where it has been regarded as an oncogene, as it appeared to be essential for the growth and survival of these cancers (reviewed by [201]).

1.5.3.1 Breast Cancer

KDM5B has been most widely studied in breast cancer. Upon discovery of KDM5B as a gene regulated by HER2 signalling (**See section 1.5**), high expression of the gene was also reported in breast cancer tissue and cell lines [183]. Knockdown of KDM5B in the MCF-7 ER+ breast cancer cell line reduced cell proliferation, colony formation and tumour formation in a mouse mammary tumour model [146]. It was later shown that KDM5B promoted estrogen dependent tumour growth of MCF-7 cells in immune suppressed mice[188]. Thus, these findings demonstrated the importance of KDM5B in the MCF-7 ER+ breast cancer cells. Indeed, KDM5B has been described as a 'luminal lineage driving oncogene' in breast cancer[202]. The authors showed that KDM5B was amplified and overexpressed in luminal breast cancers, and that KDM5B was enriched on promoters and enhancers of the luminal genes ER, GATA3, FOXA1 and TFAP2C in luminal cells [202]. Other KDM5B target genes in MCF-7 ER+ cells include BRCA1, CAV1 and metallothionein genes (MT1H, MT1F and MT1X), where KDM5B was shown to bind their promoters repressing their expression via its demethylase activity [146,156]. Additionally, high KDM5B activity in ER+ tumours was associated with poor outcome and endocrine resistance [202], suggesting KDM5B as a potential therapeutic target in ER+ breast cancer.

In the triple negative breast cancer subtype, KDM5B expression was downregulated in both tumours and cell lines [159]. Genome-wide gene expression analysis of MDA-MB-231 cells, showed that KDM5B knockdown increased expression of genes involved in cell proliferation, migration and inflammatory response [159]. Indeed, overexpression of KDM5B was shown to suppress migration and invasion of this cell line [159]. This corresponds with findings showing suppression of metastasis and angiogenesis by KDM5B, in MDA-MB-231 cells[203]. Thus, in triple negative breast cancer cells KDM5B may have a different function which can lead to tumour inhibition.

1.5.3.2 Melanoma

A sub-population of slow-cycling melanoma cells were found to express high levels of KDM5B ($KDM5B^{high}$), which was required for their continuous growth [204]. Depletion of KDM5B in $KDM5B^{high}$ cells, initially accelerated tumour growth but was followed by exhaustion, suggesting that KDM5B confers a stem cell-like function in melanoma cells [204]. Thus, in melanoma cells, KDM5B seems to be required for the maintenance of continuous growth rather than initiation of tumours [204].

1.5.3.3 Prostate Cancer

Bioinformatics analysis using the Oncomine Cancer database revealed upregulation of KDM5B in prostate cancer, particularly in metastatic prostate cancer [205]. KDM5B was shown to associate with and regulate the transcriptional activity of the androgen receptor [205]. Inhibiting the expression of KDM5B via binding of microRNA-29a in the 3'-untranslated region of KDM5B, significantly reduced prostate cancer cell proliferation and induced apoptosis[206].

1.5.3.4 Other cancers

Overexpression of KDM5B has been reported in bladder and lung cancer, where it was shown to promote proliferation, survival and/or invasion of these cells [207,208]. In gastric cancer, KDM5B is upregulated and promotes cell growth and metastasis through activation of the AKT pathway[209]. Increased expression of KDM5B in hepatocellular carcinoma (HCC) correlated with tumour size and was associated with poor prognosis. Consistently, knockdown of KDM5B significantly suppressed HCC cell proliferation[210]. KDM5B knockdown in oral squamous cell carcinoma (OSCC) cells, reduced stemness, migration, invasion and increased radiation sensitivity [211]. Similarly, silencing of KDM5B

in neuroblastoma cell lines downregulated Notch/Jaggged signalling, thus demonstrating that KDM5B promotes a stemness in these cell lines [212]

In general, it is evident that KDM5B is mostly upregulated in cancer where it acts to promote tumour progression. However, target gene identification analyses have also revealed a cell-type specific function of KDM5B, that needs to be considered when targeting KDM5B for cancer therapy.

1.6 Genes regulated by KDM5B in the normal and malignant mammary gland: CAV1

Genome-wide expression analysis performed to identify KDM5B target genes, revealed a number of genes that were either up- or down-regulated in the ER+ breast cancer cell line, MCF-7 [146,156,202]. From the genes that are down-regulated by KDM5B, CAV1 is of particular interest in this project. Recent data from our laboratory using a mouse model lacking KDM5B demethylase activity, termed ΔARID, showed upregulation of CAV1 in the mid-pregnant mammary gland (Steven Catchpole personal communication). These findings suggest that KDM5B regulates CAV1 expression in the normal and malignant mammary gland, and so indicates that similar networks may be operative in normal and cancer cells. Therefore, the extent of CAV1 regulation by KDM5B needs to be studied further to understand its importance in normal development, as well as, in cancer.

1.6.1 CAV1

Caveolins, the main components of caveolae-enriched plasma membranes, are a protein family consisting of three proteins, caveolin 1, 2 and 3 [213–215]. Caveolin proteins organise and concentrate lipids (i.e. cholesterol and glycosphingolipids) [216–218] and signalling molecules [213] within caveolar membranes and are thought to act as scaffolding proteins. CAV1 is abundantly expressed in myoepithelial, endothelial, adipocytes and fibroblast cells [219,220] and is co-expressed with CAV2 [214,221], whereas CAV3 is expressed in muscle cells[215]. CAV1 maps to chromosome 7q31.1, which is a fragile region that is frequently deleted in many cancers including breast cancer [222]. Proteins that interact with CAV1 such as EGFR, G protein and G-protein coupled receptors, HER2 and H-ras, bind to a cytoplasmic region of CAV1 that is proximal to the membrane, known as caveolin scaffolding domain (CSD) [213,223–225]. Functionally, CAV1 is involved in controlling signalling, which can lead to effects on various cellular processes such as, cell growth[226], lipid transport and signal transduction [227].

1.6.2 CAV1 in the normal mammary gland

Documentation of CAV1 protein expression during mouse mammary gland development, showed that it steadily declines during mid to late pregnancy remaining downregulated during lactation, only re-emerging during weaning and being restored to non-pregnant levels, at involution[228].

The JAK2/STAT5 pathway is required for alveologenesis (development of alveoli structures in the mammary gland) [229] and lactogenesis (milk production) [230], during pregnancy. Interestingly, a CAV1 knockout mouse model showed extensive proliferation of the mammary gland and hyperphosphorylation of STAT5a[231]. Therefore, CAV1 was characterised as a negative regulator of the Prl-R/JAK2/STA5a signalling pathway[231]. Indeed, in the ΔARID mouse, phosphorylated STAT5 was found to be downregulated [196] and this correlated with upregulation of CAV1 (Steven Catchpole personal communication), in the mid-pregnant mammary gland.

1.6.3 CAV1 in Breast Cancer

In breast cancer, CAV1 expression is generally low[232] in tumours that are hormone receptor positive (ER and PR) and express luminal cytokeratins [233]. Thus, in these breast cancers, CAV1 may act as a tumour suppressor gene, since its overexpression in ER+ breast cancer cell lines, results in reduction of tumour growth[234], migration and epidermal growth factor (EGF)-stimulated lamellipod extension[235]. Contrastingly, overexpression of CAV1 is often observed in aggressive breast cancers such as basal-like and triple negative breast cancers[233,236]. These differences in CAV1 expression in different subtypes of breast cancer, have been shown to be due to promoter methylation [237], thereby demonstrating epigenetic regulation of CAV1 expression in breast cancer. Nevertheless, CAV1 expression in breast cancer cells is not associated with patient survival[238,239]. However, recently CAV1 was identified as a marker for Herceptin resistance in HER2+ breast cancer [240,241].

On the other hand, CAV1 expression in breast cancer stroma is associated with good clinical outcome. High CAV1 expression in breast cancer-associated fibroblasts, is associated with good clinical outcome [242]. This also includes triple negative breast cancers, where stromal CAV1 expression predicts good overall survival[238,239] and so is a prognostic marker[238]. Taken together, these findings suggest a multifaceted and cell-type specific role of CAV1 in breast cancer.

The studies from KDM5B KD in breast cancer cell lines such as MCF-7, indicate that KDM5B can normally downregulate CAV1 expression. Similarly, studies in the KDM5B

demethylase null mouse model also indicate that KDM5B can downregulate CAV1, in the normal mouse mammary gland. It will be important to know just how general the regulation of CAV1 by KDM5B is in different cell phenotypes, and this question will be addressed in this thesis in chapter 4, focusing on HER2 positive cell lines.

1.7 KDM5 proteins in drug resistance

The KDM5 proteins have been implicated in drug resistance of several cancers and are therefore potential therapeutic targets. During their investigations in modelling response to anti-cancer drugs, Sharma and colleagues observed a small subpopulation of reversible 'drug tolerant' cells that maintained viability [243]. Using lung cancer cell lines, the authors investigated the underlying mechanisms of the reversibility of drug tolerant cells, and identified KDM5A as a gene that was upregulated in these cells. Indeed, knockdown of KDM5A in PC9 lung cancer cells significantly reduced the emergence of drug tolerant cells and likewise, transient expression of KDM5A in PC9 cells decreased sensitivity to anti-cancer drugs [243]. Chronic drug exposure to a prostate cancer cell line also resulted in drug tolerant cells that had high expression of KDM5A [244]. Amplification and increased expression of KDM5A in breast cancer, has also been shown to promote resistance to the EGFR inhibitor, erlotinib, since its knockdown significantly reduced the number of drug-tolerant cells[170]. A recent study by [245], demonstrated that expression of KDM5A was upregulated in gliobastoma resistant cells, and that inactivating or overexpressing KDM5A resulted in increased sensitivity or resistance, to the DNA alkylating agent temozolomide.

Cytotoxic treatment of melanoma cells resulted in enrichment of therapy resistant cells that had high KDM5B expression [246]. These observations were also seen *in vivo*, and it was demonstrated that knockdown of KDM5B increased sensitivity to anti-melanoma treatment [246]. In neuroblastoma, KDM5B expression was found to correlate with sensitivity to chemotherapy, since cell lines with a higher KDM5B expression were more resistant to doxorubicin, etoposide and cisplatin [212]. Indeed, KDM5B silencing led to increased sensitivity to cisplatin [212]. KDM5D has recently been implicated in resistance of prostate cancer cell lines to docetaxel. RNA-seq analysis of two prostate cancer cell lines, identified KDM5D as a gene that mediated docetaxel sensitivity [181]. Indeed, silencing KDM5D in a sensitive cell line led to docetaxel resistance. This corresponded to the observation that KDM5D was deleted in a castration resistant prostate cancer (CRPC) cell line, which was insensitive to docetaxel [181]. The authors demonstrated that interaction of KDM5D with the androgen receptor was necessary for docetaxel sensitivity.

1.8 KDM5B as a target for cancer therapy

Accumulating evidence showing dysregulated histone demethylases in human cancers, has led to the development of small molecule inhibitors that target the demethylase activity of these proteins, for anti-cancer therapy. As discussed herein, KDM5 demethylases are upregulated in various cancers where they promote tumour growth and drug resistance. Thus, there have been major efforts within academia and industry to develop compounds targeting the demethylase activity of KDM5 proteins. To date, several KDM5 small molecule inhibitors have been reported however, some lack cytotoxicity or selectively between KDM4 and KDM5 histone demethylases[114,115,247–256].

Selective and potent KDM5 inhibitors that have been shown to prevent drug tolerance in various cancer cell lines include CPI-455 [115], YUKA1 [114], KDOAM-25 [254] (**Table 1.4**). CPI-455 is a pan-KDM5 inhibitor with a 200-fold selectivity for KDM5 enzymes over KDM4 demethylases, and a >500-fold selectivity over other JmjC-containing demethylases. Treatment of lung, melanoma, colon and breast cancer cell lines with CPI-455 in combination with targeted therapies, reduced the number of drug tolerant cells demonstrating that the demethylase activity of KDM5 proteins is required for drug resistance [115]. YUKA1 is a KDM5A and KDM5C inhibitor with an IC_{50} of 2.66μM and 7.12μM for KDM5A and KDM5C respectively. An EGFR-mutant lung cancer cell line and a HER2+ breast cancer cell line treated with gefitinib and Herceptin respectively, in combination with YUKA1, reduced the number of drug tolerant cells [114]. These findings also demonstrated that requirement of the demethylase activity of KDM5A/C in promoting drug resistance of these cell lines. KDOAM-25 is a pan-KDM5 inhibitor with potencies of <100nM for KDM5 enzymes, but has a higher potency for KDM5B (19nM). KDOAM-25 was shown to reduce cell proliferation of a multiple myeloma cell line [254]. The authors did not investigate the effect of this inhibitor on drug tolerance. Recently, a potent, selective and orally bioavailable KDM5 inhibitor, that showed high potency for KDM5B (IC_{50} 4.7nM) and KDM5C (IC_{50} 65.5nM) *in vivo,* was developed[247]. This compound known as 48, can now be used to study KDM5 functions *in vivo.*

Since KDM5 demethylases have been shown to downregulate tumour suppressor genes via their demethylase activity, the use of demethylase inhibitors can be viewed as a means of suppressing tumour growth [152]. This therefore requires a comprehensive analysis of target genes for specific KDM5 enzymes. However, since member specific KDM5 demethylase inhibitors are currently unavailable, gene editing techniques such as CRISPR, can be used to identify genes regulated by individual KDM5 demethylases, and to further study their function in cancer cell lines [152].

Table 1.4: Small molecule inhibitors targeting KDM5 histone demethylases

Inhibitor	Specificity	Effects
CPI-455 [115]	Selectively inhibits demethylase activity of the four KDM5 proteins	Prevents drug tolerance in multiple cancer cell line models including breast and lung
YUKA1 [114]	Selectively inhibits demethylase activity of KDM5A and KDM5C proteins	Prevents drug tolerance in breast and lung cancer cell lines
KDOAM-25 [254]	Selectively inhibits demethylase activity of KDM5B with a higher potency, than KDM5A and KDM5C proteins	Inhibits cell growth of the MM1S multiple myeloma cell line
48 (Liang et al. 2016)	Potent inhibitor to KDM5B and KDM5C	Oral dosage given twice a day in mice shows unbound maximal plasma concentration (C_{max}) >15-fold over its cell EC_{50}

1.9 Gene editing technologies in drug target validation

According to data analysis from pharmaceutical companies, a major factor contributing to the failure of drug candidates at the late stages of clinical development, is lack of efficacy attributed to erroneous hypotheses about the linkage of the drug target to disease[257]. Thus, the need to better understand the role of drug targets in disease biology is important, to ensure success during drug development. Genome editing technology has currently gained momentum as one of the methods to study gene function in human disease, since it allows precise modification of genes[257].

Genome editing using customized nucleases provides a system through which targeted deletions, insertions or specific sequence changes can be induced in organisms and cell types [258]. The first step in genome editing is the creation of a DNA DSB at a desired genomic locus, followed by repair of the DSB via homology directed repair (HDR) or NHEJ [258]. HDR is used for precise genome editing, where a DNA fragment with a complementary sequence to the target site is used to repair DSBs via homologous recombination [259]. This DNA fragment can harbour any alteration, therefore allowing integration of any desired DNA sequence at the target site [259]. NHEJ is an error-prone repair mechanism which introduces insertions or deletions (indels) of varying lengths which can cause frameshifts, altering the gene product and abolishing gene function [259].

A number of genome editing tools such as zinc-finger nucleases (ZFN), transcription activator-like effector nucleases (TALENs) have been used extensively over the years however, they have remained a niche technology. ZFNs and TALENs utilise the same principle: fusion of a sequence-specific DNA binding domain to the nuclease domain of Fok1 restriction enzyme [258,259]. Contrastingly, the recently developed clustered, regularly

interspaced, short palindromic repeat-CRISPR associated (CRISPR-Cas), has resulted in widespread adoption of nuclease based genome editing, owing to its simplicity, high-throughput capabilities and ability to target multiple genomic sites [259]. CRISPR-Cas is an RNA-guided system, that utilises Watson-Crick base pairing between an engineered RNA and the target DNA sequence [258,260]. CRISPR-Cas is a prokaryotic adaptive immune system that has been manipulated for genome editing. This technique has been simplified to consist of a single guide RNA (sgRNA) and a Cas9 endonuclease. The sgRNA directs the Cas9 endonuclease to induce DNA DSBs at homologous sites, which are then repaired via NHEJ or HDR leading to introduction of insertions or deletions (indels) or precise gene editing, respectively (**Fig 1.7**).

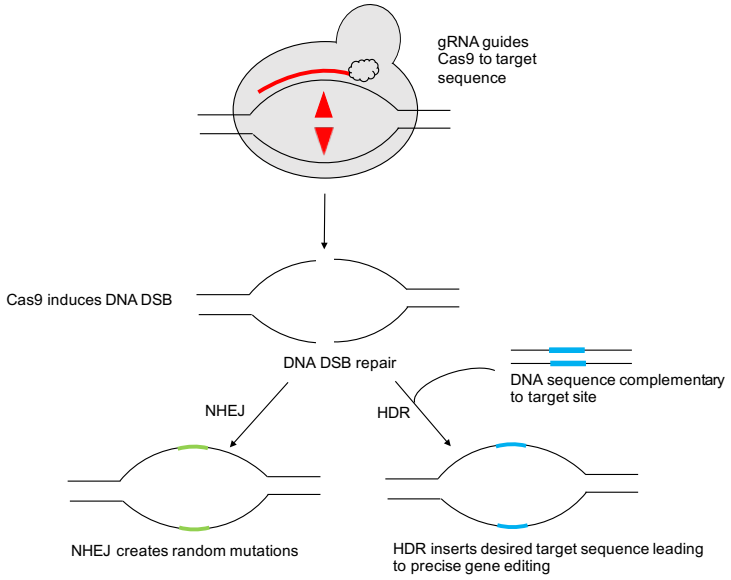

Figure 1.7: CRISPR-Cas9 technology. A single gRNA (sgRNA) guides the Cas9 nuclease to a target site with a complementary DNA sequence. Cas9 then cleaves the DNA inducing a double strand break (DSB). The DSB is repaired via non-homologous end joining (NHEJ) leading to introduction of mutations, insertions or deletions. Repair can also occur through homology directed repair (HDR) when a short DNA sequence that is complementary to the target site is inserted, thus allowing precise gene editing [259].

1.9.1 CRISPR-Cas9 for drug target validation

Advances in DNA sequencing technologies have provided insight into the genetic variation among patients in human disease, thus enabling improvement in treatment strategies [261]. These advances have therefore driven the need for personalised or precision medicine, where a patient's information is combined with their genetic data, to inform on individual treatment regimens [261]. However, hypotheses generated from these studies require testing using specific genetic models. CRISPR-Cas technology has enabled the study of gene function in disease relevant cell types, through development

of cell line and animal models [262]. These models have been used to evaluate drug targets and model drug resistance. CRISPR-Cas has also been simplified for use in genome-wide screens. CRISPR screens study phenotypes produced upon gene knockout, with the aim of identifying genes involved in metabolic or pathogenetic processes [261]. CRISPR screens have been used to identify candidate drug targets in cancer and human pathogens [261]. Thus, the adoption of CRISPR-Cas technology in cancer research for example, should enable acceleration of drug discovery and development of more effective cancer therapies [262].

1.10 Overview of PhD project

1.10.1 Rationale

Breast cancer is the most common cancer in women in the UK, and high incidence rates have been reported worldwide. Recent advances in treatment strategies owing to improved molecular characterisation of breast cancer, as well as, early detection of the disease, has increased survival rates of breast cancer patients. However, breast cancer still remains the second most common cause of cancer death in women, in the UK. One of the major factors contributing to the high mortality rate is resistance (*de novo* or acquired) to administered treatments.

A role for epigenetics in contributing to drug resistance, stems from observing development of drug tolerance and the reversibility of this tolerance by epigenetic manipulation. The reversible nature of drug tolerance by epigenetic factors has led to the development of epigenetic-based therapies, some of which (e.g. histone deacetylase inhibitors) have been approved for cancer treatment. However, targeting the epigenome, can be challenging due to the wide involvement of epigenetic factors in biological processes [263]. Recent technological advances such as gene editing, may allow further characterisation of these genes in specific cell-types thus, fine-tuning their function. Such insights will allow better drug design, thereby enabling further exploration of the utility of epigenetic drugs, as well as, investigating their potential in improving the effects of current drugs [263].

KDM5B is a histone demethylase that is overexpressed in a majority of breast cancers, particularly those belonging to the ER+ and HER2+ molecular subtypes [202]. KDM5B is considered a promising target for a number of reasons. First, KDM5B is overexpressed in many malignancies. Second, KDM5B promotes drug resistance in a number of cancers, by maintaining the growth of a sub-population of cancer cells, that serve to initiate therapeutic relapse. Third, since KDM5B regulates expression of genes involved in biological processes such as, cell cycle, DNA repair and development, its aberrant expression can result in dysregulation of these processes and eventually disease development or progression.

Based on the above, KDM5B is a possible target for anti-cancer therapy. Although there have been advances towards development of small molecule inhibitors targeting KDM5B, these inhibitors lack specificity since they also target other members of the KDM5 family[114,115,247,254]. Thus, understanding the function of KDM5B in normal and cancer cells, could provide to the knowledge required to develop specific KDM5B inhibitors, since multiple enzymes can demethylate the H3K4me2/me3 marks, thereby regulating various networks [152].

1.10.2 Hypothesis

The aim of this project was to further investigate the role of KDM5B in the normal and malignant mammary gland. KDM5B has been widely studied in ER+ breast cancer, with a few studies being done in triple negative breast cancer cells. However, the function of KDM5B in HER2+ breast cancer cells, has not been widely investigated. Furthermore, although KDM5B has been shown to promote resistance to anti-cancer drugs in various malignancies, its involvement in breast cancer drug resistance, particularly in HER2 targeted therapy, has not yet been demonstrated.

KDM5B has been shown to downregulate CAV1 in the normal mammary gland at mid pregnancy and in ER+ breast cancers. Thus, suggesting similar networks are operative in development of the normal gland and in breast cancer. However, it is not clear how widespread the downregulation of CAV1 by KDM5B is seen in different breast cancer cell lines, nor is it clear, which cell types in the developing mammary gland (luminal, myoepithelial and fat cells), could be responsible for the downregulation of CAV1 by KDM5B. Given the above, this PhD project was directed towards testing the following hypotheses:

1. Since KDM5B can enhance signalling by the ERα and HER2 receptors operative in some cancer cells, knockout of KDM5B will reduce cell growth, increase efficacy of therapeutic targeting of the HER2 receptor and impede development of drug resistance.

2. Since KDM5B can downregulate expression of CAV1, which when expressed in stromal tissue is inhibitory to breast cancer growth, they may be expressed in the same cell types and their expression could be inversely correlated. Thus, targeting KDM5B could restore levels of CAV1, therefore inhibiting other signalling pathways regulated by paracrine signalling.

1.10.3 Aims

The specific aims of this thesis were to:

1) Develop KDM5B KOs in two HER2+ breast cancer cell lines using CRISPR-Cas9 technology

2) Investigate the molecular effect of KDM5B KO by performing transcriptomic analysis, in a HER2+ breast cancer cell line

3) Investigate phenotypic effects of KDM5B KO on cell growth and drug resistance, in two HER2+ breast cancer cell lines

4) Investigate KDM5B regulation of CAV1 by examining their expression levels in a) parental and KDM5B KO HER2+ breast cancer cells and b) normal and breast cancer-associated fibroblast cells. Furthermore, the cellular localisation of KDM5B and CAV1 will be examined in the mouse mammary gland, to decipher the cell types responsible for CAV1 downregulation by KDM5B.

2 : Materials and Methods

2.1 Cell culture and conditions

2.1.1 Cell culture Reagents

Table 2.1: Cell culture reagents

Reagent	Supplier
Trypsin (2.5%), no phenol red	Life Technologies
Trypan blue solution 0.4%	Sigma-Aldrich
Penicillin-Streptomycin/Glutamine 100X	Life Technologies
Insulin solution human	Sigma-Aldrich
Fetal Bovine Serum (FBS)	Life Technologies
Dulbecco's Modified Eagle's Medium (DMEM)	VWR International
Roswell Park Memorial Institute 1640 (RPMI)	VWR International
Dimethyl sulfoxide (DMSO)	Sigma-Aldrich
Trastuzumab (Herceptin)	Kindly provided by the Breast Clinic at Guy's Hospital, London
Lapatinib	Selleckchem

2.1.2 Cell culture media

Table 2.2 Cell culture media

Media	Reagents	Concentration
DMEM (500ml)	FBS	10% (v/v)
	Penicillin-Streptomycin/Glutamine	1% (v/v)
RPMI (500ml)	FBS	10% (v/v)
	Penicillin-Streptomycin/Glutamine	1% (v/v)
	Insulin	10µg/mL
DMEM Conditioned media	Fresh complete media Conditioned media Penicillin- Streptomycin/Glutamine	70% 30% 1%
RPMI Conditioned media	Fresh complete media Conditioned media Penicillin- Streptomycin/Glutamine Insulin	70% 30% 1% 10µg/mL

2.1.3 Cell culture maintenance

The breast cancer cell lines BT- 474, HCC1143 and T47D were maintained in RPMI medium. MCF-7, MDA-MB-231 and SKBr3 cell lines were maintained in DMEM medium. BT-474 and SKBr3 Herceptin resistant cells were maintained using the same medium as the parental cells, with further addition of 40µg/ml Herceptin. BT-474 and SKBr3

KDM5B knockout cell lines were maintained using the same conditions as the parental cells. The normal breast fibroblast line, HMFU19 and the breast cancer-associated fibroblast lines, LS11-045 and LS11-088 were maintained in DMEM medium. All cells were incubated at 37°C with 5% CO_2. The characteristics of these cell lines are shown in **Table 2.3** [264]**.** All cell lines were authenticated using short-tandem repeat (STR) profiling. To maintain the cells' authenticity a master cell bank was created. Cells were kept in culture for no more than 10 weeks and were regularly checked for mycoplasma contamination using the MycoAlert Mycoplasma Detection Kit (Lonza).

Table 2.3: Description of cell lines.

Name	Immunoprofile	Subtype	Source
BT-474	ER^+/ $PR^{+/-}$/$HER2^+$	Luminal B	CRUK Cell Service laboratory
HCC1143	ER^-/$HER2^-$/PR^-	Basal	ATCC
MCF-7	ER^+/$PR^{+/-}$/$HER2^-$	Luminal A	ATCC
MDA-MB-231	ER^-/$HER2^-$/PR^-	Basal	ATCC
SKBr3	ER^-/PR^-/$HER2^+$	HER2+	Memorial Sloan Kettering Cancer Centre
T47D	ER^+/$PR^{+/-}$/$HER2^-$	Luminal A	Kindly provided by the Keydar group
BT-474 Herceptin resistant	ER^+/ $PR^{+/-}$/$HER2^+$	Luminal B	Kindly provided by Professor Anthony Kong, University of Oxford, UK
SKBr3 Herceptin resistant	ER^-/PR^-/$HER2^+$	HER2+	Kindly provided by Professor Anthony Kong, University of Oxford, UK
HMFU19 Normal breast fibroblast line			Kindly provided by Professor Valerie Speirs, University of Leeds, UK
LS11-045 and LS11-088 breast cancer-associated fibroblast lines			Kindly provided by Professor Valerie Speirs, University of Leeds, UK

2.2 CRISPR-Cas9 Gene Editing

2.2.1 Reagents

Table 2.4: Reagents used for CRISPR gene editing

Reagent	Supplier
T4 ligase buffer	Thermo Fisher Scientific
T4 DNA ligase	Thermo Fisher Scientific
Fast digestion buffer	New England Biolabs
BbsI	New England Biolabs
SOC media	Thermo Fisher Scientific
Ammonium buffer	Amplicon
$MgCl_2$	Amplicon
dNTP mix	Amplicon
TEMPase Hot Start DNA polymerase	Amplicon

2.2.2 Plasmids

Table 2.5: Plasmids used for CRISPR gene editing

Plasmid Name	Source
U6-gRNA PX458	Asst. Prof. Eric Bennett, Copenhagen Centre for Glycomics, University of Copenhagen
Cas9-2A-GFP pBKS	Asst. Prof. Eric Bennett, Copenhagen Centre for Glycomics, University of Copenhagen

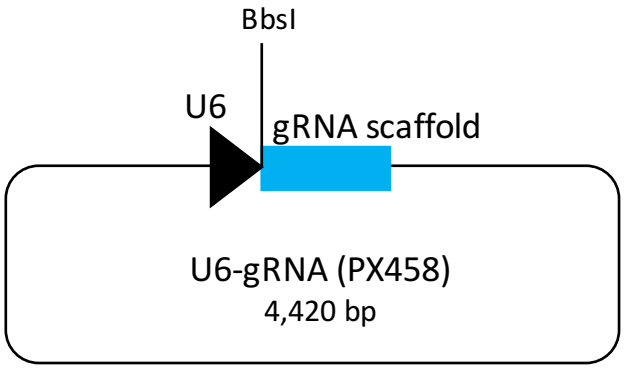

Figure 2.1: U6-gRNA PX458 plasmid map. KDM5B gRNAs were inserted into the BbsI site. U6 promoter is shown as a black arrow head. The gRNA scaffold (blue rectangle) is a sequence required for Cas9 binding.

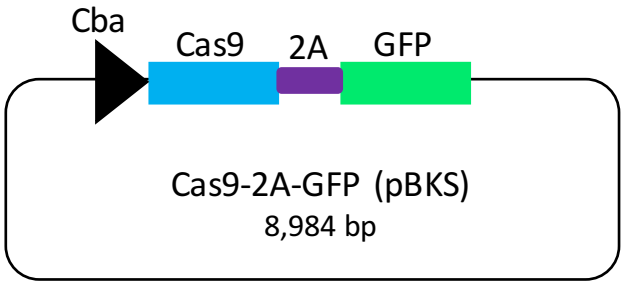

Figure 2.2: Cas9-2AGFP pBKS plasmid map. Plasmid map showing features of the Cas9-2AGFP pBKS plasmid. Cas9 endonuclease is driven by the chicken beta actin (cba) promoter. The Green fluorescent protein (GFP) reporter gene was used to allow isolation of transfected cells. The 2A peptide sequence (2A) allows simultaneous expression of Cas9 and GFP genes.

2.2.3 KDM5B PCR primers

Table 2.6: KDM5B Primers to Exons 1, 4, 5 and 6

Target	Primer Sequence
6-FAM 5'-labelled (FamF)	5'-GAGCTGACCGGCAGCAAAATTG-3'
KDM5B Exon 1	For: 5'-GAGCTGACCGGCAGCAAAATTGGTACAACTCGGACTTGCTGTTGCTC-3' Rev: 5'-CTCAACTCCGACCTTCTAGGC-3'
KDM5B Exon 4	For: 5'-GAGCTGACCGGCAGCAAAATTGCAGAAGAAGGTGGATTTGCAGTTGT-3' Rev: 5'-CAAGGTCTTCCAAACACAATCAAGG-3'
KDM5B Exon 5	For: 5'-GAGCTGACCGGCAGCAAAATTGGTGCAGCCTCTGGAAGTAGATCAAA-3' Rev: 5'-ACATGAGAGAAATCCAGTGCCAGAC-3'
KDM5B Exon 6	For: 5'-GAGCTGACCGGCAGCAAAATTGAAGGCCATGAATATTAAAATAGAAC-3' Rev: 5'-CAAAGCCCAACCCAGTGACTACT-3'

For – Forward; Rev – Reverse. The forward primer has a FAMF target sequence extension (red).

2.2.4 Design of candidate KDM5B gRNAs

gRNAs targeting four exons of KDM5B were selected (**Table 2.7**) using a Cas9/gRNA target prediction tool (https://chopchop.rc.fas.harvard.edu/). Chopchop ranks gRNA sequences according to specific parameters including 1) number of off-targets and mismatches 2) GC content (gRNAs are most effective when they have a GC content of between 40-70%) and 3) location of gRNA within the gene (5' (best) and 3' (worst)). KDM5B gRNAs were tested for their cutting efficiency, and a suitable guide was chosen to develop KDM5B KO cell lines.

Table 2.7: KDM5B gRNA target sequences with corresponding target exon.

KDMB gRNA sequence	Targeted Exon
CGGCCCATAGCCGAGCAGACTGG	1
GTTTGCTCCTGGCAAAGCAGTGG	4
CCCAGAGGCAGTCTGTGCAGCCT	5
TCATAATCTGAGACGTCGAATGG	6

PAM sequence is highlighted in red.

2.2.5 Generation of KDM5B gRNA expression plasmid

For each gRNA targeting one of the four exons of KDM5B, a 25-base pair (bp) sequence was synthesised as two complementary oligonucleotides (**Table 2.8**). The oligonucleotides were annealed and inserted into the U6-gRNA plasmid (**Fig 2.1**) which was cut with BbsI, to generate single KDM5B gRNA expression constructs, as described below.

Table 2.8: KDM5B gRNA oligonucleotide sequences

KDM5B Targeted Exon	Sequence
1	For: 5'-CACCGCGGCCCATAGCCGAGCAGAC-3'
	Rev: 5'-AAACGTCTGCTCGGCTATGGGCCGC-3'
4	For: 5'-CACCGGTTTGCTCCTGGCAAAGCAG-3'
	Rev: 5'-AAACCTGCTTTGCCAGGAGCAAACC-3'
5	For: 5'-CACCGAGGCTGCACAGACTGCCTCT-3'
	Rev: 5'-AAACAGAGGCAGTCTGTGCAGCCTC-3'
6	For: 5'-CACCGTCATAATCTGAGACGTCGAA-3'
	Rev: 5'-AAACTTCGACGTCTCAGATTATGAC-3'

For – Forward Rev – Reverse. The selected guide RNA sequences are underlined.

2.2.5.1 Oligonucleotide annealing

Forward and reverse oligonucleotide (oligo) gRNA sequences targeting exons 1, 4, 5 or 6 of KDM5B (**Table 2.8**), were first annealed together to form a double stranded DNA molecule. Oligonucleotides were mixed with the appropriate buffer (**Table 2.9**) and annealed in a thermocycler using the following conditions: 95°C for 5 minutes followed by a ramp down to 25°C at 5°C/minute.

Table 2.9: Components of oligo annealing reaction

Reagent	Final Concentration	Volume
100μM Oligonucleotide (Forward)	10μM	1μl
100μM Oligonucleotide (Reverse)	10μM	1μl
10X T4 ligase buffer	1X	1μl
ddH_2O	Make up to 10μl	7μl

2.2.5.2 Digestion of U6-gRNA expression plasmid

The U6-gRNA plasmid was digested with the BbsI restriction enzyme (**Table 2.10**) and incubated for 1 hour at 37°C.

Table 2.10: Components of U6-gRNA expression plasmid digest

Reagent	Final Concentration	Volume
10X Fast digestion buffer	1X	0.8 μl
U6-gRNA plasmid	300ng	6.7 μl
10U BbsI	0.625U	0.5 μl

2.2.5.3 Ligation of annealed oligonucleotides with the U6-gRNA plasmid

The annealed KDM5B gRNA oligonucleotides were mixed directly with the digested U6-gRNA plasmid in a ligation reaction (**Table 2.11**) and incubated at 16°C overnight. This allowed insertion of the KDM5B gRNA oligonucleotides into the BbsI site of the U6-gRNA plasmid (**Fig 2.1**).

Table 2.11: Components of ligation reaction

Reagent	Final Concentration	Volume
10μM Annealed oligonucleotides	50nM	0.5μl
BbsI digested U6-gRNA plasmid	300ng	8 μl
10X T4 ligase buffer	1X	1 μl
5U/μl T4 DNA ligase	0.3U	0.6μl

2.2.5.4 Transformation of competent cells

15µl of Top 10 chemically competent *E. coli* cells (Thermo Fisher Scientific) were transformed with 1µl of the ligation mixture. Reaction was incubated on ice for 30 minutes, followed by heat shock at 42°C for 60 seconds and immediate incubation on ice for 2 minutes. 90µl of super optimal broth with catabolite repression (SOC) media (Thermo Fisher Scientific) was added and cells incubated at 37°C for 30 minutes with shaking. Thereafter, cells were spread on Lysogeny broth (LB) agar plates containing ampicillin and incubated at 37°C overnight, to allow for the growth of antibiotic-resistant clones.

2.2.6 Hot PCR Screen

To check whether the gRNAs had been inserted correctly in the U6-gRNA plasmid, a few colonies were picked and lysed in 5µl of 0.5µM sodium hydroxide (NaOH) for 2 minutes, neutralised with 10µl of 1M Tris pH 8.0 and diluted in 100µl H_2O. 1µl of the lysed cells was used in a 12.5µl PCR reaction utilising primers outlined in **Table 2.6**. 1µl of 10ng/µl positive (correct vector – B4GALT7; provided by Asst. Prof. Eric Benett) and negative (empty vector - PX458) controls were also included in the PCR reaction (**Table 2.12**) using thermocycling conditions shown in **Table 2.13**.

Positive colonies containing the correct sized inserts, were identified by fragment analysis using the ABI3010 DNA Analyzer (ABI/Life Technologies) according to manufacturer's instructions. 1µl PCR product was mixed with 0.3µl of GeneScan-LIZ600 standard (ABI/Life Technologies) and 10µl Hi-Di Formamide (Thermo Fisher Scientific), incubated at 90°C for 2 minutes then subjected to fragment analysis. Analysis of raw data was performed on the Peak Scanner Software (ABI/Life Technologies). Positive colonies with correct sized inserts were purified using the Qiagen Miniprep Kit according to manufacturer's instructions and DNA concentration was measured using the NanoDrop 1000 spectrophotometer (Thermo Fisher Scientific). Positive colonies were also validated by Sanger sequencing, which confirmed correct orientation of inserts. For this purpose, 5µl DNA (100ng/µl stock) and 5µl forward primer (5µM stock) were mixed and sent for sequencing (BGI Europe, Denmark).

Table 2.12: Tri-primer PCR Reaction

PCR component	Volume (µl)	Final concentration
10x Ammonium buffer	1.25	1x
$MgCl_2$ (25mM)	0.7	2.5mM
dNTP (25mM)	0.1	200µM
TEMPase Hot Start DNA Polymerase	0.12	0.5
FamF primer (25µM)	0.125	0.25µM
Forward primer (2.5µM)	0.125	0.025µM
Reverse primer (25µM)	0.125	0.25µM
H_2O	8.955	
Template	1	

Table 2.13: Tri-primer PCR thermocycling conditions

Temperature	Time	Number of cycles
95°C	15 minutes	
95°C	30 seconds	X15
72°C	30 seconds	
72°C*	30 seconds	
95°C	30 seconds	X25
58°C	30 seconds	
72°C	30 seconds	
72°C	7 minutes	
4°C	Forever	

*Touchdown 72°C to 1°C per cycle

2.2.7 Screening of KDM5B gRNAs

2.2.7.1 Transfection and fluorescence-activated cell sorting (FACS)

To examine the cutting efficiency of the KDM5B gRNAs, positive gRNA sequences prepared by Miniprep were co-transfected with the Cas9-2AGFP pBKS plasmid (**Fig 2.2**), into SKBr3 cells. Plasmid DNA was delivered into the cells by nucleofection using AMAXA solution kit C (Lonza), and program E-09 on the AMAXA Cell Nucleofector 2b device. $1x10^6$ cells were harvested and nucleofected with 2µg U6-KDM5B gRNA and 2µg Cas9-2AGFP plasmid DNA. Cells were incubated for 72 hours at 37°C with 5% CO_2 and thereafter subjected to FACS analysis to identify cells with high GFP expression (intensity between $>10^4$) (**Chapter 3 Section 3.2.4**). $1x10^4$ parental and bulk sorted

KDM5B KO cells were subjected to DNA extraction using the Quick Extract DNA solution kit (Epicentre) according to manufacturer's instructions. The cells were centrifuged for 5 minutes at 200 x g and supernatant discarded. Cell pellet was re-suspended in 30µl Quick Extract DNA solution and cells incubated at 72°C for 20 min then 90°C for 10 min. DNA was amplified by PCR as described below.

2.2.7.2 Identification of indels using Indel detection by amplicon analysis (IDAA)

For the identification of gRNAs that generated indels with Cas9, indel detection by amplicon analysis (IDAA) was used. This techniques was recently developed by[265,266] (**Fig 2.3**). Tri-primer amplification was used to fluorescently label amplicons through the use of a universal 6-FAM 5'-labelled primer (FamF), whose sequence was complementary to the 5' overhang sequence of the forward primer and, the forward (F) and reverse (R) primers that flanked the gene editing target site. The assay primers are shown on **Table 2.6.** A PCR tri-primer ratio of 10:1:10 (FamF:F:R) was previously suggested as the ratio that produces optimal amplicon yields[265]. PCR was performed on the extracted DNA in a 12.5µl reaction using the recipe shown on **Table 2.12** and a touchdown thermocycling profile as shown on **Table 2.13**. Thereafter, 1µl of the PCR reaction was mixed with 0.3µl of GeneScan-LIZ600 standard (ABI/Life Technologies) and 10µl Hi-Di Formamide (Thermo Fisher Scientific), incubated at 90°C for 2 minutes then subjected to fragment analysis on the 3730xl DNA Analyzer (ABI/Life Technologies) according to manufacturer's instructions. Analysis of raw data was performed on the Peak Scanner Software (ABI/Life Technologies).

2.2.8 Development of KDM5B knockout cells

2.2.8.1 Selection of KDM5B gRNA

The gRNA targeting KDM5B exon 4, was the only gRNA that produced edited cells (**Chapter 3 section 3.2.4.2**), and so was used to develop KDM5B knockout (KO) cells in BT-474 and SKBr3 cell lines.

2.2.8.2 Transfection, FACS and cell cloning

To generate KDM5B KO cells, cells were co-transfected with the U6-gRNA expression plasmid targeting KDM5B exon 4 and the Cas9-2AGFP pBKS plasmid, as described in

Section 2.2.7.1. 72 hours post transfection, cells with a GFP intensity of between 10^3-10^4 were isolated by FACS (**Chapter 3 Section 3.2.5.1**) and either 3 cells per well or 10 cells per well were seeded into 96 well plates. Cells were maintained with the appropriate media conditioned on WT cells (RPMI for BT-474 cells and DMEM for SKBr3 cells; **Table 2.2**) at 37°C and 5% CO_2. Only wells with single colonies were selected and expanded into 24 well plates and thereafter subjected to IDAA analysis to identify KDM5B KO clones.

2.2.8.3 IDAA screening of KDM5B edited clones

DNA from single colonies growing in 24 well plates was extracted using the Quick Extract DNA solution as described in **Section 2.2.7.1.** DNA was PCR amplified and PCR products were subjected to IDAA as described in **Section 2.2.7.2.** A total of 17 BT-474 and 29 SKBr3 KDM5B edited clones were screened by IDAA (**Chapter 3 Section 3.2.5.2**). Selected KDM5B KO clones were further validated by Sanger sequencing, western blot and RT-qPCR as described in the sections below.

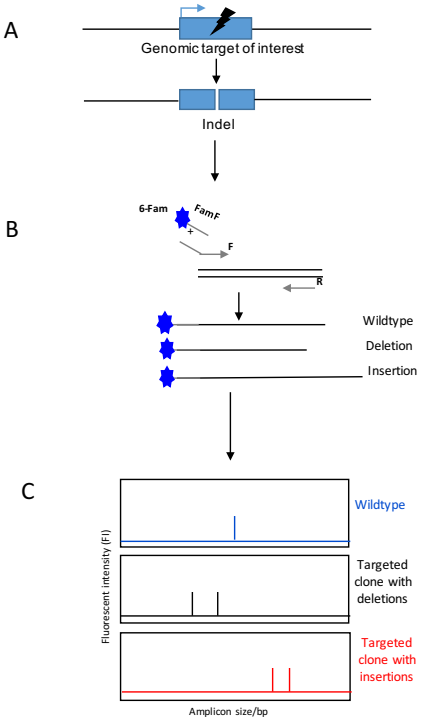

Figure 2.3: Schematic representation of the IDAA technique. (a) Precise gene editing creates DSBs that are repaired by NHEJ, thus introducing indels at the target site. **(b)** Amplification occurs through tri-primer PCR, using primers flanking the target region (Forward (F)/Reverse (R)) and a universal 5'-FAM labelled primer (FAMF) that is complementary to the 5' overhang sequence attached to the forward primer. This results in fluorescently labelled amplicons. **(c)** Fragment analysis detects indels produced in fluorescently labelled amplicons. Y axis represents fluorescent intensity (FI) and X axis represents amplicon size in base pairs (bp).

2.2.9 Sanger sequencing of KDM5B KO clones

2.2.9.1 Purification of PCR Product

PCR products of KDM5B KO clones generated in **Section 2.2.8.3**, were purified using the ExoSAP-IT™ PCR product cleanup reagent (Thermo Fisher Scientific), according to manufacturer's instructions. 5µl PCR product was mixed with 2µl ExoSAP-IT™ reagent and incubated at 37°C for 15 minutes, to degrade any remaining primers and nucleotides. The reaction was then incubated at 80°C for 15 minutes to inactivate the ExoSAP-IT™ reagent. Purified PCR products were subjected to Sanger sequencing or stored at -20°C for later analysis.

2.2.9.2 Sanger Sequencing

DNA sequencing of KDM5B KO clones was performed using the BigDye terminator v3.1 Cycle Sequencing kit (Thermo Fisher Scientific) with either the forward or reverse primer targeting KDM5B Exon 4 (**Table 2.6**). The sequencing reaction was set up in a 96 well plate as shown in **Table 2.14.**

Table 2.14: Sequencing reaction components

Reagent	Amount (µL)
Sequencing buffer	1.25
BigDye 3.1	0.25
F or R primer	0.25-0.50
ExoSAP-cleaned PCR product	3.5
Total	5.25-5.5

The plate was sealed, vortexed for 5 seconds and spun briefly for 30 seconds at 300 x g, to collect contents. The sequencing reaction was then run in a thermal cycler with conditions outlined on **Table 2.15.** The sequencing reaction was then purified by ethanol/sodium acetate (NaOAc) precipitation. 26µl of precipitation solution (50ml 100% ethanol and 2ml 3M NaOAc) was added to the sequencing reaction, vortexed gently for 2-3 seconds and incubated for 10 minutes at room temperature. The plate was sealed and centrifuged at 600 x g for 10 minutes. The plate was then centrifuged uncovered, upside down, at 13 x g for 5 seconds and air-dried upright and protected from light for 10-15 minutes at room temperature or stored at -20°C. Dried samples were re-suspended in 10µl Hi-Di Formamide (Thermo Fisher Scientific) and incubated at 90°C for 2 minutes. Plate was run on the ABI3730xl DNA analyzer (ABI/Life Technologies), in the NIHR BRC Genomics Laboratory at Guy's Hospital, London. Sanger sequencing

analysis was performed on the CodonCode Aligner software. Sequences of KDM5B KO clones were determined by the assistance of Dr Zhang Yang, Copenhagen Centre for Glycomics, University of Copenhagen.

Table 2.15: Sequencing reaction conditions

Time	Temperature	
30 seconds	96°C	X 30 cycles
15 seconds	50°C	
60 seconds	60°C	
Hold	4°C	

2.3 Copy number and Gene expression analysis of breast tumours

The two largest publicly available breast cancer datasets with both genomic and transcriptomic data namely, Molecular Taxonomy of Breast Cancer International Consortium (METABRIC) and The Cancer Genome Atlas (TCGA) were used. METABRIC contains genomic and transcriptomic information for 2509 breast tumours whereas, TCGA information data for 825 breast tumours. These data were downloaded from the cBioportal platform. Plots were generated on GraphPad Prism® 7 software.

2.4 Protein Analysis

2.4.1 Whole cell lysate extraction of proteins

Confluent T75cm^2 flask was trypsinised and cell pellet collected by centrifugation at 200 x g for 5 minutes. The cell pellet was re-suspended in appropriate media, counted and 1x10^6 cells transferred to a 1.5ml Eppendorf tube. Cells were centrifuged at 200 x g for 5 minutes to collect the cell pellet, which was subsequently lysed in 100µl 1X Laemmli sample buffer (0.01% (w/v) bromophenol blue, 2% SDS, 60mM Tris-HCl pH 6.8, 10% (w/v) glycerol) containing 5% β−mercaptoethanol. Protein lysates were heated at 95°C for 3 minutes and passed through a 25-gauge needle to shear the DNA. Protein lysates were either stored at -20°C for later analysis or subjected immediately to sodium dodecyl sulfate polyacrylamide gel electrophoresis (SDS-PAGE) and western blot, as described below.

2.4.2 Histone protein extraction

Confluent T75cm^2 flask was trypsinised and cell pellet collected by centrifugation at 200 x g for 5 minutes. The cell pellet was re-suspended in appropriate media, counted and 2x10^6 cells transferred to a 1.5ml Eppendorf tube. Histone proteins were then extracted according to the Abcam histone extraction protocol http://www.abcam.com/ps/pdf/protocols/histone%20extraction%20protocol.pdf. The cell pellet was washed twice in ice-cold PBS by centrifugation at 200 x g for 5 minutes. Cells were re-suspended in 200µl Triton Extraction buffer (TEB) (PBS containing: 0.5% Triton X-100, 2mM phenylmethylsulfonyl fluoride (PMSF), 0.02% Sodium Azide (NaN_3)) and lysed on ice for 10 minutes with gentle mixing. Following lysis, cells were centrifuged at 200 x g for 10 minutes at 4°C and supernatant discarded. Cells were washed in 100µl TEB and centrifuged at 200 x g for 10 minutes at 4°C. Pellet was re-suspended in 50µl 0.2M hydrochloric acid (HCl) and incubated at 4°C overnight, with gentle rotation to acid extract histones. The following day, samples were centrifuged at 200 x g for 10 minutes at 4°C and supernatant was transferred to a fresh 1.5ml Eppendorf tube. Concentration of histone protein lysate was determined using the Nanodrop One spectrophotometer (ThermoFisher Scientific) on the Protein A280 setting. Histone lysates were stored at -20°C for later analysis or subjected immediately to SDS-PAGE and western blot, as described below.

2.4.3 SDS-PAGE Gel and Western blot

10μl of protein lysate was separated on either a 7.5% or 12.5% SDS-PAGE gel according to their molecular weight using SDS-PAGE running buffer. 5μg of histone protein lysate was separated on a 15% SDS-PAGE gel. Samples were run on the Mini-PROTEAN Tetra Cell system (Bio-Rad) at 150V for approximately 60-75 minutes.

Proteins were transferred onto an Amersham Protran 0.45μm nitrocellulose membrane (GE Healthcare Life Sciences) using the Mini-transfer blot system (Biorad) in 1X Transfer buffer at 30V, overnight at 4°C. Alternatively, proteins were transferred using the TransBlot® Turbo™ Transfer System (Bio-Rad) for 30 minutes. Membranes were incubated in blocking buffer (5% non-fat milk powder, 0.1% Tween-20 in TBS or 5% bovine serum albumin (BSA), 0.1% Tween-20 in tris-buffered saline (TBS)) for 1 hour at room temperature, with gentle shaking. Blots were incubated in appropriate primary antibodies (**Table 2.16**) diluted in binding buffer (1% non-fat milk powder, 0.1% Tween-20 in TBS or 1% BSA, 0.1% Tween-20 in TBS). Following primary antibody incubation, membranes were washed three times in 0.1% Tween-20 in TBS at room temperature, for 10 minutes per wash. Membranes were then incubated with appropriate secondary antibody diluted in binding buffer (**Table 2.17**) for 1 hour at room temperature, with gentle shaking. Membranes were washed three times in 0.1% Tween-20 in TBS at room temperature, for 10 minutes per wash. Immune-complexes bound to the membrane were detected using enhanced chemiluminescence (ECL) (Pierce) and visualised using the GeneGnome XRQ chemiluminescence imaging system (SYNGENE) or, on autoradiography film (GE Healthcare) after developing the film on an X-ray developer. Blots were quantified using the ImageJ software.

2.4.4 Stripping membranes

To remove membrane bound antibodies, the stripping buffer (62.5mM Tris-HCl, pH6.7, 2% SDS, 100mM 2-Mercaptoethanol) was heated to 50°C in a water bath or in the microwave for 15 seconds. Membranes were incubated in stripping buffer for 15 minutes with shaking, in the fume hood. Membranes were washed in several washes of PBS, and the removal of antibodies was confirmed by visualisation on the GeneGnome XRQ chemiluminescence imaging system (SYNGENE) or, on autoradiography film (GE Healthcare), after ECL detection.

2.4.5 Antibodies and Buffers used for Protein Analysis

Table 2.16: Primary antibodies used in western blot analysis

Primary Antibody	Immunogen	Dilution	Diluent	Source
CAV1 Rabbit polyclonal to Caveolin-1 (ab2910)	Synthetic peptide corresponding to Human Caveolin-1 aa 1-17	1:1000	1% non-fat milk powder, 0.1% Tween-20 in TBS	Abcam
KDM5A Rabbit polyclonal A300-897A	Synthetic peptide corresponding to Human KDM5A aa 1640-1690	1:2000	1% non-fat milk powder, 0.1% Tween-20 in TBS	Bethyl Laboratories
KDM5B LC03 Rabbit polyclonal	Raised against the C-terminus domain of human KDM5B corresponding to aa 1283-1473	1:1500	1% non-fat milk powder, 0.1% Tween-20 in TBS	In-house
KDM5C JARID1C (D29B9) Rabbit monoclonal	Synthetic peptide corresponding to residues surrounding Leu830 of human JARID1C protein.	1:1000	1% BSA, 0.1% Tween-20 in TBS	Cell Signaling Technology
Histone H3, C-terminal Rabbit polyclonal	Raised against a C-terminal peptide of histone H3	1:5000	1% BSA, 0.1% Tween-20 in TBS	Active Motif
H3K4me3 Mouse monoclonal Anti-histone H3 (tri-methyl K4) (ab1012)	Synthetic peptide corresponding to Human Histone H3 aa 1-100 (tri methyl K4)	1:1000	1% BSA, 0.1% Tween-20 in TBS	Abcam
HER2 Rabbit monoclonal 29D8	Synthetic peptide corresponding to residues surrounding tyrosine 1248 of HER2 protein	1:1000	1% BSA, 0.1% Tween-20 in TBS	Cell Signaling Technology
Phospho-HER2 (Tyr 1221/1222) Rabbit polyclonal	Synthetic peptide corresponding to residues surrounding tyrosine 1221/1222 of HER2 protein	1:1000	1% BSA, 0.1% Tween-20 in TBS	Cell Signaling Technology
HSC70 Mouse monoclonal Sc-7298	Synthetic peptide corresponding to human HSC70 aa 583-601	1:10,000	1% non-fat milk powder, 0.1% Tween-20 in TBS	Santa Cruz

Table 2.17: Secondary antibodies used in western blot analysis

Secondary Antibody	Dilution	Source
Swine-anti Rabbit HRP	1:1000	DAKO
Goat anti-Mouse HRP	1:1000	DAKO

Buffer recipes used for western blot are as listed below. All chemicals were purchased from Sigma Aldrich unless otherwise stated.

1x SDS-PAGE running buffer

1. 25mM Tris pH8.3
2. 192mM Glycine
3. 0.1% SDS

1x Transfer buffer

1. 25mM Tris pH 8.3
2. 192mM Glycine
3. 20% methanol (Thermo Fisher Scientific)

1x Tris-buffered saline-Tween (TBST) buffer

1. 20mM Tris pH 7.6
2. 150mM NaCl
3. 0.1% Tween-20

Blocking buffer

1. TBST buffer
2. 5% skimmed milk powder (Oxoid) or 5% Bovine Serum Albumin (BSA)

2.5 Histology

2.5.1 Tissue Fixation

Thoracic mammary glands of 12.5 day pregnant mice were dissected by Dr Gianfranco Picco. Once excised, mammary glands were formalin-fixed in 10% neutral buffered formalin (Sigma-Aldrich), overnight at room temperature. Fixed mammary glands were subsequently paraffin embedded by the King's Health Partners (KHP) Cancer Biobank group at Guy's Hospital, London. Paraffin-embedded glands were stored at room temperature until required for tissue sectioning.

2.5.2 Tissue sectioning

Paraffin-embedded mammary glands were chilled on ice block before sectioning. The block was first trimmed at a thickness of 10μm to expose the tissue surface. Thereafter, tissue sections were cut at a thickness of 3μm to produce a ribbon of sections. The ribbon of sections was placed on the surface of the water of a 35°C water bath to flatten them out. Consecutive sections were separated using tweezers and mounted onto a microscope slide. Mounted sections were placed on a slide rack and allowed to dry overnight in a 37°C oven. Sections can then be stored at 4°C or immediately subjected to immunohistochemistry.

2.5.3 Immunohistochemistry

Tissue sections were baked at 60°C for 2 hours and de-waxed by incubating in two changes of xylene for 2 minutes each. To hydrate the sections, they were incubated in two changes of absolute ethanol for 2 minutes per incubation and thereafter in one change of 70% ethanol for 2 minutes. The sections were washed in water and subjected to antigen retrieval for 20 minutes in 10mM sodium citrate buffer pH6.0 in the pressure cooker. Whilst still in the racks, sections were placed in slow running water to allow them to cool for 10 minutes. Sections were incubated in blocking buffer (50% FBS in phosphate buffered saline (PBS)) for 30 minutes. Following blocking, sections were incubated with appropriate primary antibody (**Table 2.18**) diluted in blocking buffer, for 60 minutes at room temperature. The sections were washed in three changes of PBS for 3 minutes per wash and incubated with the appropriate secondary antibody (**Table 2.18**) for 60 minutes at room temperature. The sections were washed in three changes of PBS for 3 minutes per wash and incubated in 3,3'-Diaminobenzidine (DAB) (DAKO) for

horseradish peroxidase (HRP) antibodies for 3 minutes or in liquid permanent red (DAKO) for alkaline phosphatase for 10 minutes. Sections were placed on a slide rack and washed once in distilled water. The sections were then counterstained with Mayer's Haematoxylin (Sigma-Aldrich) for 5 minutes, placed in a tray of running water to wash off the haematoxylin and then incubated in 1% acid alcohol for 5 seconds. Sections were serially dehydrated in 70% ethanol for 5 seconds and incubated in two changes of 100% ethanol for 1 minute per incubation. Following dehydrations, sections were incubated in xylene for 2 minutes to remove the alcohol. Slides were mounted onto a coverslip and left to dry. Immunostaining of sections was visually inspected using the Olympus BX50 microscope (Olympus). Slides were scanned using the Hamamatsu NanoZoomer (Hamamatsu Photonics) by Patryjca Gazinska from the Breast Cancer Now Unit at Guy's Cancer Centre, London. Images were viewed with the Hamamatsu NDP.view2 software.

Table 2.18: Antibodies and reagents used for immunohistochemistry

	Caveolin-1	**KDM5B**	**SMA**
Primary antibody	Rabbit polyclonal to Caveolin-1 (ab2910)	Rabbit 3 antibody. Rabbit polyclonal to KDM5B	Smooth muscle actin monoclonal mouse anti-human clone 1A4 (M0851)
Immunogen	Synthetic peptide corresponding to Human Caveolin-1 aa 1-17	Raised against the C-terminus domain of human KDM5B corresponding to aa 1283-1473	N-terminal synthetic decapeptide of α-smooth muscle actin (4)
Supplier	Abcam	In-house	DAKO
Dilution	1:100	1:700	1:500
Primary antibody diluent	2% FBS/PBS	2% FBS/PBS	2% FBS/PBS
Secondary antibody	Swine anti-rabbit HRP (P021702-2)	Swine anti-rabbit HRP (P021702-2)	Goat anti-mouse alkaline phosphatase (ab7069)
Supplier	DAKO	DAKO	Abcam
Dilution	1:100	1:100	1:300
Secondary antibody diluent	2% FBS/PBS	2% FBS/PBS	2% FBS/PBS
Detection substrate	Liquid DAB+ (K3468)	Liquid DAB+ (K3468)	Liquid permanent red (K064011-2)
Supplier	DAKO	DAKO	DAKO
Wash buffer	PBS	PBS	PBS
Blocking buffer	50% FBS/PBS	50% FBS/PBS	50% FBS/PBS

HRP: Horseradish peroxidase; PBS: phosphate buffered saline

2.6 Gene Expression

2.6.1 RNA Extraction

RNA was extracted from WT and KDM5B KO cells of BT-474 and SKBr3, using the RNeasy mini kit (Qiagen) according to manufacturer's instructions. $2x10^5$ WT and KDM5B KO cells of BT-474 or SKBr3, were seeded in a well of a 6-well plate, and incubated at 37°C and 5% CO_2 for three days. Media was aspirated from wells and cells were lysed directly in the well using 350μl of lysis buffer supplied. Cells were scraped using a cell scraper and lysate was transferred into an Eppendorf tube and vortexed for a one minute to homogenize the lysate. 1 volume (350μl) of 70% ethanol was added to the homogenized lysate and mixed by pipetting. 700μl of the sample was transferred into an RNeasy spin column (made of silica membrane that binds RNA) placed inside a 2ml collection tube. Samples were centrifuged for 15 seconds at ≥8000 x g and the flow-through discarded. To wash the membrane of the spin column, 700μl of the supplied wash buffer was added to the RNeasy spin column and centrifuged for 15 seconds at ≥8000 x g and flow-through discarded. The membrane was washed again using 500μl of a second wash buffer, centrifuged for 15 seconds at ≥8000 x g and flow-through discarded. The membrane was washed a second time with 500μl wash buffer and centrifuged for 2 minutes at ≥8000 x g. The spin column was placed in a fresh collection tube and spun for 1 minute at full speed to prevent any carryover of wash buffer. The spin column was then placed in a new 1.5ml Eppendorf tube and 42μl RNase free water (Thermo Fisher Scientific) was added directly onto the spin column membrane. Samples were centrifuged for 1 minute at ≥8000 x g to elute RNA. RNA was stored at -80°C. RNA concentration was measured using the Nanodrop One spectrophotometer (Thermo Fisher Scientific) on the RNA setting.

2.6.2 Bioanalyzer analysis of RNA samples

The Agilent 2100 Bioanalyzer on-chip electrophoresis platform, was used to further check the quality and quantity of RNA. RNA samples were run on the Agilent RNA 6000 Nano chip according to manufacturer's instructions. RNA integrity was expressed using the RNA integrity number (RIN). Good quality, non-degraded RNA was demonstrated by a RIN greater than 7, as well as, the presence of distinct bands of 18S and 28S rRNA in the gel image and their corresponding peaks on the electropherogram (**Figure 2.4**). RNA concentration was expressed as pg/μl.

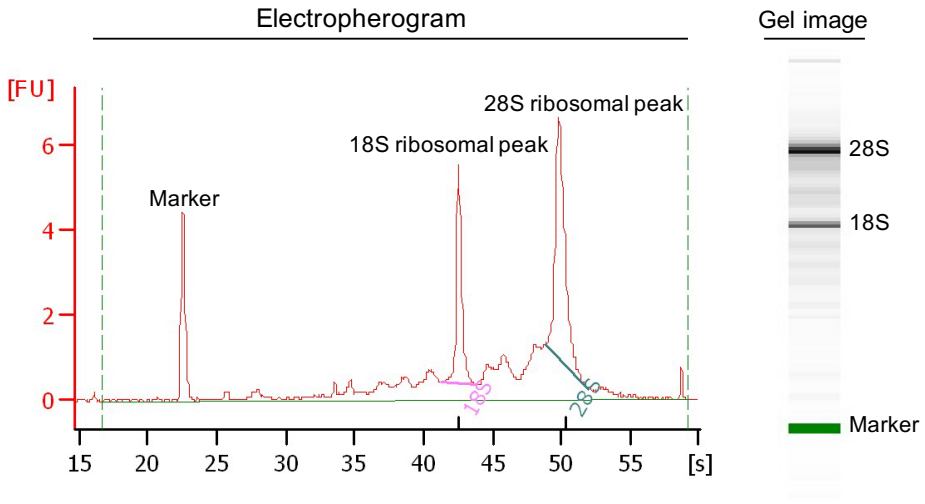

Figure 2.4: Electropherogram trace and gel image from the Agilent 2100 Bioanalyzer. An example of electropherogram and corresponding gel image of the SKBr3 wild-type (WT) RNA sample with a RIN number of 8.2.

2.6.3 cDNA synthesis for RT-qPCR analysis

Complementary DNA (cDNA) was generated from the isolated total RNA using the qScript cDNA Supermix kit (Quantabio), according to manufacturer's instructions. A 20μl reaction consisting of 1μg of total RNA, 1X qScript cDNA supermix and RNase free water (where appropriate), was gently mixed by vortexing and briefly centrifuged to collect contents. The mixture was then incubated as follows to generate cDNA:

- 25°C for 5 minutes
- 42°C for 30 minutes
- 85°C for 5 minutes

Samples were then stored at -20°C.

2.6.4 RT-qPCR analysis

Relative quantification of genes was determined using the Precision qPCR SYBR green Master mix (Primer Design) and Quantitect primers (Qiagen) according to manufacturer's instructions. The primers used in the RT-qPCR reactions are listed in **Table 2.19.** PUM1 primer (Eurofins) was used as the reference gene. cDNA was diluted to 5ng/μl and a total of 25ng was used for each qPCR reaction. A master mix of each individual primer and the qPCR mastermix was prepared (**Tables 2.20 and 2.21**) and pipetted into triplicate wells of a 96 well plate. 5μl of cDNA (5ng/μl) was then added to each well and mixed well by pipetting. Plate was sealed and spun at 300 x g for 2 minutes prior to running on the Opticon 2 continuous fluorescence detector (MJ Research). The PCR

cycle conditions for all primers listed in **Table 2.19** were: 95°C for 5 minutes, then 40 cycles at 95°C for 15 seconds, 60°C for 30 seconds, 72°C for 30 seconds.

Data values were averaged prior to further analysis. Cycle threshold (Ct) was set above the background but within the linear phase of amplification for all samples. Data was normalised to the PUM1 expression and subsequently analysed using the comparative $2^{-\Delta\Delta Ct}$ method: ΔΔCT = ΔCT (target gene) − ΔCT(reference gene) [267].

Table 2.19: Primers used in RT-qPCR reactions

Target gene	ID and Source
ABCC2	Hs_ABCC2_1_SG QuantiTect Primer Assay (QT00056294; Qiagen)
EGR1	Hs_EGR1_1_SG QuantiTect Primer Assay (QT00218505; Qiagen)
FOS	Hs_FOS_1_SG QuantiTect Primer Assay (QT00007070; Qiagen)
KDM5B	Hs_KDM5B_1_SG QuantiTect Primer Assay (QT00060648; Qiagen)
LCN2	Hs_LCN2_1_SG QuantiTect Primer Assay (QT00028098; Qiagen)
MYC	Forward: 5'- GCC ACG TCT CCA CAC ATC AG-3' Reverse: 5'- TCT TGG CAG CAG GAT AGT CCT-3' (Eurofins Genomics)
PUM1	Forward: 5'- GAT TAT TCA GGC ACG CAG GT -3' Reverse: 5'- AGC AGC GCT GAT GAT GTA TG -3' (Eurofins Genomics)
SLC40A1	Hs_SLC40A1_1_SG QuantiTect Primer Assay (QT00094843: Qiagen)

Table 2.20: RT-qPCR master mix components for each reaction using QuantiTect Primers

	1X Master mix (per reaction)
2X Precision qPCR SYBR green Master mix (PrimerDesign)	10μl
10X QuantiTect primers	2μl
cDNA (5ng/μl)	5μl
RNase free water	3μl
Total	20μl

Table 2.21: RT-qPCR master mix components for each reaction using PUM1 or MYC primers

	1X Master mix (per reaction)
2X Precision qPCR SYBR green Master mix (PrimerDesign)	10μl
2μM PUM1 or MYC primer	5μl
cDNA (5ng/μl)	5μl
Total	20μl

2.7 Microarray Gene Expression analysis

2.7.1 cDNA synthesis and amplification

The Ovation® PicoSL WTA system V2 kit (NuGEN Technologies) was used to prepare cDNA for gene expression analysis, following cDNA amplification with the Ribo-Single Isotheral Amplification (Ribo-SPIA) technology, according to manufacturer's instructions. The Ribo-SPIA technology was used to amplify SKBr3 WT and KDM5B KO cDNA using three main steps (**Fig 2.5**):

1) The first strand of cDNA is generated using reverse transcriptase producing a cDNA/mRNA hybrid molecule with an RNA tag sequence (SPIA tag), at the 5' end of the cDNA strand.
2) Heat induced fragmentation of mRNA within the cDNA/mRNA complex then creates priming sites that allow for second strand synthesis of cDNA by DNA polymerase. DNA complementary to the 5' SPIA tag sequence is also synthesized. This generates double stranded cDNA with a DNA/RNA heteroduplex that corresponds to the SPIA tag.
3) Addition of RNase H results in removal of the RNA portion of the SPIA tag sequence allowing binding of the SPIA primer (DNA/RNA chimeric primer). cDNA synthesis by DNA polymerase at the 3' end of the SPIA primer displaces the forward strand, producing a DNA/RNA heteroduplex. This results in subsequent removal of the RNA portion of the SPIA primer by RNase H, and so initiates the next round of cDNA synthesis. This process results in rapid cDNA amplification producing 2-5μg of cDNA from 500 picograms of RNA.

Following amplification, cDNA purification was performed using the MinElute Reaction Cleanup kit (Qiagen) according to manufacturer's instructions. Purity of the amplified cDNA samples were run on the 2100 Bioanalyzer platform using the Agilent RNA 6000 Nano chip. cDNA yield was determined using the NanoDrop 1000 spectrophotometer (Thermo Scientific) on the single-stranded DNA setting.

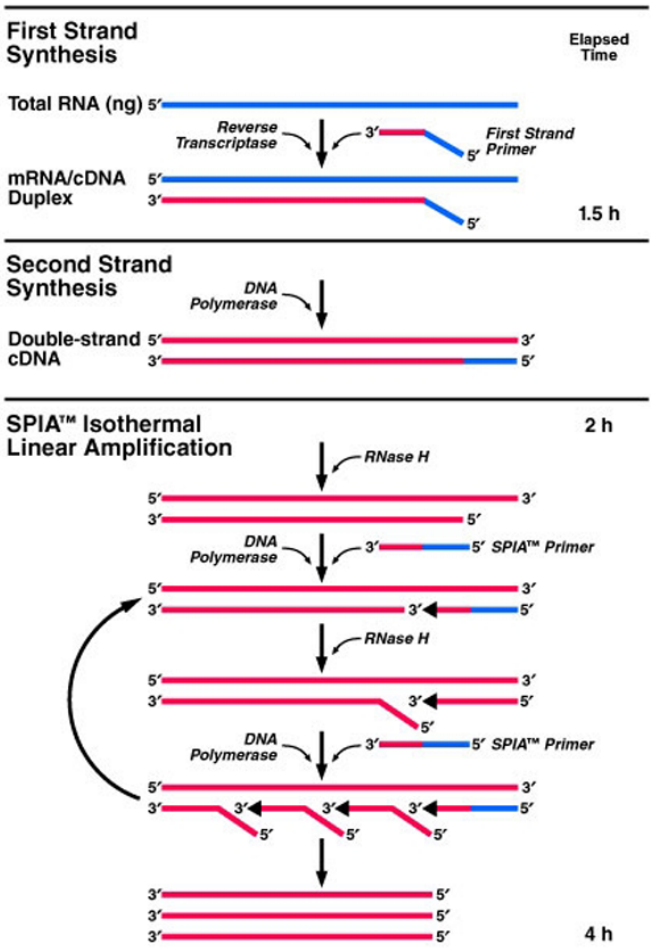

Figure 2.5: Ribo-SPIA process for synthesizing single stranded cDNA. Modified image from [268].

2.7.2 Biotinylation of amplified cDNA

Amplified cDNA was biotinylated using the Encore BiotinIL Module (NuGEN) according to manufacturer's instructions. Removal of the uracil base incorporated during the amplification process was achieved through addition of the uracil-DNA glycosylase (UNG) enzyme, which resulted in creation of abasic sites in the cDNA strand. Subsequent chemical attachment of a biotin moiety onto the abasic site, resulted in labelling of the cDNA. Biotin labelled cDNA was purified using the MinElute Reaction Cleanup kit (Qiagen) according to manufacturer's instructions and concentration of eluted cDNA (10μl) was determined using the NanoDrop 1000 spectrophotometer (Thermo Fisher Scientific) on the single-stranded DNA setting. The labelled cDNA was

diluted with RNase-free water or concentrated using the Vacufuge vacuum concentrator (Eppendorf) to a final concentration of 150ng/μl in a total volume of 5μl.

2.7.3 Hybridisation of biotin-labelled cDNA on Microarray

One biological repeat of SKBr3 WT and KDM5B KO was analysed by microarray. The Illumina HumanHT-12 v4 Expression BeadChip array (Illumina) which targets more than 47,000 genes, was used. Hybridisation of biotin labelled cDNA on to this array was performed by the NIHR BRC Genomics Facility at Guy's Hospital, London. Scanning of the BeadChip was done on the iScan system (Illumina) using GenomeStudio software (Illumina). Data analysis was done by Dr Paul Lavender, who used the Partek Genomics Suite software (Partek Incorporated) using the 2 way-ANOVA model. Genes were considered to be differentially expressed if they had a ≥1.5-fold difference in expression. Differentially expressed genes that had a fold change ≥1.5 were analysed for enriched biological processes using the ToppGene Suite bioinformatics tool [269]. Gene Ontology (GO) terms were considered to be statistically significant by using the Benjamini-Hochberg (BH) false discovery rate (FDR) model for multiple test adjustment.

2.8 Cell Viability Assays

2.8.1 MTT cell growth assay

$1x10^4$ cells of SKBr3 parental and KDM5B KO cells, were seeded in duplicate in 24 well plates and cell growth determined at day 1, 4 and 7 using the thiazolyl blue tetrazolium bromide (MTT) (Sigma-Aldrich) assay according to manufacturer's instructions. At the end of each time point, 5μg/ml MTT was added to each well and incubated for 3 hours at 37°C with 5% CO_2. Cell viability was subsequently determined by measuring absorbance at 595nm on the FLUOstar Omega plate reader (BMG Labtech). All optical density (OD) values were corrected by subtraction of background values generated using the media alone control.

2.8.2 Methylene Blue Assay

$1x10^4$ cells of WT and KDM5B KO cells of BT-474 or SKBr3, were seeded in duplicate in 24 well plates and cells left to adhere overnight at 37°C with 5% CO_2. The following day, cells were treated with control (DMSO or PBS), Herceptin (10μg/ml), Lapatinib (100nM) or Herceptin/Lapatinib (10μg/ml and 100nM respectively) combination for 0,3 and 6 days. Media and control or drug was changed every three days. At the end of each time point, media was aspirated from wells and cells were fixed with 4% glutaraldehyde (Sigma-Aldrich) for 20 minutes at room temperature. Cells were washed twice with PBS and subsequently stained with 0.05% Methylene Blue (Sigma-Aldrich) for 20 minutes at room temperature, with gentle shaking. Cells were washed three times in a tray of running water then air-dried upside down, overnight at room temperature. The following day, methylene blue dye was extracted by addition of 3% HCl and incubation for 30 minutes with gentle shaking, at room temperature. Cell viability was determined by measuring absorbance at 655nm on the FLUOstar Omega plate reader (BMG Labtech). All OD values were corrected by subtraction of background values generated using the media alone control.

For the analysis of BT-474 parental and KDM5B KO cell growth, cells were seeded in duplicate in 24 well plates and cell growth was determined at day 1, 4 and 7. At the end of each time point, the methylene blue assay was performed as aforementioned.

2.8.3 Crystal violet assay

$2.5x10^3$ WT and KDM5B KO cells of BT-474 or SKBr3, were seeded in duplicate onto 6-well plates and 5μg/ml Herceptin was immediately added to the wells. Cells were incubated for 14 days at 37°C with 5% CO_2, with media and Herceptin changes every three to four days. At the end of the 14-day period, media was aspirated from wells and cells were fixed with 4% glutaraldehyde (Sigma-Aldrich) for 20 minutes at room temperature. Cells were washed twice with PBS and subsequently stained with 0.05% Crystal Violet (Sigma-Aldrich) for 20 minutes at room temperature, with gentle shaking. Cells were washed three times in a tray of running water then air-dried upside down, overnight at room temperature. The following day, the crystal violet dye was extracted by addition of 10% acetic acid and incubation for 30 minutes with gentle shaking, at room temperature. Cell viability was determined by measuring absorbance at 570nm on the FLUOstar Omega plate reader (BMG Labtech). Viability was calculated as:

$$Relative\ absorbance = \left(\frac{\text{average OD of treated}}{\text{average OD of control}}\right)$$

2.9 Statistical Analysis

Unpaired two-sided Student *t*-test was used to determine whether the means of the parental and KDM5B KO cells were significantly different. ANOVA with Sidak multiple comparisons test, was used to determine whether there were any statistically significant differences between three or more groups. Results were considered statistically significant if $p<0.05$. All statistical analysis was performed using GraphPad Prism® 7 software. Experiments were performed at least twice to confirm observations.

3 : Development of KDM5B KO in HER2+ Breast Cancer Cell Lines using CRISPR-Cas9 technology

3.1 Introduction

To begin studies in understanding the role of KDM5B in HER2+ breast cancer, gene editing was employed to knock out KDM5B. Genome editing using endonucleases that target specific genomic sequences, have become powerful tools for biological research, allowing genetic manipulation of a wide range of organisms and cell types. Here, the selected gene editing tool CRISPR-Cas9 was used to develop KDM5B KO cells and so will be discussed in more detail below.

3.1.1 CRISPR-Cas system in prokaryotes

CRISPR-Cas is a prokaryotic adaptive immune system, that uses RNA-guided nucleases to destroy invading nucleic acids such as viruses and plasmids [270–272]. To date, two main classes of CRISPR-Cas systems exist, which are classified according to the occurrence of the CRISPR-associated (Cas) proteins. These classes are divided into six types (I-VI) and multiple subtypes, of which type I-III and V, have been well characterized. Class 1 CRISPR-Cas systems consist of type I, III and IV and utilise a multi-protein effector complex whereas, class 2 systems (type II, V and VI) use one effector protein (**Fig 3.1**) (reviewed by [259]. In this work, the type II CRISPR system was used and so will be the main system discussed hereafter. The mechanism of the CRISPR-Cas system can be divided into three main stages: 1) Protospacer acquisition 2) CRISPR RNA (crRNA) biogenesis and 3) crRNA guided interference.

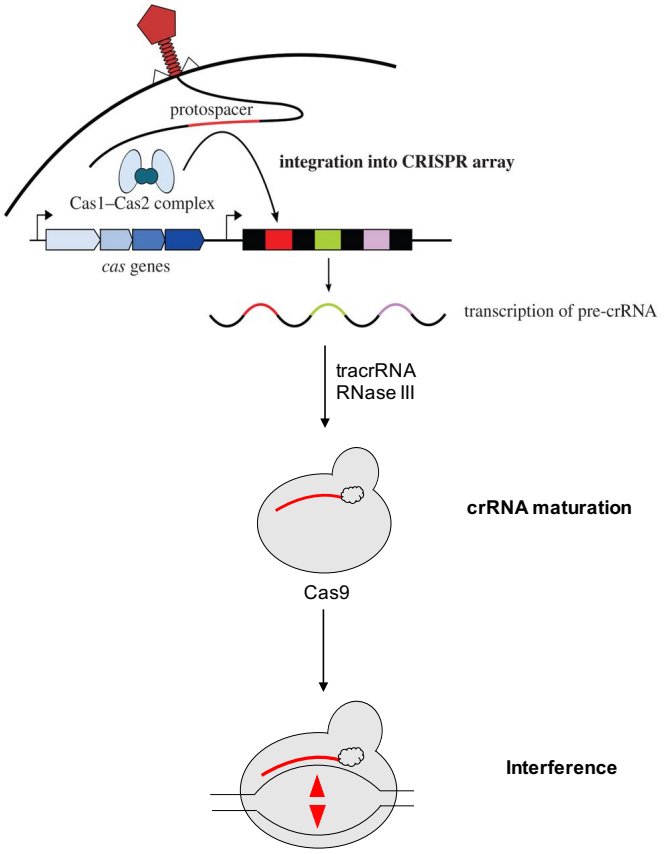

Figure 3.1: CRISPR-Cas immune systems in bacteria. Upon viral or phage infection, a sequence of foreign DNA (protospacer), the Cas1-Cas2 complex incorporates the DNA into the CRISPR array. The CRISPR array consists of identical repeat sequences (black rectangles) interspersed by phage-derived spacers (coloured rectangles) and is flanked by the *cas* genes (blue). To acquire immunity, the CRISPR array is transcribed into a long precursor CRISPR RNA (pre-crRNA) which is subsequently processed into short mature CRISPR RNA (crRNA). Type II systems, require Cas9, RNase III and tracrRNA for pre-crRNA processing. During interference, Cas9, RNase III and tracrRNA:crRNA duplex target and cleave invading DNA. Red triangles represent cleavage sites of the interference machinery. Modified image from [259].

3.1.1.1 Protospacer acquisition

In this stage, invading DNA known as protospacers, are incorporated in-between CRISPR repeat sequences (20-50 base pairs), thereby generating a CRISPR array [273,274]. CRISPR arrays are flanked by *cas* genes that encode Cas proteins, and are preceded by an AT-rich leader sequence. Protospacers are usually integrated at the leader end of the CRISPR array and for each integrated protospacer, the first CRISPR repeat sequence is duplicated, to maintain the repeat-spacer-repeat architecture [273,274]. Selection of protospacers is dependent on the protospacer adjacent motif (PAM); a short sequence located directly next to the protospacer [275,276]. In the type II-A system, it has been demonstrated that protospacer selection, occurs through the PAM-recognizing domain of the Cas9 protein [277,278]. Following protospacer selection, Cas9 is thought to recruit Cas1, Cas2 and possibly Csn2, for integration of the protospacer into the CRISPR array [259].

3.1.1.2 crRNA biogenesis

The second stage of the CRISPR-Cas adaptive immune system, involves acquisition of immunity. This involves the transcription of the CRISPR array into a long precursor crRNA (pre-crRNA), followed by processing into short guide crRNAs, which requires the *trans* activating CRISPR RNA (tracrRNA) [279]. tracrRNA is a 24-nucleotide sequence that is complementary to the CRISPR repeat [279]. tracrRNA and pre-crRNA form an RNA-duplex, which is stabilized by Cas9 and processed by the host RNase III, resulting in an intermediate crRNA that is further processed to a mature small guide crRNA [279]. These guide crRNAs contain protospacer sequences required for adaptive immune response.

3.1.1.3 crRNA guided interference

The third stage of CRISPR-Cas adaptive immunity involves crRNA guided interference of invading nucleic acids. crRNAs guide the Cas9 effector protein to invading nucleic acids, which are identified through complementary base-pairing [280]. Cas9 subsequently cleaves the invading DNA through introduction of a DSB [280]. Cleavage by Cas9 occurs if the invading sequence is adjacent to a PAM sequence, thus preventing self-targeting.

3.1.2 Applications of CRISPR-Cas9 technology

CRISPR-Cas9 has been exploited in different fields of biological research and medicine, to introduce precise gene modifications in cells or organisms. In this context, the type II CRISPR system from *Streptococcus pyogenes* has been simplified to consist of two components: Cas9 nuclease protein and a guide RNA (gRNA), which is a hybrid of the crRNA: tracrRNA duplex [280]. The gRNA, a 20-nucleotide (nt) sequence, directs Cas9 to a specific complementary DNA sequence where Cas9 induces a DSB (**see Fig 1.7 in Chapter 1 section 1.9**). The gRNA must lie upstream of a PAM sequence to allow cleavage of the target DNA by Cas9. PAM sequences in *S. pyogenes* are in the form 5'-NGG, thus any DNA sequence in the form N_{20}-NGG can be targeted by Cas9, by altering the 20-nt gRNA sequence to correspond to a target of interest. Type II CRISPR systems from other bacterial species that have different crRNA and tracrRNA sequences and recognise different PAM sequences, have also been used [281,282]. However, the *S. pyogenes* is the most commonly used and well characterised type II CRISPR system. Genome editing using the CRISPR-Cas9 system takes advantage of eukaryotic DNA repair mechanisms, to repair Cas9-induced DSB by NHEJ. NHEJ is an error-prone mechanism that results in the introduction of deletions, insertions, point mutations or

frameshifts, that can alter the gene product leading to loss of function [283]. This loss of gene function is what is termed as genetic knockout (KO), and is the desired outcome of CRISPR-Cas9 targeting. For precise gene editing, homology directed repair (HDR) pathway is used. This is achieved by using, a DNA sequence that shares sequence homology with the target site, to repair the Cas9-induced DSB via homologous recombination. The DNA sequence can contain any alteration e.g. insertion or deletion, thus allowing precise editing of the target sequence [284,285].

CRISPR-Cas9 has also been used to regulate gene transcription by mutating the nuclease domain of Cas9 thus resulting in a nuclease 'dead' protein (dCas9) (reviewed by [259]). Targeting a gene's promoter region or open reading frame using dCas9 prevents binding of RNA polymerase and inhibits mRNA elongation. Alternatively, dCas9 can be fused to a transcriptional activator or repressor thus allowing gene expression or inhibition, respectively. CRISPR-Cas9 has also been utilised in genome-wide screens through reverse genetics, whereby the resultant phenotype from a gene knockout, is used to study the function of the gene.

3.1.3 Aims

In this Chapter, development of KDM5B KO in HER2+ breast cancer cell lines using CRISPR-Cas9, is documented. This was achieved by:

1) Examining expression of KDM5B in breast tumours and cell lines. This was to enable selection of suitable cell lines for KDM5B gene editing
2) Investigating expression of KDM5B in Herceptin sensitive and resistant cell lines
3) Selection of suitable guide RNAs for KDM5B gene editing
4) Co-transfection of selected gRNA and Cas9 in HER2+ breast cancer cell lines, followed by single cell cloning
5) Screening and selection of KDM5B KO clones using indel analysis, followed by validation of KDM5B KO in selected cones

3.2 Results

3.2.1 KDM5B expression is upregulated in Luminal A and HER2+ breast tumours and cell lines

3.2.1.1 Copy number and gene expression analysis of KDM5B in breast cancer

Upon discovery of KDM5B,[183] first showed that KDM5B mRNA expression was upregulated in breast cancer cell lines. Later, studies using Single Nucleotide Polymorphism (SNP) array analysis, identified KDM5B as a gene with copy number gain in breast cancer [286]. More recently, it was demonstrated that increased KDM5B mRNA expression is associated with copy number gain [202]. To confirm these observations, two published breast cancer databases containing copy number (CN) and gene expression (GE) data were used.

The first database, Molecular Taxonomy of Breast Cancer International Consortium (METABRIC) contains CN and GE profiles of 2509 tumours [46,287]. The second, The Cancer Genome Atlas (TCGA), contains CN and GE profiles of 825 breast tumours [288]. These datasets were downloaded from the cBioPortal platform [289,290]. Increased KDM5B mRNA expression was found to be associated with copy number gain or amplification in both datasets (**Fig 3.2A**). It was further investigated whether KDM5B expression was associated with breast cancer subtypes (luminal A, luminal B, HER2-enriched, basal-like and normal-like), as classified by the PAM50 gene classifier [45]. KDM5B mRNA expression was significantly higher in the HER2+ tumours compared to the other subtypes in the METABRIC dataset (**Fig 3.2B**), thus corresponding with previous observations [202]. In the TCGA dataset, there was no significant difference in KDM5B expression between HER2+ and luminal A subtypes. These findings suggest that KDM5B may play an important role in luminal A and HER2+ breast cancers. Indeed, KDM5B has been shown to be an oncogenic driver of the luminal lineage in breast cancer [202]. Here, the role of KDM5B in HER2+ breast cancer is further examined.

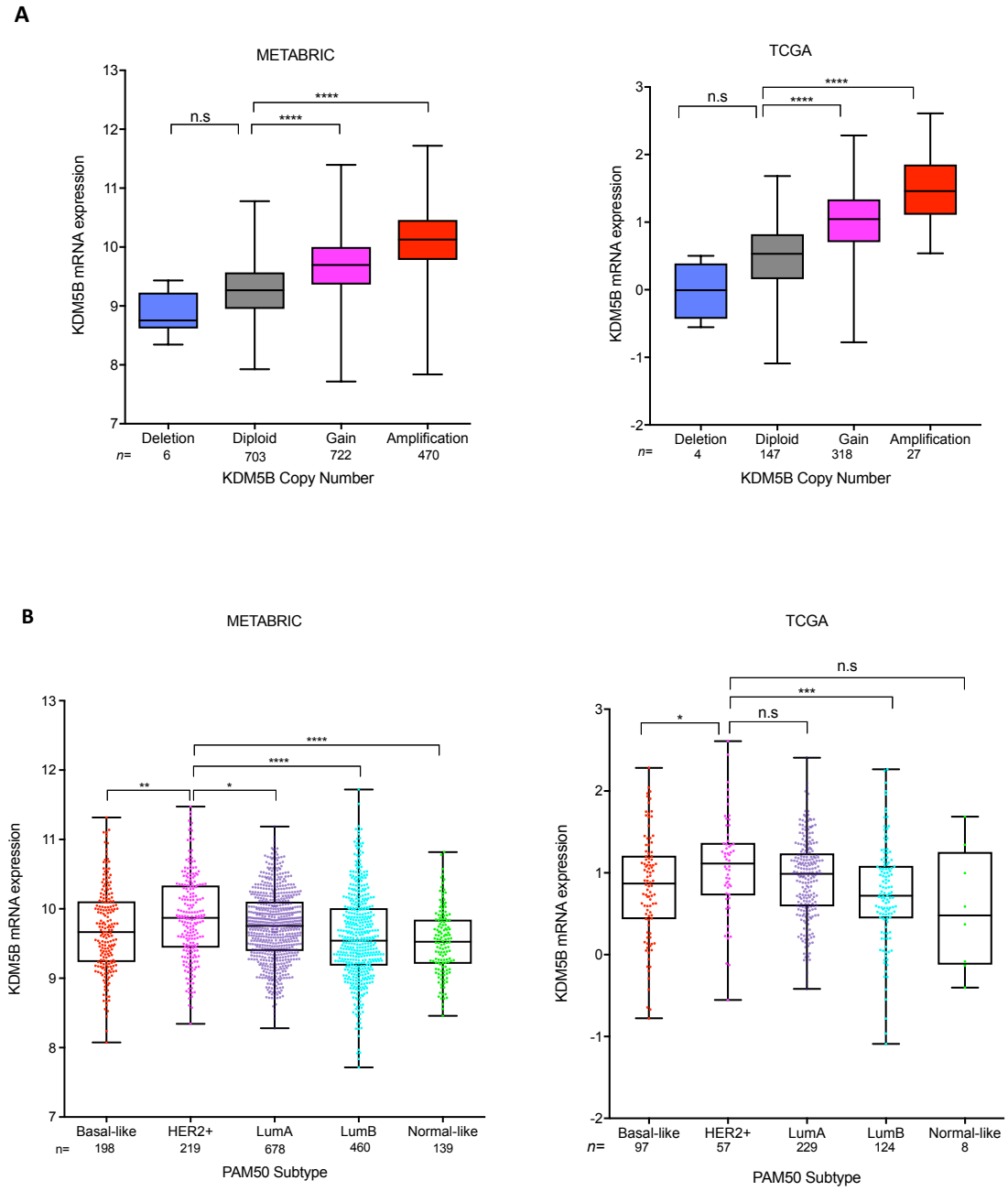

Figure 3.2: KDM5B expression is upregulated in luminal A and HER2 breast cancer. A) Increased KDM5B mRNA expression is associated with copy number gain or amplification in the METABRIC and TCGA datasets. Sample numbers are indicated below each copy number alteration. B) KDM5B mRNA expression is significantly upregulated in luminal A and HER2+ breast tumours. Sample numbers are indicated below each PAM50 subtype. METABRIC and TCGA data was downloaded from the cBioportal platform. Asterisks indicate significance where *=p≤0.05, **=p≤0.01, ***=p≤0.001, ****=p≤0.0001. n.s = not significant. Statistical significance was calculated using One-way ANOVA with Sidak correction.

3.2.1.2 KDM5B protein expression in breast cancer cell lines

The expression of KDM5B was then examined in a panel of breast cancer cell lines. These cell lines are representative of the PAM50 breast cancer subtypes. KDM5B protein levels were high in ER+ (luminal) and HER2+ (HER2-enriched) cell lines, and low in the triple negative (TN; basal-like) cells (**Fig 3.3**), agreeing with the gene expression analysis in primary breast tumours (**Fig 3.2B)**. BT-474 and SKBr3 were the two chosen HER2+ breast cancer cell lines used in this project.

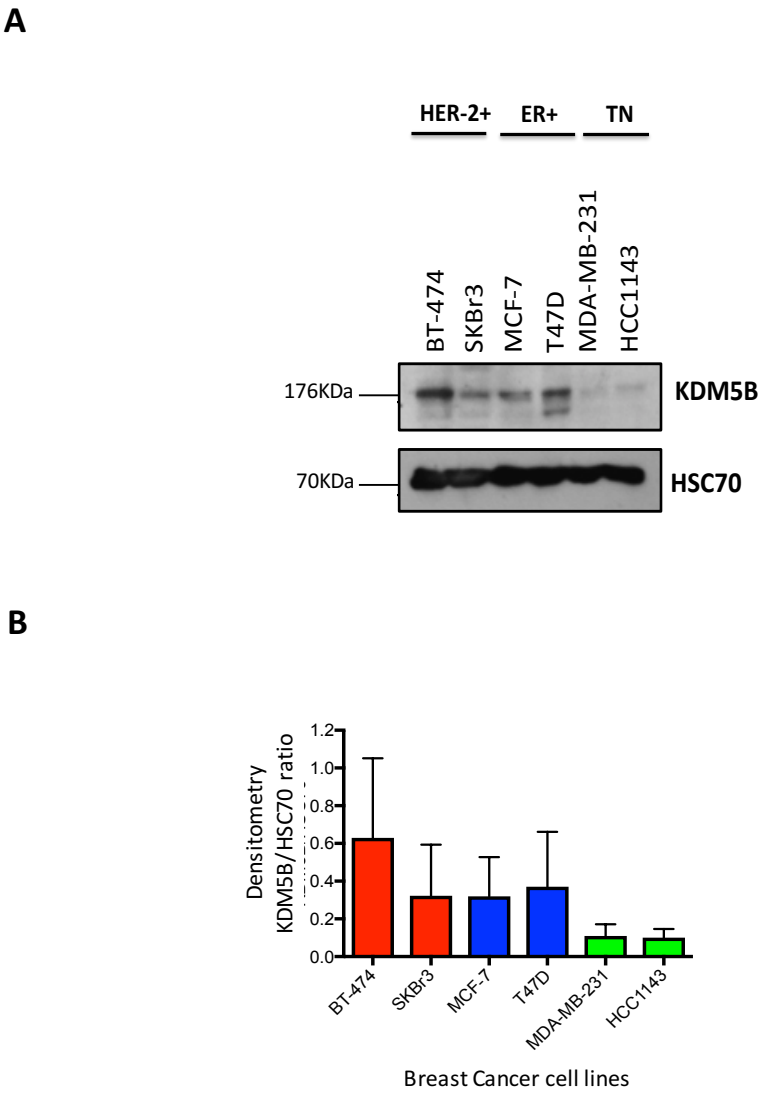

Figure 3.3: Protein expression of KDM5B in breast cancer cell lines. A) Whole cell lysates of six breast cancer cell lines were subjected to western blot and probed with KDM5B antibody. HSC70 was used as a loading control. B) Blots were quantified using ImageJ. Values represent means ± s.e.m. Blots are representative of three independent experiments.

3.2.2 Expression of KDM5B in Herceptin resistance breast cancer cell lines

To begin studies in understanding the role of KDM5B in resistance of HER2+ breast cancer, protein expression of KDM5B was examined in Herceptin sensitive and Herceptin resistant cell lines.

Treatment of SKBr3 cells with 20nM Herceptin for 48 hours, resulted in down-regulation of KDM5B expression (**Fig 3.4**). Similarly, a 48-hour treatment with 100nM Lapatinib, a dual EGFR/HER2 tyrosine kinase inhibitor, also down-regulated KDM5B expression (**Fig 3.4**). These findings confirm observations by [183], who showed that KDM5B is downregulated by Herceptin treatment, suggesting involvement of KDM5B in HER2 signalling. Interestingly, phosphorylated HER2 (pHER2) was downregulated by Lapatinib, but not by Herceptin (**Fig 3.4**). This corresponds with previous data showing no effect on HER2 phosphorylation following Herceptin treatment, in SKBr3 cells [291].

Next, KDM5B expression was examined in Herceptin resistant cells, that had been developed by weekly treatment with 40μg/ml Herceptin, for 8 months [109]. KDM5B protein levels in both BT-474 and SKBr3 Herceptin resistant cell lines (BT-474-HR and SKBr3-HR respectively) did not change, in comparison to WT cells (**Fig 3.5**), suggesting that KDM5B may play a role in Herceptin resistance.

Interestingly, SKBr3-HR cells did not express detectable pHER2 (**Fig 3.5**) and HER2 (data not shown). Loss of HER2 amplification and overexpression has been observed in a BT-474 Herceptin resistant clone, and in patients who have undergone Herceptin-based neoadjuvant therapy [103], suggesting a mechanism of resistance operating through enhancement of other signalling pathways. HER2 protein expression was undetected in 3 out of 4 independent experiments and because of this inconsistency, this result could be an effect of culturing conditions. Therefore, it is important to regularly assess HER2 status of HR cells, to ensure that the phenotype is the same in all experiments.

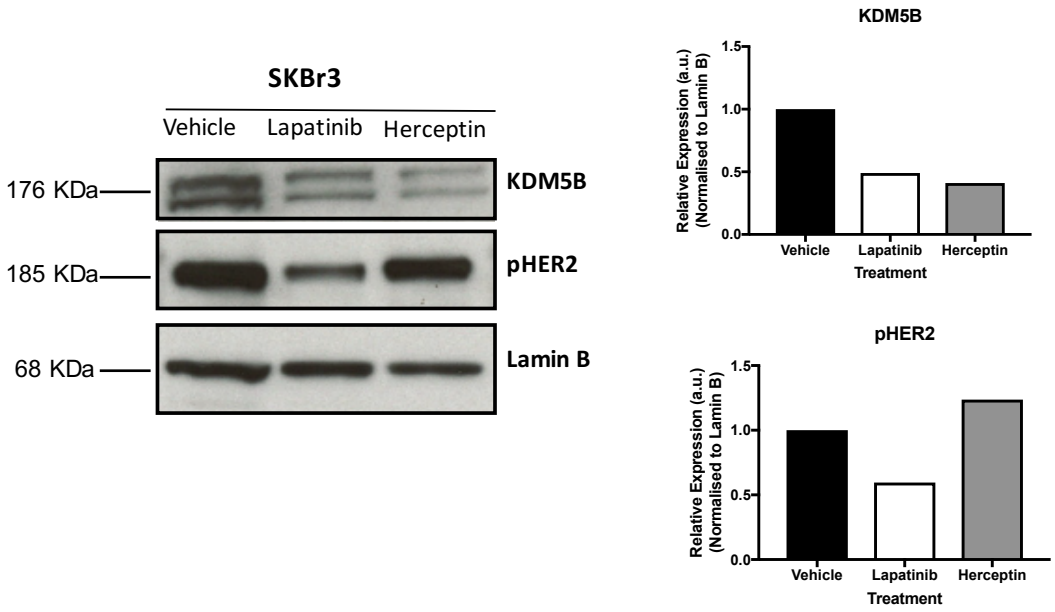

Figure 3.4: Herceptin and Lapatinib treatment reduces KDM5B expression in SKBr3 cells. Whole cell lysates of SKBr3 cells treated with vehicle, 100nM Lapatinib or 20nM Herceptin were subjected to western blot and probed with KDM5B and pHER2 antibodies. Lamin B was used as a loading control. Blots were quantified on image J software. Values show relative expression to vehicle control after normalising to Lamin B. Blots represent one experiment.

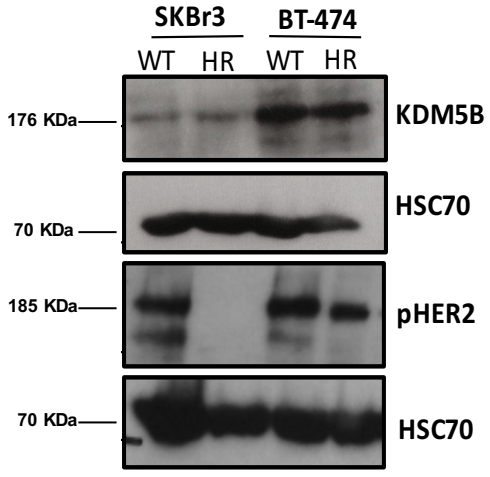

Figure 3.5: KDM5B expression in Herceptin resistant breast cancer cell lines. Whole cell lysates of parental and Herceptin resistant BT-474 and SKBr3 cells were subjected to western blot and probed with KDM5B and pHER2 antibodies. HSC70 was used as a loading control. Blots represent three independent experiments.

3.2.3 Generating KDM5B knockout breast cancer cell lines using the CRISPR-Cas9 gene editing technique

3.2.3.1 CRISPR Workflow

To examine the function of KDM5B in HER2+ breast cancer, KDM5B was knocked out in BT-474 and SKBr3 HER2+ cell lines, using CRISPR-Cas9 technology. The CRISPR workflow used to develop KDM5B KO cell lines is shown in **Figure 3.6**, with each being illustrated in more detail.

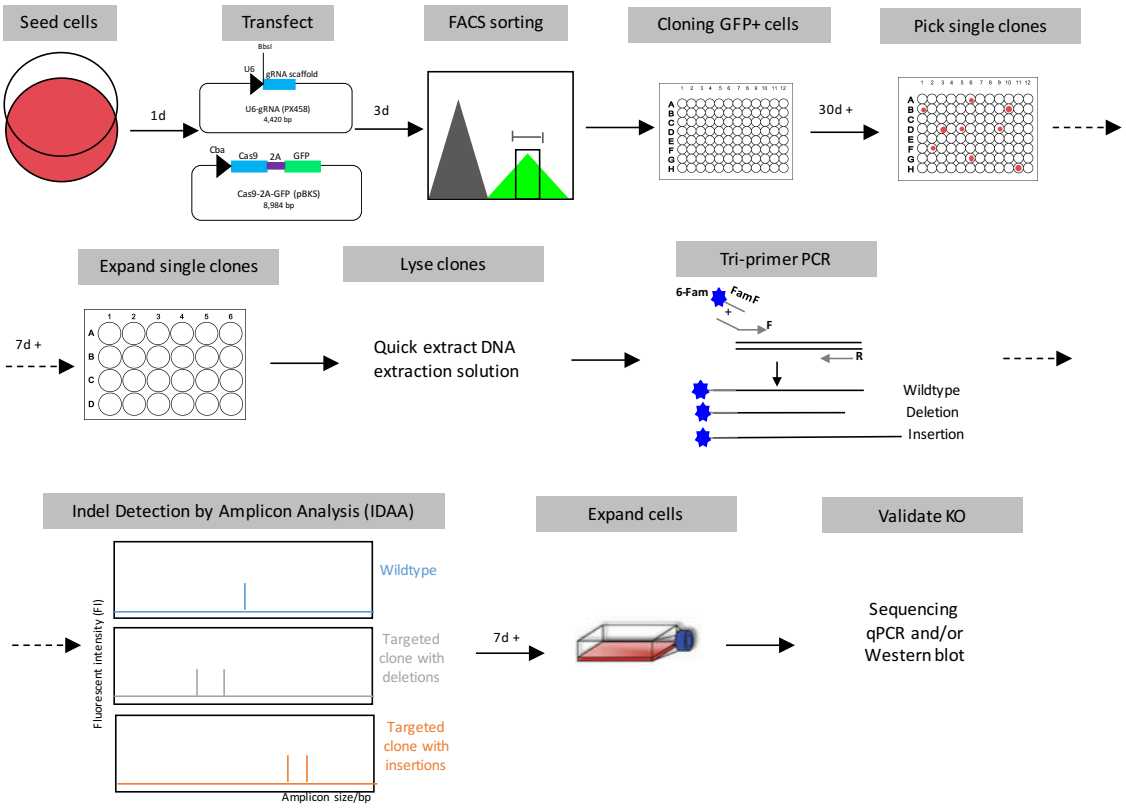

Figure 3.6: CRISPR workflow. Cells are transfected with Cas9 and KDM5B gRNAs, the day after seeding. Three days post transfection, cells are subjected to FACS to sort for cells with a specific GFP intensity. Sorted cells are single cell cloned into 96-well plates for approximately 5-8 weeks. Single cell clones are identified, picked and expanded in 24-well plates. Once confluent, DNA is extracted from cells using the Quick extract DNA solution. DNA samples are subsequently amplified by tri-primer PCR using forward (F) and reverse (R) primers that flank the targeted gRNA site, and a FAM labelled primer. Fluorescently labelled amplicons are analysed by capillary electrophoresis to identify indels produced. KO clones are selected, expanded and confirmed by various methods such as sanger sequencing, western blot and qPCR.

3.2.3.2 Design and construction of CRISPR-Cas9 KDM5B gRNAs

Four gRNA sequences targeting KDM5B (**Table 3.1**) were selected using the CRISPR-Cas9 target site selection tool CHOPCHOP (https://chopchop.rc.fas.harvard.edu/). gRNAs were targeted to exons 1, 4, 5 and 6 of KDM5B as shown in **Figure 3.7**. The gRNA sequences were cloned into the PX458 vector which was co-transfected with the Cas9 vector into breast cancer cell lines as described in **Chapter 2**.

Table 3.1: KDM5B gRNA target sequence.

gRNA	Target sequence	PAM	Exon	Strand
1	CGGCCCATAGCCGAGCAGAC	TGG	1	+
2	GTTTGCTCCTGGCAAAGCAG	TGG	4	+
3	AGGCTGCACAGACTGCCTCT	GGG	5	-
4	TCATAATCTGAGACGTCGAA	TGG	6	+

List of KDM5B target sequences, PAM sequences, targeted exons and strand orientation of gRNAs. gRNA 1 (green) targets exon 1, gRNA 2 (blue) targets exon 4, gRNA 3 (red) targets exon 5 and gRNA 4 (purple) targets exon 6.

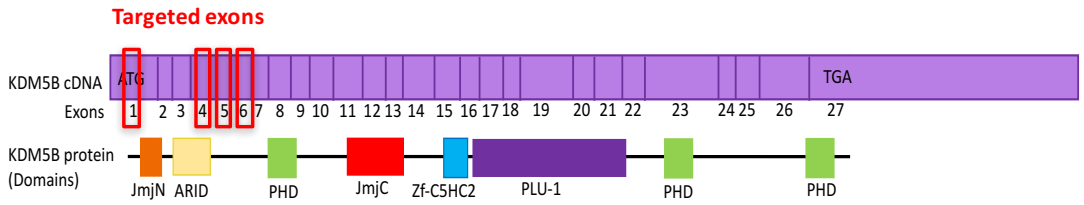

Figure 3.7: Schematic structure of KDM5B showing gRNA targeted exons and the corresponding position of the exons on the KDM5B protein.

3.2.4 Experimental selection of KDM5B gRNA

3.2.4.1 FACS Analysis of Cas9 and KDM5B gRNAs transfected in SKBr3 cells

Plasmids containing the four gRNAs targeting KDM5B, were individually co-transfected with the Cas9 plasmid into SKBr3 cells by nucleofection. 72 hours post transfection, cells were subjected to fluorescence activated cell sorting (FACS), to select fluorescent GFP expressing cells. All of the gRNAs tested had a transfection efficiency of approximately 50-60% of the total population, as detected by GFP expression in the Cas9 plasmid. 12-15% of these cells had a high GFP intensity (>10^4) (**Fig 3.8**) and were therefore sorted and subjected to indel analysis as described in the following section.

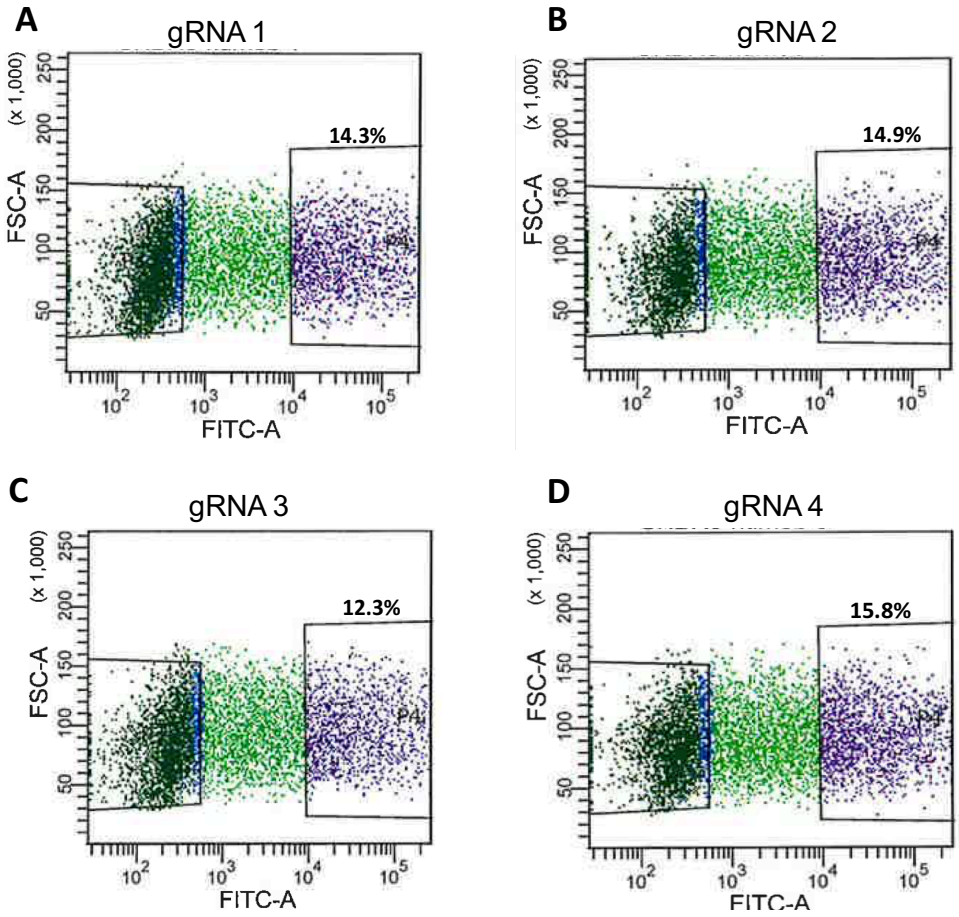

Figure 3.8: FACS analysis of SKBr3 cells transfected with KDM5B gRNAs and Cas9. Transfection efficiency of all gRNAs was approximately 60%, of which 12-15% of this population was selected for sorting as they had a high GFP intensity. A) gRNA targeting exon 1 B) gRNA targeting exon 4 C) gRNA targeting exon 5 and D) gRNA targeting exon 6.

3.2.4.2 Screening of KDM5B gRNAs cutting efficiency using indel detection by amplicon analysis (IDAA)

Bulk sorted SKBr3 cells were validated by IDAA as described in **Chapter 2**. DNA was extracted from cells and amplified by tri-primer PCR. Fluorescently labelled PCR amplicons were subsequently analysed by capillary electrophoresis. Fragment analysis showed induction of indels with gRNA 2, that was targeting exon 4 (**Fig 3.9A**). This gRNA produced various indels i.e. 1, 2, 3, 4, 5, 6 and 7bp deletions and a 1bp insertion. gRNAs 3 and 4 that were targeting exons 5 and 6 respectively, did not produce any indels (**Fig 3.9B and C**). No data was available for samples targeted with gRNA 1, due to technical issues. gRNA 2 was therefore selected and used to develop KDM5B knockout cell lines.

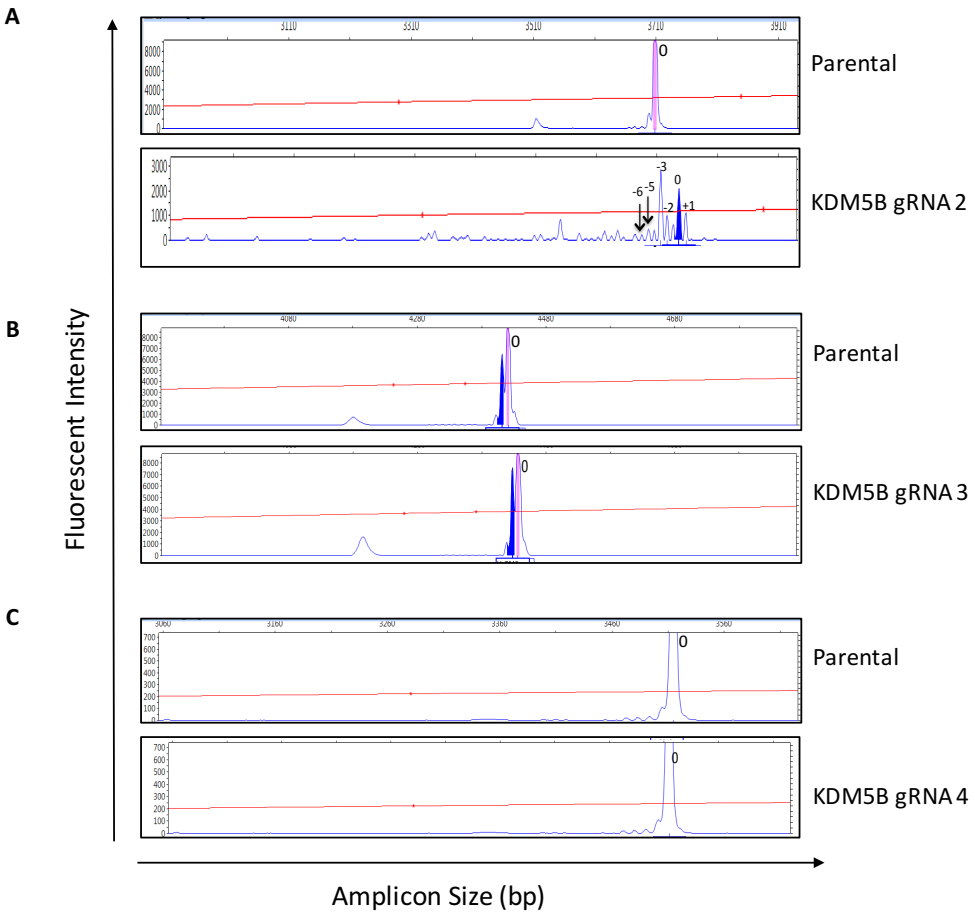

Figure 3.9: IDAA screening of KDM5B gRNAs cutting efficiency. SKBr3 cells transfected with Cas9 and KDM5B gRNA targeting exons 1, 4, 5 and 6 were bulk sorted and analysed by Indel Detection by Amplicon Analysis (IDAA). A) gRNA 2 targeting exon 4 successfully induced indels in the KDM5B gene. Deletions denoted as -1, -2, -3, -4, -5, -6 and -7 correspond to the number of deleted base pairs. Insertions are denoted as +1, corresponding to the number of base pairs inserted. B) gRNA 3 and C) gRNA 4 targeting exon 5 and 6 respectively, did not induce any indels in the KDM5B gene. Analysis was done on the Peak Scanner Software.

3.2.5 Development of KDM5B Knockout cell lines

3.2.5.1 FACS analysis of CRISPR targeted KDM5B in BT-474 and SKBr3 cells

The selected gRNA 2 (targeting exon 4 of KDM5B) and Cas9 plasmids were co-transfected into BT-474 and SKBr3 cells, by nucleofection. 72 hours post transfection, cells were subjected to FACS analysis. For this experiment, cells with a GFP intensity of between 10^3-10^4 were selected, to reduce the selection of clones with potential off target site, which can occur with high Cas9 transfection. The sorted population was 1% and 13.3% for BT-474 and SKBr3 cells, respectively (**Fig 3.10**). These cells were subsequently single cell sorted into 96-well plates.

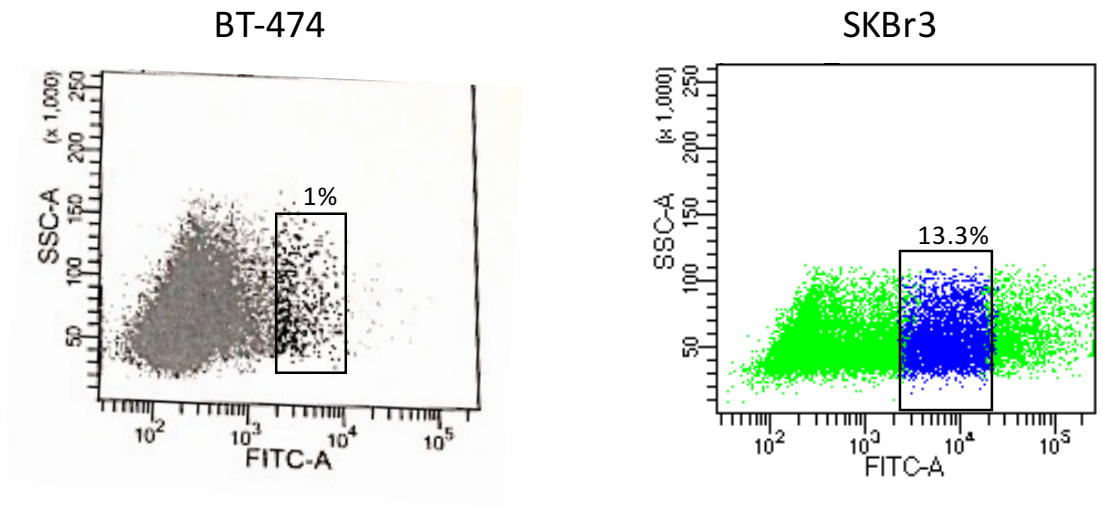

Figure 3.10: FACS analysis of BT-474 and SKBr3 cells transfected with KDM5B gRNA 2 and Cas9 plasmids. Gating of transfected cells with specific GFP fluorescent intensity levels. Values indicate percentage of cells in the selected gate. Cells were analysed on the FACS Aria II instrument.

3.2.5.2 IDAA screening of CRISPR-Cas9 targeted KDM5B single cell clones in BT-474 and SKBr3 cells

CRISPR-Cas9 targeted KDM5B single cell clones were cultured for approximately 8 weeks prior to IDAA, to obtain sufficient number of cells to split allowing half to be used for IDAA. In total, 17 single cell clones were analysed in BT-474 cells (**Fig 3.11**) and 29 single cell clones in SKBr3 cells (**Fig 3.12**).

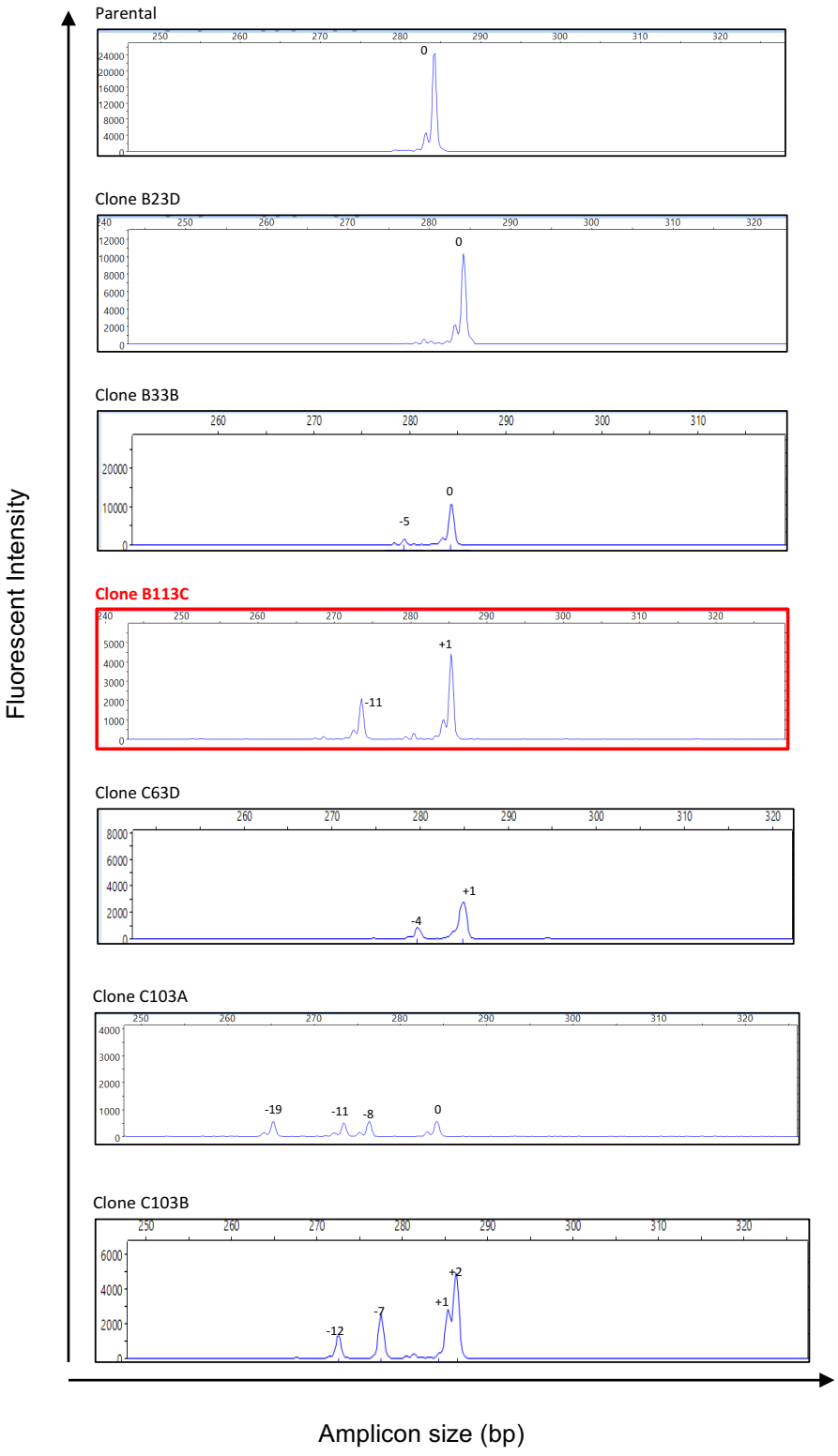

Figure 3.11: IDAA screening of CRISPR targeted KDM5B single cell clones in BT-474 cells. DNA was extracted from single cell clones and amplified by tri-primer PCR. Fluorescently labelled amplicons were run on a capillary electrophoresis sequencer and thereafter data was analysed on the Peak Scanner software. The selected KDM5B KO clones, B113C and G113C are shown in a red box.

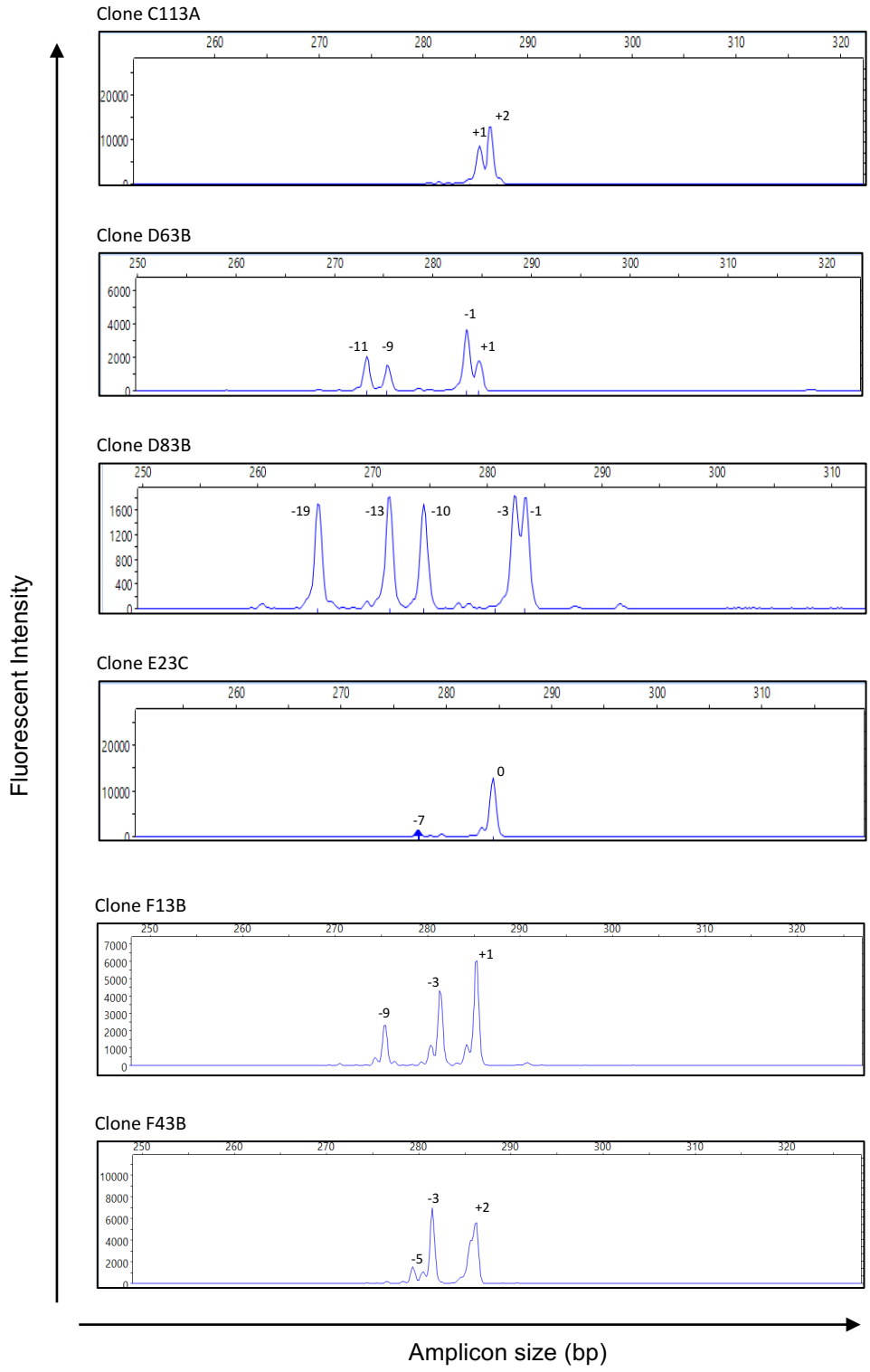

Figure 3.11: IDAA screening of CRISPR targeted KDM5B single cell cline in BT-474 cells (continued).

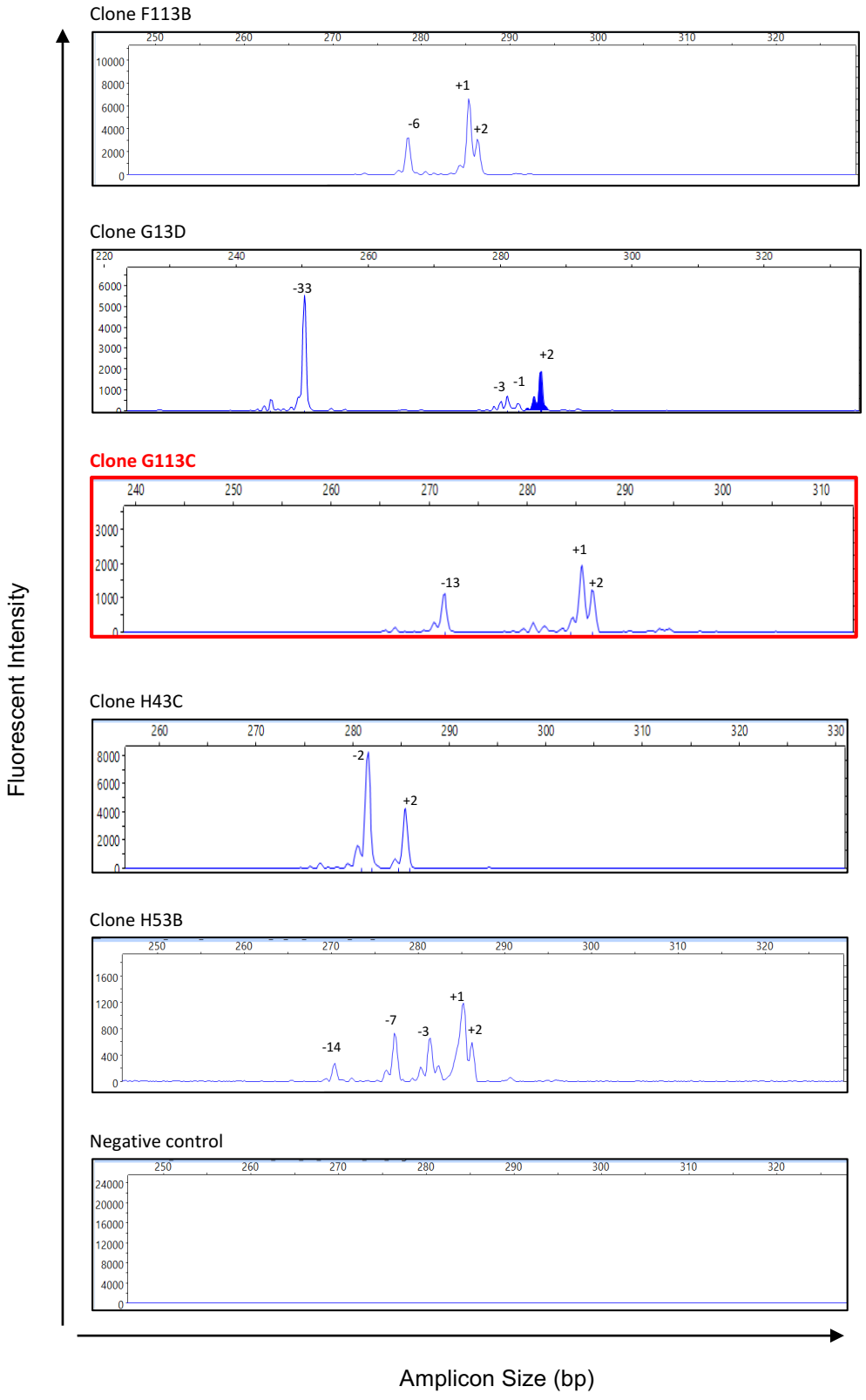

Figure 3.11: IDAA screening of CRISPR targeted KDM5B single cell clones in BT-474 cells (continued).

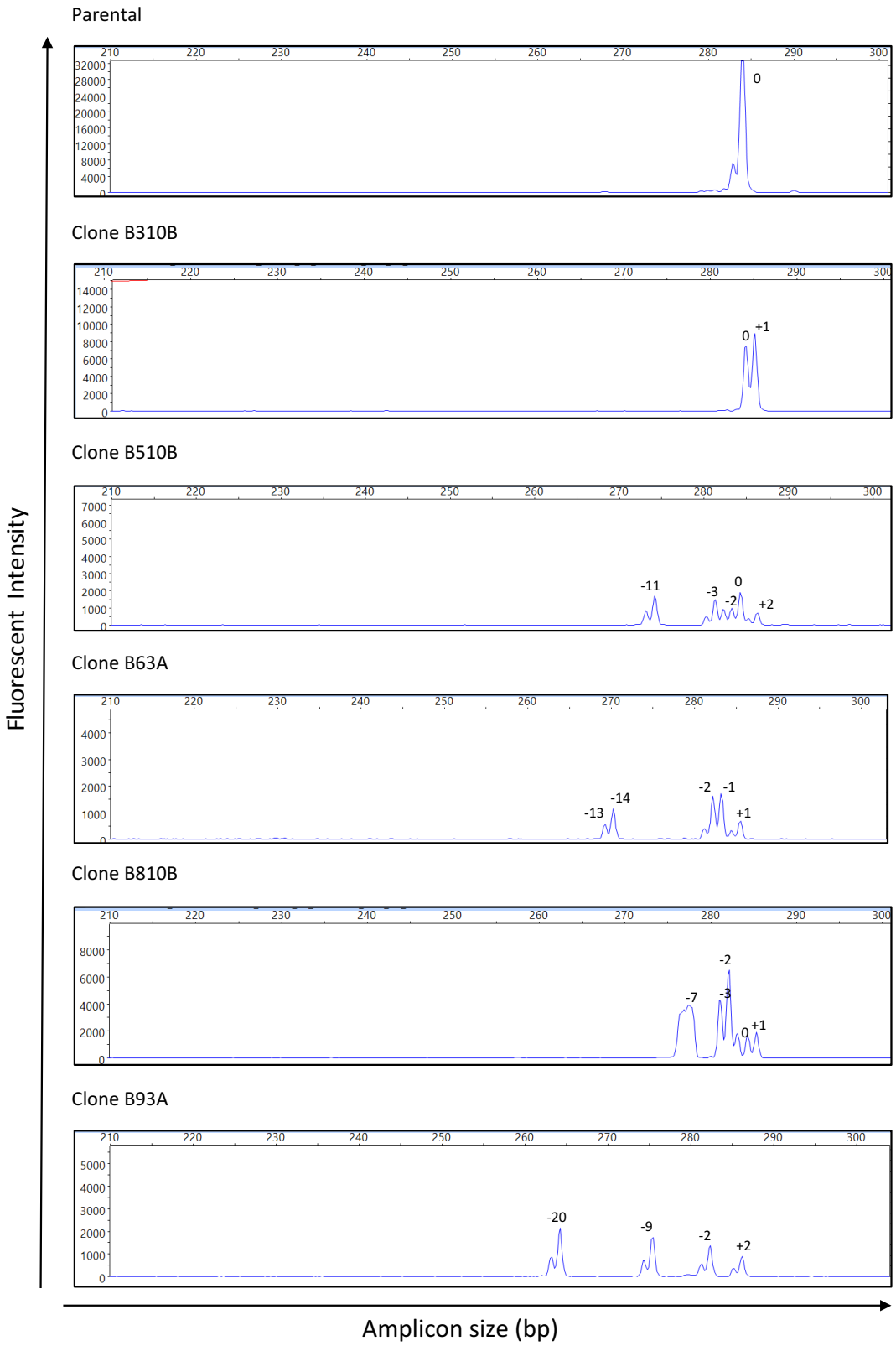

Figure 3.12: IDAA screening of CRISPR targeted KDM5B single cell clones in SKBr3 cells. DNA was extracted from single cell colonies and amplified by tri-primer PCR. Fluorescently labelled amplicons were run on a capillary electrophoresis sequencer and thereafter data was analysed on the Peak Scanner software. The selected KDM5B KO clone, F113E, is shown in a red box.

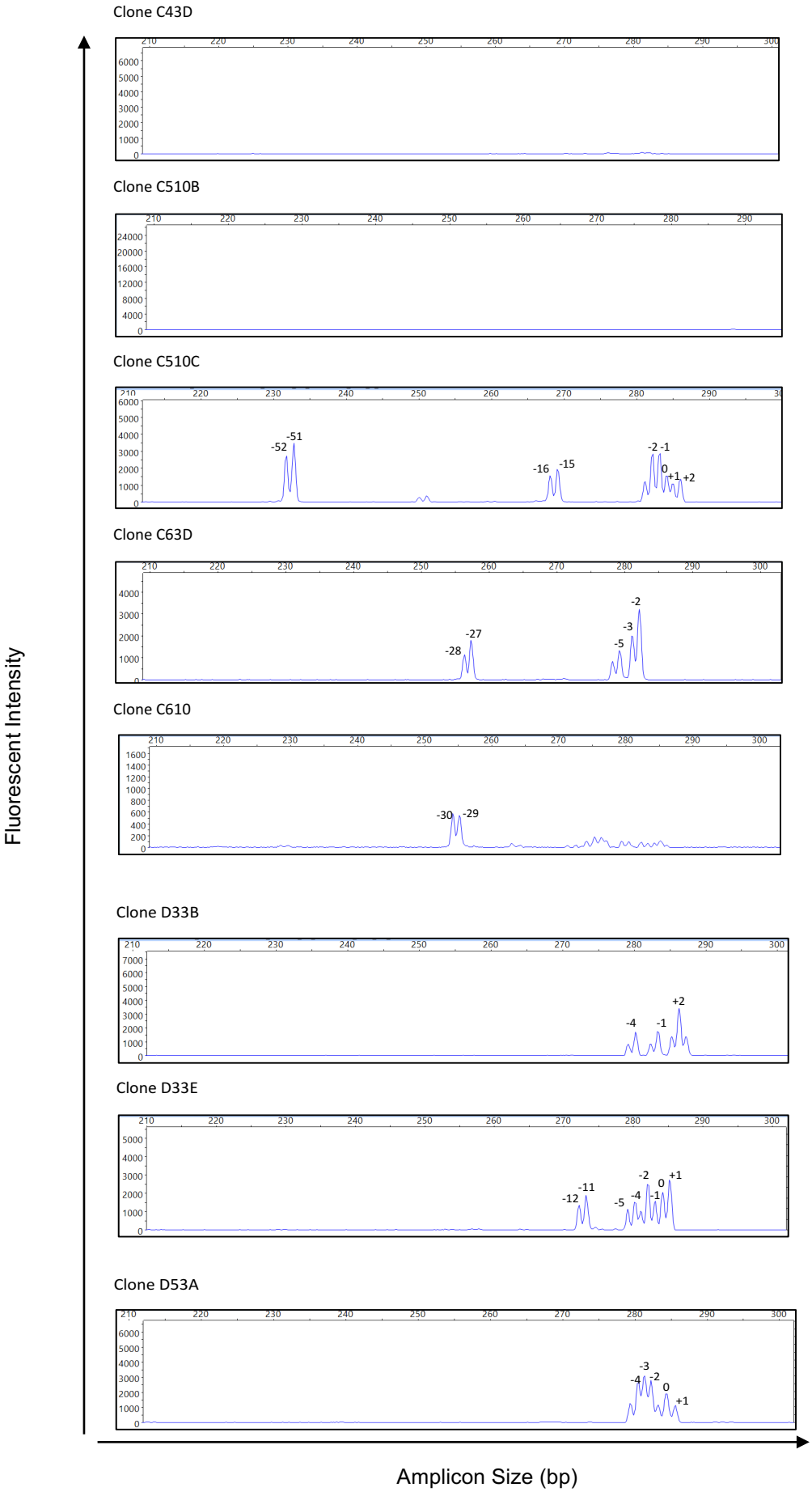

Figure 3.12: IDAA screening of CRISPR targeted KDM5B clones in SKBr3 cells (continued).

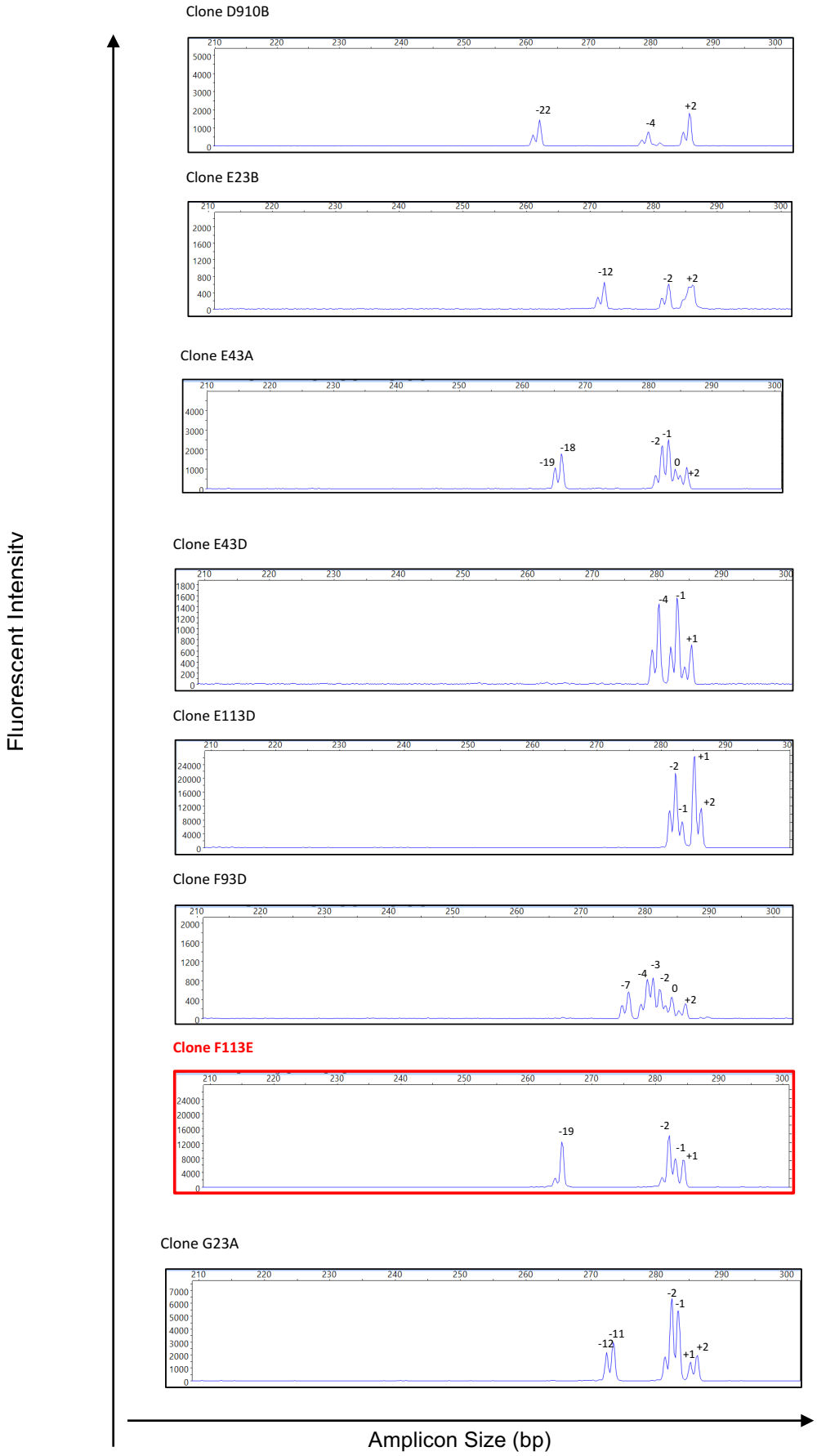

Figure 3.12: IDAA screening of CRISPR targeted KDM5B clones in SKBr3 cells (continued).

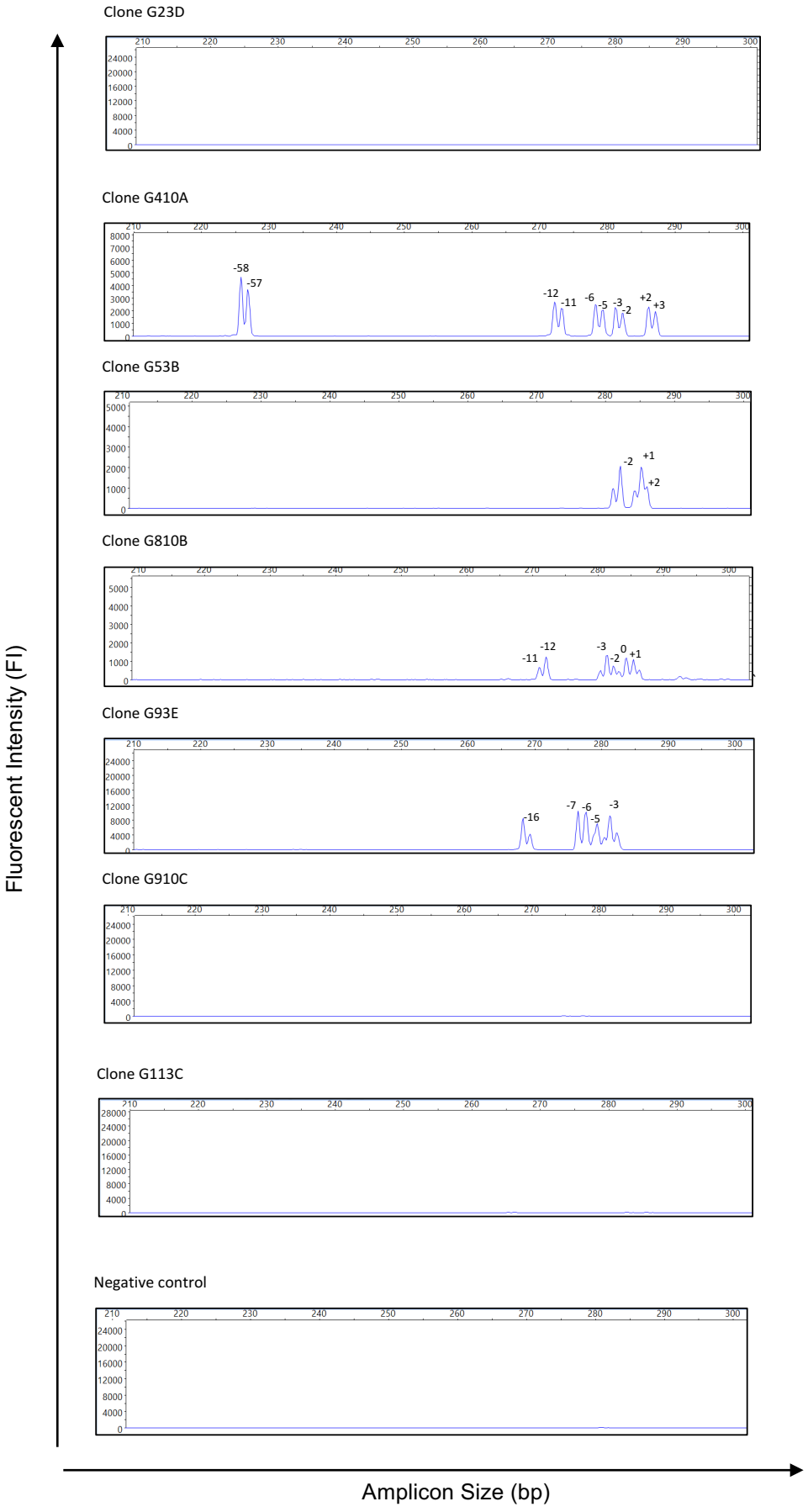

Figure 3.12: IDAA screening of CRISPR targeted KDM5B single cell clones in SKBr3 cells (continued).

Clones were selected as potential KOs if they did not have the parental allele or in-frame indels. Furthermore, the growth rate was also a determining factor in selecting KDM5B KO clones, as clones that did not grow very well were not selected. In BT-474, this resulted in 10 clones being selected as potential KOs. These clones were subsequently screened by western blot for KDM5B expression, which identified B113C and G113C clones as KDM5B KOs, since they did not have any detectable KDM5B protein (**Fig 3.13**). In SKBr3 cells, 2 clones (D910B and F113E) were selected as potential KOs and screened by western blot. The D910B clone showed expression of KDM5B, whereas the F113E did not have any detectable KDM5B and so was selected as a KDM5B KO (**Fig 3.14**).

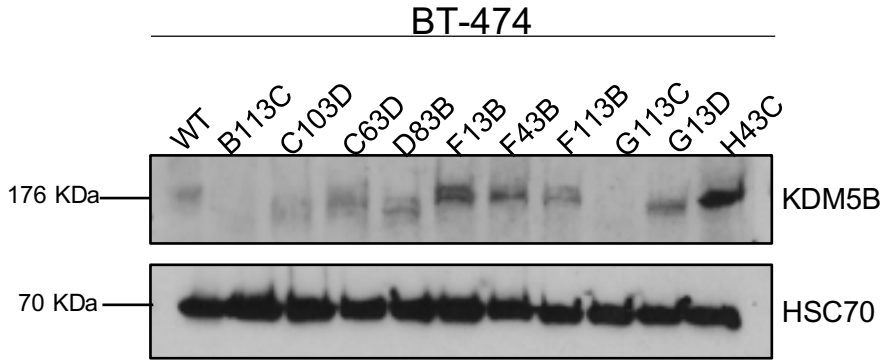

Figure 3.13: Screening of KDM5B CRISPR targeted clones in BT-474. Whole cell lysates of BT-474 WT and KDM5B CRISPR targeted clones were subjected to western blot and probed with a KDM5B antibody. HSC70 was used as a loading control. Blots represent one independent experiment.

Figure 3.14: Screening of KDM5B CRISPR targeted clones in SKBr3. Whole cell lysates of SKBr3 WT and KDM5B CRISPR targeted clones were subjected to western blot and probed with a KDM5B antibody. HSC70 was used as a loading control. Blots represent one independent experiment.

3.2.5.3 Validation of CRISPR-Cas9 targeted KDM5B KO clones by Sanger Sequencing

To confirm the presence of the indels identified in the CRISPR targeted KDM5B clones (BT-474 B113C, BT-474 G113C and SKBr3 F113E), DNA of the targeted site (Exon 4) was PCR amplified and sequenced. Sanger sequencing data was analysed using the CodonCode Aligner software and was in agreement with IDAA, as the sequences identified in each of the clones had the exact indels shown by IDAA. Two sequences were identified in the BT-474 B113C clone, 3 sequences in the BT-474 G113C clone and 4 sequences in the SKBr3 F113E clone. The sequences and their corresponding indels are shown in (**Fig 3.15**), and were identified with the assistance of Dr. Zhang Yang, University of Copenhagen. Furthermore, the number of sequences identified in BT-474 G113C and in SKBr3 F113E correspond to KDM5B copy number in these cell lines, where the copy number of KDM5B is three in BT-474 and four in SKBr3, as analysed in the cancer cell line encyclopedia (CCLE) [292]. However, since only two sequences were identified in the BT-474 B113C clone, it suggests that this clone may not be a complete KO.

A

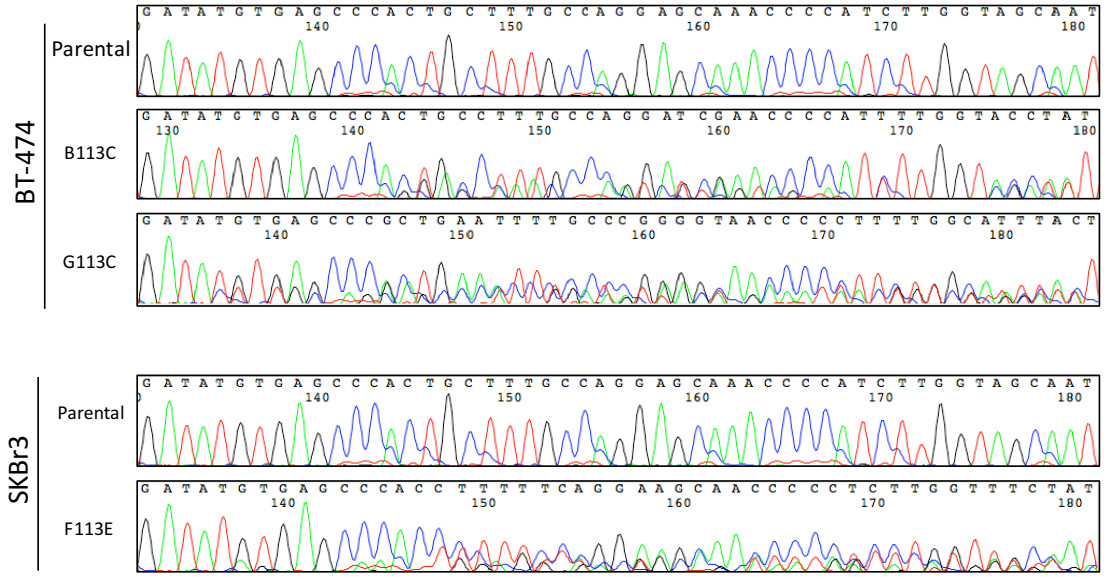

B

gRNA 2 target sequence | PAM

Cut site

		Indels
Parental	CCAAGATGGGgtttgctcctggcaaagcagtggGCTCACATATCAGAGGGATTATGAACGAATTCTCAACCCCTA	0
BT-474 B113C	CCAAGATGGGgtttgctcctggcaaag**G**cagtggGCTCACATATCAGAGGGATTATGAACGAATTCTCAACCCCTA	+1
	CCAAGATGGGgtttgctcc_____tggGCTCACATATCAGAGGGATTATGAACGAATTCTCAACCCCTA	-11
BT-474 G113C	CCAAGATGGGgtttgctcctggcaaag**G**cagtggGCTCACATATCAGAGGGATTATGAACGAATTCTCAACCCCTA	+1
	CCAAGATGGGgtttgctcctggcaaag_____TATCAGAGGGATTATGAACGAATTCTCAACCCCTA	-13
	CCAAGATGGGgtttgctcctggcaaag**GG**cagtggGCTCACATATCAGAGGGATTATGAACGAATTCTCAACCCCTA	+2
SKBr3 F113E	CCAAGATGGGgtttgctcctggcaaag_ _gtggGCTCACATATCAGAGGGATTATGAACGAATTCTCAACCCCTA	-2
	CCAAGATGGGgtttgctcctggcaaag**G**cagtggGCTCACATATCAGAGGGATTATGAACGAATTCTCAACCCCTA	+1
	CCAAGATGGGgtttgctcct_____ATATCAGAGGGATTATGAACGAATTCTCAACCCCTA	-19
	CCAAGATGGGgtttgctcctggcaaagc_gtggGCTCACATATCAGAGGGATTATGAACGAATTCTCAACCCCTA	-1

Figure 3.15: Sanger sequencing of CRISPR targeted KDM5B clones. A) Sequencing traces of Parental and CRISPR targeted KDM5B clones showing KDM5B gene disruption in the clones. B) Sequences of CRISPR targeted KDM5B clones with their respective indels. Red: gRNA 2 target sequence and PAM sequence; Bold red uppercase: Inserted bases; dashed line: deleted bases. The position of Cas9 cutting site is indicated with an orange arrow. Sequences were analysed on the CodonCode Aligner software.

3.2.5.4 Validation of CRISPR-Cas9 targeted KDM5B clones by western blot and RT-qPCR

KDM5B KO clones were further validated by western blot and RT-qPCR. KDM5B protein was not detected in the BT-474 and SKBr3 KO clones by western blot analysis (**Fig 3.16 and 3.17**). Protein expression of KDM5A and KDM5C were also examined to determine whether they compensated for KDM5B KO. Expression levels of KDM5A and KDM5C did not change in the KDM5B KO clones in comparison to parental cells (**Fig 3.16 and Fig 3.17**). KDM5D was not examined as being located on the Y chromosome[168] it is not expressed in females.

KDM5B mRNA expression by RT-qPCR in the KO clones showed a fold change of 0.28 in BT-474 B113C, 0.07 in BT-474 G113C and 0.13 in the SKBr3 F113E clones (**Fig 3.18A and 3.18B**). Taken together, these findings confirm complete KDM5B KO in the SKBr3 F113E clone and BT-474 G113C clone. Whereas, the low KDM5B mRNA expression in the BT-474 B113C clone, suggests a partial/incomplete KO. Thus, further studies utilizing this clone needs to consider this low mRNA expression, when making conclusions on any molecular and/or phenotypic observations. These clones will hereafter be referred to as BT-474 KO1* (B113C), BT-474 KO2 (G113C) and SKBr3 KO (F113E).

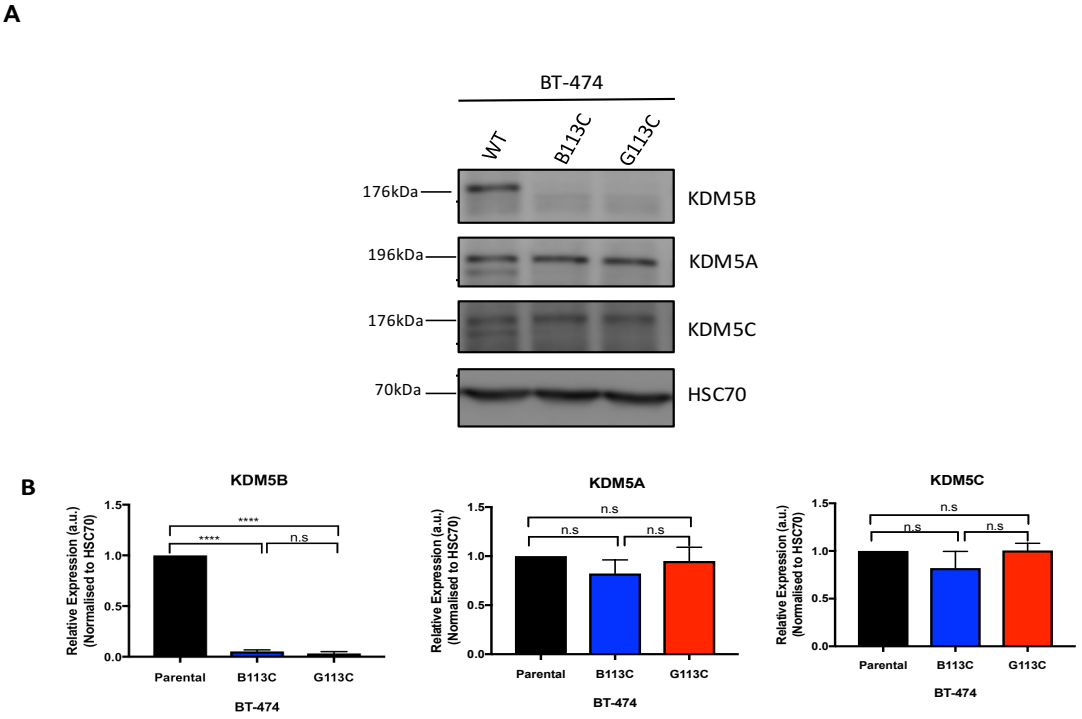

Figure 3.16: Validation of KDM5B KO in BT-474 cells by western blot. A) Western blot analysis showing no detectable KDM5B protein in the KO clones. Expression of KDM5A and KDM5C was not changed in the KDM5B KO clones. HSC70 was used as a loading control. Blots are representative of 3 independent experiments. B) Quantification of blots on imageJ software. Error bars indicate s.e.m of 3 independent experiments. Asterisks show significance where **** = $p \leq 0.0001$ and n.s=not significant. Statistical significance was calculated using unpaired Student's *t*-test.

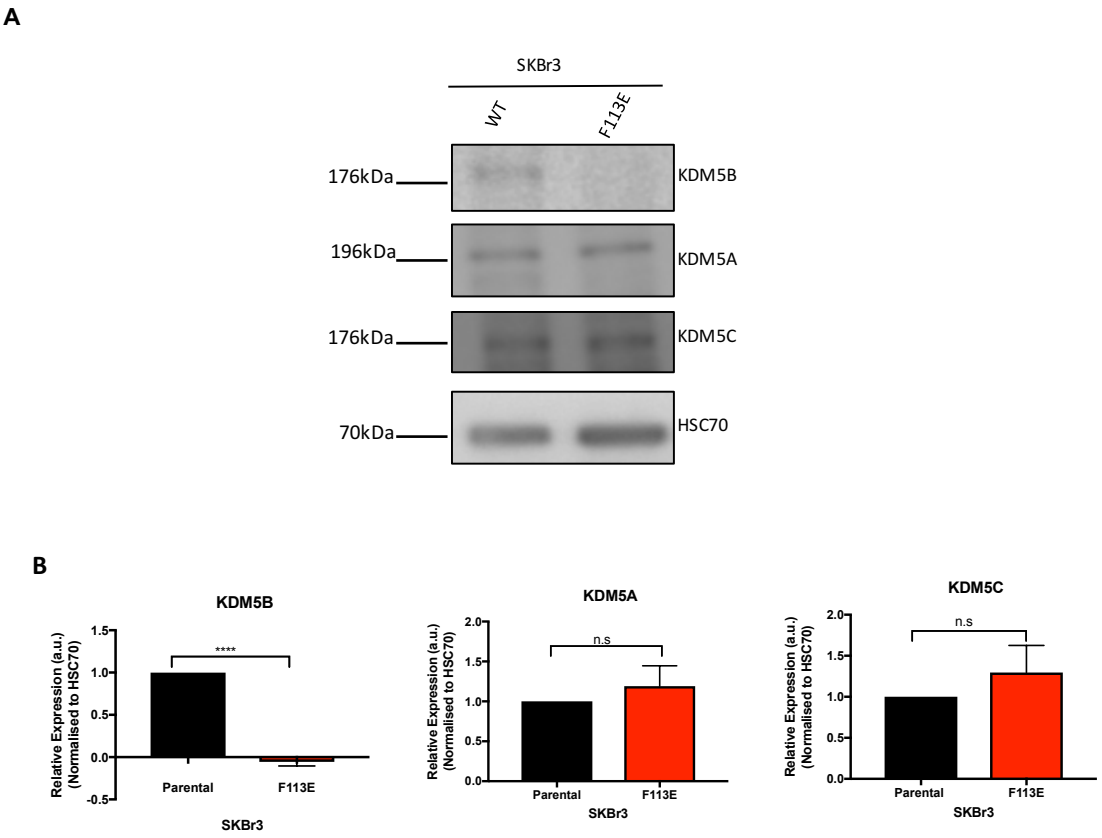

Figure 3.17: Validation of KDM5B KO in SKBr3 cells by western blot. A) Western blot analysis showing no detectable KDM5B protein in the KO clones. Expression of KDM5A and KDM5C was not changed in the KDM5B KO clones. HSC70 was used as a loading control. Blots are representative of 3 independent experiments. B) Quantification of blots on imageJ software. Error bars indicate s.e.m of 3 independent experiments. Asterisks show significance where **** = p≤0.0001 and n.s=not significant. Statistical significance was calculated using unpaired Student's *t*-test.

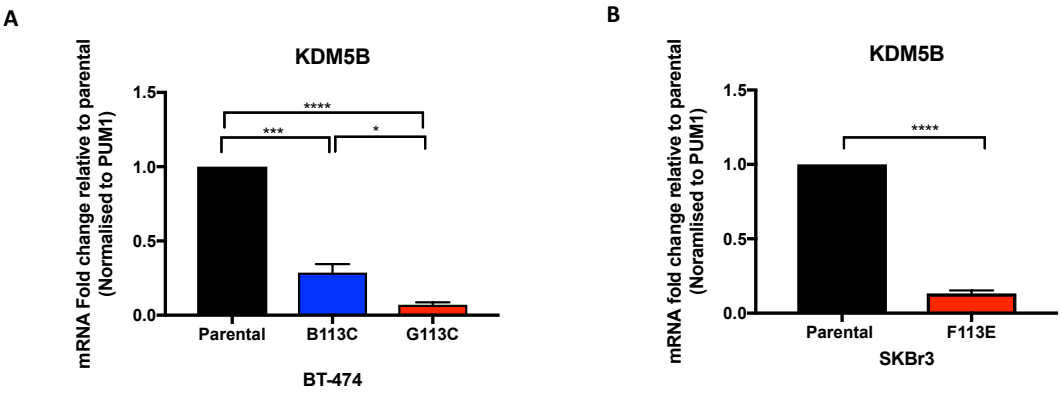

Figure 3.18: Validation of KDM5B KO clones by RT-qPCR. Expression of KDM5B in the KO clones was quantitated relative to parental cells. Cells were normalised to expression of the housekeeping gene PUM1. Values are fold changes ± s.e.m. of 3 independent experiments. Asterisks show significance where * = p≤0.05, *** = p≤0.001 and **** = p≤0.0001. Statistical significance was calculated using unpaired Student's *t*-test.

3.3 Discussion

In this Chapter, upregulation of KDM5B in breast tumours is shown and this increased expression was found to be associated with copy number gain and/or amplification. Furthermore, KDM5B was found to be particularly increased in HER2+ and ER+ breast tumours and cell lines, suggesting it may play an important role in these tumours. Since KDM5B has been implicated in drug resistance of various cancers [204,212], its expression was examined in Herceptin resistant HER2+ breast cancer cells. KDM5B protein levels in BT-474 and SKBr3 Herceptin resistant cells was similar to WT cells. This is in contrast to its downregulation in SKBr3 Herceptin sensitive cells, thus suggesting that KDM5B may play a role in Herceptin resistance in these cells.

The study of gene function in various biological processes, has been accelerated by the development of genome editing tools such as CRISPR-Cas9. To understand the role of KDM5B in HER2+ breast cancer cells including drug resistance, CRISPR-Cas9 was employed to develop KDM5B KO breast cancer cell lines. KDM5B KO was successfully achieved in BT-474 and SKBr3 cells. Confirmation of gene inactivation by RT-qPCR revealed substantial reduction of KDM5B in the KO cell lines, which could be due to degradation of nonsense mRNAs via the nonsense-mediated decay (NMD) pathway [293]. However, in the BT-474 KO1* cells there is still some mRNA expression. The difference between BT-474 KO1* and BT-474 KO2 cells could relate to the number of targeted alleles, i.e. two versus three alleles, respectively, as observed by IDAA. Since KDM5B has a copy number of three in BT-474 cells, it suggests that one of the alleles was not targeted in the BT-474 KO1* cells. Since KDM5B protein in the BT-474 KO1* cells was not detected on western blot, this may be a reflection on the sensitivity of the assay therefore, it is important to consider the mRNA expression in any differences observed between the two clones in future experiments.

In this first round of targeting KDM5B using CRISPR-Cas9, only one KDM5B KO clone was developed in SKBr3 cells. It would have been ideal to have a second KDM5B KO clone, to enable validation of any phenotypes observed in these cells. Although the D910B was a potential KO as visualised by IDAA, western blot analysis showed the presence of KDM5B protein. Re-targeting of nuclease edited cells has been shown to increase editing efficiency [294]. Thus, this clone could be re-targeted to assess whether complete KDM5B KO can eventually be achieved. Unfortunately, the other potential KO clones B63A, D33B, E43D, E113D and G53B were discarded as it was initially thought that they were not KOs, therefore they cannot be further analysed or re-targeted. These KDM5B KO cell lines will now be used to study the function of KDM5B in gene expression and response to HER2 targeted therapies in HER2+ breast cancer cell lines.

4 : KDM5B regulation of Caveolin1 in the normal and malignant mammary gland

4.1 Introduction

Genome-wide analyses looking at KDM5B occupancy, have revealed its association with transcriptional start sites, where it binds at the regions containing the H3K4me3 mark on promoters of target genes [146,202]. Clearly demonstrating that KDM5B can repress target genes via its demethylase activity. One of the target genes that was found to have increased expression upon KDM5B KD which correlated with increased H3K4me3 levels in the MCF-7 breast cancer cell line, is CAV1 [146]. Understanding KDM5B regulation of CAV1 is of particular interest because, recent data from our laboratory using a mouse model suggests that CAV1 may normally be downregulated by KDM5B, during normal mammary gland development.

In the mouse mammary gland, CAV1 negatively regulates STAT5a expression since its knockout resulted in hyperactivation of JAK2/STAT5 signalling [231]. Interestingly, in the mid-pregnant mammary gland of the ΔARID mouse which lacks KDM5B demethylase activity, pSTAT5 is downregulated [196] and this correlates with upregulation of CAV1 (Steven Catchpole personal communication). Therefore, KDM5B could play a role in downregulating CAV1 expression, thus enabling activation of the JAK2/STAT5 signalling pathway and in turn alveologenesis.

CAV1 expression is generally downregulated in breast cancer [232,233], where it may act as a tumour suppressor [234]. However, in the aggressive basal-like and triple negative breast cancers CAV1 expression has been reported to be upregulated [233,236]. In contrast, high expression of CAV1 in breast cancer associated fibroblasts has been found to be associated with good prognosis [239,242]. More recently, stromal CAV1 expression in TNBC was shown to predict better overall survival in Asian women [238]. Taken together, these findings suggest a multifaceted and cell-type specific role of CAV1 in breast cancer.

4.1.1 Aims

Data from previous studies, suggest a possible role for KDM5B in repression of CAV1 expression, during normal mammary gland development and in some breast cancer cell lines. However, it is not clear how widespread the downregulation of CAV1 by KDM5B is seen in different breast cancer cell lines, nor is it clear, which cell types in the developing mammary gland (luminal, myoepithelial and fat cells), could be responsible for downregulation of CAV1 by KDM5B. This chapter aims to further understand KDM5B regulation of CAV1 in mammary gland development and breast cancer by examining:

1) Expression and copy number of CAV1 in breast tumours
2) Expression of CAV1 and KDM5B in breast tumours and cell lines
3) CAV1 expression in KDM5B KO breast cancer cell lines
4) Expression of CAV1 and KDM5B in normal breast fibroblasts and breast cancer-associated fibroblasts
5) Cellular distribution of CAV1 and KDM5B in the mouse mammary gland during mid-pregnancy

4.2 Results

4.2.1 CAV1 expression in breast tumours and cell lines

4.2.1.1 Copy number and gene expression analysis of CAV1 in breast tumours

CAV1 is downregulated in a majority of breast cancers and cell lines [232,237], with the exception of aggressive subtypes such as basal-like and triple negative [233,236]. To confirm these observations and to determine whether *CAV1* expression was driven by copy number aberrations, the METABRIC breast cancer database was used. Decreased *CAV1* mRNA expression was found to be associated with copy number deletion in a fraction of breast cancers (186 out of 1903) (**Fig 4.1A**). However, since a majority of the tumours were diploid (1478 out of 1903), it suggests that other factors may be driving downregulation of *CAV1*. It was further investigated whether *CAV1* expression was associated with breast cancer molecular subtypes (luminal A (LumA), luminal B (LumB), HER2+ (HER2+), basal-like and normal-like), as classified by the PAM50 gene classifier [45]. *CAV1* expression was found to be downregulated in all breast cancer subtypes, in comparison to the normal-like subtype (**Fig 4.1B**). *CAV1* expression was however significantly lower in the basal-like, HER2+ and LumB subtypes in comparison to the LumA subtype (**Fig 4.1B**).

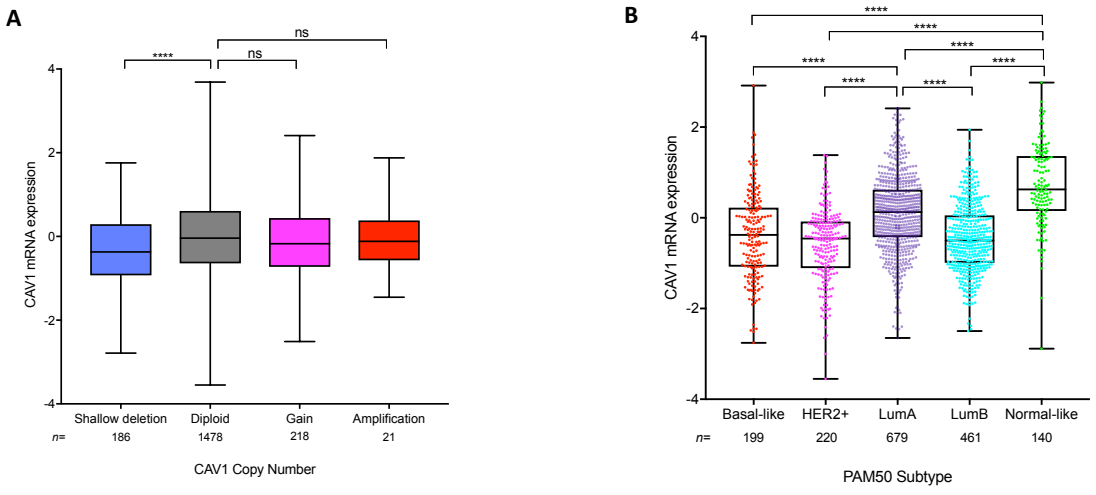

Figure 4.1: *CAV1* expression is downregulated in breast cancers. A) Decreased *CAV1* mRNA expression is associated with copy number deletion in the METABRIC dataset. Sample numbers are indicated below each copy number alteration. B) *CAV1* mRNA expression is significantly downregulated in breast cancer tumours. Sample numbers are indicated below each PAM50 subtype. METABRIC data was downloaded from the cBioportal platform. Asterisks indicate significance where, ****=p≤0.0001. ns=not significant. Statistical significance was calculated using One-way ANOVA with Sidak correction.

4.2.1.2 CAV1 and KDM5B expression in breast cancer

In order to determine whether CAV1 and KDM5B expression correlate in breast cancer, their expression was examined in breast tumours and a panel of breast cancer cell lines. Further analysis using the METABRIC dataset to validate whether *CAV1* and *KDM5B* genes are inversely correlated in breast cancers, showed a weak negative correlation between the two proteins (**Fig 4.2A**). CAV1 expression was examined in six breast cancer cell lines that were representative of the breast cancer molecular subtypes. CAV1 was abundantly expressed in the triple negative cells (TN; most TN are associated with the basal-like subtype) (MDA-MB-231 and HCC1143), moderately expressed in the ER+ (luminal) cell line (MCF-7), but not in the ER+ T47D cell line (**Fig 4.2B**). Very low expression was observed in the HER2+ cell lines (BT-474 and SKBr3) (**Fig 4.2B**). Interestingly, expression of CAV1 was generally inversely correlated with KDM5B expression in these cells lines. In particular, the TN cells had very low levels of KDM5B, whereas the HER2+ cells had moderate to high levels of KDM5B expression (**Figure 3.3A section 3.2.1.2**). The difference in the level of CAV1 expression in the two ER+ cell lines, indicates that even within a subtype, phenotypic variation is seen.

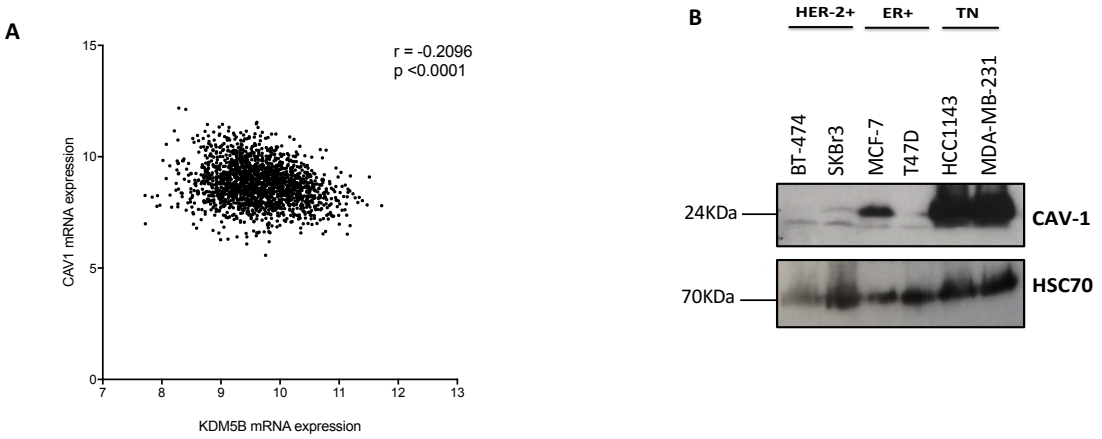

Figure 4.2: KDM5B and CAV1 expression in breast cancer. A) Correlation between *CAV1* and *KDM5B* mRNA expression in breast tumours from the METABRIC dataset. N=1904 pairs. B) Whole cell lysates of breast cancer cell lines were subjected to western blot and probed for CAV1. HSC70 was used as a loading control. Blots are representative of two independent experiments for CAV1. Statistical significance and the correlation coefficient r, was calculated using Pearson correlation.

4.2.2 Global H3K4me3 expression in KDM5B KO breast cancer cell lines

Transcriptional repression by KDM5B on its target genes, has been shown to occur through its demethylase activity acting on the active H3K4me3 mark, found on the promoters of these genes [146]. Thus, prior to examining CAV1 expression in the KDM5B KO cells, global H3K4me3 levels were examined in these cells. H3K4me3 levels was high in BT-474 KO2 cells and moderately increased in the BT-474 KO1* cells, in comparison to WT cells (**Fig 4.3A**). Contrastingly, KDM5B KO in SKBr3 cells did not alter global H3K4me3 levels (**Fig 4.3B**). Lack of increased global H3K4me3 levels upon KDM5B silencing has previously been observed in MCF-7 cells [146]. The authors did however observe increased H3K4me3 levels on the promoters of KDM5B target genes including CAV1, and this was related to their increased expression.

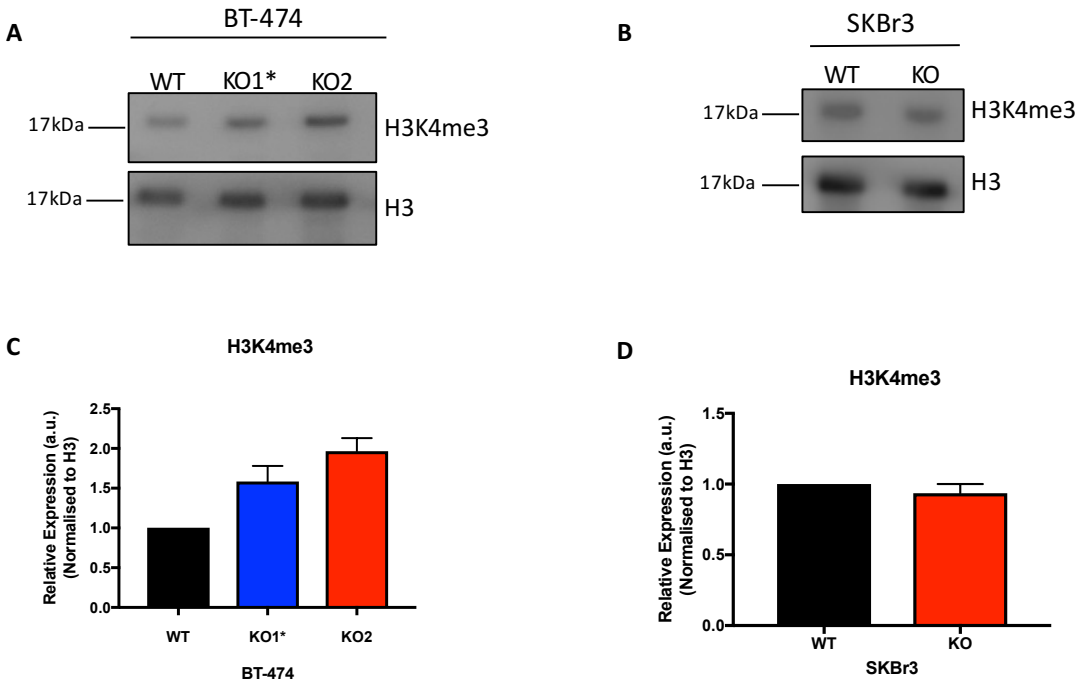

Figure 4.3: Global H3K4me3 expression in KDM5B KO cells. Acid extracted histone proteins from wildtype (WT) and KDM5B KO cells of A) BT-474 and B) SKBr3 cells, were subjected to western blot and probed with the H3K4me3 antibody. Histone H3 was used as a loading control. C) and D) Quantification of blots was done on imageJ software. Blots were normalised to histone H3 and thereafter to WT cells. Error bars indicate s.e.m of two independent experiments. Blots are representative of two independent experiments.

4.2.3 KDM5B transcriptionally represses CAV1 expression in SKBr3 cells

Since silencing of KDM5B activates CAV1 expression in MCF-7 breast cancer cells [146,156], CAV1 expression was examined in the BT-474 and SKBr3 KDM5B KO cells, to determine whether KDM5B regulates its expression in these cell lines. CAV1 was markedly upregulated upon KDM5B KO in SKBr3 cells (**Fig 4.4A**). Interestingly, KDM5B KO did not alter CAV1 expression in BT-474 cells (**Fig 4.4B**). This data demonstrates that KDM5B regulates CAV1 in a cell phenotype dependent manner since, BT-474 being an ER+/HER2+ cell line, has different signalling pathways in comparison to SKBr3, an ER-/HER2+ cell line.

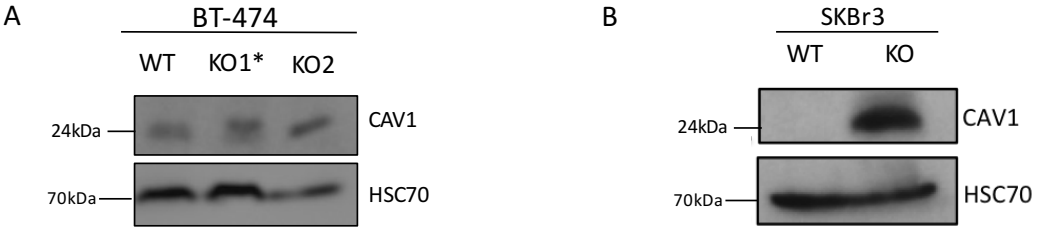

Fig 4.4: CAV1 expression upon KDM5B KO in SKBr3 and BT-474 cells. Whole cell lysates of A) BT-474 WT KO1* and KO2 cells and B) SKBr3 WT and KO cells were subjected to western blot and probed with CAV1 antibody. HSC70 was used as a loading control. Blots represent three independent experiments.

4.2.4 KDM5B and CAV1 expression in normal breast fibroblast and breast cancer-associated fibroblasts

Studies have shown that high CAV1 expression in breast cancer-associated fibroblasts (CAFs), is associated with good clinical outcome [239]. However, the mechanism of CAV1 downregulation in the stroma, is still poorly understood. Since KDM5B can repress CAV1 expression in some cell types (**Fig 4.4**), and this can be reflected as an inverse correlation between CAV1 and KDM5B expression, the level of expression in two strains of breast CAFs was examined. Levels of these proteins were compared to levels found in the cell line derived from a normal breast fibroblast. KDM5B expression in breast CAFs (LS11-045 and LS11-088) was downregulated in comparison to the normal breast fibroblast line (HMFU19). Conversely, CAV1 expression was upregulated in these breast CAFs in comparison to the normal breast fibroblast line (**Fig 4.5**). Clearly the levels of CAV1 in these two CAFs are high and so would predict a good clinical outcome. The inverse relationship between KDM5B and CAV1 allows for the interpretation that KDM5B

could be involved in downregulation of CAV1 expression in breast fibroblasts. Thus, inhibiting KDM5B in breast CAFs that have a low CAV1 expression, could potentially be beneficial in the clinic.

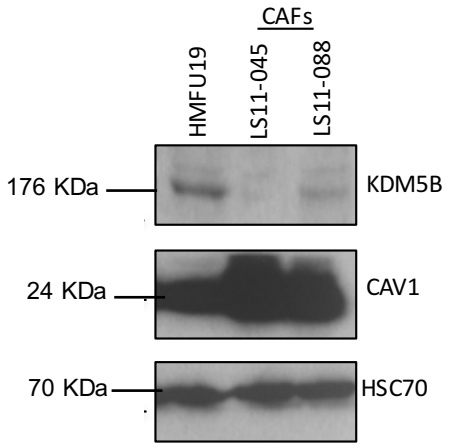

Figure 4.5: Expression of CAV1 and KDM5B in the normal breast fibroblast and breast cancer-associated fibroblasts. Whole cell lysates of the normal breast fibroblast line HMFU19 and breast CAFs were subjected to western blot and probed with KDM5B and CAV1 antibodies. HSC70 was used as a loading control. Blots are from one experiment.

4.2.5 Cellular distribution of KDM5B and CAV1 in the mouse mammary gland

At mid-pregnancy, data from our laboratory has shown that deletion of the demethylase activity of KDM5B, activates CAV1 expression (Steven Catchpole personal communication) and downregulates pSTAT5 [196] in the mouse mammary gland. Since KDM5B represses CAV1 expression by demethylating the H3K4me3 active mark found on the CAV1 promoter, it requires that KDM5B and CAV1 are expressed in the same cells. Therefore, to investigate the cellular distribution of these proteins, immunohistochemical staining was performed on the mid-pregnant (day 12.5) mammary glands of WT mice.

Serial sections were stained with antibodies to CAV1, KDM5B and smooth muscle actin (α-SMA), which was used to identify myoepithelial cells. **Fig 4.6A** shows strong KDM5B expression in the nuclei of luminal epithelial cells of alveoli, but a moderate and heterogeneous expression of the same, in the ducts (**Fig 4.6D**). KDM5B was also expressed in the myoepithelial and fat cells (**Fig 4.6A and D**). A strong CAV1 expression was observed in the myoepithelial and fat cells, but was completely absent in the luminal cells (**Fig 4.6G**). The adjacent serial sections show α-SMA staining in myoepithelial cells (**Fig 4.6B, E, H**). This data demonstrates that KDM5B could regulate CAV1 in myoepithelial and/or fat cells, in the mid-pregnant mammary gland. However, phosphorylation of STAT5 occurs in, and leads to proliferation of luminal cells and in their

subsequent production of milk at lactation. It follows therefore that signals from CAV1, which controls the JAK/STAT5 pathway, occurs in a paracrine fashion.

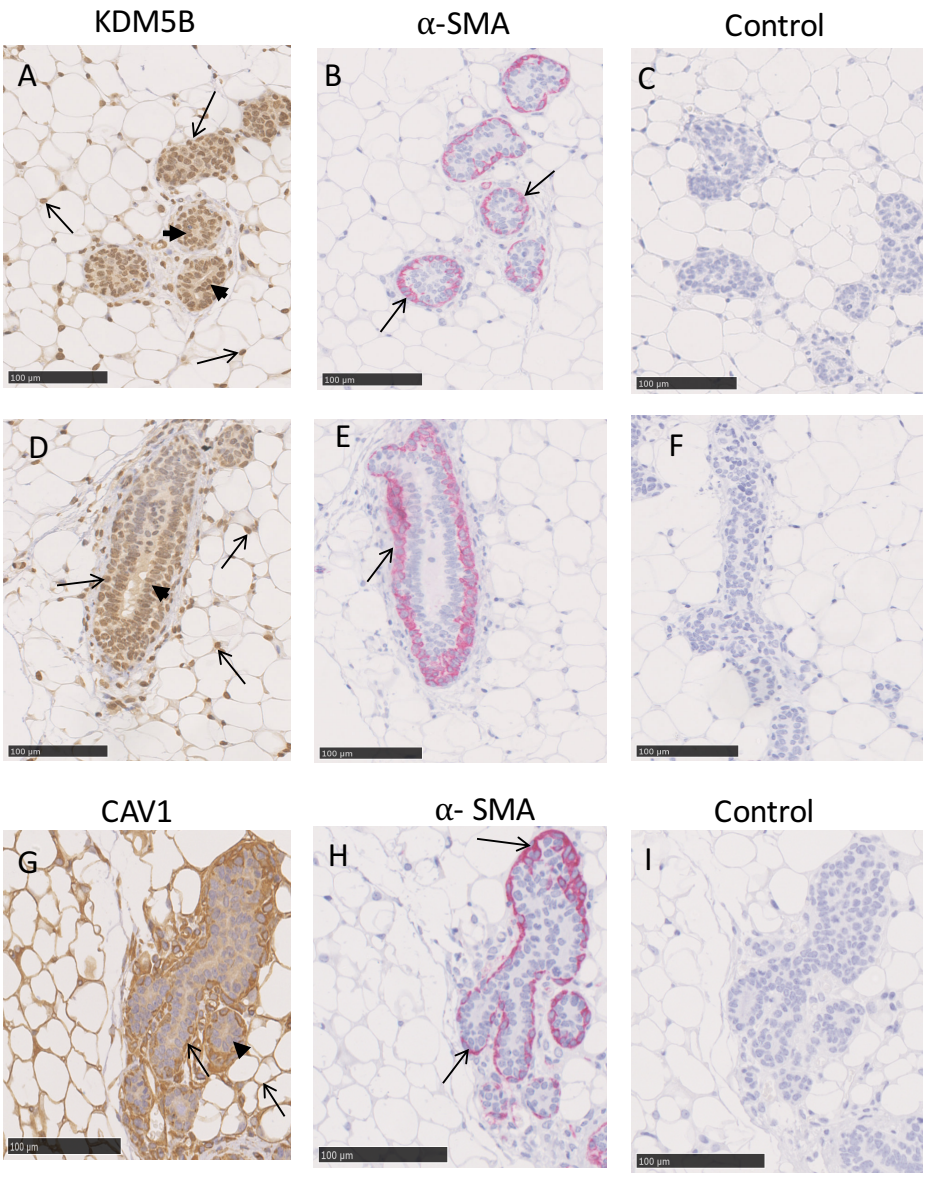

Figure 4.6: Cellular distribution of CAV1 and KDM5B in the mouse mammary gland at pregnancy day 12.5. (A-C) Consecutive sections showing staining of lobules. A) KDM5B expression in luminal (arrow heads), myoepithelial and fat cells (black arrows). B) α-SMA expression in myoepithelial cells (black arrow) and C) Secondary antibody control. **(D-F)** Consecutive sections showing staining of ducts. D) KDM5B expression in luminal (arrow heads), myoepithelial and fat cells (black arrows). E) α-SMA expression in myoepithelial cells (black arrow) and F) Secondary antibody control. **(G-I)** Consecutive sections showing G) CAV1 expression in myoepithelial and fat cells (black arrows) and lack of staining in luminal cells (arrow heads). H) α-SMA expression in myoepithelial cells (black arrow) and I) Secondary antibody control. Representative images taken from mammary glands of 2 mice.

4.3 Discussion

The aim of this chapter was to further understand KDM5B regulation of CAV1 in the normal and malignant mammary gland, by looking at their cellular distribution in the mid-pregnant mammary gland and their expression in different breast cancer cell types (i.e. epithelial and fibroblasts), respectively.

4.3.1 CAV1 expression in breast tumours

Studies on the expression of CAV1 and KDM5B in breast tumours using the METABRIC dataset revealed that, CAV1 gene expression is downregulated in HER2+ and luminal B breast cancer subtypes (**see Fig 4.1**). However, CAV1 mRNA expression in the METABRIC dataset was unexpectedly low in the basal-like subtype, which can also include triple negative breast cancers. However, it has previously been suggested that analysis using expression arrays such as METABRIC, should be interpreted with caution. This is because, samples constituting the normal-like subtype may have been derived from cell types expressing high CAV1 (adipocytes, fibroblasts and endothelial cells), and so may distort analysis [233]. Therefore, to precisely measure CAV1 mRNA, Elsheikh and colleagues, suggested the use of microdissection or *in situ* methods [233]. It was observed that expression of CAV1 in the luminal A subtype, was not as downregulated as in the other subtypes. This difference particularly between luminal A (ER+/HER2-) and, HER2+ (ER-/HER2+) and luminal B (ER+/HER2+ or ER+/HER2-) subtypes, may be attributed to HER2 expression, as CAV1 has been shown to negatively associate with HER2 [232].

Given that CAV1 is located in a region that is frequently deleted in many malignancies including breast cancer [295], it was investigated whether CAV1 gene deletion was the underlying mechanism driving CAV1 downregulation. CAV1 was significantly deleted in 186 out of 1903 (9.8%) breast tumours, suggesting that CAV1 expression is driven by copy number deletion in a fraction of breast cancers. Since the majority of breast cancers were diploid for CAV1 expression, it suggests that other factors such as epigenetics as discussed below, may be driving CAV1 expression in breast cancer.

4.3.2 CAV1 expression in breast cancer cell lines is subtype specific

CAV1 expression in breast cancer cell lines, appeared to be subtype specific. These differences in CAV1 expression between different breast cancer subtypes (high in TN and moderate to low in ER+ and HER2+ cells), has previously been explained to be due to methylation of CpG Islands (CGI) shores on the CAV1 promoter [237]. CGI shores are regions that flank CGI with less CG-density. The authors demonstrated that

hypermethylation of CAV1 CGI shores, is mostly observed in cell lines that have low CAV1 expression and is characteristic of some luminal breast cancer cell lines. Contrastingly, hypomethylation of CAV1 CGI shore is characteristic of the basal-like subtype and is hypothesized as contributing to the enhanced aggressiveness of some cancers in this subtype. To investigate whether the CGI and CGI shores chromatin environment influenced CAV1 gene expression, the authors performed chromatin immunoprecipitation sequencing (ChIP-seq) analysis of histone modifications in MCF-7 cells. Although the H3K4me2 active mark, a substrate of KDM5B was tested, only minimal enrichment at CGI shores was observed and so it was concluded that this mark was not sufficient to activate CAV1 expression. This is in agreement with the observation that CAV1 expression is controlled by the H3K4me3 mark and not H3K4me2 or H3Kme1 [146]. Thus, it is not known whether the H3K4me3 mark is enriched at these CGI shores thereby regulating CAV1 expression. If so, this may also implicate KDM5B at these regions, since KDM5B and H3K4me3 bind at the same regions [146,202].

4.3.3 KDM5B regulates CAV1 in SKBr3 cells

In breast tumours, there was a weak inverse correlation between CAV1 and KDM5B expression. However, in breast cancer cell lines, there was an indication that KDM5B may regulate CAV1, since cell lines with a high KDM5B expression, had a very low CAV1 expression. Indeed, I now find that KDM5B regulates CAV1 expression in SKBr3 cells, as demonstrated by its increased expression upon KDM5B KO. This is the first study to show that KDM5B can regulate CAV1 in a HER2+ breast cancer cell line, since previous studies have used the ER+ cell line, MCF-7 [146,156]. Although global H3K4me3 levels did not change in SKBr3 KO cells, the increased CAV1 expression implies increased H3K4me3 levels on the CAV1 promoter, due to the absence of KDM5B. Further work using ChIP-PCR assays should confirm this.

Surprisingly, CAV1 expression did not change in BT-474 KDM5B KO cells. BT-474 cells have a high KDM5B expression, and so its KO is expected to result in gene expression changes of target genes. Thus, the lack of a change in CAV1 expression in BT-474 cells, reflects the cell phenotype. Being an ER+/HER2+ cell line, BT-474 has both the ER and HER2 pathways active, and this allows for molecular cross-talk between the two pathways, which in turn influences gene expression amongst other cellular behaviours [296]. In contrast, in the ER-/HER2+ SKBr3 cell line, the HER2 signalling pathway may dominate and so knockout of KDM5B can result in more dramatic changes of target genes.

4.3.4 KDM5B may regulate CAV1 in normal and breast cancer-associated fibroblasts

In breast cancer-associated fibroblasts, CAV1 upregulation is often associated with good clinical outcome [239,242]. However, the underlying mechanism of CAV1 expression is not known. Similar to breast cancer epithelial cells, an inverse correlation between CAV1 and KDM5B expression was observed in the breast fibroblast and CAF lines. This suggests that CAV1 in breast cancer fibroblasts, may be epigenetically regulated by KDM5B. Therefore, targeting KDM5B in breast CAFS that have low CAV1 expression, could improve clinical outcome of patients. Given more time, I would have confirmed this hypothesis by gene editing of KDM5B in breast fibroblast lines.

4.3.5 KDM5B may regulate CAV1 in myoepithelial and/or fat cells in the mouse mammary gland

To elucidate the CAV1 and KDM5B axis in breast cancer, an understanding of their association in the normal mammary gland needs to be examined. A mouse model lacking KDM5B demethylase activity, showed upregulation of CAV1 in the mammary gland during mid-pregnancy (Steven Catchpole personal communication). Investigations into the cellular distribution of CAV1 and KDM5B in the mouse mammary gland, revealed expression of both proteins in fat and myoepithelial cells at mid pregnancy. This suggests that KDM5B regulates CAV1 through its demethylase activity, in one or both of these cell types. The fact that CAV1 is not expressed in the luminal epithelial cells is in agreement with previous data [220], and coincides with the notion that CAV1 may be regulating signalling pathways in mammary epithelial cells through the stroma, in a paracrine fashion. Indeed, observations in our laboratory show that phosphorylation of STAT5, which is inhibited by CAV1 [231], is expressed in the luminal epithelial cells [196], which are involved in alveologenesis and lactation. Therefore, during mid-pregnancy KDM5B may be downregulating CAV1 expression in the fat and/or myoepithelial cells, which in turn results in activation of the STAT5a signalling pathway, in luminal cells. The importance of this pathway has been demonstrated by accelerated mammary gland development and premature lactation during pregnancy, as a result of CAV1 knockout [231].

4.3.6 Conclusion

In conclusion, the data presented here suggests that, downregulation of CAV1 in breast cancer cell lines can be mediated by KDM5B in a cell phenotype dependent manner. It is also possible that this regulation is extended to normal fibroblast and breast cancer-

associated fibroblasts. Furthermore, during normal mammary gland development as demonstrated in the mouse, KDM5B could regulate CAV1 in the myoepithelial and fat cells. Thus, the regulation of CAV1 by KDM5B seems to span across different cell types, in the normal and malignant mammary gland. Elucidating this molecular axis may enable us to understand the opposite roles of CAV1 in different breast cancer phenotypes and may in turn, lead to development of novel therapies.

5 : Molecular Effects of KDM5B KO in HER2+ Breast Cancer Cells

5.1 Introduction

Previous studies looking at KDM5B-induced gene expression changes in ER+ or triple negative breast cancer cell lines, have used knockdown (KD) cells for their analysis [146,156,159,202]. These functional studies which aimed to identify KDM5B target genes in breast cancer cells, have shown that KDM5B regulates genes involved in various processes such as proliferation, mitotic cell cycle and immune response [146,156,159]. Some of KDM5B target genes identified in the ER+ breast cancer cell line MCF-7, include *BRCA1, CAV1* and *HOXA5* [146,156]. These studies have shown that KDM5B regulates these target genes, through its demethylase activity. Furthermore, global gene expression analysis of KDM5B knockdown in luminal and basal-like breast cancer cells, resulted in specific gene expression changes associated with the luminal lineage showing that KDM5B can drive specific lineage-associated gene expression patterns [202]. To date, global gene expression changes induced by KDM5B in HER2+ breast cancer cells, has not yet been reported.

5.1.1 Aims

KDM5B was first identified as a gene that was downregulated upon inhibition of HER2 signalling [183]. This suggests that KDM5B is positively regulated by HER2 signalling and may therefore be involved in HER2 tumorigenesis in the breast. It is therefore hypothesized that, loss of KDM5B function in HER2+ breast cancer cells will result in global gene expression changes. These gene expression changes may in turn lead to inhibition of hallmarks of cancer such as, uncontrolled cell growth.

In **Chapter 4**, it was shown that KDM5B regulates its target gene *CAV1*, in the HER2+ breast cancer cell line SKBr3, but not in BT-474 cells. This demonstrates that KDM5B may regulate target genes in a cell phenotype dependent manner, even within HER2+ cell lines, possibly by forming different biological complexes. This chapter aimed to 1) identify KDM5B target genes in HER2+ breast cancer cells and 2) determine whether HER2+ breast cancer cell lines have common genes regulated by KDM5B. These aims were investigated by:

1) Performing transcriptomic analysis on SKBr3 WT and KDM5B KO cells
2) Validating expression array analysis in selected KDM5B target genes by RT-qPCR
3) Examining expression of selected target genes in BT-474 WT and KDM5B KO cells by RT-qPCR
4) Performing gene ontology analysis in SKBr3 KDM5B KO cells to identify enriched biological processes of differentially expressed genes

5.2 Results

5.2.1 Genome wide expression profiling of KDM5B KO cells by microarray analysis

5.2.1.1 KDM5B-induced gene expression changes in SKBr3 cells

Whole genome expression profile was assessed in one biological repeat of SKBr3 parental and KDM5B KO cells, using the Illumina Human HT-12 v4 Expression BeadChip array, as described in **Chapter 2**. Comparison of SKBr3 parental and KDM5B KO cells, identified 99 upregulated genes and 105 downregulated genes, that showed expression differences of 1.5-fold or greater (**Fig 5.1**) in the KO cells. These findings show that *KDM5B* is involved in both gene activation and repression, in SKBr3 cells. Importantly, these differentially expressed genes are constitutive changes, since KDM5B is constitutively knocked out in the SKBR3 KO cell line.

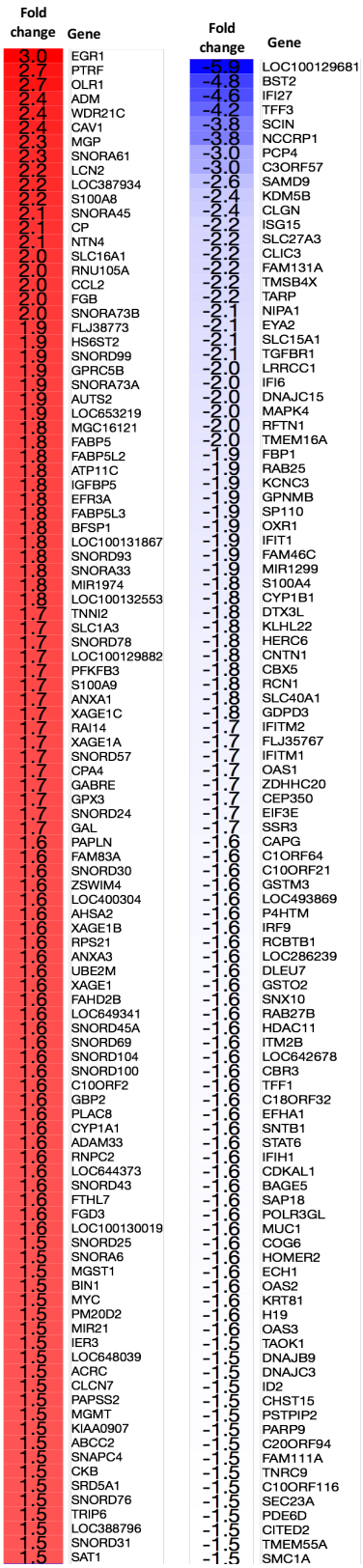

Fold change	Gene
3.0	EGR1
2.7	PTRF
2.7	OLR1
2.4	ADM
2.4	WDR21C
2.4	CAV1
2.3	MGP
2.3	SNORA61
2.2	LCN2
2.2	LOC387934
2.2	S100A8
2.1	SNORA45
2.1	CP
2.1	NTN4
2.0	SLC16A1
2.0	RNU105A
2.0	CCL2
2.0	FGB
2.0	SNORA73B
1.9	FLJ38773
1.9	HS6ST2
1.9	SNORD99
1.9	GPRC5B
1.9	SNORA73A
1.9	AUTS2
1.9	LOC653219
1.8	MGC16121
1.8	FABP5
1.8	FABP5L2
1.8	ATP11C
1.8	IGFBP5
1.8	EFR3A
1.8	FABP5L3
1.8	BFSP1
1.8	LOC100131867
1.8	SNORD93
1.8	SNORA33
1.8	MIR1974
1.8	LOC100132553
1.7	TNNI2
1.7	SLC1A3
1.7	SNORD78
1.7	LOC100129882
1.7	PFKFB3
1.7	S100A9
1.7	ANXA1
1.7	XAGE1C
1.7	RAI14
1.7	XAGE1A
1.7	SNORD57
1.7	CPA4
1.7	GABRE
1.7	GPX3
1.7	SNORD24
1.7	GAL
1.6	PAPLN
1.6	FAM83A
1.6	SNORD30
1.6	ZSWIM4
1.6	LOC400304
1.6	AHSA2
1.6	XAGE1B
1.6	RPS21
1.6	ANXA3
1.6	UBE2M
1.6	XAGE1
1.6	FAHD2B
1.6	LOC649341
1.6	SNORD45A
1.6	SNORD69
1.6	SNORD104
1.6	SNORD100
1.6	C10ORF2
1.6	GBP2
1.6	PLAC8
1.6	CYP1A1
1.6	ADAM33
1.6	RNPC2
1.6	LOC644373
1.6	SNORD43
1.6	FTHL7
1.6	FGD3
1.6	LOC100130019
1.5	SNORD25
1.5	SNORA6
1.5	MGST1
1.5	BIN1
1.5	MYC
1.5	PM20D2
1.5	MIR21
1.5	IER3
1.5	LOC648039
1.5	ACRC
1.5	CLCN7
1.5	PAPSS2
1.5	MGMT
1.5	KIAA0907
1.5	ABCC2
1.5	SNAPC4
1.5	CKB
1.5	SRD5A1
1.5	SNORD76
1.5	TRIP6
1.5	LOC388796
1.5	SNORD31
1.5	SAT1

Fold change	Gene
-5.9	LOC100129681
-4.8	BST2
-4.6	IFI27
-4.2	TFF3
-3.8	SCIN
-3.8	NCCRP1
-3.0	PCP4
-3.0	C3ORF57
-2.6	SAMD9
-2.4	KDM5B
-2.4	CLGN
-2.2	ISG15
-2.2	SLC27A3
-2.2	CLIC3
-2.2	FAM131A
-2.2	TMSB4X
-2.2	TARP
-2.1	NIPA1
-2.1	EYA2
-2.1	SLC15A1
-2.1	TGFBR1
-2.0	LRRCC1
-2.0	IFI6
-2.0	DNAJC15
-2.0	MAPK4
-2.0	RFTN1
-2.0	TMEM16A
-1.9	FBP1
-1.9	RAB25
-1.9	KCNC3
-1.9	GPNMB
-1.9	SP110
-1.9	OXR1
-1.9	IFIT1
-1.9	FAM46C
-1.9	MIR1299
-1.8	S100A4
-1.8	CYP1B1
-1.8	DTX3L
-1.8	KLHL22
-1.8	HERC6
-1.8	CNTN1
-1.8	CBX5
-1.8	RCN1
-1.8	SLC40A1
-1.8	GDPD3
-1.7	IFITM2
-1.7	FLJ35767
-1.7	IFITM1
-1.7	OAS1
-1.7	ZDHHC20
-1.7	CEP350
-1.7	EIF3E
-1.7	SSR3
-1.6	CAPG
-1.6	C1ORF64
-1.6	C10ORF21
-1.6	GSTM3
-1.6	LOC493869
-1.6	P4HTM
-1.6	IRF9
-1.6	RCBTB1
-1.6	LOC286239
-1.6	DLEU7
-1.6	GSTO2
-1.6	SNX10
-1.6	RAB27B
-1.6	HDAC11
-1.6	ITM2B
-1.6	LOC642678
-1.6	CBR3
-1.6	TFF1
-1.6	C18ORF32
-1.6	EFHA1
-1.6	SNTB1
-1.6	STAT6
-1.6	IFIH1
-1.6	CDKAL1
-1.6	BAGE5
-1.6	SAP18
-1.6	POLR3GL
-1.6	MUC1
-1.6	COG6
-1.6	HOMER2
-1.6	ECH1
-1.6	OAS2
-1.6	KRT81
-1.6	H19
-1.6	OAS3
-1.5	TAOK1
-1.5	DNAJB9
-1.5	DNAJC3
-1.5	ID2
-1.5	CHST15
-1.5	PSTPIP2
-1.5	PARP9
-1.5	C20ORF94
-1.5	FAM111A
-1.5	TNRC9
-1.5	C10ORF116
-1.5	SEC23A
-1.5	PDE6D
-1.5	CITED2
-1.5	TMEM55A
-1.5	SMC1A

Figure 5.1: Differentially expressed genes upon KDM5B KO in SKBr3 cells. Differentially expressed genes with their respective fold changes (only fold changes ≥1.5 or ≥-1.5 are shown). Comparison of SKBr3 WT cells with KDM5B KO cells (n=1 per group) identified 99 upregulated genes (red) and 105 downregulated genes (blue). Data analysis was performed in Partek Genomics Suite software using a 2-way ANOVA model.

5.2.1.2 RT-qPCR validation of microarray analysis

To confirm the microarray analysis, RT-qPCR was performed on three upregulated genes, *EGR1* (fold change = 3), *FOS* (fold change = 1.27) and *MYC* (fold change = 1.5) and one downregulated gene, *SLC40A1* (fold change = -1.8). Early response gene 1 *(EGR1)* was selected as it was the top upregulated gene, and has previously been shown to be a KDM5B target gene in mouse embryonic stem cells (mESCs) [190]. *FOS* was selected since it is also an early response gene and is co-regulated with EGR1 [297], although its fold change was below 1.5. *MYC* was selected as it has previously been shown to exist in a transcriptional repressor complex with KDM5B [298]. Solute carrier family 40 member 1 *(SLC40A1)* was one of the downregulated genes chosen to confirm results.

Total RNA was isolated from cells and processed as described in **Chapter 2**. RT-qPCR analysis of the genes confirmed upregulation of *EGR1, FOS and MYC* (**Fig 5.2A, B, C**) however, due to large variations between experiments, particularly in the two early response genes (*EGR1 and FOS*), the upregulation was not statistically significant (**Fig 5.2A, B**). *SLC40A1* showed a trend towards downregulation by RT-qPCR (**Fig 5.2D**). KDM5B KO was confirmed in the KO cells (**Fig 5.2E**).

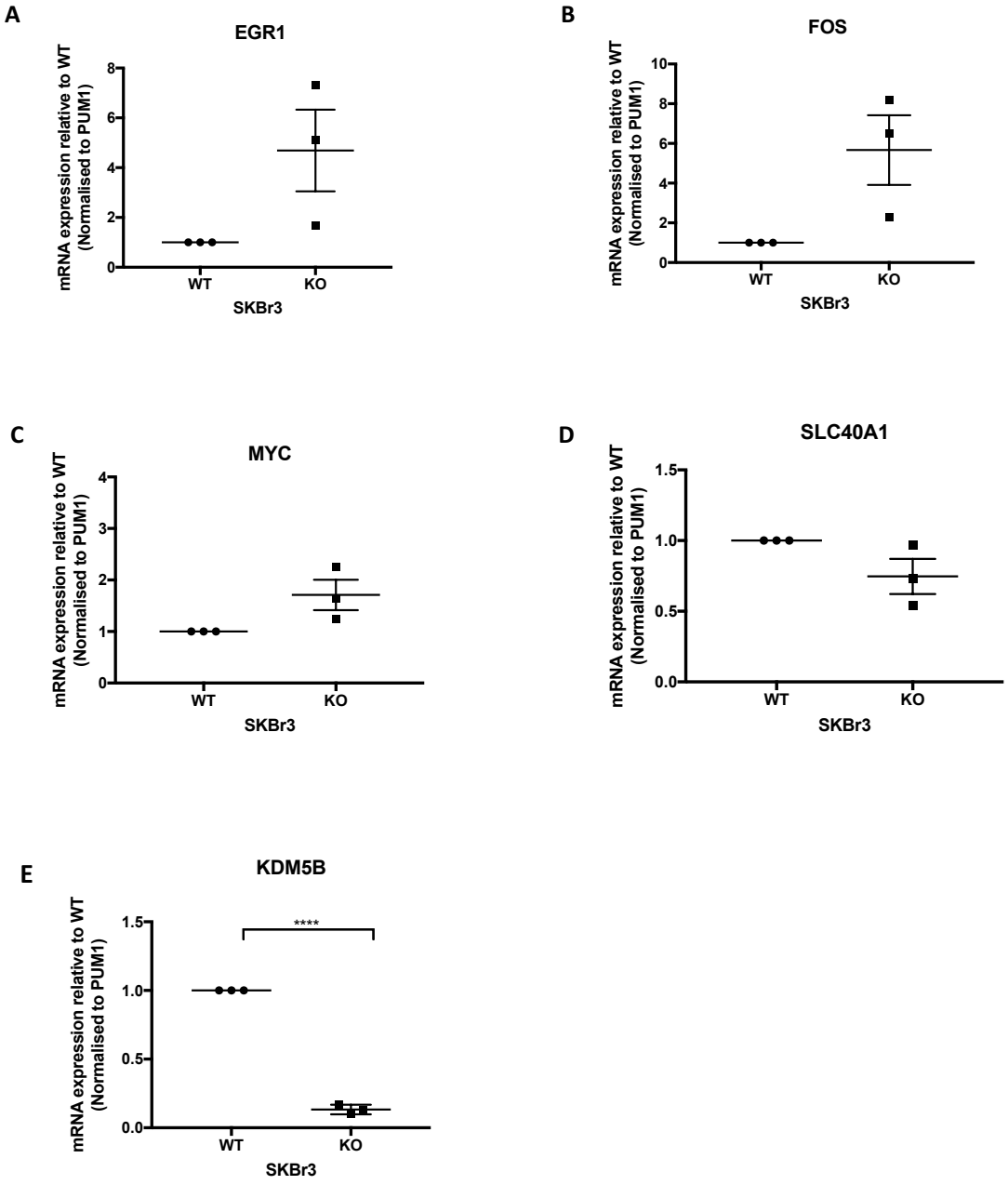

Figure 5.2: RT-qPCR validation of microarray analysis. RNA extracted from SKBr3 WT and KO cells was reverse transcribed, and A) *EGR1*, B) *FOS*, C) *MYC*, D) *SLC40A1* and E) *KDM5B* genes examined using Qiagen Quantitect primers. Samples were run in triplicate in each experiment. Data represents three independent experiments. Errors bars denote standard error of the mean (s.e.m). Asterisks show significance where ****= $p \leq 0.0001$. Statistical significance was calculated using unpaired Student's *t*-test.

5.2.1.3 Expression of selected microarray genes in BT-474 cells

To determine whether the genes selected above (i.e. *EGR1, FOS, MYC* and *SLC40A1*) are regulated by KDM5B in another HER2+ cell line, their expression in BT-474 WT and KDM5B KO cells was examined by RT-qPCR.

EGR1, FOS and *MYC* expression were upregulated in the BT-474 KO2 cells, in comparison to WT cells (**Fig 5.3A, B, C**), with *EGR1* and *MYC* showing statistical significance. However, due to large variations between experiments, the increased expression in *FOS* was not statistically significant, although a clear trend can be observed. These genes were however not upregulated in the BT-474 KO1* cells, in comparison to WT cells (**Fig 5.3A, B, C**). Comparison of SKBr3 KO and BT-474 KO2 cells, suggest that KDM5B can be a transcriptional repressor of *EGR1, FOS* and *MYC,* in these two phenotypically different cell types.

SLC40A1 was downregulated in both BT-474 KO cells in comparison to WT cells however, downregulation was only significant in the BT-474 KO1* cells (**Fig 5.3D**). This data suggests that KDM5B can be a transcriptional activator of *SLC40A1* in BT-474 and SKBr3 cells. KDM5B KO was confirmed in the BT-474 KO cell lines (**Fig 5.3E**).

The differences observed between BT-474 KO1* and KO2 are likely to be due to the higher *KDM5B* mRNA expression in the former. For genes where *KDM5B* appears to be acting as an activator (i.e. they are downregulated in the knockouts), the influence of the low level of *KDM5B* mRNA still present in the BT-474 KO1* cells, could be expanded through indirect activation or repression of other factors influencing *SLC40A1* expression. However, it cannot be ruled out that these differences may also be attributed to a clonal effect. Taken together, these data suggest that KDM5B can regulate *EGR1, FOS, MYC* and *SLC40A1* in BT-474 and SKBr3 cells. However, further validation using additional clones in both cell lines is required.

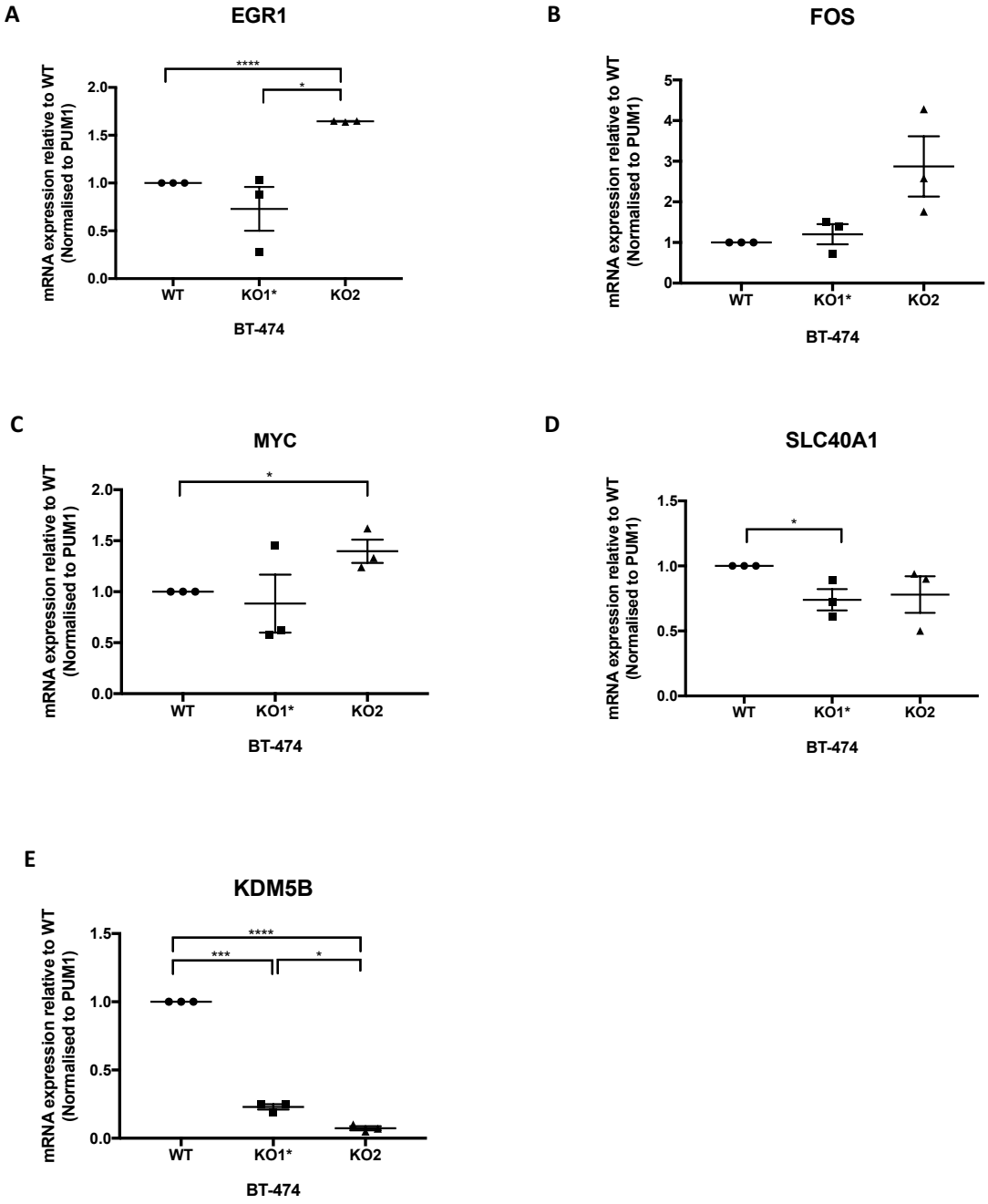

Figure 5.3: Expression of selected microarray genes in BT-474 cells. RNA extracted from BT-474 WT, KO1* and KO2 cells was reverse transcribed and A) *EGR1*, B) *FOS*, C) *MYC*, D) *SLC40A1* and E) K*DM5B* genes examined, using Qiagen Quantitect primers. Samples were run in triplicate in each experiment. Data represents three independent experiments. Errors bars denote standard error of the mean (s.e.m). Only significant differences are shown. Asterisks show significance where *= $p \leq 0.05$, ***= $p \leq 0.001$, ****= $p \leq 0.0001$. Statistical significance was calculated using unpaired Student's *t*-test.

5.2.2 Cell culture methods can affect expression of early response genes

EGR1 and *FOS* are early response genes that are normally expressed in response to stress stimuli [299]. Since large variations were observed particularly in *EGR1* and/or *FOS* expression in SKBr3 KO and BT-474 KO2 cells, it suggested that cell culture methods could be affecting their expression. Indeed, a previous study by Yang and colleagues, found that *EGR1* expression was rapidly induced when cells were rinsed with PBS or media, prior to cell lysis [300]. Upon closer observation of *EGR1* expression from two independent RT-qPCR experiments of BT-474 WT cells for example, it was noticed that the cycle threshold (Ct) values differed (i.e. 19.3 and 24.2 in experiment 1 and experiment 2 respectively). Ct values are inversely correlated to the amount of RNA in the sample. Lower Ct values indicate high amounts of targeted gene, whereas higher Ct values indicate low amounts of targeted gene. It was thus hypothesized that these differences in Ct values, may be attributed to the method of cell lysis used for RNA preparation. This is because in experiment 1, cell lysis was performed on a cell pellet after trypsinisation, whereas in experiment 2, cells were directly lysed on the plate by scraping. Therefore, these two methods of cell lysis (trypsin and scraping), were re-examined in BT-474 WT cells, to validate the initial observations. **Figure 5.4** shows the Ct values of *EGR1* and the control gene *PUM1* in the two experiments.

EGR1 was detected at lower cycles in the trypsinised samples (**Fig 5.4**). Contrastingly, in the scraped samples, *EGR1* expression was detected at higher cycles (**Fig 5.4**). Thus, demonstrating induction of *EGR1* expression when cells are trypsinised. Expression of the housekeeping gene *PUM1* was detected at relatively similar cycles in both the trypsinised and scraped samples (**Fig 5.4**). This suggests that, trypsinising cells prior to lysis, can induce expression of early response genes such as *EGR1*. Therefore, care should be taken in manipulating cells when working with early response genes. The microarray and RT-qPCR data shown in **Figures 5.1, 5.2 and 5.3,** were performed on samples that were lysed using the cell scraping method. Thus, the reported gene expression data are constitutive changes, and not a response to stress stimuli.

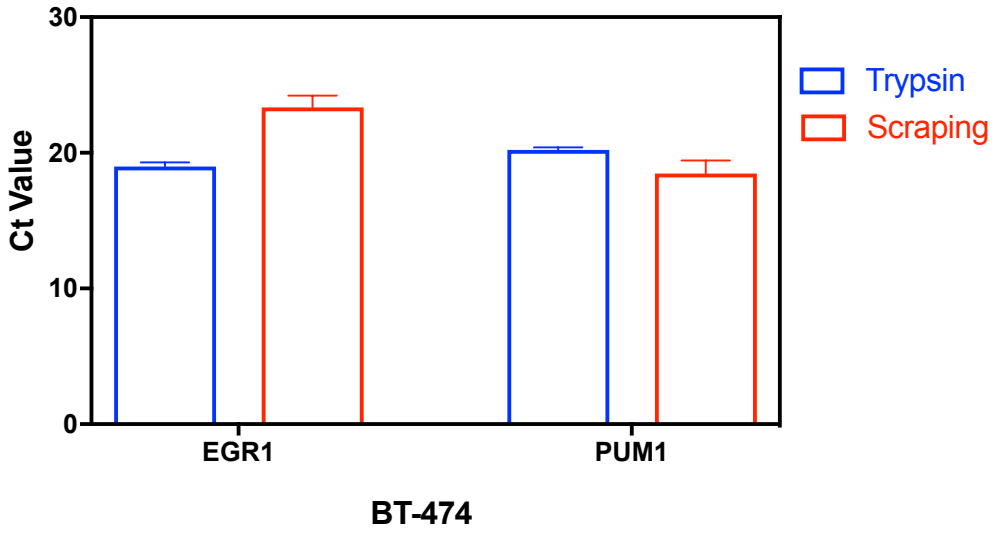

Figure 5.4: Cell culture methods can affect expression of early response genes. Comparison of two cell lysis methods (trypsin or scraping) on *EGR1* expression in BT-474 WT cells. Graph shows detection of *EGR1* in lower cycle numbers in trypsinised samples, in comparison to scraped samples. In contrast, *PUM1* was detected at similar cycle numbers in trypsinised and scraped samples. Data represents two independent experiments. Errors bars denote standard error of the mean (s.e.m).

5.2.3 Gene ontology of differentially expressed genes in SKBr3 KDM5B KO cells

Further analysis on the differentially expressed genes (**Fig 5.1**) was performed using the ToppGene Suite tool to identify enriched biological processes. Interestingly, gene ontology showed that upregulated genes were enriched for the biological process 'response to drug' (**Fig 5.5**). Closer examination of the 12 genes identified in this group, revealed that 5 of the genes i.e. ATP binding cassette (ABC) transporter (*ABCC2*), Annexin A1 (*ANXA1*), *CAV1*, *MYC* and Lipocalin 2 (*LCN2*), promote resistance to Herceptin or Lapatinib [240,301–303].

The downregulated genes in the SKBr3 KDM5B KO cells were enriched for various biological processes including mammary gland epithelial cell proliferation (**Fig 5.6**). These genes included inhibitor of differentiation 2 (*ID2*) and *STAT6*, which belong to the transforming growth factor-beta (TGFβ) and JAK/STAT pathways respectively. A full list of biological processes enriched in differentially expressed genes in SKBr3 KO cells is shown in **Appendix Tables 8.1 and 8.2**.

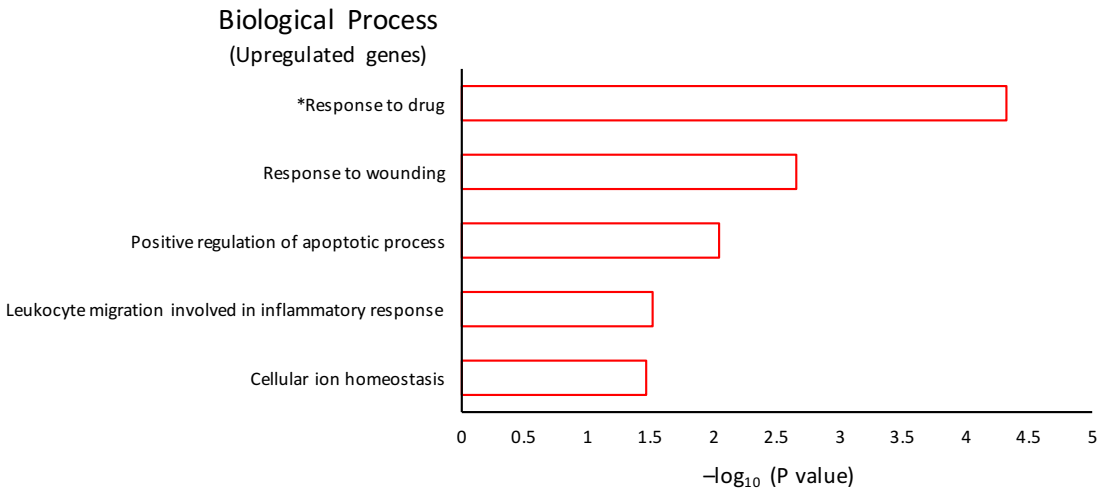

Fig 5.5: Gene ontology of upregulated genes in SKBr3 KDM5B KO cells. Representative enriched biological processes in upregulated genes upon KDM5B KO in SKBr3 cells, as reported by ToppGene. P-values are log transformed ($-\log_{10}(p\ value)$) and were corrected by the Benjamini-Hochberg (B&H) false discovery rate (FDR) method.

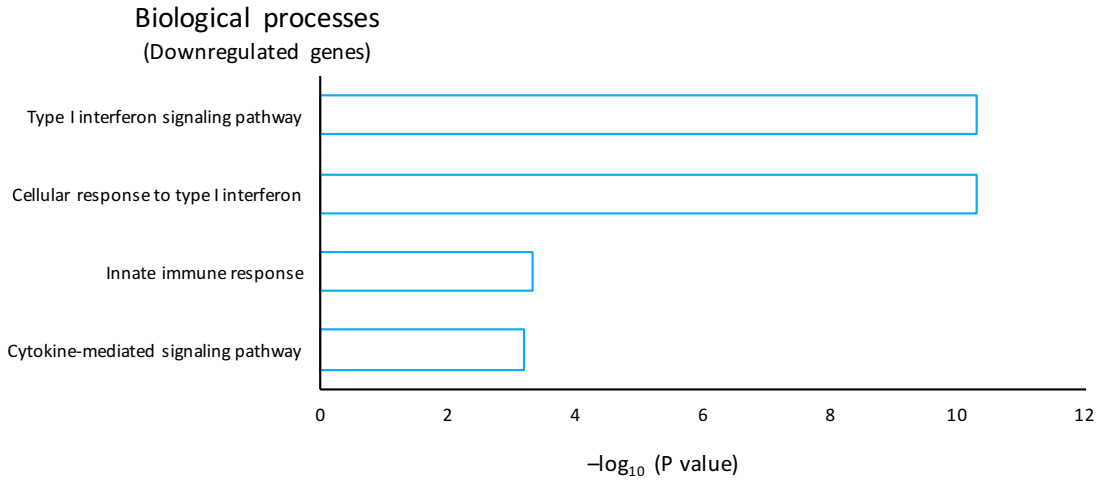

Figure 5.6: Gene ontology of downregulated genes in SKBr3 KDM5B KO cells. Representative enriched biological processes in upregulated genes upon KDM5B KO in SKBr3 cells, as reported by ToppGene. P-values are log transformed ($-\log_{10}(p\ value)$) and were corrected by the Benjamini-Hochberg (B&H) false discovery rate (FDR) method.

5.3 DISCUSSION

Since its discovery, studies have shown that KDM5B is a transcriptional regulator that is overexpressed in breast cancers. To further understand its function in this disease, different studies have aimed to identify genes that are regulated by KDM5B. Identification of KDM5B target genes and their specific roles, has enabled identification of biological processes involving this enzyme. To date, KDM5B target genes have been identified in either ER+ or triple negative breast cancer cell lines [146,156,159,202]. These studies have mainly used RNAi to silence KDM5B expression and subsequently study its function. This is the first study to my knowledge, to use KDM5B KO cells to identify KDM5B target genes on a whole genome level, in the SKBr3 HER2+ breast cancer cells.

5.3.1 KDM5B-induced gene expression changes in SKBr3 and BT-474 HER2+ breast cancer cells

A total of 204 genes were differentially expressed upon KDM5B KO (99 upregulated and 105 downregulated genes) in the SKBr3 HER2+ cells. From the selected genes used to validate the microarray, *EGR1, FOS, and MYC* have previously been associated with KDM5B in different cell types [146,156,190,195,298]. Furthermore, assessment of these genes in BT-474 KO cells, revealed a similar expression pattern to SKBr3 KO cells for BT-474 KO2 cells, but not BT-474 KO1* cells. The difference between the two BT-474 KO cells supports the interpretation that the BT-474 KO1* cells are not a complete KO, retaining expression of a low amount of *KDM5B* mRNA.

EGR1 is an early response gene encoding for a zinc finger transcription factor, and is expressed in response to various stimuli [297]. *EGR1* is transcriptionally repressed by *KDM5B* through its demethylase activity, in mESCs [190]. The authors demonstrated that by overexpressing KDM5B or silencing by siRNA, KDM5B directly inhibits EGR1 expression. They showed that binding of KDM5B led to decreased levels of H3K4me3 at the EGR1 promoter, thereby decreasing EGR1 expression. Furthermore, of the three cell lineage markers examined (*EGR1, p27 and BMI1*), *EGR1* was the only gene found to be affected by inhibition of KDM5B, emphasising a crucial role for KDM5B in downregulating this gene [190].

In breast cancer, expression of EGR1 is decreased at the RNA and protein levels compared to normal mammary epithelial cells, as well as, in breast tumours [304,305]. Overexpression of EGR1 suppresses breast cancer cell proliferation, by arresting cell cycle progression at the G0/G1 phase [304]. The data reported in this chapter indicates that KDM5B normally represses EGR1 expression in SKBr3 cells, and so contributes to their proliferation (**See Chapter 6**).

FOS is an immediate early response gene and is co-regulated with *EGR1* during growth and differentiation [297]. FOS is part of the activator protein 1 (AP-1) complex and acts as a transcription factor. Knockout of KDM5b in mouse mammary epithelial cells (MECs), showed that fos expression did not change in comparison to wildtype MECs [195]. This suggests that the function of KDM5B in regulating FOS may differ in normal and tumour cells, since *FOS* was upregulated upon KDM5B KO in BT-474 and SKBr3 breast cancer cells. Furthermore, regulation of FOS by KDM5B in human and mouse mammary cells may also differ.

MYC is a protooncogene involved in many signal transduction pathways that promote cell growth, cell cycle and adhesion [306]. Not surprisingly, abnormal expression of MYC is often observed in cancers, including breast cancer [307]. Using the MCF-7 breast cancer cell line, MYC was found to exist in a complex with KDM5B and the transcription factor AP-2 gamma (TFAP2C) [298]. This KDM5B-MYC-TFAP2C complex was shown to repress the cell cycle inhibitor p21, and it was proposed that this complex might promote cell cycle progression in breast cancer. In glioblastoma cells, MYC expression was found to correlate with H3K4me3 abundance on its locus, suggesting epigenetic regulation of MYC [308]. An RT-PCR screen showed a moderate association between KDM5B and H3K4me3 expression on the Myc locus. Thus, the upregulation of *MYC* observed here in SKBr3 KO and BT-474 KO2 cells, suggests that KDM5B could regulate MYC expression via its demethylase activity.

An association of KDM5B with SLC40A1 has not yet been documented. SLC40A1 (Ferroportin) is an iron exporter that is decreased in some breast cancer cells and tissues [309,310]. Since *SLC40A1* was downregulated in KDM5B KO cells, it implies that it is normally upregulated in BT-474 and SKBr3 cells. The expression of *SLC40A1* still needs validating, as the RT-qPCR only showed a slight trend in reduction in BT-474 and SKBr3 KO cells.

5.3.2 KDM5B normally represses genes associated with Herceptin or Lapatinib resistance in SKBr3 cells

Knock out of KDM5B in SKBr3 cells resulted in upregulation of *CAV1, ABCC2, ANXA1, LCN2 and MYC*, all of which have been implicated in Herceptin or Lapatinib resistance. This suggests that KDM5B normally represses these genes and so knocking out KDM5B in SKBr3 cells, may not be a good therapeutic target in these cells since expression of these genes upon loss of KDM5B function may not enhance sensitivity to HER2 targeted therapies (**see Chapter 6**).

CAV1 was recently identified as a gene that promotes Herceptin resistance [240]. Sekhaar and colleagues, had previously shown that CAV1 contributes to Herceptin resistance by mediating endocytosis of HER2[241]. The authors proposed that endocytosis of HER2 contributed to Herceptin resistance by attenuating antibody dependent cellular cytotoxicity (ADCC). Increased ABCC2 expression promotes resistance of gastric cancer cells to Trastuzumab emtansine (TDM1), since its inhibition sensitized cells to TDM1 and reduced cell viability [301]. LCN2, a chaperone protein, was identified as a gene upregulated in the Herceptin resistant cell line HCC1954, and so is associated with Herceptin resistance [240]. Upregulation of ANXA1 was found to confer resistance to Herceptin in HER2+ breast cancer cells as well as, HER2+ breast cancer patients who had received adjuvant Herceptin-based therapy [303]. Thus, ANXA1 was identified as a predictive marker of Herceptin treatment response.

MYC has previously been implicated in Lapatinib resistance since activation of the FOXO/c-Myc axis via the MLL2 protein, reduced sensitivity to Lapatinib[302]. Indeed, inhibition of this axis using an inhibitor to the chromatin associating protein BRD4, re-sensitized cells to Lapatinib[302].

5.3.3 KDM5B normally activates genes associated with the TGFβ and JAK/STAT pathways in SKBr3 cells

The JAK/STAT and TGFβ pathways consists of diverse proteins that regulate cell proliferation and differentiation. Constitutive activation of these pathways is correlated with tumour development and/or progression including breast cancer. Downregulation of *STAT6* and *ID2* which belong to the JAK/STAT and TGFβ pathways, respectively, in SKBr3 KO cells, suggests that KDM5B normally activates their expression. This corresponds to data showing decreased TGFβ pathway activity in siKDM5B basal-like breast cancer cells [202]. Therefore, downregulation of members of the JAK/STAT and TGFβ could result in reduced proliferation of SKBr3 cells (**See Chapter 6**). Contrastingly however, KDM5B knockdown in luminal breast cancer cells, led to upregulation of genes associated with the TGFβ pathway [202]. These findings show the importance of cell phenotype on KDM5B function.

5.3.4 Conclusion

Global gene expression profiling in SKBr3 parental and KDM5B KO cells has revealed that, KDM5B may contribute to proliferation of SKBr3 cells. It is possible that these functions of KDM5B extends to BT-474 cells, since at least *EGR1, FOS* and *MYC* were

also upregulated upon KDM5B KO in this cell line. Thus, the effect of KDM5B KO in proliferation in BT-474 and SKBr3 cells, was examined (**see Chapter 6**). Furthermore, KDM5B may mediate proliferation of SKBr3 cells through activation of the JAK/STAT and TGFβ pathways however, the underlying mechanisms need to be experimentally determined. Additionally, knocking out KDM5B in SKBr3 revealed that KDM5B normally represses genes implicated in Herceptin or Lapatinib resistance and so suggests that this loss of KDM5B function may not increase sensitivity to HER2 targeted therapies in SKBr3 cells (**see chapter 6**).

In order to understand whether KDM5B regulates similar genes in HER2+ breast cancer cells, genome wide expression analysis needs to be performed in WT and KDM5B KO of BT-474 and other HER2+ breast cancer cell lines. Additionally, it would be important to determine whether KDM5B regulates its target genes via its demethylase activity. Such information will enable us to determine whether the demethylase activity is the prominent mechanism through which KDM5B downregulates gene expression. This information will have bearing on the use of KDM5B small molecule inhibitors in the clinic, since these inhibitors target the demethylase domain.

6 : Phenotypic Effects of KDM5B KO in HER2+ Breast Cancer Cells

6.1 Introduction

The KDM5 family of histone demethylases have increasingly gained the spotlight as novel targets for anti-cancer therapy. Their attractiveness comes from studies showing their genetic amplification, aberrant expression, promotion of tumour growth and of drug resistance in various cancers. Since the KDM5 proteins are well characterised for their H3K4me3 demethylase activity, there are currently major efforts aimed at developing small molecules which inhibit their enzymatic activity for application to cancer therapy. These inhibitors can also be used to study the biological function of this activity. Identifying whether these proteins are involved in drug resistance could lead to the development of novel therapeutic strategies.

6.1.1 Role of KDM5B in promoting cell proliferation of cancers

Studies have shown that KDM5B promotes proliferation of various cancers, since its downregulation can lead to reduced cell growth. For example, silencing of KDM5B has been shown to reduce cell growth of bladder and lung cancer cell lines [208]. The authors proposed that KDM5B silencing may be inducing apoptosis of bladder and lung cancer cells, since most of the cells were in the sub-G1 phase. Further analysis using microarray expression data, showed that KDM5B could be regulating cell cycle progression of bladder and lung cancer cell lines via activation of the E2F/RB pathway [208]. Similarly, knockdown of KDM5B in hepatocellular carcinoma cells (HCC) inhibited cell proliferation and colony formation [210]. Reduced tumour growth of HCC upon KDM5B knockdown was also observed *in vivo* [210]. In melanoma cells, KDM5B expression in a sub-population of slow-cycling cells was found to be necessary for maintenance of tumour growth [204].

In breast cancer, KDM5B has been shown to promote proliferation of the MCF-7 ER+ cells [146,188,202]. Yamamoto and colleagues demonstrated that reduction of cell proliferation in KDM5B knockdown MCF-7 cells, was due to activation of the TGFβ signalling pathway[202]. KDM5B knockdown in the ER-/HER2+ breast cancer cell line, UACC812, has also been shown to result in reduced cell growth [253].

6.1.2 KDM5B and drug resistance in cancer

A role for epigenetic factors in promoting drug resistance is emerging, implicating various epigenetic modifiers including KDM5B. High KDM5B expression in a subpopulation of melanoma cells was found to confer resistance to various anti-cancer drugs [246]. Similarly, MYCN amplified neuroblastoma cells with a high KDM5B expression, were resistant to chemotherapy drugs [212]. Although a role for KDM5B in breast cancer drug resistance has

not yet been determined experimentally, using gene expression and copy number data from public databases, it has been shown that positive KDM5B activity in patients with ER+ tumours, was associated with poor outcome and endocrine resistance[202].

6.1.3 Aims

In Chapter 5 (**Section 5.2.3**), gene expression analysis in SKBr3 KO cells revealed that downregulated genes were enriched for genes associated with cell proliferation. Whereas upregulated genes were enriched for genes involved in Herceptin or Lapatinib resistance. The aim of this chapter was therefore to investigate the effect of KDM5B KO on cell proliferation of SKBr3 and BT-474 cells. Furthermore, it was also determined whether KDM5B KO affected drug sensitivity to HER2 targeted therapies (Herceptin and Lapatinib) in SKBr3, as well as, BT-474 cells. These aims were achieved by examining:

1) Cell proliferation of BT-474 and SKBr3 WT and KDM5B KO cells, at different time points
2) Cell viability of BT-474 and SKBr3 WT and KDM5B KO cells, following treatment with Herceptin or Lapatinib alone, or in combination, at different time points. The effect of KDM5B KO on the emergence of drug tolerant cells following long-term treatment with Herceptin, was also evaluated.

6.2 Results

6.2.1 Effect of KDM5B KO on cell proliferation of BT-474 and SKBr3 cells

Studies utilising RNA interference (RNAi) technology, have shown that KDM5B promotes cell proliferation of the ER+ breast cancer cells, MCF-7 [146,188,202]. In the experiment described below, KDM5B KO cell lines that were developed using CRISPR (**Chapter 3 Section 3.2.5**), were used to investigate the role of KDM5B in proliferation of HER2+ breast cancer cells. It was observed that KDM5B KO did not compromise cell proliferation of BT-474 cells (**Fig 6.1A**). In contrast, KDM5B KO significantly reduced proliferation of SKBr3 cells (**Fig 6.1B**). Thus, suggesting that KDM5B can promote proliferation of some but not all, HER2+ breast cancer cell lines. It is should be noted however, the differences observed in cell proliferation between the two cell lines, may be a reflection of the different methodologies used and so requires further validation using the same assay.

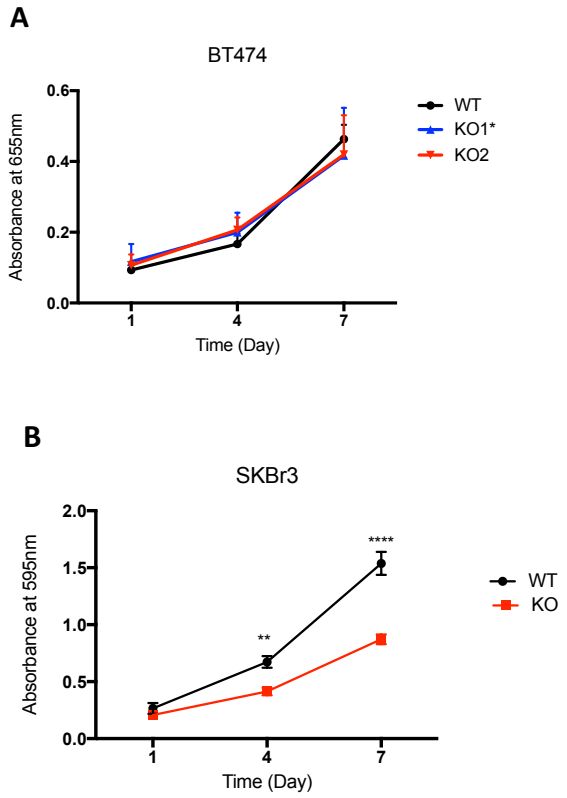

Figure 6.1: Effect of KDM5B KO on cell proliferation of BT-474 and SKBr3 HER2+ breast cancer cells. A) Methylene blue cell viability assay of BT-474 WT, KDM5B KO1* and KO2 cells and B) MTT cell viability assay of SKBr3 WT and KDM5B KO cells. Cell viability was assessed at days 1, 4 and 7. Absorbance was read at 595nm for the MTT assay and 655nm for the methylene blue assay. Data shows the mean from three independent experiments and error bars standard error of the mean (± s.e.m). Asterisks indicate significance where ***P*=0.01 and *****P*=0.0001. Statistical significance was calculated using 2-way ANOVA with Sidak correction.

6.2.2 Effect of KDM5B KO on response to HER2 targeted therapies

The effect of KDM5B KO on response to the HER2 targeted therapies Herceptin and Lapatinib, was examined. $1x10^4$ WT and KDM5B KO cells of BT-474 or SKBr3, were seeded in 24-well plates and 24 hours later after adhesion to the wells, cells were treated with control (PBS or DMSO), Herceptin (10μg/ml) or Lapatinib (100nM) alone, or in combination. Cell viability was then examined using the methylene blue assay at day 0, 3 and 6.

BT-474 KO2 cells were significantly more sensitive to Herceptin in comparison to WT cells, as seen at day 6 (**Fig 6.2A**). However, BT-474 KO1* cells did not show enhanced Herceptin sensitivity at the dose and time tested, in comparison to WT cells (**Fig 6.2A**). Interestingly, KDM5B KO did not enhance sensitivity to Lapatinib alone in BT-474 cells (**Fig 6.2B**). However, enhanced sensitivity was observed in BT-474 KO2 cells in comparison to WT cells, upon combined Herceptin and Lapatinib treatment (**Fig 6.2C**), probably because of the increased sensitivity observed with Herceptin treatment. BT-474 KO1* cells did not show enhanced sensitivity upon combined Herceptin and Lapatinib treatment, in comparison to WT cells (**Fig 6.2C**), supporting the suggestion that KDM5B is not completely knocked out in these cells.

In contrast, KDM5B KO in SKBr3 cells did not show enhanced sensitivity to either Herceptin (**Fig 6.3A**) or Lapatinib (**Fig 6.3B**) alone, or in combination (**Fig 6.3C**), at the dose and time tested. These data suggest that features of the cell phenotype other than HER2 expression, are determining factors in response to Herceptin treatment, in the HER2+ breast cancer subtype.

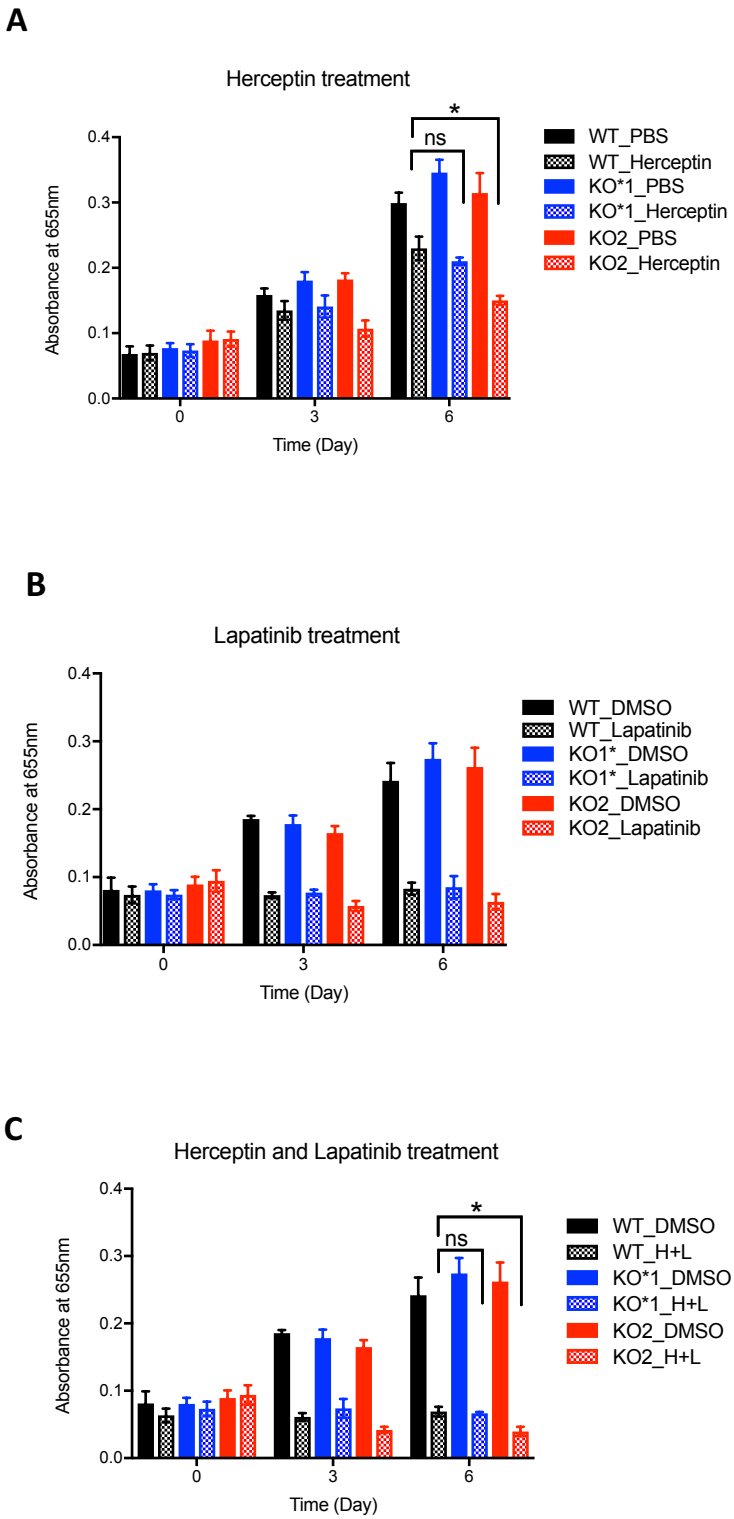

Figure 6.2: KDM5B KO increases sensitivity to HER2 targeted therapies in BT-474 cells. BT-474 parental, KDM5B KO1* and KDM5B KO2 cells were treated with A) 10μg/ml Herceptin B) 100nM Lapatinib or C) 10μg/ml Herceptin and 100nM Lapatinib for 0, 3 and 6 days. PBS and DMSO were used as controls. Bars denote mean from three independent experiments and errors bars standard error of the mean (± s.e.m.). Statistical significance was calculated using unpaired Student's *t*-test. Asterisks indicate significance where, *=p<0.05 and ns=not significant. Significance was only observed at day 6.

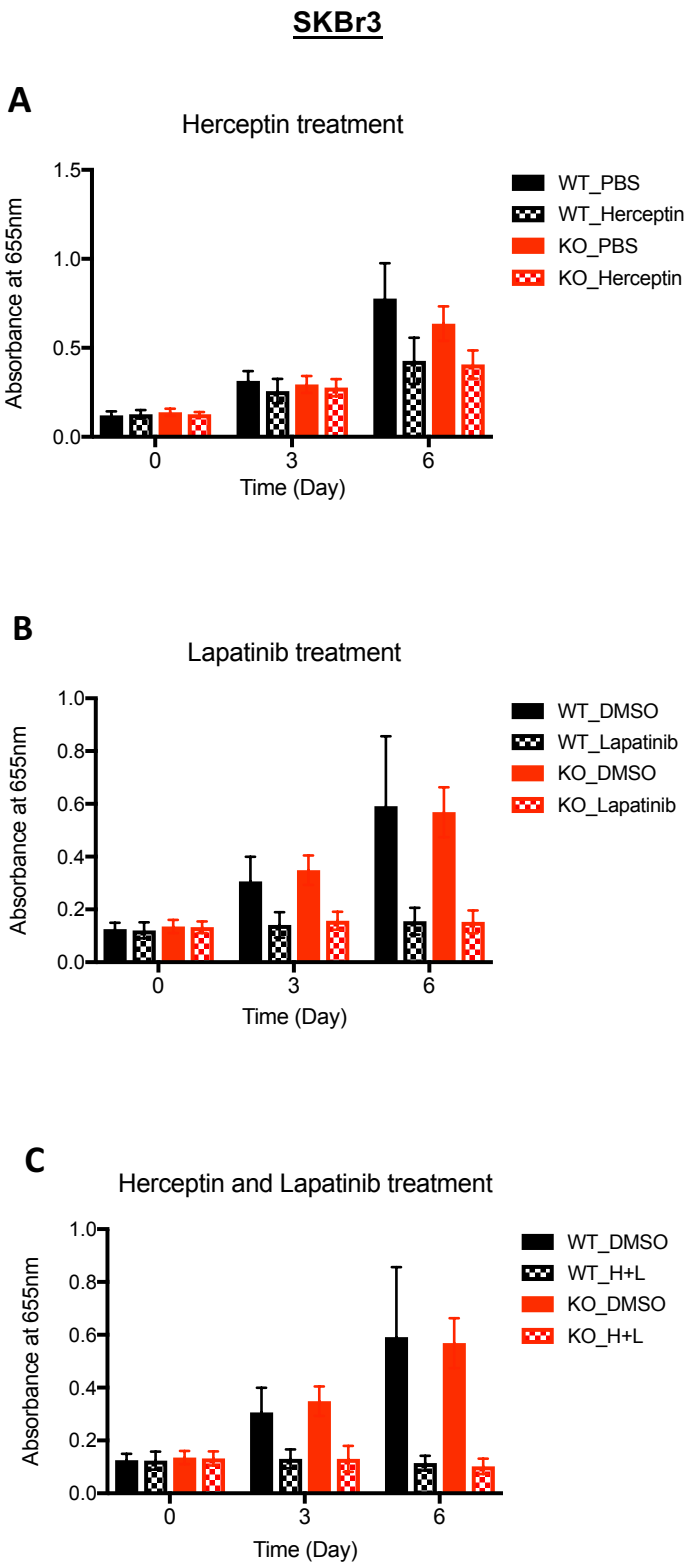

Figure 6.3: KDM5B KO does not affect response to HER2 targeted therapies in SKBr3 cells. SKBr3 parental and KDM5B KO cells were treated with A) 10μg/ml Herceptin B) 100nM Lapatinib or C) 10ug/ml Herceptin and 100nM Lapatinib for 0, 3 and 6 days. PBS and DMSO were used as controls. Bars denote mean from three independent experiments and errors bars standard error of the mean (± s.e.m.).

6.2.3 Effect of KDM5B KO on emergence of drug tolerant cells in BT-474 and SKBr3 cells

Since increased sensitivity to Herceptin was observed in BT-474 KO2 cells and not SKBr3 KO cells, it suggested that KDM5B may be contributing to the survival of drug tolerant cells in BT-474 cells. To evaluate this observation, low numbers ($2.5x10^3$) of WT and KDM5B KO cells of BT-474 or SKBr3, were seeded onto 6-well plates and immediately treated with a low dose of Herceptin (5μg/ml) for 14 days. Media and Herceptin or PBS control, was changed every three to four days. After 14 days, cells were fixed and stained with crystal violet and absorbance read at 595nm, following extraction of the dye with 10% acetic acid.

BT-474 KO2 cells were significantly more sensitive to Herceptin after the 14-day treatment, in comparison to WT cells (**Fig 6.4A**). In contrast, there was no difference in Herceptin sensitivity between BT-474 WT and KO1* cells (**Fig 6.4A**). Similarly, no difference in Herceptin sensitivity was observed between SKBr3 WT and KO cells (**Fig 6.4B**). These experiments provide the first evidence that KDM5B can contribute to emergence of drug tolerance to Herceptin in BT-474 cells.

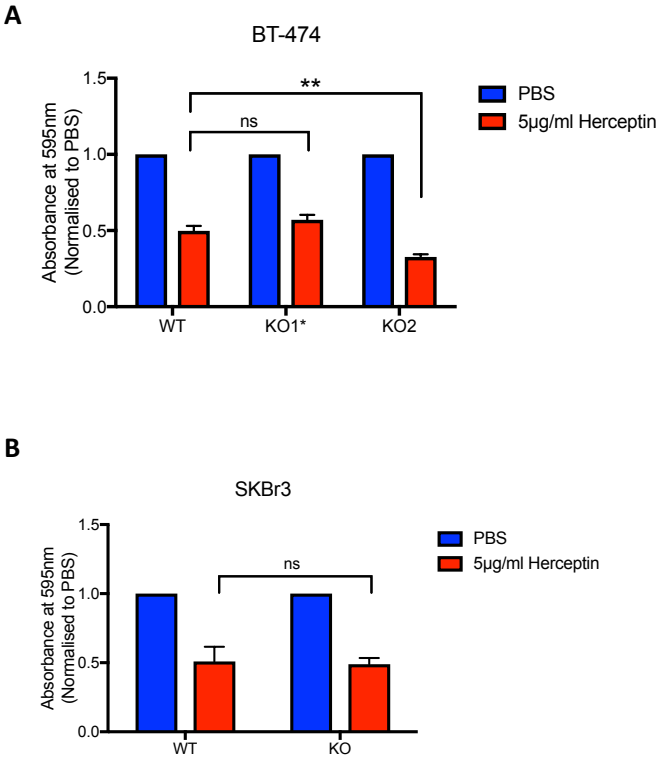

Figure 6.4: Effect of KDM5B KO on emergence of drug tolerant cells in BT-474 and SKBr3 cells. A) $2.5x10^3$ BT-474 WT, KDM5B KO1* and KDM5B KO2 cells and B) $2.5x10^3$ SKBr3 WT and KDM5B KO cells, were seeded in 6-well plates and treated with PBS (blue bars) or 5μg/ml Herceptin (red bars) for 14 days. Bars denote mean from three independent experiments and errors bars show standard error of the mean (± s.e.m.). Asterisks indicate significance where **P=0.01 and ns=not significant. Statistical significance was calculated using 2-way ANOVA, with Sidak correction.

6.2.4 Dosage effect of Herceptin on cell viability of SKBr3 WT and KDM5B KO cells

As enhanced sensitivity was not observed in SKBr3 KDM5B KO cells treated with either 5μg/ml or 10μg/ml Herceptin, it was determined whether increasing Herceptin concentration would increase sensitivity. To this end, both SKBr3 WT and KO cells were treated with control (PBS), 40μg/ml, 100μg/ml or 200μg/ml Herceptin for 3 and 6 days. As shown in **figure 6.5,** treatment with Herceptin at the indicated doses did not enhance sensitivity in SKBr3 KO cells, in comparison to WT cells. Thus, suggesting that the maximum dose that induced a response had been reached.

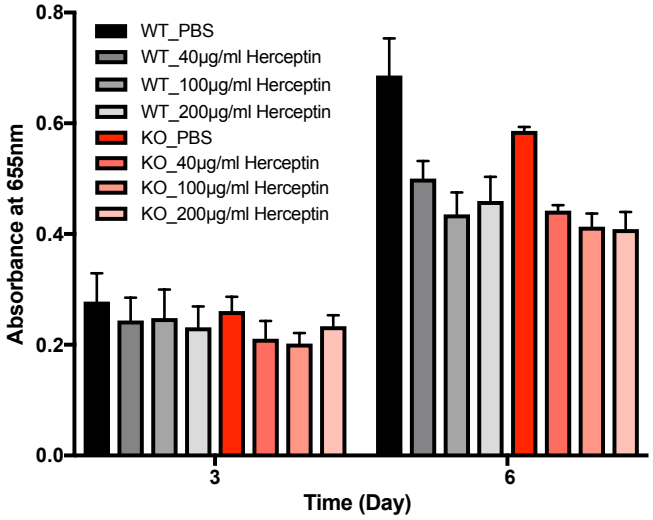

Figure 6.5: Dosage effect of Herceptin on cell viability of SKBr3 WT and KDM5B KO cells. SKBr3 parental and KO cells were treated with PBS control or Herceptin at the indicated doses for 3 and 6 days. Bars denote mean from three independent experiments and errors bars standard error of the mean (± s.e.m.).

6.2.5 KDM5B represses genes associated with drug response in SKBr3 cells

Gene expression studies have shown association between expression of particular genes and Herceptin response [240]. In Chapter 5, gene ontology analysis revealed that some upregulated genes (*CAV1, ABCC2, ANXA1, LCN2* and *MYC*) are involved in resistance to Herceptin or Lapatinib (**Chapter 5 Section 5.2.3**). To determine whether gene expression profile could explain the differences observed in Herceptin sensitivity between SKBr3 KO and BT-474 KO2 cells, mRNA expression of these genes was examined in these cells.

Upregulation of *ABCC2* and *LCN2* mRNA expression in SKBr3 KO cells was confirmed by RT-qPCR (**Fig 6.6A and B**). Upregulation of CAV1 and *MYC* in SKBr3 KO cells has previously been confirmed by western blot and RT-qPCR, as shown in **Chapters 4 Section 4.2.3 and Chapter 5 Section 5.2.1.2**, respectively.

In BT-474 KO2 cells, *LCN2* mRNA expression (**Fig 6.6B**) and CAV1 protein expression (**Chapter 4 Section 4.2.3**) did not change in comparison to WT cells. However, *ABCC2* (**Fig 6.6A**) and *MYC* mRNA expression (**Chapter 5 Section 5.2.1.3**) were upregulated in BT-474 KO2 cells but to a lesser extent than in SKBr3 KO cells. These results suggest that gene expression/cell phenotype could determine KDM5B function in conferring Herceptin resistance in HER2+ breast cancer cell lines. Further functional experiments are required to test this hypothesis.

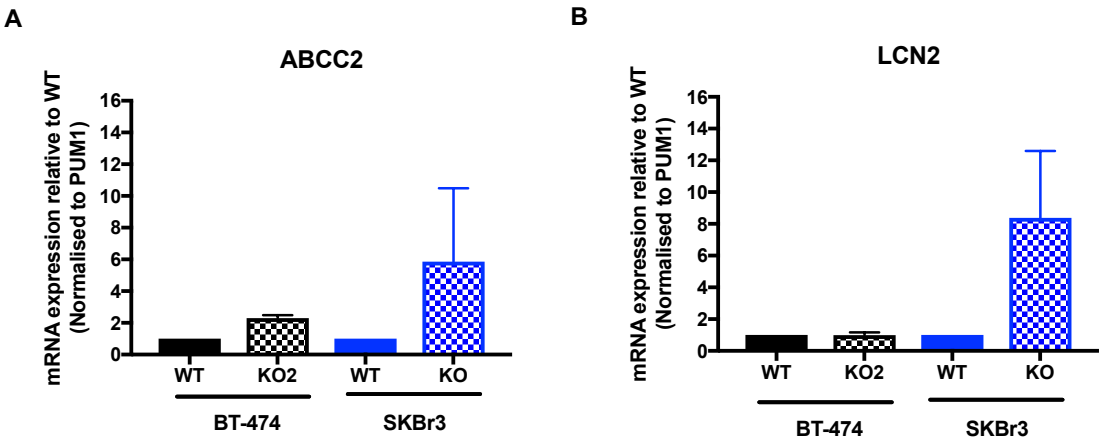

Figure 6.6: Expression of *ABCC2* and *LCN2* in SKBr3 and BT-474 WT and KDM5B KO cells. RNA extracted from SKBr3 WT and KO cells and BT-474 WT and KO2 cells was reverse transcribed and *ABCC2* and *LCN2* genes examined, using Qiagen Quantitect primers. Samples were run in triplicate in each experiment. Data represents three independent experiments. Errors bars denote standard error of the mean (s.e.m).

6.3 Discussion

In this chapter, the phenotypic effects of KDM5B KO on 1) cell proliferation and 2) sensitivity to the HER2 targeted therapies, Herceptin and Lapatinib was investigated. The findings show that KO of KDM5B inhibits cell growth of the ER-/HER2+ SKBr3 cells and reveals a potential novel role for KDM5B in promoting resistance to Herceptin, in the ER+/HER2+ BT-474 cells. These results demonstrate that KDM5B functions in a phenotypic specific manner.

6.3.1 KDM5B promotes cell proliferation of SKBr3 cells

The finding that KDM5B KO results in reduced proliferation of SKBr3 cells, confirms Gene Ontology analysis showing involvement of some of the downregulated genes in mammary epithelial cell proliferation (**Chapter 5 Section 5.2.3**). These genes included ID2 and STAT6 which are part of the TGFβ and JAK-STAT signalling pathways, respectively. Both of these pathways are involved in promoting cell proliferation, suggesting that KDM5B normally activates these genes potentially leading to increased cell growth. This is in contrast to the finding that KDM5B knockdown activated the TGF pathway in the ER+ cell line, MCF-7[202]. Thus, these data demonstrate that KDM5B function is dependent on cell phenotype.

Furthermore, the result that KDM5B KO reduces cell proliferation of SKBr3 cells, demonstrates the advantages of the CRISPR/Cas9 gene editing technology in functional studies. A KDM5B shRNA screen for cellular viability in a panel of breast cancer cell lines, that included BT-474 and SKBr3, showed that the growth of these cells was not inhibited by KDM5B knockdown [202]. Using CRISPR it is now evident that KDM5B KO reduces the growth of SKBr3 cells, and thus shows the limitations of RNAi technology, which only partially silences genes that may still therefore have residual functionality. This observation however, needs to be validated using another clone or by performing rescue experiments to confirm that observations are not a clonal effect.

Although KDM5B is highly expressed in BT-474 cells, it was surprising that its knockout did not have an effect on cell growth. Furthermore, since BT-474 is an ER+/HER2+ cell line and KDM5B has been shown to control cell growth of ER+ cells [188,202], this lack of reduced cell growth was surprising. However, these results are in agreement with those of Gale and colleagues who found that treatment of BT-474 cells with a small molecule inhibitor to KDM5A and KDM5C, did not affect cell proliferation[114]. Thus, taken together these findings suggest that KDM5B and indeed other KDM5 family members, may not have a direct role in controlling the growth of BT-474 cells.

6.3.2 A role for KDM5B in Herceptin resistance of BT-474 cells

This is the first study to demonstrate a role for KDM5B in Herceptin resistance of BT-474 breast cancer cells. Increased sensitivity to Herceptin in BT-474 KO2 cells was also observed in a long-term assay (**Fig 6.4**), where fewer drug tolerant cells were seen after 14-day Herceptin treatment. Herceptin has previously been shown to enhance apoptotic cell death induced by Lapatinib [311,312]. The data shown here is in agreement with these studies, since cell viability was further reduced when BT-474 KO2 cells were treated with a combination of Herceptin and Lapatinib. Taken together it is clear that multiple targeting is important in achieving enhanced therapeutic response and that determination of tumour phenotype is vital.

Surprisingly, KDM5B KO did not increase efficacy to Herceptin in SKBr3 cells but gene ontology analysis revealed that upregulated genes in SKBr3 KO cells, were enriched for genes involved in Herceptin resistance (**see Chapter 5 Section 5.2.3**), thus demonstrating that KDM5B normally represses expression of these genes. Interestingly, expression of CAV1 and *LCN2* which have previously been associated with Herceptin resistance, were not upregulated in BT-474 KO2 cells, whereas *ABCC2* was marginally upregulated in these cells. Therefore, the difference in Herceptin sensitivity observed between BT-474 and SKBr3 KDM5B KO cells could be explained by cell phenotype, since KDM5B represses some resistance associated genes in SKBr3 cells but not in BT-474 cells.

6.3.3 KDM5B KO does not enhance sensitivity to Lapatinib

KDM5B KO in both BT-474 and SKBr3 cells did not enhance sensitivity to Lapatinib. Lapatinib influences cell proliferation by 1) slowing down cycling cells and 2) driving cells into quiescence through apoptosis [312]. This phenomenon was observed here, where Lapatinib had an initial cytotoxic effect at day 3 resulting in reduced cell viability, which was later cytostatic by day 6, in both BT-474 and SKBr3 cells. Although BT-474 KO2 cells seemed to be slightly more sensitive to Lapatinib, this response was not significant. Thus, other factors which could include other KDM5 family members, may be influencing Lapatinib sensitivity. Indeed, a recent study has shown that treatment of SKBr3 cells with Lapatinib in combination with a pan-KDM5 small molecule inhibitor significantly reduced survival of drug tolerant cells [115]. Thus, inhibition of other KDM5 enzymes, perhaps coupled with other therapies, may be required to overcome drug tolerance to Lapatinib in this cell line.

Furthermore, the lack of increased sensitivity to Lapatinib could be explained by upregulation of MYC which has been shown to confer resistance to Lapatinib [302]. Since

MYC expression was also upregulated in both SKBr3 KO and BT-474 KO2 cells, this could explain why both cell lines did not show enhanced sensitivity to Lapatinib. Therefore, this increased expression of *MYC* upon KDM5B KO, may be contributing to the maintenance of Lapatinib resistance at day 6, in BT-474 and SKBr3 cells (**Fig 6.2 and 6.3 respectively**). Inhibition of MYC may therefore re-sensitise these cells to Lapatinib however, this needs to be experimentally tested.

6.3.4 Conclusion

The data shown here, demonstrate a novel observation that KDM5B promotes proliferation of SKBr3 cells which had not been previously shown using RNAi. This effect in proliferation is not universal in HER2+ breast cancer cells, since BT-474 cell growth was not affected by KDM5B KO. Gene expression profiling of SKBr3 KO cells, showed that KDM5B normally activates genes involved in the TGFβ (i.e. *ID2*) and JAK-STAT (i.e. *STAT6*) pathways, in this ER-/HER2+ cell line. Thus, it remains to be experimentally tested whether KDM5B may be promoting cell proliferation of SKBr3 cells through these signalling pathways. Furthermore, it remains to be determined whether KDM5B regulation of these genes depends on its demethylase activity, since in contrast to gene repression which has been shown to occur mainly via KDM5B demethylase function, the mechanism through which KDM5B activates gene expression is not known.

One of the hypotheses of this PhD was that, loss of KDM5B could increase efficacy to HER2 targeted therapies. This is the first study to show that KDM5B can promote resistance to Herceptin in BT-474 cells, and thus this finding warrants further validation by testing KDM5B KO in other HER2+/ER+ cell lines. Surprisingly, in SKBr3 cells, KDM5B appears to have the opposite effect in that, it represses genes associated with drug resistance and so KO does not therefore increase efficacy to HER2 targeted therapies, and could in fact increase drug resistance. Given the increasing interest in the clinical potential of KDM5 small molecule inhibitors, it is crucial that these results be validated. The findings demonstrate the importance of cell phenotype when investigating function of KDM5B. As discussed in the introduction, considerable effort is being focused on the development of small molecule inhibitors of KDM5B as cancer therapeutics. If these are to be translated into the clinic, the data here suggests that patient stratification would be vital. Therefore, pending *in vivo* validation, it is possible that the recently developed KDM5B small molecule inhibitor, KDOAM-25 [254] can indeed find utility in the clinical setting, for the treatment of some HER2+ breast cancers, providing careful patient selection is carried out.

7 : General Discussion

7.1 Overview of PhD project

KDM5B is regulated by HER2 signalling [183] however, its function in HER2+ breast cancer has not been widely studied. One of the aims of this PhD thesis, was to investigate the role of KDM5B in HER2+ breast cancer cells by developing KDM5B KO cells and examining their effect on, 1) gene expression levels 2) cell proliferation and 3) response to Herceptin or Lapatinib, alone or in combination. The second aim was to investigate CAV1 regulation by KDM5B in normal and malignant breast cancer cells, as well as the cellular distribution of CAV1 and KDM5B in the developing mammary gland. Beyond ER+ cells it is not known how widespread KDM5B downregulation of CAV1 is in breast cancer. This is of importance as CAV1 expression in the stroma of breast cancers is associated with a good prognosis [238,239,242]. Additionally, in the normal gland it is not clear in which cells downregulation of CAV1 by KDM5B can occur.

During this PhD, I have:

- Developed the first reported KDM5B knockout cell lines produced by gene editing.
- Shown that the early response genes EGR1 and FOS are down-regulated by KDM5B.
- Demonstrated that KDM5B enhances the growth of the HER2+ SKBr3 cell line.
- Shown for the first time that KDM5B can promote resistance to Herceptin, adding to the evidence that KDM5B may be a suitable therapeutic target. However, this effect was cell phenotype dependent and in the SKBr3 cell line where KDM5B knockout did not increase Herceptin sensitivity, KDM5B appears to downregulate genes involved in drug resistance in the parental SKBr3 cells. It is crucial that these results be extended and validated in other cell lines, if inhibitors of KDM5B are to enter the clinic.
- Shown that the down-regulation of CAV1 by KDM5B in breast cancer cells lines is phenotype dependent.
- Identified in the mouse mammary gland the cellular distribution of KDM5b and CAV1.

The specific phenotypes of the KDM5B KO cells in BT-474 and SKBr3 are shown in Table 7.1.

Table 7.1: Summary of observed phenotypes in KDM5B KO cells

	BT-474 KDM5B KO1*	BT-474 KDM5B KO2	SKBr3 KDM5B KO
Global H3K4me3 levels	Not changed	Not changed	**Increased**
Gene Expression 1. CAV1 2. Early response genes (EGR1 and FOS) 3. MYC	1. Not changed 2. Not changed 3. Not changed	1. Not changed **2. Increased** **3. Increased**	**1. Increased** **2. Increased** **3. Increased**
Cell growth	Not changed	Not changed	**Reduced growth**
Drug resistance	No increase in sensitivity to Herceptin or Lapatinib alone, or in combination.	**Increased sensitivity to Herceptin alone or in combination with Lapatinib, but not to Lapatinib alone.**	No increase in sensitivity to Herceptin or Lapatinib alone, or in combination.
Herceptin resistant genes (i.e. ABCC2 and LCN2)	Not tested	No change in expression	**Increased expression**

7.2 Genes controlled by KDM5B

Disruption of KDM5B function was achieved by using a gRNA targeting exon 4 of KDM5B. This resulted in development of KDM5B KO cell lines in BT-474 and SKBr3. An additional cell line BT-474 KO1* did express low levels of KDM5B mRNA as determined by RT-qPCR. As discussed in chapter 3, in the IDAA analysis only two indels were detected for this clone in contrast to BT474 KO2 that showed three indels, and this was confirmed by sequencing. As BT474 has three copies of KDM5B this may suggest that a single copy of KDM5B is being transcribed. This may explain the differing results obtained with BT474 KO1* and BT474 KO2 in the sensitivity of these cells to Herceptin, and its contribution to resistance where BT474 KO1* is acting more like wild-type cells. Although the possibility of the effects being due to clonal variation cannot be ruled out, given that *EGR1, FOS and MYC* are upregulated in both the SKBr3 KO and BT474 KO2 but not in BT473 KO1*, the most likely explanation for the phenotype of the BT474 KO1* is that it is not a full knockout.

7.2.1 KDM5B regulation of early response genes

The global gene expression analysis of the SKBr3 KO showed that KDM5B down regulates the early response genes *EGR1* and *FOS*. This was also observed in BT474 KO2. Early response genes are typically induced transiently and rapidly when cells are exposed to external stimuli [299] such as mitogens, for example EGF and platelet-derived growth factor (PDGF). Using 14 breast cancer datasets Li and colleagues showed that *EGR1* and *FOS* are down-regulated in breast cancer [313]. It is tempting to speculate that this is the result of KDM5B expression by these breast cancers.

Analyses of published papers looking at global gene expression analysis after knockdown of KDM5B in breast cancer cell lines do not reveal EGR1 to be a target of KDM5B [156,159,202]. However, the work of Dey and colleagues in mouse embryonic stem cells also shows that KDM5B suppresses the expression of *EGR1*, thus inhibiting differentiation [190]. It is interesting to note the discordance between gene expression profiles of KDM5B knock-downs which is seen between different groups of investigators using the same breast cancer cell line (in many cases MCF-7). While this could be due to a drift in the cell phenotype it may also be due to the variation in levels of KDM5B that are seen in RNAi or short hairpin RNA (shRNA) knockdowns and illustrates the advantage of using a gene editing technique such as CRISPR/Cas9.

7.2.2 KDM5B regulation of CAV1 expression

The precise role of CAV1 in breast cancer is currently under much debate. Although there have been numerous reports examining CAV1 expression in breast cancer tissues and cell lines, there is no consensus regarding how CAV1 expression in tumour cells relates to prognosis [314]. Furthermore, whilst some studies suggest that CAV1 is a tumour suppressor in breast cancer, others report an oncogenic function of CAV1 in breast cancer [232,315,236,295]. Taken together with controversial reports on the CAV1 P132L mutation[316–318], progress in understanding the specific role of CAV1 in different breast cancer subtypes has been confounded. There is however consensus that expression of CAV1 in breast cancer stromal fibroblasts is associated with a good prognosis [238,239,242]. Thus, CAV1 function is highly dependent on the context of the cell.

The data obtained from the KO clones of two HER2+ cell lines, and on CAV1 and KDM5B expression in breast cancer fibroblasts, are relevant to these issues. CAV1 protein expression varied in cell lines obtained from different breast cancer subtypes, and regulation of CAV1 expression by KDM5B was seen in SKBr3 KO cells but not, BT-474 KO cells. These data demonstrate that KDM5B regulates CAV1 expression in a cell phenotype dependent manner, in HER2+ breast cancer cells. Others have shown that

CAV1 is also transcriptionally repressed by KDM5B in ER+ breast cancer cells [146,156], indicating that regulation of CAV1 is operating in different pathways in different breast cancer subtypes.

In the two strains of cancer associated fibroblasts that were examined here, high CAV1 and low KDM5B expression was observed in comparison to normal breast fibroblast cells. An inverse correlation was also observed in breast cancer cell lines. Nevertheless, the inverse ratio does not necessarily indicate that KDM5B is regulating gene expression as the knockouts of BT474 and SKBr3 showed. Indeed, although both wild-type cells show low levels of CAV1, knocking out KDM5B increased CAV1 expression only in the SKBr3KO cells.

Studies in mice have provided data relating to the role of CAV1 in normal mammary gland. CAV1 has been found to inhibit the proliferation and extension of the mouse luminal epithelial cells in pregnancy, and this inhibition relates to CAV1 inhibition of phosphorylated STAT5 signalling[231]. Data from an analysis of mice that are null for KDM5b demethylase activity showed an increase in CAV1 expression in the mid-pregnant mammary gland (Steven Catchpole personal communication). The data reported here showed that in the mouse mammary gland at mid-pregnancy, CAV1 and KDM5B are both expressed in the myoepithelial and fat cells, allowing the interpretation that KDM5B may be regulating CAV1 in one or both of these cells. However, the increased proliferation of the mammary luminal epithelial cells (where CAV1 is not expressed) at mid pregnancy is driven by the STAT5 signalling pathway [231], and activation of STAT5 was found to be inhibited in the KDM5B demethylase null mouse at mid pregnancy [196]. Thus, if CAV1 is normally downregulated by KDM5B in stromal or myoepithelial cells, any effects of CAV1 on mammary epithelial cell proliferation driven by pSTAT5, would have to be regulated in a paracrine fashion.

These findings in the normal mouse mammary gland could relate to the effect of high levels of CAV1 expression in breast cancer fibroblasts correlating with good prognosis. Thus, CAV1 effects on tumour proliferation may also be operating through a paracrine mechanism. Constitutive activation of STAT5a has been reported in many malignancies including breast cancer, and this could be due to KDM5B down-regulation of CAV1. However, this hypothesis needs to be tested. Using the gRNA we have identified for CRISPR gene editing, it should be possible to develop KDM5B KOs from strains of breast cancer fibroblasts, to determine whether KDM5B regulates CAV1 expression in these cells. Demonstration of downregulation of CAV1 by KDM5B would add to the argument for inhibitor targeting of this demethylase.

7.2.3 KDM5B regulation of MYC expression

In Drosophila the homologue of KDM5- Lid, was found to interact with dmyc and was required for activation of mitochondrial genes by Myc; a function which was independent of KDM5 demethylase activity [319]. This connection with Myc has not been reported in mammalian KDM5 proteins. However, upregulation in enzymes of mitochondrial oxidative-ATP-synthesis (oxidative phosphorylation) have been found in long-term tumor-maintaining melanoma cells with high KDM5B expression [246]. Moreover, using the MCF-7 breast cancer cell line, MYC was found to exist in a complex with KDM5B and TFAP2C [298]. This KDM5B-MYC-TFAP2C complex was shown to repress the cell cycle inhibitor p21, and it was proposed that this complex might promote cell cycle progression in breast cancer. In this thesis, knocking out KDM5B in two HER2 expressing breast cancer cell lines, induced increased expression of *MYC* (**Chapter 5**), suggesting that *KDM5B* normally downregulates *MYC* in these cells. It will be important to investigate the relevance of effects of KDM5 proteins and the role of MYC on mitochondrial gene expression in the context of targeting KDM5 demethylases.

7.3 The role of KDM5B in sensitivity to HER2 targeted therapies

The epigenetic changes that are induced by HER2 signalling are dramatic [320] altering the chromatin state and changing the global profile of genes expressed. Thus, targeting elements of epigenetic change, for example the methyl mark (H3K4me3) removed by KDM5B, could affect multiple pathways including those reported to be involved in the development of resistance to HER2 targeting. In order to examine the phenotypic effects of KDM5B KO, its role in cell proliferation and drug resistance was investigated. KDM5B KO in SKBr3 cells reduced cell proliferation, but did not increase sensitivity to Herceptin or Lapatinib alone or in combination. In contrast, whereas KDM5B KO in BT-474 cells did not compromise their proliferation, sensitivity to Herceptin alone or in combination with Lapatinib, was increased in BT-474 KO2 cells. Furthermore, treatment of BT-474 KO2 cells with Herceptin in a long-term assay, resulted in reduction of drug tolerant cells. To my knowledge, this is the first report showing a role of KDM5B in drug resistance of BT-474 cells.

Interestingly, in SKBr3, knockout of KDM5B increased the expression of some genes involved in drug resistance including *ABCC2, CAV1* and *LCN2*. ABCC2, CAV1 and LCN2 were validated by qPCR or western blot and shown to be elevated in SKBr3 KO. Although, ABCC2 was elevated to a much lesser extent in BT474 KO2 knockout, CAV1 and LCN2 levels did not change in this cell line. ABCC2 is involved in the efflux of

chemicals from the cells such as the chemotherapeutics doxorubicin and cisplatin. While it is hard to see an association with the ABCC2 expression and resistance to Herceptin, LCN2 has been associated with resistance to Herceptin. LCN2 is a chaperone protein that is upregulated during the unfolded protein response (UPR). It has been associated with drug resistance in a number of systems and is highly expressed in the intrinsically Herceptin resistant line HCC1954 [240], and there is evidence to suggest that LCN2 can override Herceptin inhibition of HER2 [321]. The upregulation of ABCC2, CAV1 and LCN2 in the SKBr3 KO but not in the BT474 KO2, correlates with the observation that KDM5B silencing does not enhance sensitivity to Herceptin in SKBr3, but does in BT474.

Owing to its various reported roles in tumorigenesis and drug resistance, KDM5B has been proposed to be a suitable target for cancer therapy. Although considerable effort has been made to develop small molecule inhibitors to KDM5B to study its clinical utility, currently none of these inhibitors are specific to KDM5B. To enable validation and application of these inhibitors, a proper understanding of the tumorigenic function of KDM5B is required. The knockout lines developed in this thesis can now be used to further characterise and fine-tune the function of KDM5B in HER2+ breast cancer. Furthermore, they can be used to complement work using small molecule inhibitors, to investigate the importance of the KDM5B demethylase activity in drug resistance. Indeed, this strategy has been used to validate the effect of a KDM5A/C inhibitor on cell proliferation [114]. The authors compared the effect of inhibiting the demethylase activity of KDM5A with knockout of KDM5A. Both strategies showed reduced proliferation of HeLa cells but minimal effect on MCF-7 cells, thus demonstrating that KDM5A promotes proliferation of KDM5A-dependent cells, through its demethylase activity [114]. Adopting similar strategies will therefore enable better drug design and thus improve success of these inhibitors in the clinic. The unexpected result that in SKBr3 cells KDM5B appears to downregulate genes encoding proteins involved in drug resistance needs to be extended and validated to other HER2+/ER- cell lines, if small molecule inhibitors of KDM5B are to be introduced to the clinic. Moreover, the involvement of the demethylase activity of KDM5B in repressing these genes needs to be established. These results emphasise the importance of performing extensive preclinical studies before phase I trials are initiated.

7.4 Future work

The interest in developing small molecular weight inhibitors of the demethylase activity of KDM5B proteins, stems from the fact that these proteins are often elevated in many cancers, and that they can change the profile of genes transcribed by a cell by demethylating the active H3K4me3/2 marks. Although some inhibitors have been

developed that specifically inhibit the KDM5 family of demethylases, as yet inhibitors showing reliable specificity for inhibiting a specific KDM5 member have yet to be developed, although inhibitors with some preferences for individual family members have been reported [114,254]. Without such inhibitor specificity, investigating the effects of an individual KDM5 protein on the phenotype of cells from different tissues and cancers and the role of the demethylase activity can be approached through gene editing.

7.4.1 KDM5B

In this thesis, we have taken the first step in examining how deleting the KDM5B gene in two cell lines from the subtype of HER2+ breast cancers, affects cell phenotype. To pursue the validation of KDM5B affecting cell proliferation and upregulation of genes associated with drug resistance, in the HER2+/ER- cell line SKBr3, another KO clone should be developed. KDM5B KO in other HER2+/ER- cell lines should also be developed with the gRNA used here, to investigate the extent of these observations. A similar approach should be taken to validate the increased Herceptin sensitivity induced by knocking out KDM5B in BT474 cells (i.e. isolate another KO clone and delete KDM5B in other HER2+/ER+ cell lines). Furthermore, RNA-seq can be performed to analyse global gene expression changes induced upon KDM5B KO. The importance of the demethylase activity in these effects can be addressed by gene mutation, rather than deleting the KDM5B gene, for example replacing the WT gene with a demethylase null mutant. Additionally, rescue experiments should be performed to demonstrate that the phenotype of the knockout clones is dependent on KDM5B loss. Furthermore, functional testing through knockdown of genes involved in Herceptin resistance (e.g. *ABC22* and *LCN2*), is required to make conclusions about the mechanisms behind any effects of KDM5B.

To further understand the role of KDM5B in drug resistance, the effect of KDM5B loss with and without HER2 targeted therapies, on apoptosis, metastasis, migration, stem cell activities and *in vivo* tumour growth, should be examined. These studies will enable identification of specific mechanisms and in turn, genetic targets that can be further explored for therapy. To make these observations more clinically relevant, similar experiments should be performed using patient-derived organoids/xenografts.

7.4.2 Other Cell types and other KDM5 family members

The epigenome defines cell phenotype and specific epigenetic factors are expressed and regulated differently in different cell types. The KDM5 family members form

complexes regulating transcription which can vary with cell phenotype. We have focused on the effects of one KDM5 protein in two cell lines which represent two HER2+ subtypes of breast cancer. With the guide RNA already established, the effects of silencing KDM5B can readily be examined in cell lines derived from different cancers and different breast cancer subtypes. It will be important to knockout KDM5B in strains of breast cancer fibroblasts to determine whether CAV1 expression is regulated by KDM5B. These studies would give a picture of the importance of this family member in regulating phenotype in different cancers and could guide the choice of cancers to be targeted in the clinic- should specific inhibitors become available. However, in many cells of female origin KDM5 A, B and C can be expressed, and all four members can be expressed in males. Depending on which family members are expressed, gene editing can be used to silence the other family members both individually and consecutively if necessary. Thus, extensive pre-clinical testing of the importance of the individual family members in regulation of cell phenotype in different cancers should ideally be carried out before moving to the clinic.

7.4.3 Use of current inhibitors

It is not clear whether KDM5B promotes cell proliferation in SKBr3 cells or Herceptin resistance in BT-474 cells through its demethylase activity. While knocking in ΔJmjC KDM5B into the KO cells, could resolve this issue, comparing the effect of total KDM5B KO with the effect of the inhibitor KDOAM-25 (has higher potency for inhibiting KDM5B demethylase activity but is not completely specific for KDM5B) [254] on cell phenotype would also be informative. The KDM5B KO cells will lose any important functions governed by other domains and unrelated to the demethylase activity, and these could be important for the phenotypic changes seen in the KO. This should indicate whether the effect on increased sensitivity seen in the KO is dependent or independent of the demethylase activity. Moreover, to investigate whether KDM5B is the prominent KDM5 protein in SKBr3 and/or BT474 cells, the KDM5A/C inhibitor, YUKA1 [114], can be used to study the effects on cell proliferation, regulation of target genes and drug resistance. These findings can then be compared to the effects seen with the KDM5B KO and the pan-KDM5 inhibitor, KDOAM-25. Taken together, these investigations could provide an analysis of KDM5B function in the two breast cancer cell lines and the utility of the currently available small molecule inhibitors. Gathering information on the effects of silencing individual KDM5 family members in different cell types (using gene editing techniques) and analysing whether the effects on phenotype are attributable to, or independent of, the demethylase activity will be a crucial and necessary preclinical activity. These studies will also expand the basic knowledge relating to the regulatory

activity of this family of demethylases, which may relate to the potential importance of other domains in the proteins.

7.5 Conclusion

The results presented in this PhD thesis demonstrate a cell phenotype dependent function of KDM5B in HER2+ breast cancer cell lines, where KDM5B KO can result in either reduced proliferation in HER2+/ER- cells or increased sensitivity to Herceptin in HER2+/ER+ cells. Thus, it is very important to investigate whether this data will predict the same phenotypes in other HER2+/ER- and HER2+/ER+ breast cancer cell lines. The data shown in this thesis suggests that KDM5B could be a potential therapeutic target in HER2+ breast cancers however, patient stratification would be vital and ER positivity could be used as a predictive marker for response to HER2 targeted therapies. Therefore, it is imperative to investigate further and validate the function of KDM5B in HER2+ breast cancer.

8 : Appendix

DNA sequence of U6-gRNA (PX458) and Cas9-2AGFP-pBKS plasmids

U6-gRNA (PX458) plasmid sequence

gagggcctatttcccatgattccttcatatttgcatatacgatacaaggctgttagagagataattggaattaatttgactgtaa
acacaaagatattagtacaaaatacgtgacgtagaaagtaataatttcttgggtagtttgcagttttaaaattatgttttaaaat
ggactatcatatgcttaccgtaacttgaaagtatttcgatttcttggctttatatatcttgtggaaaggacgaaacaccgggtctt
cgagaagacctgttttagagctagaaatagcaagttaaaataaggctagtccgttatcaacttgaaaaagtggcaccga
gtcggtgctttttgttttagagctagaaatagcaagttaaaataaggctagtccgtttttagcgcgtgcgccaattctgcagac
aaatggctctagaggtacccgttacataacttacggtaaatggcccgcctggctgaccgcccaacgacccccgcccatt
gacgtcaatagtaacgccaatagggactttccattgacgtcaatgggtggagtatttacggtaaactgcccacttggcagt
acatcaagtgtatcatatgccaagtacgccccctattgacgtcaatgacggtaaatggcccgcctggcattgtgcccagta
catgaccttatgggactttcctacttggcagtacatctacgtattagtcatcgctattaccatggtcgaggtgagccccacgtt
ctgcttcactctccccatctcccccccctccccacccccaattttgtatttatttatttttttaattattttgtgcagcgatgggggcgg
ggggggggggggggcgcgcgccaggcggggcggggcggggcgaggggcggggcggggcgaggcggagaggt
gcggcggcagccaatcagagcggcgcgctccgaaagtttccttttatggcgaggcggcggcggcggcccctataa
aaagcgaagcgcgcggcgggcgggagtcgctgcgacgctgccttcgccccgtgccccgctccgccgccgcctcgcg
ccgcccgccccggctctgactgaccgcgttactcccacaggtgagcgggcgggacggcccttctcctccgggctgtaatt
agctgagcaagaggtaagggtttaagggatggttggttggtggggtattaatgtttaattacctggagcacctgcctgaaat
cacttttttcaggttggaccggtgccaccatggactataaggaccacgacggagactacaaggatcatgatattgattac
aaagacgatgacgataagatggccccaaagaagaagcggaaggtcggtatccacggagtcccagcagccaaaag
gccggcggccacgaaaaaggccggccaggcaaaaaagaaaaaggaattcggcagtggagaattctaactagagct
cgctgatcagcctcgactgtgccttctagttgccagccatctgttgtttgcccctcccccgtgccttccttgaccctggaaggtg
ccactcccactgtcctttcctaataaaatgaggaaattgcatcgcattgtctgagtaggtgtcattctattctgggggggtgggg
tggggcaggacagcaagggggaggattgggaagagaatagcaggcatgctggggagcggccgcaggaacccctа
gtgatggagttggccactccctctctgcgcgctcgctcgctcactgaggccgggcgaccaaaggtcgcccgacgcccgg
gctttgcccgggcggcctcagtgagcgagcgagcgcgcagctgcctgcaggggcgcctgatgcggtattttctccttacg
catctgtgcggtatttcacaccgcatacgtcaaagcaaccatagtacgcgccctgtagcggcgcattaagcgcggcggg
tgtggtggttacgcgcagcgtgaccgctacacttgccagcgccctagcgcccgctcctttcgctttcttcccttcctttctcgcc
acgttcgccggctttccccgtcaagctctaaatcgggggctcccttagggttccgatttagtgctttacggcacctcgaccc
caaaaaacttgatttgggtgatggttcacgtagtgggccatcgccctgatagacggtttttcgccctttgacgttggagtcca
cgttctttaatagtggactcttgttccaaactggaacaacactcaaccctatctcgggctattcttttgatttataagggattttgc
cgatttcggcctattggttaaaaaatgagctgatttaacaaaaatttaacgcgaattttaacaaaatattaacgtttacaatttt
atggtgcactctcagtacaatctgctctgatgccgcatagttaagccagccccgacacccgccaacacccgctgacgcg
ccctgacgggcttgtctgctcccggcatccgcttacagacaagctgtgaccgtctccgggagctgcatgtgtcagaggtttt
caccgtcatcaccgaaacgcgcgagacgaaagggcctcgtgatacgcctatttttataggttaatgtcatgataataatgg
tttcttagacgtcaggtggcacttttcggggaaatgtgcgcggaacccctatttgtttatttttctaaatacattcaaatatgtatc
cgctcatgagacaataaccctgataaatgcttcaataatattgaaaaaggaagagtatgagtattcaacatttccgtgtcgc
ccttattcccttttttgcggcattttgccttcctgtttttgctcacccagaaacgctggtgaaagtaaaagatgctgaagatcagtt
gggtgcacgagtgggttacatcgaactggatctcaacagcggtaagatccttgagagttttcgccccgaagaacgttttcc
aatgatgagcacttttaaagttctgctatgtggcgcggtattatcccgtattgacgccgggcaagagcaactcggtcgccgc
atacactattctcagaatgacttggttgagtactcaccagtcacagaaaagcatcttacggatggcatgacagtaagaga
attatgcagtgctgccataaccatgagtgataacactgcggccaacttacttctgacaacgatcggaggaccgaaggag
ctaaccgcttttttgcacaacatgggggatcatgtaactcgccttgatcgttgggaaccggagctgaatgaagccatacca
aacgacgagcgtgacaccacgatgcctgtagcaatggcaacaacgttgcgcaaactattaactggcgaactacttactc
tagcttcccggcaacaattaatagactggatggaggcggataaagttgcaggaccacttctgcgctcggcccttccggct
ggctggtttattgctgataaatctggagccggtgagcgtggaagccgcggtatcattgcagcactggggccagatggtaa
gccctcccgtatcgtagttatctacacgacggggagtcaggcaactatggatgaacgaaatagacagatcgctgagata
ggtgcctcactgattaagcattggtaactgtcagaccaagtttactcatatatactttagattgatttaaaacttcatttttaattta

aaaggatctaggtgaagatccttttgataatctcatgaccaaaatcccttaacgtgagttttcgttccactgagcgtcagac
cccgtagaaaagatcaaaggatcttcttgagatccttttttttctgcgcgtaatctgctgcttgcaaacaaaaaaaccaccgct
accagcggtggtttgtttgccggatcaagagctaccaactctttttccgaaggtaactggcttcagcagagcgcagatacc
aaatactgtccttctagtgtagccgtagttaggccaccacttcaagaactctgtagcaccgcctacatacctcgctctgctaa
tcctgttaccagtggctgctgccagtggcgataagtcgtgtcttaccgggttggactcaagacgatagttaccggataagg
cgcagcggtcgggctgaacgggggttcgtgcacacagcccagcttggagcgaacgacctacaccgaactgagata
cctacagcgtgagctatgagaaagcgccacgcttcccgaagggagaaaggcggacaggtatccggtaagcggcag
ggtcggaacaggagagcgcacgagggagcttccagggggaaacgcctggtatctttatagtcctgtcgggtttcgccac
ctctgacttgagcgtcgatttttgtgatgctcgtcaggggggcggagcctatggaaaaacgccagcaacgcggccttttac
ggttcctggccttttgctggccttttgctcacatgt

Cas9-2AGFP-pBKS plasmid sequence

ORIGIN

1 gcacttttcg gggaaatgtg cgcggaaccc ctatttgttt atttttctaa atacattcaa

61 atatgtatcc gctcatgaga caataaccct gataaatgct tcaataatat tgaaaaagga

121 agagtatgag tattcaacat ttccgtgtcg cccttattcc ctttttgcg gcattttgcc

181 ttcctgtttt tgctcaccca gaaacgctgg tgaaagtaaa agatgctgaa gatcagttgg

241 gtgcacgagt gggttacatc gaactggatc tcaacagcgg taagatcctt gagagttttc

301 gccccgaaga acgttttcca atgatgagca cttttaaagt tctgctatgt ggcgcggtat

361 tatcccgtat tgacgccggg caagagcaac tcggtcgccg catacactat tctcagaatg

421 acttggttga gtactcacca gtcacagaaa agcatcttac ggatggcatg acagtaagag

481 aattatgcag tgctgccata accatgagtg ataacactgc ggccaactta cttctgacaa

541 cgatcggagg accgaaggag ctaaccgctt ttttgcacaa catgggggat catgtaactc

601 gccttgatcg ttgggaaccg gagctgaatg aagccatacc aaacgacgag cgtgacacca

661 cgatgcctgt agcaatggca acaacgttgc gcaaactatt aactggcgaa ctacttactc

721 tagcttcccg gcaacaatta atagactgga tggaggcgga taaagttgca ggaccacttc

781 tgcgctcggc ccttccggct ggctggttta ttgctgataa atctggagcc ggtgagcgtg

841 ggtctcgcgg tatcattgca gcactggggc cagatggtaa gccctcccgt atcgtagtta

901 tctacacgac ggggagtcag gcaactatgg atgaacgaaa tagacagatc gctgagatag

961 gtgcctcact gattaagcat tggtaactgt cagaccaagt ttactcatat atactttaga

1021 ttgatttaaa acttcatttt taatttaaaa ggatctaggt gaagatcctt tttgataatc

1081 tcatgaccaa aatcccttaa cgtgagtttt cgttccactg agcgtcagac cccgtagaaa

1141 agatcaaagg atcttcttga gatccttttt ttctgcgcgt aatctgctgc ttgcaaacaa

1201 aaaaaccacc gctaccagcg gtggtttgtt tgccggatca agagctacca actcttttc

1261 cgaaggtaac tggcttcagc agagcgcaga taccaaatac tgtccttcta gtgtagccgt

1321 agttaggcca ccacttcaag aactctgtag caccgcctac atacctcgct ctgctaatcc

1381 tgttaccagt ggctgctgcc agtggcgata agtcgtgtct taccgggttg gactcaagac

1441 gatagttacc ggataaggcg cagcggtcgg gctgaacggg gggttcgtgc acacagccca

1501 gcttggagcg aacgacctac accgaactga gatacctaca gcgtgagcta tgagaaagcg

1561 ccacgcttcc cgaagggaga aaggcggaca ggtatccggt aagcggcagg gtcggaacag

1621 gagagcgcac gagggagctt ccagggggaa acgcctggta tctttatagt cctgtcgggt

1681 ttcgccacct ctgacttgag cgtcgatttt tgtgatgctc gtcaggggg cggagcctat

1741 ggaaaaacgc cagcaacgcg gccttttac ggttcctggc cttttgctgg ccttttgctc

1801 acatgttctt tcctgcgtta tcccctgatt ctgtggataa ccgtattacc gcctttgagt

1861 gagctgatac cgctcgccgc agccgaacga ccgagcgcag cgagtcagtg agcgaggaag

1921 cggaagagcg cccaatacgc aaaccgcctc tccccgcgcg ttggccgatt cattaatgca

1981 gctggcacga caggtttccc gactggaaag cgggcagtga gcgcaacgca attaatgtga

2041 gttagctcac tcattaggca ccccaggctt tacactttat gcttccggct cgtatgttgt

2101 gtggaattgt gagcggataa caatttcaca caggaaacag ctatgaccat gattacgcca

2161 agctcgaaat taaccctcac taaagggaac aaaagctggg tacccgttac ataacttacg

2221 gtaaatggcc cgcctggctg accgcccaac gacccccgcc cattgacgtc aatagtaacg

2281 ccaataggga ctttccattg acgtcaatgg gtggagtatt tacggtaaac tgcccacttg

2341 gcagtacatc aagtgtatca tatgccaagt acgccccta ttgacgtcaa tgacggtaaa

2401 tggcccgcct ggcattgtgc ccagtacatg accttatggg actttcctac ttggcagtac

2461 atctacgtat tagtcatcgc tattaccatg gtcgaggtga gccccacgtt ctgcttcact

2521 ctccccatct ccccccccctc cccaccccca attttgtatt tatttatttt ttaattattt

2581 tgtgcagcga tgggggcggg ggggggggggg gggcgcgcgc caggcggggc ggggcggggc

2641 gaggggcggg gcggggcgag gcggagaggt gcggcggcag ccaatcagag cggcgcgctc

2701 cgaaagtttc cttttatggc gaggcggcgg cggcggcggc cctataaaaa gcgaagcgcg

2761 cggcgggcgg gagtcgctgc gacgctgcct tcgccccgtg ccccgctccg ccgccgcctc

2821 gcgccgcccg ccccggctct gactgaccgc gttactccca caggtgagcg ggcgggacgg

2881 cccttctcct ccgggctgta attagctgag caagaggtaa gggtttaagg gatggttggt

2941 tggtggggta ttaatgttta attacctgga gcacctgcct gaaatcactt ttttttcaggt

3001 tggaccggtg ccaccatgga ctataaggac cacgacggag actacaagga tcatgatatt

3061 gattacaaag acgatgacga taagatggcc ccaaagaaga agcggaaggt cggtatccac

3121 ggagtcccag cagccgacaa gaagtacagc atcggcctgg acatcggcac caactctgtg

3181 ggctgggccg tgatcaccga cgagtacaag gtgcccagca agaaattcaa ggtgctgggc

3241 aacaccgacc ggcacagcat caagaagaac ctgatcggag ccctgctgtt cgacagcggc

3301 gaaacagccg aggccacccg gctgaagaga accgccagaa gaagatacac cagacggaag

3361 aaccggatct gctatctgca agagatcttc agcaacgaga tggccaaggt ggacgacagc

3421 ttcttccaca gactggaaga gtccttcctg gtggaagagg ataagaagca cgagcggcac

3481 cccatcttcg gcaacatcgt ggacgaggtg gcctaccacg agaagtaccc caccatctac

3541 cacctgagaa agaaactggt ggacagcacc gacaaggccg acctgcggct gatctatctg

3601 gccctggccc acatgatcaa gttccggggc cacttcctga tcgagggcga cctgaacccc

3661 gacaacagcg acgtggacaa gctgttcatc cagctggtgc agacctacaa ccagctgttc

3721 gaggaaaacc ccatcaacgc cagcggcgtg gacgccaagg ccatcctgtc tgccagactg

3781 agcaagagca gacggctgga aaatctgatc gcccagctgc ccggcgagaa gaagaatggc

3841 ctgttcggaa acctgattgc cctgagcctg ggcctgaccc ccaacttcaa gagcaacttc

3901 gacctggccg aggatgccaa actgcagctg agcaaggaca cctacgacga cgacctggac

3961 aacctgctgg cccagatcgg cgaccagtac gccgacctgt ttctggccgc caagaacctg

4021 tccgacgcca tcctgctgag cgacatcctg agagtgaaca ccgagatcac caaggccccc

4081 ctgagcgcct ctatgatcaa gagatacgac gagcaccacc aggacctgac cctgctgaaa

4141 gctctcgtgc ggcagcagct gcctgagaag tacaaagaga ttttcttcga ccagagcaag

4201 aacggctacg ccggctacat tgacggcgga gccagccagg aagagttcta caagttcatc

4261 aagcccatcc tggaaaagat ggacggcacc gaggaactgc tcgtgaagct gaacagagag

4321 gacctgctgc ggaagcagcg gaccttcgac aacggcagca tcccccacca gatccacctg

4381 ggagagctgc acgccattct gcggcggcag gaagattttt acccattcct gaaggacaac

4441 cgggaaaaga tcgagaagat cctgaccttc cgcatcccct actacgtggg ccctctggcc

4501 aggggaaaca gcagattcgc ctggatgacc agaaagagcg aggaaaccat caccccctgg

4561 aacttcgagg aagtggtgga caagggcgct tccgcccaga gcttcatcga gcggatgacc

4621 aacttcgata agaacctgcc caacgagaag gtgctgccca agcacagcct gctgtacgag

4681 tacttcaccg tgtataacga gctgaccaaa gtgaaatacg tgaccgaggg aatgagaaag

4741 cccgccttcc tgagcggcga gcagaaaaag gccatcgtgg acctgctgtt caagaccaac

4801 cggaaagtga ccgtgaagca gctgaaagag gactacttca agaaaatcga gtgcttcgac

4861 tccgtggaaa tctccggcgt ggaagatcgg ttcaacgcct ccctgggcac ataccacgat

4921 ctgctgaaaa ttatcaagga caaggacttc ctggacaatg aggaaaacga ggacattctg

4981 gaagatatcg tgctgaccct gacactgttt gaggacagag agatgatcga ggaacggctg

5041 aaaacctatg cccacctgtt cgacgacaaa gtgatgaagc agctgaagcg gcggagatac

5101 accggctggg gcaggctgag ccggaagctg atcaacggca tccgggacaa gcagtccggc

5161 aagacaatcc tggatttcct gaagtccgac ggcttcgcca acagaaactt catgcagctg

5221 atccacgacg acagcctgac ctttaaagag gacatccaga aagcccaggt gtccggccag

5281 ggcgatagcc tgcacgagca cattgccaat ctggccggca gccccgccat taagaagggc

5341 atcctgcaga cagtgaaggt ggtggacgag ctcgtgaaag tgatgggccg gcacaagccc

5401 gagaacatcg tgatcgaaat ggccagagag aaccagacca cccagaaggg acagaagaac

5461 agccgcgaga gaatgaagcg gatcgaagag ggcatcaaag agctgggcag ccagatcctg

5521 aaagaacacc ccgtggaaaa cacccagctg cagaacgaga agctgtacct gtactacctg

5581 cagaatgggc gggatatgta cgtggaccag gaactggaca tcaaccggct gtccgactac

5641 gatgtggacc atatcgtgcc tcagagcttt ctgaaggacg actccatcga caacaaggtg

5701 ctgaccagaa gcgacaagaa ccggggcaag agcgacaacg tgccctccga agaggtcgtg

5761 aagaagatga agaactactg gcggcagctg ctgaacgcca agctgattac ccagagaaag

5821 ttcgacaatc tgaccaaggc cgagagaggc ggcctgagcg aactggataa ggccggcttc

5881 atcaagagac agctggtgga aacccggcag atcacaaagc acgtggcaca gatcctggac

5941 tcccggatga acactaagta cgacgagaat gacaagctga tccgggaagt gaaagtgatc

6001 accctgaagt ccaagctggt gtccgatttc cggaaggatt tccagtttta caaagtgcgc

6061 gagatcaaca actaccacca cgcccacgac gcctacctga acgccgtcgt gggaaccgcc

6121 ctgatcaaaa agtaccctaa gctggaaagc gagttcgtgt acggcgacta caaggtgtac

6181 gacgtgcgga agatgatcgc caagagcgag caggaaatcg gcaaggctac cgccaagtac

6241 ttcttctaca gcaacatcat gaacttttтc aagaccgaga ttaccctggc caacggcgag

6301 atccggaagc ggcctctgat cgagacaaac ggcgaaaccg gggagatcgt gtgggataag

6361 ggccgggatt ttgccaccgt gcggaaagtg ctgagcatgc cccaagtgaa tatcgtgaaa

6421 aagaccgagg tgcagacagg cggcttcagc aaagagtcta tcctgcccaa gaggaacagc

6481 gataagctga tcgccagaaa gaaggactgg gaccctaaga agtacggcgg cttcgacagc

6541 cccaccgtgg cctattctgt gctggtggtg gccaaagtgg aaaagggcaa gtccaagaaa

6601 ctgaagagtg tgaaagagct gctggggatc accatcatgg aaagaagcag cttcgagaag

6661 aatcccatcg actttctgga agccaagggc tacaaagaag tgaaaaagga cctgatcatc

6721 aagctgccta agtactccct gttcgagctg gaaaacggcc ggaagagaat gctggcctct

6781 gccggcgaac tgcagaaggg aaacgaactg gccctgccct ccaaatatgt gaacttcctg

6841 tacctggcca gccactatga gaagctgaag ggctcccccg aggataatga gcagaaacag

6901 ctgtttgtgg aacagcacaa gcactacctg gacgagatca tcgagcagat cagcgagttc

6961 tccaagagag tgatcctggc cgacgctaat ctggacaaag tgctgtccgc ctacaacaag

7021 caccgggata agcccatcag agagcaggcc gagaatatca tccacctgtt taccctgacc

7081 aatctgggag cccctgccgc cttcaagtac tttgacacca ccatcgaccg gaagaggtac

7141 accagcacca aagaggtgct ggacgccacc ctgatccacc agagcatcac cggcctgtac

7201 gagacacgga tcgacctgtc tcagctggga ggcgacaaaa ggccggcggc cacgaaaaag

7261 gccggccagg caaaaaagaa aaaggaattc ggcagtggag agggcagagg aagtctgcta

7321 acatgcggtg acgtcgagga gaatcctggc ccagtgagca agggcgagga gctgttcacc

7381 ggggtggtgc ccatcctggt cgagctggac ggcgacgtaa acggccacaa gttcagcgtg

7441 tccggcgagg gcgagggcga tgccacctac ggcaagctga ccctgaagtt catctgcacc

7501 accggcaagc tgcccgtgcc ctggcccacc ctcgtgacca ccctgaccta cggcgtgcag

7561 tgcttcagcc gctaccccga ccacatgaag cagcacgact tcttcaagtc cgccatgccc

7621 gaaggctacg tccaggagcg caccatcttc ttcaaggacg acggcaacta caagacccgc

7681 gccgaggtga agttcgaggg cgacaccctg gtgaaccgca tcgagctgaa gggcatcgac

7741 ttcaaggagg acggcaacat cctggggcac aagctggagt acaactacaa cagccacaac

7801 gtctatatca tggccgacaa gcagaagaac ggcatcaagg tgaacttcaa gatccgccac

7861 aacatcgagg acggcagcgt gcagctcgcc gaccactacc agcagaacac ccccatcggc

7921 gacggccccg tgctgctgcc cgacaaccac tacctgagca cccagtccgc cctgagcaaa

7981 gaccccaacg agaagcgcga tcacatggtc ctgctggagt tcgtgaccgc cgccgggatc

8041 actctcggca tggacgagct gtacaaggaa ttctaactag agctcgctga tcagcctcga

8101 ctgtgccttc tagttgccag ccatctgttg tttgcccctc ccccgtgcct tccttgaccc

8161 tggaaggtgc cactcccact gtcctttcct aataaaatga ggaaattgca tcgcattgtc

8221 tgagtaggtg tcattctatt ctgggggggtg gggtggggca ggacagcaag ggggaggatt

8281 gggaagagaa tagcaggcat gctggggagc ggccgccacc gcggtggagc tccaattcgc

8341 cctatagtga gtcgtattac aattcactgg ccgtcgtttt acaacgtcgt gactgggaaa

8401 accctggcgt tacccaactt aatcgccttg cagcacatcc ccctttcgcc agctggcgta

8461 atagcgaaga ggcccgcacc gatcgccctt cccaacagtt gcgcagcctg aatggcgaat

8521 gggacgcgcc ctgtagcggc gcattaagcg cggcgggtgt ggtggttacg cgcagcgtga

8581 ccgctacact tgccagcgcc ctagcgcccg ctcctttcgc tttcttccct tcctttctcg

8641 ccacgttcgc cggctttccc cgtcaagctc taaatcgggg gctcccttta gggttccgat

8701 ttagtgcttt acggcacctc gaccccaaaa aacttgatta gggtgatggt tcacgtagtg

8761 ggccatcgcc ctgatagacg gtttttcgcc ctttgacgtt ggagtccacg ttctttaata

8821 gtggactctt gttccaaact ggaacaacac tcaaccctat ctcggtctat tcttttgatt

8881 tataagggat tttgccgatt tcggcctatt ggttaaaaaa tgagctgatt taacaaaaat

8941 ttaacgcgaa ttttaacaaa atattaacgc ttacaattta ggtg

Table 8.1: ToppGene Gene Ontology analysis of upregulated genes in SKBr3 KDM5B KO cells

Category	ID	Name	Source	p-value	q-value Bonferroni	q-value FDR B&H	q-value FDR B&Y	Hit Count in Query List	Hit Count in Genome	Hit in Query List
GO: Biological Process	GO:0042493	response to drug		1.89E-08	4.78E-05	4.78E-05	4.02E-04	12	481	MYC,CYP1A1,ANXA1,SRD5A1,CAV1,LCN2,SLC1A3,GAL,MGMT,MGST1, CCL2,ABCC2
GO: Biological Process	GO:0009636	response to toxic substance		1.18E-07	2.97E-04	1.48E-04	1.25E-03	9	269	CYP1A1,SRD5A1,GPX3,LCN2,SLC1A3,S100A9,MGMT,MGST1,CCL2
GO: Biological Process	GO:1901700	response to oxygen-containing compound		8.06E-07	2.03E-03	4.74E-04	3.99E-03	18	1614	CYP1A1,ANXA1,SRD5A1,GPX3,GBP2,CAV1,LCN2,SLC1A3,OLR1,ADM,S100A8,GAL,MGMT,IGFBP5,MGST1,EGR1,CCL2, ABCC2
GO: Biological Process	GO:0009611	response to wounding		8.95E-07	2.26E-03	4.74E-04	3.99E-03	14	967	MYC,CYP1A1,ANXA1,CAV1,PAPSS2,SLC1A3,FABP5,ADM,S100A8,S100A9,IER3,FGB,CCL2,GPRC5B
GO: Biological Process	GO:0043207	response to external biotic stimulus		1.13E-06	2.85E-03	4.74E-04	3.99E-03	14	986	CYP1A1,ANXA3,GBP2,CAV1,LCN2,SLC1A3,PLAC8,ADM,S100A8,S100A9,MGST1,IER3,FGB,CCL2
GO: Biological Process	GO:0051707	response to other organism		1.13E-06	2.85E-03	4.74E-04	3.99E-03	14	986	CYP1A1,ANXA3,GBP2,CAV1,LCN2,SLC1A3,PLAC8,ADM,S100A8,S100A9,MGST1,IER3,FGB,CCL2
GO: Biological Process	GO:0009617	response to bacterium		1.44E-06	3.64E-03	5.01E-04	4.21E-03	11	590	CYP1A1,ANXA3,GBP2,CAV1,PLAC8,ADM,S100A8,S100A9,MGST1,FGB,CCL2
GO: Biological Process	GO:0010243	response to organonitrogen compound		1.59E-06	4.01E-03	5.01E-04	4.21E-03	13	866	MYC,ANXA1,SRD5A1,CAV1,SLC1A3,ADM,GAL,MGMT,IGFBP5,MGST1,EGR1,CCL2,ABCC2
GO: Biological Process	GO:0009607	response to biotic stimulus		1.83E-06	4.61E-03	5.12E-04	4.30E-03	14	1027	CYP1A1,ANXA3,GBP2,CAV1,LCN2,SLC1A3,PLAC8,ADM,S100A8,S100A9,MGST1,IER3,FGB,CCL2
GO: Biological Process	GO:0043065	positive regulation of apoptotic process		3.63E-06	9.15E-03	9.08E-04	7.64E-03	11	649	MYC,BIN1,ANXA1,UBE2M,CAV1,ADM,S100A8,S100A9,GAL,EGR1,FGD3
GO: Biological Process	GO:0043068	positive regulation of programmed cell death		3.96E-06	9.99E-03	9.08E-04	7.64E-03	11	655	MYC,BIN1,ANXA1,UBE2M,CAV1,ADM,S100A8,S100A9,GAL,EGR1,FGD3
GO: Biological Process	GO:0006952	defense response		5.34E-06	1.35E-02	1.12E-03	9.43E-03	17	1651	ANXA1,ANXA3,GBP2,CAV1,LCN2,SLC1A3,OLR1,PLAC8,ADM,S100A8,S100A9,GAL,EGR1,IER3,FGB,CCL2,GPRC5B
GO: Biological Process	GO:1901698	response to nitrogen compound		6.25E-06	1.58E-02	1.21E-03	1.02E-02	13	981	MYC,ANXA1,SRD5A1,CAV1,SLC1A3,ADM,GAL,MGMT,IGFBP5,MGST1,EGR1,CCL2,ABCC2
GO: Biological Process	GO:0010942	positive regulation of cell death		6.96E-06	1.76E-02	1.22E-03	1.03E-02	11	695	MYC,BIN1,ANXA1,UBE2M,CAV1,ADM,S100A8,S100A9,GAL,EGR1,FGD3

GO: Biological Process	GO:0046916	cellular transition metal ion homeostasis		7.25E-06	1.83E-02	1.22E-03	1.03E-02	5	88	MYC,CP,LCN2,S100A8,S100A9
GO: Biological Process	GO:0042981	regulation of apoptotic process		8.23E-06	2.08E-02	1.23E-03	1.04E-02	16	1519	MYC,BIN1,ANXA1,UBE2M,CAV1,PLAC8,ADM,S100A8,S100A9,GAL,MGMT,EGR1,ER3,FGB,CCL2,FGD3
GO: Biological Process	GO:0010212	response to ionizing radiation		8.30E-06	2.09E-02	1.23E-03	1.04E-02	6	157	MYC,ANXA1,CAV1,MGMT,EGR1,CCL2
GO: Biological Process	GO:0043067	regulation of programmed cell death		9.47E-06	2.39E-02	1.33E-03	1.12E-02	16	1536	MYC,BIN1,ANXA1,UBE2M,CAV1,PLAC8,ADM,S100A8,S100A9,GAL,MGMT,EGR1,IER3,FGB,CCL2,FGD3
GO: Biological Process	GO:0002523	leukocyte migration involved in inflammatory response		1.21E-05	3.04E-02	1.48E-03	1.25E-02	3	15	S100A8,S100A9,CCL2
GO: Biological Process	GO:1903034	regulation of response to wounding		1.22E-05	3.08E-02	1.48E-03	1.25E-02	9	472	MYC,ANXA1,CAV1,S100A8,S100A9,IER3,FGB,CCL2, GPRC5B
GO: Biological Process	GO:0014070	response to organic cyclic compound		1.24E-05	3.11E-02	1.48E-03	1.25E-02	13	1045	CYP1A1,ANXA1,ANXA3,SRD5A1,CAV1,ADM,GAL,MGMT,IGFBP5, EGR1,SLC16A1,CCL2,ABCC2
GO: Biological Process	GO:0006873	cellular ion homeostasis		1.36E-05	3.44E-02	1.56E-03	1.31E-02	10	607	MYC,CP,CAV1,LCN2,CKB,ADM,S100A8,S100A9,CCL2, ABCC2
GO: Biological Process	GO:0051384	response to glucocorticoid		1.64E-05	4.15E-02	1.80E-03	1.52E-02	6	177	ANXA1,ANXA3,SRD5A1,CAV1,ADM,CCL2
GO: Biological Process	GO:0042742	defense response to bacterium		1.86E-05	4.69E-02	1.95E-03	1.64E-02	7	272	ANXA3,GBP2,PLAC8,ADM,S100A8,S100A9,FGB

Table 8.2: Table ToppGene Gene Ontology analysis of downregulated genes in SKBr3 KDM5B KO cells

Category	ID	Name	Source	p-value	q-value Bonferroni	q-value FDR B&H	q-value FDR B&Y	Hit Count in Query List	Hit Count in Genome	Hit in Query List
GO: Biological Process	GO:0060337	type I interferon signaling pathway		4.9E-14	8.9E-11	5.1E-11	4.1E-10	11	81	IFITM1,OAS1,OAS2,OAS3,IFITM2,IFI27, IFIT1,IRF9,ISG15,BST2,IFI6
GO: Biological Process	GO:0071357	cellular response to type I interferon		5.7E-14	1.0E-10	5.1E-11	4.1E-10	11	82	IFITM1,OAS1,OAS2,OAS3,IFITM2,IFI27,IFIT1 ,IRF9,ISG15,BST2,IFI6
GO: Biological Process	GO:0034340	response to type I interferon		9.8E-14	1.8E-10	5.9E-11	4.7E-10	11	86	IFITM1,OAS1,OAS2,OAS3,IFITM2,IFI27,IFIT1, IRF9,ISG15,BST2,IFI6
GO: Biological Process	GO:0045071	negative regulation of viral genome replication		2.6E-09	4.6E-06	1.2E-06	9.4E-06	7	52	IFITM1,OAS1,OAS3,IFITM2,IFIT1,ISG15,BST2
GO: Biological Process	GO:0045069	regulation of viral genome replication		5.6E-08	1.0E-04	2.0E-05	1.6E-04	7	80	IFITM1,OAS1,OAS3,IFITM2,IFIT1,ISG15,BST2
GO: Biological Process	GO:1903901	negative regulation of viral life cycle		1.5E-07	2.6E-04	4.4E-05	3.6E-04	7	92	IFITM1,OAS1,OAS3,IFITM2,IFIT1,ISG15,BST2

GO: Biological Process	GO:0048525	negative regulation of viral process		1.8E-07	3.3E-04	4.7E-05	3.8E-04	7	95	IFITM1,OAS1,OAS3,IFITM2,IFIT1,ISG15,BST2
GO: Biological Process	GO:0051607	defense response to virus		2.7E-07	4.9E-04	6.0E-05	4.8E-04	11	343	IFITM1,OAS1,OAS2,OAS3,IFITM2,IFIT1,IFIH1, IRF9,ISG15,BST2,DNAJC3
GO: Biological Process	GO:0019079	viral genome replication		3.0E-07	5.4E-04	6.0E-05	4.8E-04	7	102	IFITM1,OAS1,OAS3,IFITM2,IFIT1,ISG15,BST2
GO: Biological Process	GO:0009615	response to virus		2.4E-06	4.3E-03	4.3E-04	3.4E-03	11	428	IFITM1,OAS1,OAS2,OAS3,IFITM2,IFIT1,IFIH1, IRF9,ISG15,BST2,DNAJC3
GO: Biological Process	GO:0035455	response to interferon-alpha		2.8E-06	5.0E-03	4.5E-04	3.6E-03	4	23	IFITM1,OAS1,IFITM2,BST2
GO: Biological Process	GO:0045087	innate immune response		3.2E-06	5.7E-03	4.7E-04	3.8E-03	15	846	IFITM1,OAS1,OAS2,OAS3,IFITM2,IFI27,SP110, IFIT1,IFIH1,IRF9,RFTN1,ISG15,BST2,HERC6,IFI6
GO: Biological Process	GO:0019221	cytokine-mediated signaling pathway		4.6E-06	8.2E-03	6.3E-04	5.1E-03	12	553	IFITM1,OAS1,OAS2,OAS3,IFITM2,IFI27,IFIT1, STAT6,IRF9,ISG15,BST2,IFI6
GO: Biological Process	GO:0034341	response to interferon-gamma		7.0E-06	1.3E-02	9.0E-04	7.2E-03	7	163	IFITM1,OAS1,OAS2,OAS3,IFITM2,IRF9,BST2
GO: Biological Process	GO:0043901	negative regulation of multi-organism process		7.9E-06	1.4E-02	9.4E-04	7.6E-03	7	166	IFITM1,OAS1,OAS3,IFITM2,IFIT1,ISG15,BST2

GO: Biological Process	GO:1903900	regulation of viral life cycle		1.2E-05	2.1E-02	1.3E-03	1.0E-02	7	176	IFITM1,OAS1,OAS3,IFITM2,IFIT1,ISG15,BST2
GO: Biological Process	GO:0050792	regulation of viral process		1.8E-05	3.3E-02	1.9E-03	1.6E-02	7	189	IFITM1,OAS1,OAS3,IFITM2,IFIT1,ISG15,BST2
GO: Biological Process	GO:0043903	regulation of symbiosis, encompassing mutualism through parasitism		4.8E-05	8.7E-02	4.8E-03	3.9E-02	7	220	IFITM1,OAS1,OAS3,IFITM2,IFIT1,ISG15,BST2
GO: Biological Process	GO:0071345	cellular response to cytokine stimulus		5.7E-05	1.0E-01	5.4E-03	4.3E-02	12	713	IFITM1,OAS1,OAS2,OAS3,IFITM2,IFI27,IFIT1,STAT6,IRF9,ISG15,BST2,IFI6
GO: Biological Process	GO:0098542	defense response to other organism		6.4E-05	1.1E-01	5.7E-03	4.6E-02	11	609	IFITM1,OAS1,OAS2,OAS3,IFITM2,IFIT1,IFIH1,IRF9,ISG15,BST2,DNAJC3
GO: Biological Process	GO:0002252	immune effector process		7.3E-05	1.3E-01	6.2E-03	5.0E-02	13	851	IFITM1,OAS1,OAS2,OAS3,IFITM2,IFIT1,STAT6,IFIH1,IRF9,RFTN1,ISG15,BST2,DNAJC3
GO: Biological Process	GO:0032606	type I interferon production		1.7E-04	3.1E-01	1.4E-02	1.1E-01	5	119	POLR3GL,STAT6,IFIH1,IRF9,ISG15
GO: Biological Process	GO:0034097	response to cytokine		2.2E-04	4.0E-01	1.7E-02	1.4E-01	12	825	IFITM1,OAS1,OAS2,OAS3,IFITM2,IFI27,IFIT1,STAT6,IRF9,ISG15,BST2,IFI6

GO: Biological Process	GO:0060700	regulation of ribonuclease activity		2.8E-04	5.0E-01	2.1E-02	1.7E-01	2	6	OAS1,OAS3
GO: Biological Process	GO:0035456	response to interferon-beta		3.0E-04	5.3E-01	2.1E-02	1.7E-01	3	30	IFITM1,IFITM2,BST2
GO: Biological Process	GO:0033598	mammary gland epithelial cell proliferation		3.3E-04	5.9E-01	2.3E-02	1.8E-01	3	31	KDM5B,ID2,STAT6
GO: Biological Process	GO:0060333	interferon-gamma-mediated signaling pathway		5.1E-04	9.3E-01	3.4E-02	2.8E-01	4	85	OAS1,OAS2,OAS3,IRF9
GO: Biological Process	GO:0006952	defense response		6.4E-04	1.0E+00	4.0E-02	3.2E-01	17	1651	IFITM1,OAS1,OAS2,OAS3,IFITM2, IFI27,SP110,IFIT1,TFF3,IFIH1,IRF9, RFTN1,ISG15,BST2,HERC6,IFI6,DNAJC3
GO: Biological Process	GO:0045646	regulation of erythrocyte differentiation		6.5E-04	1.0E+00	4.0E-02	3.2E-01	3	39	ID2,P4HTM,ISG15
GO: Biological Process	GO:0033629	negative regulation of cell adhesion mediated by integrin		6.6E-04	1.0E+00	4.0E-02	3.2E-01	2	9	CYP1B1,MUC1

9 : References

1. Clarke, R. B., Anderson, E. & Howell, A. Steroid receptors in human breast cancer. *Trends Endocrinol. Metab.* **15,** 316–23 (2004).

2. Anderson, E., Clarke, R. B. & Howell, A. Estrogen responsiveness and control of normal human breast proliferation. *J. Mammary Gland Biol. Neoplasia* **3,** 23–35 (1998).

3. Petersen, O. W., Høyer, P. E. & Van Deurs, B. Frequency and distribution of estrogen receptor-positive cells in normal, nonlactating human breast tissue. *Cancer Res.* **47,** 5748–5751 (1987).

4. Kuiper, G. G., Enmark, E., Pelto-Huikko, M., Nilsson, S. & Gustafsson, J. A. Cloning of a novel receptor expressed in rat prostate and ovary. *Proc. Natl. Acad. Sci. U. S. A.* **93,** 5925–30 (1996).

5. Speirs, V., Skliris, G. P., Burdall, S. E. & Carder, P. J. Distinct expression patterns of ERα and ERβ in normal human mammary gland. *J. Clin. Pathol* **55,** 371–374 (2002).

6. Graham, J. D. & Clarke, C. L. Expression and transcriptional activity of progesterone receptor A and progesterone receptor B in mammalian cells. *Breast Cancer Res.* **4,** 187–190 (2002).

7. Mote, P. A., Bartow, S., Tran, N. & Clarke, C. L. Loss of co-ordinate expression of progesterone receptors A and B is an early event in breast carcinogenesis. *Breast Cancer Res. Treat.* **72,** 163–172 (2002).

8. Clarke, R. B., Howell, A., Potten, C. S. & Anderson, E. Dissociation between steroid receptor expression and cell proliferation in the human breast. *Cancer Res.* **57,** 4987–91 (1997).

9. Russo, J., Ao, X., Grill, C. & Russo, I. H. Pattern of distribution of cells positive for estrogen receptor a and progesterone receptor in relation to proliferating cells in the mammary gland. *Breast Cancer Res. Treat.* **53,** 217–227 (1999).

10. Zeps, N., Bentel, J. M., Papadimitriou, J. M., D'Antuono, M. F. & Dawkins, H. J. Estrogen receptor-negative epithelial cells in mouse mammary gland development and growth. *Differentiation* **62,** 221–226 (1998).

11. Capuco, A. V., Ellis, S., Wood, D. L., Akers, R. M. & Garrett, W. Postnatal mammary ductal growth: Three-dimensional imaging of cell proliferation, effects of estrogen treatment, and expression of steroid receptors in prepubertal calves. *Tissue Cell* **34,** 143–154 (2002).

12. Shoker, B. S., Jarvis, C., Clarke, R. B., Anderson, E., Hewlett, J., Davies, M. P. A., Sibson, D. R. & Sloane, J. P. Estrogen receptor-positive proliferating cells in the normal and precancerous breast. *Am. J. Pathol.* **155,** 1811–1815 (1999).

13. Roger, P., Sahla, M. E., Makela, S., Gustafsson, J. A., Baldet, P. & Rochefort, H. Decreased expression of estrogen receptor beta protein in proliferative preinvasive mammary tumors. *Cancer Res.* **61,** 2537–2541 (2001).

14. Jensen, E. V, Cheng, G., Palmieri, C., Saji, S., Makela, S., Van Noorden, S., Wahlstrom, T., Warner, M., Coombes, R. C. & Gustafsson, J. A. Estrogen receptors and proliferation markers in primary and recurrent breast cancer. *Proc Natl Acad Sci U S A* **98,** 15197–15202 (2001).

15. Marotti, J. D., Collins, L. C., Hu, R. & Tamimi, R. M. Estrogen receptor-beta expression in invasive breast cancer in relation to molecular phenotype: results from the Nurses' Health Study. *Mod. Pathol.* **23,** 197–204 (2010).

16. Holland, P. A., Knox, W. F., Potten, C. S., Howell, A., Anderson, E., Baildam, A. D. & Bundred, N. J. Assessment of hormone dependence of comedo ductal

carcinoma in situ of the breast. *J. Natl. Cancer Inst.* **89,** 1059–65 (1997).

17. Ström, A., Hartman, J., Foster, J. S., Kietz, S., Wimalasena, J. & Gustafsson, J.-A. Estrogen receptor beta inhibits 17beta-estradiol-stimulated proliferation of the breast cancer cell line T47D. *Proc. Natl. Acad. Sci. U. S. A.* **101,** 1566–71 (2004).

18. Mohsin, S. K., Weiss, H., Havighurst, T., Clark, G. M., Berardo, M., Roanh, L. D., To, T. V., Zho, Q., Love, R. R. & Allred, D. C. Progesterone receptor by immunohistochemistry and clinical outcome in breast cancer: A validation study. *Mod. Pathol.* **17,** 1545–1554 (2004).

19. Ferlay, J., Soerjomataram, I., Dikshit, R., Eser, S., Mathers, C., Rebelo, M., Parkin, D. M., Forman, D. & Bray, F. Cancer incidence and mortality worldwide: Sources, methods and major patterns in GLOBOCAN 2012. *Int. J. Cancer* **136,** E359–E386 (2015).

20. Torre, L. A., Bray, F., Siegel, R. L., Ferlay, J., Lortet-tieulent, J. & Jemal, A. Global Cancer Statistics, 2012. *CA a cancer J. Clin.* **65,** 87–108 (2015).

21. Cancer Research UK. (2017). Available at: http://www.cancerresearchuk.org/health-professional/cancer-statistics/statistics-by-cancer-type/breast-cancer#heading-Four. (Accessed: 14th November 2017)

22. Office for National Statistics. Cancer Registration Statistics, England: 2015. (2017). Available at: https://www.ons.gov.uk/peoplepopulationandcommunity/healthandsocialcare/conditionsanddiseases/bulletins/cancerregistrationstatisticsengland/2015#cancer-incidences-increase-while-deaths-from-cancer-decrease-over-time. (Accessed: 6th December 2017)

23. Singletary, S. E. Rating the Risk Factors for Breast Cancer. *Ann. Surg.* **237,** 474–482 (2003).

24. Ries, L., Eisner, M., Kosary, C., Hankey, B., Miller, B., Clegg, L. & Edwards, B. SEER Cancer Statistics Review, 1973–1997, National Cancer Institute. Bethesda, MD, 2000.

25. Brinton, L. A., Schairer, C., Hoover, R. N. & Fraumeni, J. F. Menstrual factors and risk of breast cancer. *Cancer Invest.* **6,** 245–54 (1988).

26. Trichopoulos, D., MacMahon, B. & Cole, P. Menopause and breast cancer risk. *J. Natl. Cancer Inst.* **48,** 605–13 (1972).

27. White, E. Projected changes in breast cancer incidence due to the trend toward delayed childbearing. *Am. J. Public Health* **77,** 495–497 (1987).

28. Brinton, L. A., Hoover, R. & Fraumeni, J. F. Reproductive factors in the aetiology of breast cancer. *Br. J. Cancer* **47,** 757–762 (1983).

29. Ellison, R. C., Zhang, Y., McLennan, C. E. & Rothman, K. J. Exploring the relation of alcohol consumption to risk of breast cancer. *Am. J. Epidemiol.* **154,** 740–747 (2001).

30. Tretli, S. Height and weight in relation to breast cancer morbidity and mortality. A prospective study of 570,000 women in Norway. *Int. J. Cancer* **44,** 23–30 (1989).

31. Clemons, M., Loijens, L. & Goss, P. Breast cancer risk following irradiation for Hodgkin's disease. *Cancer Treat. Rev.* **26,** 291–302 (2000).

32. Boice, J. D., Preston, D., Davis, F. G. & Monson, R. R. Frequent chest X-ray fluoroscopy and breast cancer incidence among tuberculosis patients in Massachusetts. *Radiat. Res.* **125,** 214–222 (1991).

33. Pharoah, P. D., Day, N. E., Duffy, S., Easton, D. F. & Ponder, B. A. Family history and the risk of breast cancer: a systematic review and meta-analysis. *Int. J. cancer* **71,** 800–9 (1997).

34. Easton, D. F., Ford, D. & Bishop, D. T. Breast and ovarian cancer incidence in BRCA1-mutation carriers. Breast Cancer Linkage Consortium. *Am. J. Hum. Genet.* **56,** 265–271 (1995).

35. Nelson, H. D., Humphrey, L. L., Nygren, P., Teutsch, S. M. & Allan, J. D. Postmenopausal hormone replacement therapy: scientific review. *JAMA* **288,** 872–81 (2002).

36. Rosen, P. P., Groshen, S., Kinne, D. W. & Hellman, S. Contralateral breast carcinoma: an assessment of risk and prognosis in stage I (T1N0M0) and stage II (T1N1M0) patients with 20-year follow-up. *Surgery* **106,** 904–10 (1989).

37. Hankey, B. F., Curtis, R. E., Naughton, M. D., Boice, J. D. J. & Flannery, J. T. A retrospective cohort analysis of second breast cancer risk for primary breast cancer patients with an assessment of the effect of radiation therapy. *J. Natl. Cancer Inst.* **70,** 797–804 (1983).

38. Begg, C. B. On the use of familial aggregation in population-based case probands for calculating penetrance. *J. Natl. Cancer Inst.* **94,** 1221–1226 (2002).

39. Patnick, J. NHS breast screening: the progression from one to two views. *J Med Screen* **11,** 55–56 (2004).

40. PHE. NHS Breast Screening Programme Consolidated standards. (2017). Available at: https://www.gov.uk/government/uploads/system/uploads/attachment_data/file/612739/Breast_screening_consolidated_standards.pdf. (Accessed: 4th December 2017)

41. Independent UK panel on breast cancer screening. The benefits and harms of breast cancer screening: an independent review. *Lancet (London, England)* **380,** 1778–86 (2012).

42. Reis-Filho, J. S. & Pusztai, L. Gene expression profiling in breast cancer: Classification, prognostication, and prediction. *Lancet* **378,** 1812–1823 (2011).

43. Perou, C. M., Sørlie, T., Eisen, M. B., van de Rijn, M., Jeffrey, S. S., Rees, C. a, Pollack, J. R., Ross, D. T., Johnsen, H., Akslen, L. a, Fluge, O., Pergamenschikov, a, Williams, C., Zhu, S. X., Lønning, P. E., Børresen-Dale, a L., Brown, P. O. & Botstein, D. Molecular portraits of human breast tumours. *Nature* **406,** 747–752 (2000).

44. Sorlie, T., Perou, C. M., Tibshirani, R., Aas, T., Geisler, S., Johnsen, H., Hastie, T., Eisen, M. B., van de Rijn, M., Jeffrey, S. S., Thorsen, T., Quist, H., Matese, J. C., Brown, P. O., Botstein, D., Eystein Lonning, P. & Borresen-Dale, A. L. Gene expression patterns of breast carcinomas distinguish tumor subclasses with clinical implications. *Proc. Natl. Acad. Sci. U. S. A.* **98,** 10869–10874 (2001).

45. Parker, J. S., Mullins, M., Cheang, M. C., Leung, S., Voduc, D., Vickery, T., Davies, S., Fauron, C., He, X., Hu, Z., Quackenbush, J. F., Stijleman, I. J., Palazzo, J., Marron, J. S., Nobel, A. B., Mardis, E., Nielsen, T. O., Ellis, M. J., Perou, C. M. & Bernard, P. S. Supervised risk predictor of breast cancer based on intrinsic subtypes. *J Clin Oncol* **27,** 1160–1167 (2009).

46. Curtis, C., Shah, S. P., Chin, S.-F., Turashvili, G., Rueda, O. M., Dunning, M. J., Speed, D., Lynch, A. G., Samarajiwa, S., Yuan, Y., Gräf, S., Ha, G., Haffari, G., Bashashati, A., Russell, R., McKinney, S., Langerød, A., Green, A., Provenzano, E., Wishart, G., Pinder, S., Watson, P., Markowetz, F., Murphy, L., Ellis, I.,

Purushotham, A., Børresen-Dale, A.-L., Brenton, J. D., Tavaré, S., Caldas, C. & Aparicio, S. The genomic and transcriptomic architecture of 2,000 breast tumours reveals novel subgroups. *Nature* **486,** 346–52 (2012).

47. Paik, S., Shak, S., Tang, G., Kim, C., Baker, J., Cronin, M., Baehner, F. L., Walker, M. G., Watson, D., Park, T., Hiller, W., Fisher, E. R., Wickerham, D. L., Bryant, J. & Wolmark, N. A multigene assay to predict recurrence of tamoxifen-treated, node-negative breast cancer. *N. Engl. J. Med.* **351,** 2817–26 (2004).

48. NICE. Gene expression profiling and expanded immunohistochemistry tests for guiding adjuvant chemotherapy decisions in early breast cancer management: MammaPrint, Oncotype DX, IHC4 and Mammostrat. (2013). Available at: https://www.nice.org.uk/guidance/dg10. (Accessed: 6th December 2017)

49. National Institute for Health and Care Excellence. Early and locally advanced breast cancer: diagnosis and treatment. (2017). Available at: https://www.nice.org.uk/guidance/cg80/chapter/Key-priorities-for-implementation. (Accessed: 4th December 2017)

50. Wu, D., Si, M., Xue, H.-Y. & Wong, H.-L. Nanomedicine applications in the treatment of breast cancer: current state of the art. *Int. J. Nanomedicine* **12,** 5879—5892 (2017).

51. Breast Cancer Trialists, E. & Group, C. Relevance of breast cancer hormone receptors and other factors to the effi cacy of adjuvant tamoxifen: patient-level meta-analysis of randomised trials. *Lancet* **378,** 771–784 (2011).

52. Fisher, B., Costantino, J. P., Wickerham, D. L., Cecchini, R. S., Cronin, W. M., Robidoux, A., Bevers, T. B., Kavanah, M. T., Atkins, J. N., Margolese, R. G., Runowicz, C. D., James, J. M., Ford, L. G. & Wolmark, N. Tamoxifen for the Prevention of Breast Cancer: Current Status of the National Surgical Adjuvant Breast and Bowel Project P-1 Study. *JNCI J. Natl. Cancer Inst.* **97,** 1652–1662 (2005).

53. Vogel, V. G., Costantino, J. P., Wickerham, D. L., Cronin, W. M., Cecchini, R. S., Atkins, J. N., Bevers, T. B., Fehrenbacher, L., Pajon, E. R., Wade, J. L., Robidoux, A., Margolese, R. G., James, J., Runowicz, C. D., Ganz, P. A., Reis, S. E., McCaskill-Stevens, W., Ford, L. G., Jordan, V. C. & Wolmark, N. Update of the national surgical adjuvant breast and bowel project Study of Tamoxifen and Raloxifene (STAR) P-2 trial: Preventing breast cancer. *Cancer Prev. Res.* **3,** 696–706 (2010).

54. Rakha, E. A., El-Rehim, D. A., Paish, C., Green, A. R., Lee, A. H. S., Robertson, J. F., Blamey, R. W., Macmillan, D. & Ellis, I. O. Basal phenotype identifies a poor prognostic subgroup of breast cancer of clinical importance. *Eur. J. Cancer* **42,** 3149–3156 (2006).

55. Carey, L. A., Perou, C. M., Livasy, C. A., Dressler, L. G., Cowan, D., Conway, K., Karaca, G., Troester, M. A., Tse, C. K., Edmiston, S., Deming, S. L., Geradts, J., Cheang, M. C. U., Nielsen, T. O., Moorman, P. G., Earp, H. S. & Millikan, R. C. Race, Breast Cancer Subtypes, and Survival in the Carolina Breast Cancer Study. *JAMA* **295,** 2492 (2006).

56. Wahba, H. A. & El-Hadaad, H. A. Current approaches in treatment of triple-negative breast cancer. *Cancer Biol. Med.* **12,** 106–16 (2015).

57. Atchley, D. P., Albarracin, C. T., Lopez, A., Valero, V., Amos, C. I., Gonzalez-Angulo, A. M., Hortobagyi, G. N. & Arun, B. K. Clinical and pathologic characteristics of patients with BRCA-positive and BRCA-negative breast cancer. *J. Clin. Oncol.* **26,** 4282–4288 (2008).

58. Gonzalez-Angulo, A. M., Timms, K. M., Liu, S., Chen, H., Litton, J. K., Potter, J.,

Lanchbury, J. S., Stemke-Hale, K., Hennessy, B. T., Arun, B. K., Hortobagyi, G. N., Do, K.-A., Mills, G. B. & Meric-Bernstam, F. Incidence and outcome of BRCA mutations in unselected patients with triple receptor-negative breast cancer. *Clin. Cancer Res.* **17,** 1082–9 (2011).

59. Turner, N., Tutt, A. & Ashworth, A. Hallmarks of 'BRCAness' in sporadic cancers. *Nature Reviews Cancer* **4,** 814–819 (2004).

60. Farmer, H., McCabe, N., Lord, C. J., Tutt, A. N. J., Johnson, D. A., Richardson, T. B., Santarosa, M., Dillon, K. J., Hickson, I., Knights, C., Martin, N. M. B., Jackson, S. P., Smith, G. C. M. & Ashworth, A. Targeting the DNA repair defect in BRCA mutant cells as a therapeutic strategy. *Nature* **434,** 917–921 (2005).

61. Dizdar, O., Arslan, C. & Altundag, K. Advances in PARP inhibitors for the treatment of breast cancer. *Expert Opin. Pharmacother.* **16,** 2751–2758 (2015).

62. Soliman, H., Khalil, F. & Antonia, S. PD-L1 expression is increased in a subset of basal type breast cancer cells. *PLoS One* **9,** (2014).

63. Mittendorf, E. A., Philips, A. V, Meric-Bernstam, F., Qiao, N., Wu, Y., Harrington, S., Su, X., Wang, Y., Gonzalez-Angulo, A. M., Akcakanat, A., Chawla, A., Curran, M., Hwu, P., Sharma, P., Litton, J. K., Molldrem, J. J. & Alatrash, G. PD-L1 Expression in Triple-Negative Breast Cancer. *Cancer Immunol. Res.* **28,** 361–370 (2014).

64. Butte, M. J., Keir, M. E., Phamduy, T. B., Sharpe, A. H. & Freeman, G. J. Programmed Death-1 Ligand 1 Interacts Specifically with the B7-1 Costimulatory Molecule to Inhibit T Cell Responses. *Immunity* **27,** 111–122 (2007).

65. Masoud, V. & Pages, G. Targeted therapies in breast cancer: New challenges to fight against resistance. *World J Clin Oncol* **8,** 96–177 (2017).

66. Yu, L. Y., Li, M. P., Kuang, D. Bin, Zhang, C. M. & Chen, X. P. New immunotherapy strategies in breast cancer. *Chinese Pharmacol. Bull.* **32,** 1037–1040 (2016).

67. Slamon, D. J., Godolphin, W., Jones, L. A., Holt, J. A., Wong, S. G., Keith, D. E., Levin, W. J., Stuart, S. G., Udove, J., Ullrich, A. & al., et. Studies of the HER-2/neu proto-oncogene in human breast and ovarian cancer. *Science (80-.).* **244,** 707–712 (1989).

68. Roskoski, R. The ErbB/HER family of protein-tyrosine kinases and cancer. *Pharmacological Research* **79,** 34–74 (2014).

69. Slamon, D. J., Leyland-Jones, B., Shak, S., Fuchs, H., Paton, V., Bajamonde, A., Fleming, T., Eiermann, W., Wolter, J., Pegram, M., Baselga, J. & Norton, L. Use of Chemotherapy plus a Monoclonal Antibody against HER2 for Metastatic Breast Cancer That Overexpresses HER2. *N. Engl. J. Med.* **344,** 783–792 (2001).

70. Pegram, M. D., Lipton, A., Hayes, D. F., Weber, B. L., Baselga, J. M., Tripathy, D., Baly, D., Baughman, S. A., Twaddell, T., Glaspy, J. A. & Slamon, D. J. Phase II study of receptor-enhanced chemosensitivity using recombinant humanized anti-p185(HER2/neu) monoclonal antibody plus cisplatin in patients with HER2/neu-overexpressing metastatic breast cancer refractory to chemotherapy treatment. *J. Clin. Oncol.* **16,** 2659–2671 (1998).

71. Adams, C. W., Allison, D. E., Flagella, K., Presta, L., Clarke, J., Dybdal, N., McKeever, K. & Sliwkowski, M. X. Humanization of a recombinant monoclonal antibody to produce a therapeutic HER dimerization inhibitor, pertuzumab. *Cancer Immunol. Immunother.* **55,** 717–727 (2006).

72. Konecny, G. E., Pegram, M. D., Venkatesan, N., Finn, R., Yang, G., Rahmeh, M., Untch, M., Rusnak, D. W., Spehar, G., Mullin, R. J., Keith, B. R., Gilmer, T. M., Berger, M., Podratz, K. C. & Slamon, D. J. Activity of the dual kinase inhibitor lapatinib (GW572016) against HER-2-overexpressing and trastuzumab-treated breast cancer cells. *Cancer Res* **66,** 1630–1639 (2006).

73. Lewis Phillips, G. D., Li, G., Dugger, D. L., Crocker, L. M., Parsons, K. L., Mai, E., Blättler, W. A., Lambert, J. M., Chari, R. V. J., Lutz, R. J., Wong, W. L. T., Jacobson, F. S., Koeppen, H., Schwall, R. H., Kenkare-Mitra, S. R., Spencer, S. D. & Sliwkowski, M. X. Targeting HER2-positive breast cancer with trastuzumab-DM1, an antibody-cytotoxic drug conjugate. *Cancer Res.* **68,** 9280–9290 (2008).

74. Carter, P., Presta, L., Gorman, C. M., Ridgway, J. B., Henner, D., Wong, W. L., Rowland, a M., Kotts, C., Carver, M. E. & Shepard, H. M. Humanization of an anti-p185HER2 antibody for human cancer therapy. *Proc. Natl. Acad. Sci. U. S. A.* **89,** 4285–4289 (1992).

75. Moja, L., Tagliabue, L., Balduzzi, S., Parmelli, E., Pistotti, V., Guarneri, V. & D'Amico, R. Trastuzumab containing regimens for early breast cancer. *Cochrane Database of Systematic Reviews* (2012). doi:10.1002/14651858.CD006243

76. Gianni, L., Pienkowski, T., Im, Y. H., Roman, L., Tseng, L. M., Liu, M. C., Lluch, A., Staroslawska, E., de la Haba-Rodriguez, J., Im, S. A., Pedrini, J. L., Poirier, B., Morandi, P., Semiglazov, V., Srimuninnimit, V., Bianchi, G., Szado, T., Ratnayake, J., Ross, G. & Valagussa, P. Efficacy and safety of neoadjuvant pertuzumab and trastuzumab in women with locally advanced, inflammatory, or early HER2-positive breast cancer (NeoSphere): A randomised multicentre, open-label, phase 2 trial. *Lancet Oncol.* **13,** 25–32 (2012).

77. Nagata, Y., Lan, K. H., Zhou, X., Tan, M., Esteva, F. J., Sahin, A. A., Klos, K. S., Li, P., Monia, B. P., Nguyen, N. T., Hortobagyi, G. N., Hung, M. C. & Yu, D. PTEN activation contributes to tumor inhibition by trastuzumab, and loss of PTEN predicts trastuzumab resistance in patients. *Cancer Cell* **6,** 117–127 (2004).

78. Junttila, T. T., Akita, R. W., Parsons, K., Fields, C., Lewis Phillips, G. D., Friedman, L. S., Sampath, D. & Sliwkowski, M. X. Ligand-Independent HER2/HER3/PI3K Complex Is Disrupted by Trastuzumab and Is Effectively Inhibited by the PI3K Inhibitor GDC-0941. *Cancer Cell* **15,** 429–440 (2009).

79. Arnould, L., Gelly, M., Penault-Llorca, F., Benoit, L., Bonnetain, F., Migeon, C., Cabaret, V., Fermeaux, V., Bertheau, P., Garnier, J., Jeannin, J.-F. & Coudert, B. Trastuzumab-based treatment of HER2-positive breast cancer: an antibody-dependent cellular cytotoxicity mechanism? *Br. J. Cancer* **94,** 259–267 (2006).

80. Cooley, S., Burns, L. J., Repka, T. & Miller, J. S. Natural killer cell cytotoxicity of breast cancer targets is enhanced by two distinct mechanisms of antibody-dependent cellular cytotoxicity against LFA-3 and HER2/neu. *Exp. Hematol.* **27,** 1533–1541 (1999).

81. Lambert, J. M. & Chari, R. V. J. Ado-trastuzumab emtansine (T-DM1): An antibody-drug conjugate (ADC) for HER2-positive breast cancer. *J. Med. Chem.* **57,** 6949–6964 (2014).

82. Krop, I. E., Kim, S. B., González-Martín, A., LoRusso, P. M., Ferrero, J. M., Smitt, M., Yu, R., Leung, A. C. F. & Wildiers, H. Trastuzumab emtansine versus treatment of physician's choice for pretreated HER2-positive advanced breast cancer (TH3RESA): A randomised, open-label, phase 3 trial. *Lancet Oncol.* **15,** 689–699 (2014).

83. Verma, S., Miles, D., Gianni, L., Krop, I. E., Welslau, M., Baselga, J., Pegram,

M., Oh, D.-Y., Diéras, V., Guardino, E., Fang, L., Lu, M. W., Olsen, S. & Blackwell, K. Trastuzumab Emtansine for HER2-Positive Advanced Breast Cancer. *N. Engl. J. Med.* **367,** 1783–1791 (2012).

84. Scheuer, W., Friess, T., Burtscher, H., Bossenmaier, B., Endl, J. & Hasmann, M. Strongly enhanced antitumor activity of trastuzumab and pertuzumab combination treatment on HER2-positive human xenograft tumor models. *Cancer Res.* **69,** 9330–9336 (2009).

85. Blackwell, K. L., Burstein, H. J., Storniolo, A. M., Rugo, H., Sledge, G., Koehler, M., Ellis, C., Casey, M., Vukelja, S., Bischoff, J., Baselga, J. & O'Shaughnessy, J. Randomized study of lapatinib alone or in combination with trastuzumab in women with ErbB2-positive, trastuzumab-refractory metastatic breast cancer. *J. Clin. Oncol.* **28,** 1124–1130 (2010).

86. Geyer, C. E., Forster, J., Lindquist, D., Chan, S., Romieu, C. G., Pienkowski, T., Jagiello-Gruszfeld, A., Crown, J., Chan, A., Kaufman, B., Skarlos, D., Campone, M., Davidson, N., Berger, M., Oliva, C., Rubin, S. D., Stein, S. & Cameron, D. Lapatinib plus Capecitabine for HER2-Positive Advanced Breast Cancer. *N. Engl. J. Med.* **355,** 2733–2743 (2006).

87. Johnston, S., Pippen, J., Pivot, X., Lichinitser, M., Sadeghi, S., Dieras, V., Gomez, H. L., Romieu, G., Manikhas, A., Kennedy, M. J., Press, M. F., Maltzman, J., Florance, A., O'Rourke, L., Oliva, C., Stein, S. & Pegram, M. Lapatinib combined with letrozole versus letrozole and placebo as first-line therapy for postmenopausal hormone receptor - Positive metastatic breast cancer. *J. Clin. Oncol.* **27,** 5538–5546 (2009).

88. Baselga, J., Bradbury, I., Eidtmann, H., Di Cosimo, S., De Azambuja, E., Aura, C., Gómez, H., Dinh, P., Fauria, K., Van Dooren, V., Aktan, G., Goldhirsch, A., Chang, T. W., Horváth, Z., Coccia-Portugal, M., Domont, J., Tseng, L. M., Kunz, G., Sohn, J. H., Semiglazov, V., Lerzo, G., Palacova, M., Probachai, V., Pusztai, L., Untch, M., Gelber, R. D. & Piccart-Gebhart, M. Lapatinib with trastuzumab for HER2-positive early breast cancer (NeoALTTO): A randomised, open-label, multicentre, phase 3 trial. in *The Lancet* **379,** 633–640 (2012).

89. Rabindran, S. K., Discafani, C. M., Rosfjord, E. C., Baxter, M., Floyd, M. B., Golas, J., Hallett, W. A., Johnson, B. D., Nilakantan, R., Overbeek, E., Reich, M. F., Shen, R., Shi, X., Tsou, H. R., Wang, Y. F. & Wissner, A. Antitumor activity of HKI-272, an orally active, irreversible inhibitor of the HER-2 tyrosine kinase. *Cancer Res.* **64,** 3958–3965 (2004).

90. Chan, A., Delaloge, S., Holmes, F. A., Moy, B., Iwata, H., Harvey, V. J., Robert, N. J., Silovski, T., Gokmen, E., von Minckwitz, G., Ejlertsen, B., Chia, S. K. L., Mansi, J., Barrios, C. H., Gnant, M., Buyse, M., Gore, I., Smith, J., Harker, G., Masuda, N., Petrakova, K., Zotano, A. G., Iannotti, N., Rodriguez, G., Tassone, P., Wong, A., Bryce, R., Ye, Y., Yao, B. & Martin, M. Neratinib after trastuzumab-based adjuvant therapy in patients with HER2-positive breast cancer (ExteNET): A multicentre, randomised, double-blind, placebo-controlled, phase 3 trial. *Lancet Oncol.* **17,** 367–377 (2016).

91. U.S. Food and Drug Administration. FDA approves neratinib for extended adjuvant treatment of early stage HER2-positive breast cancer. (2017). Available at: https://www.fda.gov/drugs/informationondrugs/approveddrugs/ucm567259.htm. (Accessed: 6th November 2017)

92. Vu, T. & Claret, F. X. Trastuzumab: Updated Mechanisms of Action and Resistance in Breast Cancer. *Front. Oncol.* **2,** (2012).

93. Arribas, J., Baselga, J., Pedersen, K. & Parra-Palau, J. L. p95HER2 and breast

cancer. *Cancer Research* **71,** 1515–1519 (2011).

94. Scaltriti, M., Rojo, F., Ocaña, A., Anido, J., Guzman, M., Cortes, J., Di Cosimo, S., Matias-Guiu, X., Ramon y Cajal, S., Arribas, J. & Baselga, J. Expression of p95HER2, a truncated form of the HER2 receptor, and response to Anti-HER2 therapies in breast cancer. *J. Natl. Cancer Inst.* **99,** 628–638 (2007).

95. Sperinde, J., Jin, X., Banerjee, J., Penuel, E., Saha, A., Diedrich, G., Huang, W., Leitzel, K., Weidler, J., Ali, S. M., Fuchs, E. M., Singer, C. F., Köstler, W. J., Bates, M., Parry, G., Winslow, J. & Lipton, A. Quantitation of p95HER2 in paraffin sections by using a p95-specific antibody and correlation with outcome in a cohort of trastuzumab-treated breast cancer patients. *Clin. Cancer Res.* **16,** 4226–4235 (2010).

96. Kwong, K. Y. & Hung, M. C. A novel splice variant of HER2 with increased transformation activity. *Mol. Carcinog.* **23,** 62–68 (1998).

97. Castiglioni, F., Tagliabue, E., Campiglio, M., Pupa, S. M., Balsari, A. & Ménard, S. Role of exon-16-deleted HER2 in breast carcinomas. *Endocr. Relat. Cancer* **13,** 221–232 (2006).

98. Mitra, D., Brumlik, M. J., Okamgba, S. U., Zhu, Y., Duplessis, T. T., Parvani, J. G., Lesko, S. M., Brogi, E. & Jones, F. E. An oncogenic isoform of HER2 associated with locally disseminated breast cancer and trastuzumab resistance. *Mol. Cancer Ther.* **8,** 2152–2162 (2009).

99. Mayer, E. L., Baurain, J.-F., Sparano, J., Strauss, L., Campone, M., Fumoleau, P., Rugo, H., Awada, A., Sy, O. & Llombart-Cussac, A. A phase 2 trial of dasatinib in patients with advanced HER2-positive and/or hormone receptor-positive breast cancer. *Clin. Cancer Res.* **17,** 6897–904 (2011).

100. Neckers, L. Heat shock protein 90: The cancer chaperone. *J. Biosci.* **32,** 517–530 (2007).

101. Scaltriti, M., Serra, V., Normant, E., Guzman, M., Rodriguez, O., Lim, A. R., Slocum, K. L., West, K. A., Rodriguez, V., Prudkin, L., Jimenez, J., Aura, C. & Baselga, J. Antitumor Activity of the Hsp90 Inhibitor IPI-504 in HER2-Positive Trastuzumab-Resistant Breast Cancer. *Mol. Cancer Ther.* **10,** 817–824 (2011).

102. Wainberg, Z. A., Anghel, A., Rogers, A. M., Desai, A. J., Kalous, O., Conklin, D., Ayala, R., O'Brien, N. A., Quadt, C., Akimov, M., Slamon, D. J. & Finn, R. S. Inhibition of HSP90 with AUY922 Induces Synergy in HER2-Amplified Trastuzumab-Resistant Breast and Gastric Cancer. *Mol. Cancer Ther.* **12,** 509–519 (2013).

103. Mittendorf, E. A., Wu, Y., Scaltriti, M., Meric-Bernstam, F., Hunt, K. K., Dawood, S., Esteva, F. J., Buzdar, A. U., Chen, H., Eksambi, S., Hortobagyi, G. N., Baselga, J. & Gonzalez-Angulo, A. M. Loss of HER2 amplification following trastuzumab-based neoadjuvant systemic therapy and survival outcomes. *Clin Cancer Res* **15,** 7381–7388 (2009).

104. Berns, K., Horlings, H. M., Hennessy, B. T., Madiredjo, M., Hijmans, E. M., Beelen, K., Linn, S. C., Gonzalez-Angulo, A. M., Stemke-Hale, K., Hauptmann, M., Beijersbergen, R. L., Mills, G. B., van de Vijver, M. J. & Bernards, R. A Functional Genetic Approach Identifies the PI3K Pathway as a Major Determinant of Trastuzumab Resistance in Breast Cancer. *Cancer Cell* **12,** 395–402 (2007).

105. Eichhorn, P. J. A., Gili, M., Scaltriti, M., Serra, V., Guzman, M., Nijkamp, W., Beijersbergen, R. L., Valero, V., Seoane, J., Bernards, R. & Baselga, J. Phosphatidylinositol 3-kinase hyperactivation results in lapatinib resistance that is reversed by the mTOR/phosphatidylinositol 3-kinase inhibitor NVP-BEZ235.

Cancer Res. **68,** 9221–9230 (2008).

106. Giuliano, M., Hu, H., Wang, Y. C., Fu, X., Nardone, A., Herrera, S., Mao, S., Contreras, A., Gutierrez, C., Wang, T., Hilsenbeck, S. G., Angelis, C. D., Wang, N. J., Heiser, L. M., Gray, J. W., Lopez-Tarruella, S., Pavlick, A. C., Trivedi, M. V., Chamness, G. C., Chang, J. C., Osborne, C. K., Rimawi, M. F. & Schiff, R. Upregulation of ER signaling as an adaptive mechanism of cell survival in HER2-positive breast tumors treated with Anti-HER2 therapy. *Clin. Cancer Res.* **21,** 3995–4003 (2015).

107. Nahta, R., Yuan, L. X. H., Zhang, B., Kobayashi, R. & Esteva, F. J. Insulin-like growth factor-I receptor/human epidermal growth factor receptor 2 heterodimerization contributes to trastuzumab resistance of breast cancer cells. *Cancer Res.* **65,** 11118–11128 (2005).

108. Ritter, C. A., Perez-Torres, M., Rinehart, C., Guix, M., Dugger, T., Engelman, J. A. & Arteaga, C. L. Human breast cancer cells selected for resistance to trastuzumab in vivo overexpress epidermal growth factor receptor and ErbB ligands and remain dependent on the ErbB receptor network. *Clin. Cancer Res.* **13,** 4909–4919 (2007).

109. Gijsen, M., King, P., Perera, T., Parker, P. J., Harris, A. L., Larijani, B. & Kong, A. HER2 phosphorylation is maintained by a PKB negative feedback loop in response to anti-HER2 herceptin in breast cancer. *PLoS Biol* **8,** e1000563 (2010).

110. De Mattos-Arruda, L., Bottai, G., Nuciforo, P. G., Di Tommaso, L., Giovannetti, E., Peg, V., Losurdo, A., Pérez-Garcia, J., Masci, G., Corsi, F., Cortés, J., Seoane, J., Calin, G. A. & Santarpia, L. MicroRNA-21 links epithelial-to-mesenchymal transition and inflammatory signals to confer resistance to neoadjuvant trastuzumab and chemotherapy in HER2-positive breast cancer patients. *Oncotarget* **6,** 37269–80 (2015).

111. Palomeras, S., Diaz-Lagares, A., Ariadna, S., Belen, C. A., Ariadna, G.-P., Sandoval, J., Rabionet, M., Esteller, M. & Puig, T. Epigenetic silencing of TGFβ1, BCL6, KILLIN and CTSZ is related to trastuzumab resistance in HER2-positive breast cancer models. [Abstract]. *Cancer Res.* Abstract nr 2130A (2016). doi:10.1158/1538-7445.AM2016-2130A

112. Huang, X., Wang, S., Lee, C. K., Yang, X. H. & Liu, B. HDAC inhibitor SNDX-275 enhances efficacy of trastuzumab in erbB2-overexpressing breast cancer cells and exhibits potential to overcome trastuzumab resistance. *Cancer Lett.* **307,** 72–79 (2011).

113. Lee, J., Bartholomeusz, C., Mansour, O., Humphries, J., Hortobagyi, G. N., Ordentlich, P. & Ueno, N. T. A class I histone deacetylase inhibitor, entinostat, enhances lapatinib efficacy in HER2-overexpressing breast cancer cells through FOXO3-mediated Bim1 expression. *Breast Cancer Res. Treat.* **146,** 259–272 (2014).

114. Gale, M., Sayegh, J., Cao, J., Norcia, M., Gareiss, P., Hoyer, D., Merkel, J. S. & Yan, Q. Screen-identified selective inhibitor of lysine demethylase 5A blocks cancer cell growth and drug resistance. *Oncotarget* **7,** 39931–39944 (2016).

115. Vinogradova, M., Gehling, V. S., Gustafson, A., Arora, S., Tindell, C. A., Wilson, C., Williamson, K. E., Guler, G. D., Gangurde, P., Manieri, W., Busby, J., Flynn, E. M., Lan, F., Kim, H. J., Odate, S., Cochran, A. G., Liu, Y., Wongchenko, M., Yang, Y., Cheung, T. K., Maile, T. M., Lau, T., Costa, M., Hegde, G. V, Jackson, E., Pitti, R., Arnott, D., Bailey, C., Bellon, S., Cummings, R. T., Albrecht, B. K., Harmange, J. C., Kiefer, J. R., Trojer, P. & Classon, M. An inhibitor of KDM5 demethylases reduces survival of drug-tolerant cancer cells. *Nat Chem Biol* **12,**

531–538 (2016).

116. Gibney, E. R. & Nolan, C. M. Epigenetics and gene expression. *Heredity (Edinb).* **105,** 4–13 (2010).

117. Kornberg, R. D. & Thomas, J. O. Chromatin structure; oligomers of the histones. *Science (80-.).* **184,** 865–868 (1974).

118. Luger, K., Mader, A. W., Richmond, R. K., Sargent, D. F. & Richmond, T. J. Crystal structure of the nucleosome core particle at 2.8 A resolution. *Nature* **389,** 251–260 (1997).

119. Højfeldt, J. W., Agger, K. & Helin, K. Histone lysine demethylases as targets for anticancer therapy. *Nat. Rev. Drug Discov.* **12,** 917–930 (2013).

120. Jones, P. A., Issa, J.-P. J. & Baylin, S. Targeting the cancer epigenome for therapy. *Nat. Rev. Genet.* **17,** 630–641 (2016).

121. Zhang, Y. & Reinberg, D. Transcription regulation by histone methylation: interplay between different covalent modifications of the core histone tails. *Genes Dev* **15,** 2343–2360 (2001).

122. Tang, J., Gary, J. D., Clarke, S. & Herschman, H. R. PRMT 3, a type I protein arginine N-methyltransferase that differs from PRMT1 in its oligomerization, subcellular localization, substrate specificity, and regulation. *J. Biol. Chem.* **273,** 16935–16945 (1998).

123. Pollack, B. P., Kotenko, S. V., He, W., Izotova, L. S., Barnoski, B. L. & Pestka, S. The human homologue of the yeast proteins Skb1 and Hs17p interacts with Jak kinases and contains protein methyltransferase activity. *J. Biol. Chem.* **274,** 31531–31542 (1999).

124. Lin, W. J., Gary, J. D., Yang, M. C., Clarke, S. & Herschman, H. R. The mammalian immediate-early TIS21 protein and the leukemia-associated BTG1 protein interact with a protein-arginine N-methyltransferase. *J. Biol. Chem.* **271,** 15034–15044 (1996).

125. Katsanis, N., Yaspo, M. L. & Fisher, E. M. C. Identification and mapping of a novel human gene, HRMT1L1, homologous to the rat protein arginine N-methyltransferase 1 (PRMT1) gene. *Mamm. Genome* **8,** 526–529 (1997).

126. Chen, D., Ma, H., Hong, H., Koh, S. S., Huang, S. M., Schurter, B. T., Aswad, D. W. & Stallcup, M. R. Regulation of Transcription by a Protein Methyltransferase. *Science (80-.).* **284,** 2174–2177 (1999).

127. Tachibana, M., Sugimoto, K., Fukushima, T. & Shinkai, Y. SET Domain-containing Protein, G9a, is a Novel Lysine-preferring Mammalian Histone Methyltransferase with Hyperactivity and Specific Selectivity to Lysines 9 and 27 of Histone H3. *J. Biol. Chem.* **276,** 25309–25317 (2001).

128. Wang, H., Cao, R., Xia, L., Erdjument-Bromage, H., Borchers, C., Tempst, P. & Zhang, Y. Purification and functional characterization of a histone H3-lysine 4-specific methyltransferase. *Mol. Cell* **8,** 1207–1217 (2001).

129. Van Leeuwen, F., Gafken, P. R. & Gottschling, D. E. Dot1p modulates silencing in yeast by methylation of the nucleosome core. *Cell* **109,** 745–756 (2002).

130. Feng, Q., Wang, H., Ng, H. H., Erdjument-Bromage, H., Tempst, P., Struhl, K. & Zhang, Y. Methylation of H3-lysine 79 is mediated by a new family of HMTases without a SET domain. *Curr Biol* **12,** 1052–1058 (2002).

131. Kouzarides, T. SnapShot: Histone-Modifying Enzymes. *Cell* **131,** (2007).

132. Henikoff, S. & Shilatifard, A. Histone modification: cause or cog? *Trends Genet* **27,** 389–396 (2011).

133. Zhang, Z. & Pugh, B. F. High-resolution genome-wide mapping of the primary structure of chromatin. *Cell* **144,** 175–186 (2011).

134. Shi, Y., Lan, F., Matson, C., Mulligan, P., Whetstine, J. R., Cole, P. A., Casero, R. A. & Shi, Y. Histone demethylation mediated by the nuclear amine oxidase homolog LSD1. *Cell* **119,** 941–953 (2004).

135. Klose, R. J., Yamane, K., Bae, Y., Zhang, D., Erdjument-Bromage, H., Tempst, P., Wong, J. & Zhang, Y. The transcriptional repressor JHDM3A demethylates trimethyl histone H3 lysine 9 and lysine 36. *Nature* **442,** 312–316 (2006).

136. Tsukada, Y., Fang, J., Erdjument-Bromage, H., Warren, M. E., Borchers, C. H., Tempst, P. & Zhang, Y. Histone demethylation by a family of JmjC domain-containing proteins. *Nature* **439,** 811–816 (2005).

137. Whetstine, J. R., Nottke, A., Lan, F., Huarte, M., Smolikov, S., Chen, Z., Spooner, E., Li, E., Zhang, G., Colaiacovo, M. & Shi, Y. Reversal of Histone Lysine Trimethylation by the JMJD2 Family of Histone Demethylases. *Cell* **125,** 467–481 (2006).

138. Kooistra, S. M. & Helin, K. Molecular mechanisms and potential functions of histone demethylases. *Nat. Rev. Mol. Cell Biol.* (2012). doi:10.1038/nrm3327

139. Karytinos, A., Forneris, F., Profumo, A., Ciossani, G., Battaglioli, E., Binda, C. & Mattevi, A. A novel mammalian flavin-dependent histone demethylase. *J. Biol. Chem.* **284,** 17775–17782 (2009).

140. Forneris, F., Binda, C., Vanoni, M. A., Mattevi, A. & Battaglioli, E. Histone demethylation catalysed by LSD1 is a flavin-dependent oxidative process. *FEBS Lett.* **579,** 2203–2207 (2005).

141. Labbé, R. M., Holowatyj, A. & Yang, Z. Q. Histone lysine demethylase (kdm) subfamily 4: Structures, functions and therapeutic potential. *American Journal of Translational Research* **6,** 1–15 (2014).

142. Kampranis, S. & Tsichlis, P. Histone demethylases and cancer. *Adv. Cancer Res.* **102,** 103–69 (2012).

143. Cloos, P. A. C., Christensen, J., Agger, K., Maiolica, A., Rappsilber, J., Antal, T., Hansen, K. H. & Helin, K. The putative oncogene GASC1 demethylates tri- and dimethylated lysine 9 on histone H3. *Nature* **442,** 307–311 (2006).

144. Fodor, B. D., Kubicek, S., Yonezawa, M., O'Sullivan, R. J., Sengupta, R., Perez-Burgos, L., Opravil, S., Mechtler, K., Schotta, G. & Jenuwein, T. Jmjd2b antagonizes H3K9 trimethylation at pericentric heterochromatin in mammalian cells. *Genes Dev.* **20,** 1557–1562 (2006).

145. Klose, R. J., Yan, Q., Tothova, Z., Yamane, K., Erdjument-Bromage, H., Tempst, P., Gilliland, D. G., Zhang, Y. & Kaelin, W. G. The Retinoblastoma Binding Protein RBP2 Is an H3K4 Demethylase. *Cell* **128,** 889–900 (2007).

146. Yamane, K., Tateishi, K., Klose, R. J., Fang, J., Fabrizio, L. A., Erdjument-Bromage, H., Taylor-Papadimitriou, J., Tempst, P. & Zhang, Y. PLU-1 is an H3K4 demethylase involved in transcriptional repression and breast cancer cell proliferation. *Mol Cell* **25,** 801–812 (2007).

147. Gildea, J. J., Lopez, R. & Shearn, A. A screen for new trithorax group genes identified little imaginal discs, the Drosophila melanogaster homologue of human retinoblastoma binding protein 2. *Genetics* **156,** 645–663 (2000).

148. Liang, G., Klose, R. J., Gardner, K. E. & Zhang, Y. Yeast Jhd2p is a histone H3 Lys4 trimethyl demethylase. *Nat. Struct. Mol. Biol.* **14,** 243–245 (2007).

149. Lee, M. G., Norman, J., Shilatifard, A. & Shiekhattar, R. Physical and Functional Association of a Trimethyl H3K4 Demethylase and Ring6a/MBLR, a Polycomb-like Protein. *Cell* **128,** 877–887 (2007).

150. Christensen, J., Agger, K., Cloos, P. A. C., Pasini, D., Rose, S., Sennels, L., Rappsilber, J., Hansen, K. H., Salcini, A. E. & Helin, K. RBP2 Belongs to a Family of Demethylases, Specific for Tri-and Dimethylated Lysine 4 on Histone 3. *Cell* **128,** 1063–1076 (2007).

151. Iwase, S., Lan, F., Bayliss, P., de la Torre-Ubieta, L., Huarte, M., Qi, H. H., Whetstine, J. R., Bonni, A., Roberts, T. M. & Shi, Y. The X-linked mental retardation gene SMCX/JARID1C defines a family of histone H3 lysine 4 demethylases. *Cell* **128,** 1077–1088 (2007).

152. Taylor-Papadimitriou, J. & Burchell, J. JARID1/KDM5 demethylases as cancer targets? *Expert Opinion on Therapeutic Targets* **21,** 5–7 (2017).

153. Horton, J. R., Engstrom, A., Zoeller, E. L., Liu, X., Shanks, J. R., Zhang, X., Johns, M. A., Vertino, P. M., Fu, H. & Cheng, X. Characterization of a linked jumonji domain of the KDM5/JARID1 family of histone H3 lysine 4 demethylases. *J. Biol. Chem.* **291,** 2631–2646 (2016).

154. Herrscher, R. F., Kaplan, M. H., Lelsz, D. L., Das, C., Scheuermann, R. & Tucker, P. W. The immunoglobulin heavy-chain matrix-associating regions are bound by Bright: A B cell-specific trans-activator that describes a new DNA-binding protein family. *Genes Dev.* **9,** 3067–3082 (1995).

155. Gregory, S. L., Kortschak, R. D., Kalionis, B. & Saint, R. Characterization of the dead ringer gene identifies a novel, highly conserved family of sequence-specific DNA-binding proteins. *Mol. Cell. Biol.* **16,** 792–9 (1996).

156. Scibetta, A. G., Santangelo, S., Coleman, J., Hall, D., Chaplin, T., Copier, J., Catchpole, S., Burchell, J. & Taylor-Papadimitriou, J. Functional analysis of the transcription repressor PLU-1/JARID1B. *Mol Cell Biol* **27,** 7220–7235 (2007).

157. Tu, S., Teng, Y.-C., Yuan, C., Wu, Y.-T., Chan, M.-Y., Cheng, A.-N., Lin, P.-H., Juan, L.-J. & Tsai, M.-D. The ARID domain of the H3K4 demethylase RBP2 binds to a DNA CCGCCC motif. *Nat. Struct. Mol. Biol.* **15,** 419–421 (2008).

158. Torres, I. O., Kuchenbecker, K. M., Nnadi, C. I., Fletterick, R. J., Kelly, M. J. S. & Fujimori, D. G. Histone demethylase KDM5A is regulated by its reader domain through a positive-feedback mechanism. *Nat. Commun.* **6,** 6204 (2015).

159. Klein, B. J., Piao, L., Xi, Y., Rincon-Arano, H., Rothbart, S. B., Peng, D., Wen, H., Larson, C., Zhang, X., Zheng, X., Cortazar, M. A., Peña, P. V., Mangan, A., Bentley, D. L., Strahl, B. D., Groudine, M., Li, W., Shi, X. & Kutateladze, T. G. The histone-H3K4-specific demethylase KDM5B Binds to its substrate and product through distinct PHD fingers. *Cell Rep.* **6,** 325–335 (2014).

160. Wang, G. G., Song, J., Wang, Z., Dormann, H. L., Casadio, F., Li, H., Luo, J.-L., Patel, D. J. & Allis, C. D. Haematopoietic malignancies caused by dysregulation of a chromatin-binding PHD finger. *Nature* **459,** 847–851 (2009).

161. Defeo-Jones, D., Huang, P. S., Jones, R. E., Haskell, K. M., Vuocolo, G. A., Hanobik, M. G., Huber, H. E. & Oliff, A. Cloning of cDNAs for cellular proteins that bind to the retinoblastoma gene product. *Nature* **352,** 251–254 (1991).

162. Beshiri, M. L., Holmes, K. B., Richter, W. F., Hess, S., Islam, A. B. M. M. K., Yan, Q., Plante, L., Litovchick, L., Gevry, N., Lopez-Bigas, N., Kaelin, W. G. &

Benevolenskaya, E. V. Coordinated repression of cell cycle genes by KDM5A and E2F4 during differentiation. *Proc. Natl. Acad. Sci.* **109,** 18499–18504 (2012).

163. Dahl, J. A., Jung, I., Aanes, H., Greggains, G. D., Manaf, A., Lerdrup, M., Li, G., Kuan, S., Li, B., Lee, A. Y., Preissl, S., Jermstad, I., Haugen, M. H., Suganthan, R., Bjørås, M., Hansen, K., Dalen, K. T., Fedorcsak, P., Ren, B. & Klungland, A. Broad histone H3K4me3 domains in mouse oocytes modulate maternal-to-zygotic transition. *Nature* **537,** 548–552 (2016).

164. Agulnik, A. I., Mitchell, M. J., Mattei, M. G., Borsani, G., Avner, P. A., Lerner, J. L. & Bishop, C. E. A novel X gene with a widely transcribed Y-linked homologue escapes X-inactivation in mouse and human. *Hum Mol Genet* **3,** 879–884 (1994).

165. Jensen, L. R., Amende, M., Gurok, U., Moser, B., Gimmel, V., Tzschach, A., Janecke, A. R., Tariverdian, G., Chelly, J., Fryns, J.-P., Van Esch, H., Kleefstra, T., Hamel, B., Moraine, C., Gecz, J., Turner, G., Reinhardt, R., Kalscheuer, V. M., Ropers, H.-H. & Lenzner, S. Mutations in the JARID1C gene, which is involved in transcriptional regulation and chromatin remodeling, cause X-linked mental retardation. *Am. J. Hum. Genet.* **76,** 227–36 (2005).

166. Tzschach, A., Lenzner, S., Moser, B., Reinhardt, R., Chelly, J., Fryns, J.-P., Kleefstra, T., Raynaud, M., Turner, G., Ropers, H.-H., Kuss, A. & Jensen, L. R. Novel JARID1C/SMCX mutations in patients with X-linked mental retardation. *Hum. Mutat.* **27,** 389 (2006).

167. Cox, B. J., Vollmer, M., Tamplin, O., Lu, M., Biechele, S., Gertsenstein, M., Van Campenhout, C., Floss, T., Kühn, R., Wurst, W., Lickert, H. & Rossant, J. Phenotypic annotation of the mouse X chromosome. *Genome Res.* **20,** 1154–1164 (2010).

168. Agulnik, A. I., Mitchell, M. J., Lerner, J. L., Woods, D. R. & Bishop, C. E. A mouse Y chromosome gene encoded by a region essential for spermatogenesis and expression of male-specific minor histocompatibility antigens. *Hum Mol Genet* **3,** 873–878 (1994).

169. Zeng, J., Ge, Z., Wang, L., Li, Q., Wang, N., Björkholm, M., Jia, J. & Xu, D. The Histone Demethylase RBP2 Is Overexpressed in Gastric Cancer and Its Inhibition Triggers Senescence of Cancer Cells. *Gastroenterology* **138,** 981–992 (2010).

170. Hou, J., Wu, J., Dombkowski, A., Zhang, K., Holowatyj, A., Boerner, J. L. & Yang, Z. Q. Genomic amplification and a role in drug-resistance for the KDM5A histone demethylase in breast cancer. *Am. J. Transl. Res.* **4,** 247–256 (2012).

171. Li, L., Wang, L., Song, P., Geng, X., Liang, X., Zhou, M., Wang, Y., Chen, C., Jia, J. & Zeng, J. Critical role of histone demethylase RBP2 in human gastric cancer angiogenesis. *Mol. Cancer* **13,** 81 (2014).

172. Cao, J., Liu, Z., Cheung, W. K. C., Zhao, M., Chen, S. Y., Chan, S., Booth, C. J., Nguyen, D. X. & Yan, Q. Histone demethylase RBP2 is critical for breast cancer progression and metastasis. *Cell Rep.* **6,** 868–877 (2014).

173. Smith, J. A., White, E. A., Sowa, M. E., Powell, M. L. C., Ottinger, M., Harper, J. W. & Howley, P. M. Genome-wide siRNA screen identifies SMCX, EP400, and Brd4 as E2-dependent regulators of human papillomavirus oncogene expression. *Proc. Natl. Acad. Sci.* **107,** 3752–3757 (2010).

174. Dalgliesh, G. L., Furge, K., Greenman, C., Chen, L., Bignell, G., Butler, A., Davies, H., Futreal, P. A., *et al.* Systematic sequencing of renal carcinoma reveals inactivation of histone modifying genes. *Nature* **463,** 360–363 (2010).

175. Rondinelli, B., Rosano, D., Antonini, E., Frenquelli, M., Montanini, L., Huang, D., Segalla, S., Yoshihara, K., Amin, S. B., Lazarevic, D., Tean, B., Verhaak, R. G. W., Andrew Futreal, P., Di Croce, L., Chin, L., Cittaro, D. & Tonon, G. Histone demethylase JARID1C inactivation triggers genomic instability in sporadic renal cancer. *J. Clin. Invest.* **125,** 4625–4637 (2015).

176. Ji, X., Jin, S., Qu, X., Li, K., Wang, H., He, H., Guo, F. & Dong, L. Lysine-specific demethylase 5C promotes hepatocellular carcinoma cell invasion through inhibition BMP7 expression. *BMC Cancer* **15,** 801 (2015).

177. Wang, Q., Wei, J., Su, P. & Gao, P. Histone demethylase JARID1C promotes breast cancer metastasis cells via down regulating BRMS1 expression. *Biochem Biophys Res Commun* **464,** 659–666 (2015).

178. Stein, J., Majores, M., Rohde, M., Lim, S., Schneider, S., Krappe, E., Ellinger, J., Dietel, M., Stephan, C., Jung, K., Perner, S., Kristiansen, G. & Kirfel, J. KDM5C is overexpressed in prostate cancer and is a prognostic marker for prostate-specific antigen-relapse following radical prostatectomy. *Am. J. Pathol.* **184,** 2430–2437 (2014).

179. Perinchery, G., Sasaki, M., Angan, a, Kumar, V., Carroll, P. & Dahiya, R. Deletion of Y-chromosome specific genes in human prostate cancer. *J. Urol.* **163,** 1339–42 (2000).

180. Li, N., Dhar, S. S., Chen, T.-Y., Kan, P.-Y., Wei, Y., Kim, J.-H., Chan, C.-H., Lin, H.-K., Hung, M.-C. & Lee, M. G. JARID1D is a suppressor and prognostic marker of prostate cancer invasion and metastasis. *Cancer Res.* **3,** 0008-5472.CAN-15-0906- (2016).

181. Komura, K., Jeong, S. H., Hinohara, K., Qu, F., Wang, X., Hiraki, M., Azuma, H., Lee, G.-S. M., Kantoff, P. W. & Sweeney, C. J. Resistance to docetaxel in prostate cancer is associated with androgen receptor activation and loss of KDM5D expression. *Proc. Natl. Acad. Sci.* **113,** 6259–6264 (2016).

182. Arseneault, M., Monlong, J., Vasudev, N. S., Laskar, R. S., Safisamghabadi, M., Harnden, P., Egevad, L., Nourbehesht, N., Panichnantakul, P., Holcatova, I., Brisuda, A., Janout, V., Kollarova, H., Foretova, L., Navratilova, M., Mates, D., Jinga, V., Zaridze, D., Mukeria, A., Jandaghi, P., Brennan, P., Brazma, A., Tost, J., Scelo, G., Banks, R. E., Lathrop, M., Bourque, G. & Riazalhosseini, Y. Loss of chromosome Y leads to down regulation of KDM5D and KDM6C epigenetic modifiers in clear cell renal cell carcinoma. *Sci. Rep.* **7,** 44876 (2017).

183. Lu, P. J., Sundquist, K., Baeckstrom, D., Poulsom, R., Hanby, A., Meier-Ewert, S., Jones, T., Mitchell, M., Pitha-Rowe, P., Freemont, P. & Taylor-Papadimitriou, J. A novel gene (PLU-1) containing highly conserved putative DNA/chromatin binding motifs is specifically up-regulated in breast cancer. *J Biol Chem* **274,** 15633–15645 (1999).

184. Vogt, T., Kroiss, M., McClelland, M., Gruss, C., Becker, B., Bosserhoff, A. K., Rumpler, G., Bogenrieder, T., Landthaler, M. & Stolz, W. Deficiency of a novel retinoblastoma binding protein 2-homolog is a consistent feature of sporadic human melanoma skin cancer. *Lab Invest* **79,** 1615–1627 (1999).

185. Kashuba, V., Protopopov, a, Podowski, R., Gizatullin, R., Li, J., Klein, G., Wahlestedt, C. & Zabarovsky, E. Isolation and chromosomal localization of a new human retinoblastoma binding protein 2 homologue 1a (RBBP2H1A). *Eur. J. Hum. Genet.* **8,** 407–13 (2000).

186. Barrett, A., Madsen, B., Copier, J., Lu, P. J., Cooper, L., Scibetta, A. G., Burchell, J. & Taylor-Papadimitriou, J. PLU-1 nuclear protein, which is upregulated in breast cancer, shows restricted expression in normal human adult

tissues: A new cancer/testis antigen? *Int. J. Cancer* **101,** 581–588 (2002).

187. Madsen, B., Spencer-Dene, B., Poulsom, R., Hall, D., Lu, P. J., Scott, K., Shaw, A. T., Burchell, J. M., Freemont, P. & Taylor-Papadimitriou, J. Characterisation and developmental expression of mouse Plu-1, a homologue of a human nuclear protein (PLU-1) which is specifically up-regulated in breast cancer. *Gene Expr. Patterns* **2,** 275–282 (2002).

188. Catchpole, S., Spencer-Dene, B., Hall, D., Santangelo, S., Rosewell, I., Guenatri, M., Beatson, R., Scibetta, A. G., Burchell, J. M. & Taylor-Papadimitriou, J. PLU-1/JARID1B/KDM5B is required for embryonic survival and contributes to cell proliferation in the mammary gland and in ER+ breast cancer cells. *Int J Oncol* **38,** 1267–1277 (2011).

189. Barrett, A., Santangelo, S., Tan, K., Catchpole, S., Roberts, K., Spencer-Dene, B., Hall, D., Scibetta, A., Burchell, J., Verdin, E., Freemont, P. & Taylor-Papadimitriou, J. Breast cancer associated transcriptional repressor PLU-1/JARID1B interacts directly with histone deacetylases. *Int J Cancer* **121,** 265–275 (2007).

190. Dey, B. K., Stalker, L., Schnerch, A., Bhatia, M., Taylor-Papidimitriou, J. & Wynder, C. The histone demethylase KDM5b/JARID1b plays a role in cell fate decisions by blocking terminal differentiation. *Mol. Cell. Biol.* **28,** 5312–5327 (2008).

191. Xie, L., Pelz, C., Wang, W., Bashar, A., Varlamova, O., Shadle, S. & Impey, S. KDM5B regulates embryonic stem cell self-renewal and represses cryptic intragenic transcription. *EMBO J* **30,** 1473–1484 (2011).

192. Schmitz, S. U., Albert, M., Malatesta, M., Morey, L., Johansen, J. V, Bak, M., Tommerup, N., Abarrategui, I. & Helin, K. Jarid1b targets genes regulating development and is involved in neural differentiation. *EMBO J.* **30,** 4586–4600 (2011).

193. Kidder, B. L., Hu, G. & Zhao, K. KDM5B focuses H3K4 methylation near promoters and enhancers during embryonic stem cell self-renewal and differentiation. *Genome Biol.* **15,** R32 (2014).

194. Albert, M., Schmitz, S. U., Kooistra, S. M., Malatesta, M., Morales Torres, C., Rekling, J. C., Johansen, J. V, Abarrategui, I. & Helin, K. The histone demethylase Jarid1b ensures faithful mouse development by protecting developmental genes from aberrant H3K4me3. *PLoS Genet* **9,** e1003461 (2013).

195. Zou, M. R., Cao, J., Liu, Z., Huh, S. J., Polyak, K. & Yan, Q. Histone demethylase jumonji AT-rich interactive domain 1B (JARID1B) controls mammary gland development by regulating key developmental and lineage specification genes. *J Biol Chem* **289,** 17620–17633 (2014).

196. Catchpole, S. Functional analysis of the KDM5B demethylase: In vitro and in vivo studies. (King's College London, 2014). doi:https://kclpure.kcl.ac.uk/portal/en/theses/functional-analysis-of-the-kdm5b-demethylase(6517eab1-6671-41bf-8ec3-3c184469247b).html

197. Yu, J., Baron, V., Mercola, D., Mustelin, T. & Adamson, E. D. A network of p73, p53 and Egr1 is required for efficient apoptosis in tumor cells. *Cell Death Differ.* **14,** 436–446 (2007).

198. Li, X., Liu, L., Yang, S., Song, N., Zhou, X., Gao, J., Yu, N., Shan, L., Wang, Q., Liang, J., Xuan, C., Wang, Y., Shang, Y. & Shi, L. Histone demethylase KDM5B is a key regulator of genome stability. *Proc. Natl. Acad. Sci.* **111,** 7096–7101 (2014).

199. Tan, K., Shaw, A. L., Madsen, B., Jensen, K., Taylor-Papadimitriou, J. & Freemont, P. S. Human PLU-1 has transcriptional repression properties and interacts with the developmental transcription factors BF-1 and PAX9. *J. Biol. Chem.* **278,** 20507–20513 (2003).

200. Zhang, Y., Liang, J. & Li, Q. Coordinated regulation of retinoic acid signaling pathway by KDM5B and polycomb repressive complex 2. *J. Cell. Biochem.* **115,** 1528–1538 (2014).

201. Han, M., Xu, W., Cheng, P., Jin, H. & Wang, X. Histone demethylase lysine demethylase 5B in development and cancer. *Oncotarget* **8,** 8980–8991 (2017).

202. Yamamoto, S., Wu, Z., Russnes, H. G., Takagi, S., Peluffo, G., Vaske, C., Zhao, X., Moen Vollan, H. K., Maruyama, R., Ekram, M. B., Sun, H., Kim, J. H., Carver, K., Zucca, M., Feng, J., Almendro, V., Bessarabova, M., Rueda, O. M., Nikolsky, Y., Caldas, C., Liu, X. S. & Polyak, K. JARID1B is a luminal lineage-driving oncogene in breast cancer. *Cancer Cell* **25,** 762–777 (2014).

203. Li, Q., Shi, L., Gui, B., Yu, W., Wang, J., Zhang, D., Han, X., Yao, Z. & Shang, Y. Binding of the JmjC demethylase JARID1B to LSD1/NuRD suppresses angiogenesis and metastasis in breast cancer cells by repressing chemokine CCL14. *Cancer Res.* **71,** 6899–6908 (2011).

204. Roesch, A., Fukunaga-Kalabis, M., Schmidt, E. C., Zabierowski, S. E., Brafford, P. A., Vultur, A., Basu, D., Gimotty, P., Vogt, T. & Herlyn, M. A Temporarily Distinct Subpopulation of Slow-Cycling Melanoma Cells Is Required for Continuous Tumor Growth. *Cell* **141,** 583–594 (2010).

205. Xiang, Y., Zhu, Z., Han, G., Ye, X., Xu, B., Peng, Z., Ma, Y., Yu, Y., Lin, H., Chen, A. P. & Chen, C. D. JARID1B is a histone H3 lysine 4 demethylase up-regulated in prostate cancer. *Proc. Natl. Acad. Sci. U. S. A.* **104,** 19226–31 (2007).

206. Li, J., Wan, X., Qiang, W., Li, T., Huang, W., Huang, S., Wu, D. & Li, Y. MiR-29a suppresses prostate cell proliferation and induces apoptosis via KDM5B protein regulation. *Int. J. Clin. Exp. Med.* **8,** 5329–5339 (2015).

207. Shen, X., Zhuang, Z., Zhang, Y., Chen, Z., Shen, L., Pu, W., Chen, L. & Xu, Z. JARID1B modulates lung cancer cell proliferation and invasion by regulating p53 expression. *Tumor Biol.* **36,** 7133–7142 (2015).

208. Hayami, S., Yoshimatsu, M., Veerakumarasivam, A., Unoki, M., Iwai, Y., Tsunoda, T., Field, H. I., Kelly, J. D., Neal, D. E., Yamaue, H., Ponder, B. A., Nakamura, Y. & Hamamoto, R. Overexpression of the JmjC histone demethylase KDM5B in human carcinogenesis: involvement in the proliferation of cancer cells through the E2F/RB pathway. *Mol Cancer* **9,** 59 (2010).

209. Wang, Z., Tang, F., Qi, G., Yuan, S., Zhang, G., Tang, B. & He, S. KDM5B is overexpressed in gastric cancer and is required for gastric cancer cell proliferation and metastasis. *Am. J. Cancer Res.* **5,** 87–100 (2015).

210. Wang, D., Han, S., Peng, R., Jiao, C., Wang, X., Yang, X., Yang, R. & Li, X. Depletion of histone demethylase KDM5B inhibits cell proliferation of hepatocellular carcinoma by regulation of cell cycle checkpoint proteins p15 and p27. *J Exp Clin Cancer Res* **35,** 37 (2016).

211. Lin, C. S., Lin, Y. C., Adebayo, B. O., Wu, A., Chen, J. H., Peng, Y. J., Cheng, M. F., Lee, W. H., Hsiao, M., Chao, T. Y. & Yeh, C. T. Silencing JARID1B suppresses oncogenicity, stemness and increases radiation sensitivity in human oral carcinoma. *Cancer Lett.* **368,** 36–45 (2015).

212. Kuo, Y. T., Liu, Y. L., Adebayo, B. O., Shih, P. H., Lee, W. H., Wang, L. S., Liao,

Y. F., Hsu, W. M., Yeh, C. T. & Lin, C. M. JARID1B expression plays a critical role in chemoresistance and stem cell-like phenotype of neuroblastoma cells. *PLoS One* **10,** (2015).

213. Okamoto, T., Schlegel, A., Scherer, P. E. & Lisanti, M. P. Caveolins, a family of scaffolding proteins for organizing 'preassembled signaling complexes' at the plasma membrane. *J Biol Chem* **273,** 5419–5422 (1998).

214. Scherer, P. E., Okamoto, T., Chun, M., Nishimoto, I., Lodish, H. F. & Lisanti, M. P. Identification, sequence, and expression of caveolin-2 defines a caveolin gene family. *Proc. Natl. Acad. Sci. U. S. A.* **93,** 131–5 (1996).

215. Tang, Z., Scherer, P. E., Okamoto, T., Song, K., Chu, C., Kohtz, D. S., Nishimoto, I., Lodish, H. F. & Lisanti, M. P. Molecular cloning of caveolin-3, a novel member of the caveolin gene family expressed predominantly in muscle. *J. Biol. Chem.* **271,** 2255–2261 (1996).

216. Fra, A. M., Masserini, M., Palestini, P., Sonnino, S. & Simons, K. A photo-reactive derivative of ganglioside GM1 specifically cross-links VIP21-caveolin on the cell surface. *FEBS Lett.* **375,** 11–14 (1995).

217. Murata, M., Peranen, J., Schreinert, R., Wielandt, F., Kurzchalia, T. V & Simons, K. VIP21/caveolin is a cholesterol-binding protein (membrane microdomains/intracellular transport/membrane reconstitution). *Cell Biol.* **92,** 10339–10343 (1995).

218. Li, S., Song, K. S. & Lisanti, M. P. Expression and characterization of recombinant caveolin: Purification by polyhistidine tagging and cholesterol-dependent incorporation into defined lipid membranes. *J. Biol. Chem.* **271,** 568–573 (1996).

219. Sagara, Y., Mimori, K., Yoshinaga, K., Tanaka, F., Nishida, K., Ohno, S., Inoue, H. & Mori, M. Clinical significance of Caveolin-1, Caveolin-2 and HER2/neu mRNA expression in human breast cancer. *Br. J. Cancer* (2004). doi:10.1038/sj.bjc.6602029

220. Sloan, E. K., Ciocca, D. R., Pouliot, N., Natoli, A., Restall, C., Henderson, M. a, Fanelli, M. a, Cuello-Carrión, F. D., Gago, F. E. & Anderson, R. L. Stromal cell expression of caveolin-1 predicts outcome in breast cancer. *Am. J. Pathol.* **174,** 2035–2043 (2009).

221. Scherer, P. E., Lewis, R. Y., Volonté, D., Engelman, J. A., Galbiati, F., Couet, J., Kohtz, D. S., Van Donselaar, E., Peters, P. & Lisanti, M. P. Cell-type and tissue-specific expression of caveolin-2. Caveolins 1 and 2 co-localize and form a stable hetero-oligomeric complex in vivo. *J. Biol. Chem.* **272,** 29337–29346 (1997).

222. Engelman, J. A., Zhang, X. L. & Lisanti, M. P. Genes encoding human caveolin-1 and -2 are co-localized to the D7S522 locus (7q31.1), a known fragile site (FRA7G) that is frequently deleted in human cancers. *FEBS Lett.* **436,** 403–410 (1998).

223. Engelman, J. a, Zhang, X., Galbiati, F., Volonte, D., Sotgia, F., Pestell, R. G., Minetti, C., Scherer, P. E., Okamoto, T. & Lisanti, M. P. Molecular genetics of the caveolin gene family: implications for human cancers, diabetes, Alzheimer disease, and muscular dystrophy. *Am. J. Hum. Genet.* **63,** 1578–1587 (1998).

224. Li, S., Couet, J. & Lisanti, M. P. Src tyrosine kinases, Galpha subunits, and H-Ras share a common membrane-anchored scaffolding protein, caveolin. Caveolin binding negatively regulates the auto-activation of Src tyrosine kinases. *J. Biol. Chem.* **271,** 29182–29190 (1996).

225. Smart, E. J., Graf, G. a, McNiven, M. a, Sessa, W. C., Engelman, J. a, Scherer, P. E., Okamoto, T. & Lisanti, M. P. Caveolins, liquid-ordered domains, and signal transduction. *Mol. Cell. Biol.* **19,** 7289–7304 (1999).

226. Zou, W., McDaneld, L. & Smith, L. M. Caveolin-1 haploinsufficiency leads to partial transformation of human breast epithelial cells. *Anticancer Res* **23,** 4581–4586 (2003).

227. Rudick, M. & Anderson, R. G. W. Multiple functions of caveolin-1. *Journal of Biological Chemistry* **277,** 41295–41298 (2002).

228. Park, D. S., Lee, H., Riedel, C., Hulit, J., Scherer, P. E., Pestell, R. G. & Lisanti, M. P. Prolactin Negatively Regulates Caveolin-1 Gene Expression in the Mammary Gland during Lactation, via a Ras-dependent Mechanism. *J. Biol. Chem.* **276,** 48389–48397 (2001).

229. Wagner, K.-U., Krempler, A., Triplett, A. a, Qi, Y., George, N. M., Zhu, J. & Rui, H. Impaired alveologenesis and maintenance of secretory mammary epithelial cells in Jak2 conditional knockout mice. *Mol. Cell. Biol.* **24,** 5510–5520 (2004).

230. Jahn, G. a, Daniel, N., Jolivet, G., Belair, L., Bole-Feysot, C., Kelly, P. a & Djiane, J. In vivo study of prolactin (PRL) intracellular signalling during lactogenesis in the rat: JAK/STAT pathway is activated by PRL in the mammary gland but not in the liver. *Biol. Reprod.* **57,** 894–900 (1997).

231. Park, D. S., Lee, H., Frank, P. G., Razani, B., Nguyen, A. V, Parlow, A. F., Russell, R. G., Hulit, J., Pestell, R. G. & Lisanti, M. P. Caveolin-1-deficient Mice Show Accelerated Mammary Gland Development During Pregnancy, Premature Lactation, and Hyperactivation of the Jak-2/STAT5a Signaling Cascade. *Mol Biol Cell* **13,** 3416–3430 (2002).

232. Park, S. S., Kim, J. E., Kim, Y. A., Kim, Y. C. & Kim, S. W. Caveolin-1 is down-regulated and inversely correlated with HER2 and EGFR expression status in invasive ductal carcinoma of the breast. *Histopathology* **47,** 625–630 (2005).

233. Elsheikh, S. E., Green, A. R., Rakha, E. A., Samaka, R. M., Ammar, A. A., Powe, D., Reis-Filho, J. S. & Ellis, I. O. Caveolin 1 and Caveolin 2 are associated with breast cancer basal-like and triple-negative immunophenotype. *Br. J. Cancer* **99,** 327–334 (2008).

234. Wu, P., Wang, X., Li, F., Qi, B., Zhu, H., Liu, S., Cui, Y. & Chen, J. Growth suppression of MCF-7 cancer cell-derived xenografts in nude mice by caveolin-1. *Biochem. Biophys. Res. Commun.* **376,** 215–220 (2008).

235. Zhang, W., Razani, B., Altschuler, Y., Bouzahzah, B., Mostov, K. E., Pestell, R. G. & Lisanti, M. P. Caveolin-1 inhibits epidermal growth factor-stimulated lamellipod extension and cell migration in metastatic mammary adenocarcinoma cells (MTLn3). Transformation suppressor effects of adenovirus-mediated gene delivery of caveolin-1. *J Biol Chem* **275,** 20717–20725 (2000).

236. Savage, K., Lambros, M. B. K., Robertson, D., Jones, R. L., Jones, C., Mackay, A., James, M., Hornick, J. L., Pereira, E. M., Milanezi, F., Fletcher, C. D. M., Schmitt, F. C., Ashworth, A. & Reis-Filho, J. S. Caveolin 1 is overexpressed and amplified in a subset of basal-like and metaplastic breast carcinomas: A morphologic, ultrastructural, immunohistochemical, and in situ hybridization analysis. *Clin. Cancer Res.* **13,** 90–101 (2007).

237. Rao, X., Evans, J., Chae, H., Pilrose, J., Kim, S., Yan, P., Huang, R.-L., Lai, H.-C., Lin, H., Liu, Y., Miller, D., Rhee, J.-K., Huang, Y.-W., Gu, F., Gray, J. W., Huang, T.-M. & Nephew, K. P. CpG island shore methylation regulates caveolin-1 expression in breast cancer. *Oncogene* **32,** 4519–4528 (2013).

238. Yeong Joe et al. Caveolin-1 expression as a prognostic marker in triple negative breast cancers of Asian women. *J. Clin. Pathol.* (2017).

239. Witkiewicz, A. K., Dasgupta, A., Sotgia, F., Mercier, I., Pestell, R. G., Sabel, M., Kleer, C. G., Brody, J. R. & Lisanti, M. P. An absence of stromal caveolin-1 expression predicts early tumor recurrence and poor clinical outcome in human breast cancers. *Am J Pathol* **174,** 2023–2034 (2009).

240. Von Heyde, S. Der, Wagner, S., Czerny, A., Nietert, M., Ludewig, F., Salinas-Riester, G., Arlt, D. & Bei??barth, T. mRNA profiling reveals determinants of trastuzumab efficiency in HER2-positive breast cancer. *PLoS One* **10,** (2015).

241. Sekhar, S. C., Kasai, T., Satoh, A., Shigehiro, T., Mizutani, A., Murakami, H., El-Aarag, B. Y., Salomon, D. S., Massaguer, A., de Llorens, R. & Seno, M. Identification Of Caveolin-1 As A Potential Causative Factor In The Generation Of Trastuzumab Resistance In Breast Cancer Cells. *J. Cancer* **4,** 391–401 (2013).

242. Simpkins, S. A., Hanby, A. M., Holliday, D. L. & Speirs, V. Clinical and functional significance of loss of caveolin-1 expression in breast cancer-associated fibroblasts. *J. Pathol.* **227,** 490–498 (2012).

243. Sharma, S. V, Lee, D. Y., Li, B., Quinlan, M. P., Takahashi, F., Maheswaran, S., Mcdermott, U., Azizian, N., Zou, L., Fischbach, M. A., Wong, K., Brandstetter, K., Wittner, B., Ramaswamy, S., Classon, M. & Settleman, J. A chromatin-mediated reversible drug tolerant state in cancer cell subpopulations. *Cell* **141,** 69–80 (2010).

244. Yan, H., Chen, X., Zhang, Q., Qin, J., Li, H., Liu, C., Calhoun-Davis, T., Coletta, L. D., Klostergaard, J., Fokt, I., Skora, S., Priebe, W., Bi, Y. & Tang, D. G. Drug-tolerant cancer cells show reduced tumor-initiating capacity: depletion of CD44 cells and evidence for epigenetic mechanisms. *PLoS One* **6,** e24397 (2011).

245. Banelli, B., Carra, E., Barbieri, F., Würth, R., Parodi, F., Pattarozzi, A., Carosio, R., Forlani, A., Allemanni, G., Marubbi, D., Florio, T., Daga, A. & Romani, M. The histone demethylase KDM5A is a key factor for the resistance to temozolomide in glioblastoma. *Cell Cycle* **14,** 3418–3429 (2015).

246. Roesch, A., Vultur, A., Bogeski, I., Wang, H., Zimmermann, K., Speicher, D., Körbel, C., Laschke, M., Gimotty, P., Philipp, S., Krause, E., Pätzold, S., Villanueva, J., Krepler, C., Fukunaga-Kalabis, M., Hoth, M., Bastian, B., Vogt, T. & Herlyn, M. Overcoming intrinsic multidrug resistance in melanoma by blocking the mitochondrial respiratory chain of slow-cycling JARID1Bhigh cells. *Cancer Cell* **23,** 811–825 (2013).

247. Liang, J., Zhang, B., Labadie, S., Ortwine, D. F., Vinogradova, M., Kiefer, J. R., Gehling, V. S., Harmange, J. C., Cummings, R., Lai, T., Liao, J., Zheng, X., Liu, Y., Gustafson, A., Van der Porten, E., Mao, W., Liederer, B. M., Deshmukh, G., Classon, M., Trojer, P., Dragovich, P. S. & Murray, L. Lead optimization of a pyrazolo[1,5-a]pyrimidin-7(4H)-one scaffold to identify potent, selective and orally bioavailable KDM5 inhibitors suitable for in vivo biological studies. *Bioorganic Med. Chem. Lett.* **26,** 4036–4041 (2016).

248. Bavetsias, V., Lanigan, R. M., Ruda, G. F., Atrash, B., McLaughlin, M. G., Tumber, A., Mok, N. Y., Le Bihan, Y. V, Dempster, S., Boxall, K. J., Jeganathan, F., Hatch, S. B., Savitsky, P., Velupillai, S., Krojer, T., England, K. S., Sejberg, J., Thai, C., Donovan, A., Pal, A., Scozzafava, G., Bennett, J. M., Kawamura, A., Johansson, C., Szykowska, A., Gileadi, C., Burgess-Brown, N. A., von Delft, F., Oppermann, U., Walters, Z., Shipley, J., Raynaud, F. I., Westaway, S. M., Prinjha, R. K., Fedorov, O., Burke, R., Schofield, C. J., Westwood, I. M., Bountra, C., Muller, S., van Montfort, R. L., Brennan, P. E. & Blagg, J. 8-

Substituted Pyrido[3,4-d]pyrimidin-4(3H)-one Derivatives As Potent, Cell Permeable, KDM4 (JMJD2) and KDM5 (JARID1) Histone Lysine Demethylase Inhibitors. *J Med Chem* **59,** 1388–1409 (2016).

249. Gehling, V. S., Bellon, S. F., Harmange, J. C., LeBlanc, Y., Poy, F., Odate, S., Buker, S., Lan, F., Arora, S., Williamson, K. E., Sandy, P., Cummings, R. T., Bailey, C. M., Bergeron, L., Mao, W., Gustafson, A., Liu, Y., VanderPorten, E., Audia, J. E., Trojer, P. & Albrecht, B. K. Identification of potent, selective KDM5 inhibitors. *Bioorganic Med. Chem. Lett.* **26,** 4350–4354 (2016).

250. Horton, J. R., Liu, X., Gale, M., Wu, L., Shanks, J. R., Zhang, X., Webber, P. J., Bell, J. S. K., Kales, S. C., Mott, B. T., Rai, G., Jansen, D. J., Henderson, M. J., Urban, D. J., Hall, M. D., Simeonov, A., Maloney, D. J., Johns, M. A., Fu, H., Jadhav, A., Vertino, P. M., Yan, Q. & Cheng, X. Structural Basis for KDM5A Histone Lysine Demethylase Inhibition by Diverse Compounds. *Cell Chem. Biol.* **23,** 769–781 (2016).

251. Itoh, Y., Sawada, H., Suzuki, M., Tojo, T., Sasaki, R., Hasegawa, M., Mizukami, T. & Suzuki, T. Identification of Jumonji AT-Rich Interactive Domain 1A Inhibitors and Their Effect on Cancer Cells. *ACS Med. Chem. Lett.* **6,** 665–670 (2015).

252. Kristensen, L. H., Nielsen, A. L., Helgstrand, C., Lees, M., Cloos, P., Kastrup, J. S., Helin, K., Olsen, L. & Gajhede, M. Studies of H3K4me3 demethylation by KDM5B/Jarid1B/PLU1 reveals strong substrate recognition in vitro and identifies 2,4-pyridine-dicarboxylic acid as an in vitro and in cell inhibitor. *FEBS J.* **279,** 1905–1914 (2012).

253. Sayegh, J., Cao, J., Zou, M. R., Morales, A., Blair, L. P., Norcia, M., Hoyer, D., Tackett, A. J., Merkel, J. S. & Yan, Q. Identification of small molecule inhibitors of Jumonji AT-rich interactive domain 1B (JARID1B) histone demethylase by a sensitive high throughput screen. *J. Biol. Chem.* **288,** 9408–9417 (2013).

254. Tumber, A., Nuzzi, A., Hookway, E. S., Hatch, S. B., Velupillai, S., Johansson, C., Kawamura, A., Savitsky, P., Yapp, C., Szykowska, A., Wu, N., Bountra, C., Strain-Damerell, C., Burgess-Brown, N. A., Ruda, G. F., Fedorov, O., Munro, S., England, K. S., Nowak, R. P., Schofield, C. J., La Thangue, N. B., Pawlyn, C., Davies, F., Morgan, G., Athanasou, N., Muller, S., Oppermann, U. & Brennan, P. E. Potent and Selective KDM5 Inhibitor Stops Cellular Demethylation of H3K4me3 at Transcription Start Sites and Proliferation of MM1S Myeloma Cells. *Cell Chem Biol* **24,** 371–380 (2017).

255. Westaway, S. M., Preston, A. G. S., Barker, M. D., Brown, F., Brown, J. A., Campbell, M., Chung, C. W., Diallo, H., Douault, C., Drewes, G., Eagle, R., Gordon, L., Haslam, C., Hayhow, T. G., Humphreys, P. G., Joberty, G., Katso, R., Kruidenier, L., Leveridge, M., Liddle, J., Mosley, J., Muelbaier, M., Randle, R., Rioja, I., Rueger, A., Seal, G. A., Sheppard, R. J., Singh, O., Taylor, J., Thomas, P., Thomson, D., Wilson, D. M., Lee, K. & Prinjha, R. K. Cell Penetrant Inhibitors of the KDM4 and KDM5 Families of Histone Lysine Demethylases. 1. 3-Amino-4-pyridine Carboxylate Derivatives. *J. Med. Chem.* **59,** 1357–1369 (2016).

256. Wu, X., Fang, Z., Yang, B., Zhong, L., Yang, Q., Zhang, C., Huang, S., Xiang, R., Suzuki, T., Li, L.-L. & Yang, S.-Y. Discovery of KDM5A inhibitors: Homology modeling, virtual screening and structure–activity relationship analysis. *Bioorg. Med. Chem. Lett.* **26,** 2284–2288 (2016).

257. Lu, Q., Livi, G. P., Modha, S., Yusa, K., Macarrón, R. & Dow, D. J. Applications of CRISPR genome editing technology in drug target identification and validation. *Expert Opinion on Drug Discovery* **12,** 541–552 (2017).

258. Sander, J. D. & Joung, J. K. CRISPR-Cas systems for editing, regulating and

targeting genomes. *Nat. Biotechnol.* **32,** 347–355 (2014).

259. Hille, F. & Charpentier, E. CRISPR-Cas: biology, mechanisms and relevance. *Philos. Trans. R. Soc. Lond. B. Biol. Sci.* **371,** 1–12 (2016).

260. Ran, F. A., Hsu, P. D., Wright, J., Agarwala, V., Scott, D. A. & Zhang, F. Genome engineering using the CRISPR-Cas9 system. *Nat Protoc* **8,** 2281–2308 (2013).

261. Fellmann, C., Gowen, B. G., Lin, P.-C., Doudna, J. A. & Corn, J. E. Cornerstones of CRISPR–Cas in drug discovery and therapy. *Nat. Rev. Drug Discov.* **16,** 89–100 (2016).

262. Luo, J. CRISPR/Cas9: From Genome Engineering to Cancer Drug Discovery. *Trends in Cancer* **2,** 313–324 (2016).

263. Altucci, L. & Rots, M. G. Epigenetic drugs: from chemistry via biology to medicine and back. *Clin. Epigenetics* **8,** 56 (2016).

264. Dai, X., Cheng, H., Bai, Z. & Li, J. Breast Cancer Cell Line Classification and Its Relevance with Breast Tumor Subtyping. *J Cancer* **8,** 3131–3141 (2017).

265. Yang, Z., Steentoft, C., Hauge, C., Hansen, L., Thomsen, A. L., Niola, F., Vester-Christensen, M. B., Frödin, M., Clausen, H., Wandall, H. H. & Bennett, E. P. Fast and sensitive detection of indels induced by precise gene targeting. *Nucleic Acids Res.* **43,** (2015).

266. Lonowski, L. A., Narimatsu, Y., Riaz, A., Delay, C. E., Yang, Z., Niola, F., Duda, K., Ober, E. A., Clausen, H., Wandall, H. H., Hansen, S. H., Bennett, E. P. & Frödin, M. Genome editing using FACS enrichment of nuclease-expressing cells and indel detection by amplicon analysis. *Nat. Protoc.* **12,** 581–603 (2017).

267. Schmittgen, T. D. & Livak, K. J. Analyzing real-time PCR data by the comparative CT method. *Nat. Protoc.* **3,** 1101–1108 (2008).

268. Barker, C. S., Griffin, C., Dolganov, G. M., Hanspers, K., Yang, J. Y. H. & Erle, D. J. Increased DNA microarray hybridization specificity using sscDNA targets. *BMC Genomics* **6,** 57 (2005).

269. Chen, J., Bardes, E. E., Aronow, B. J. & Jegga, A. G. ToppGene Suite for gene list enrichment analysis and candidate gene prioritization. *Nucleic Acids Res.* **37,** (2009).

270. Bhaya, D., Davison, M. & Barrangou, R. CRISPR-Cas Systems in Bacteria and Archaea: Versatile Small RNAs for Adaptive Defense and Regulation. *Annu. Rev. Genet.* **45,** 273–297 (2011).

271. Terns, M. P. & Terns, R. M. CRISPR-based adaptive immune systems. *Current Opinion in Microbiology* **14,** 321–327 (2011).

272. Wiedenheft, B., Sternberg, S. H. & Doudna, J. a. RNA-guided genetic silencing systems in bacteria and archaea. *Nature* **482,** 331–338 (2012).

273. Barrangou, R., Fremaux, C., Deveau, H., Richards, M., Boyaval, P., Moineau, S., Romero, D. A. & Horvath, P. CRISPR provides acquired resistance against viruses in prokaryotes. *Science* **315,** 1709–12 (2007).

274. Garneau, J. E., Dupuis, M. E., Villion, M., Romero, D. A., Barrangou, R., Boyaval, P., Fremaux, C., Horvath, P., Magadan, A. H. & Moineau, S. The CRISPR/Cas bacterial immune system cleaves bacteriophage and plasmid DNA. *Nature* **468,** 67–71 (2010).

275. Mojica, F. J. M., Díez-Villaseñor, C., García-Martínez, J. & Almendros, C. Short

motif sequences determine the targets of the prokaryotic CRISPR defence system. *Microbiology* **155,** 733–740 (2009).

276. Swarts, D. C., Mosterd, C., van Passel, M. W. J. & Brouns, S. J. J. CRISPR interference directs strand specific spacer acquisition. *PLoS One* **7,** (2012).

277. Heler R, Samai P, Modell JW, Weiner C, Goldberg GW, Bikard D, M. LA. Cas9 specifies functional viral targets during CRISPR–Cas adaptation. *Nature* **519,** 199–202 (2015).

278. Wei, Y., Terns, R. M. & Terns, M. P. Cas9 function and host genome sampling in type II-A CRISPR-cas adaptation. *Genes Dev.* **29,** 356–361 (2015).

279. Deltcheva, E., Chylinski, K., Sharma, C. M., Gonzales, K., Chao, Y., Pirzada, Z. A., Eckert, M. R., Vogel, J. & Charpentier, E. CRISPR RNA maturation by trans-encoded small RNA and host factor RNase III. *Nature* **471,** 602–607 (2011).

280. Jinek, M., Chylinski, K., Fonfara, I., Hauer, M., Doudna, J. a. & Charpentier, E. A Programmable Dual-RNA-Guided DNA Endonuclease in Adaptive Bacterial Immunity. *Science (80-.).* **337,** 816–821 (2012).

281. Hou, Z., Zhang, Y., Propson, N. E., Howden, S. E., Chu, L.-F., Sontheimer, E. J. & Thomson, J. a. Efficient genome engineering in human pluripotent stem cells using Cas9 from Neisseria meningitidis. *Proc. Natl. Acad. Sci. U. S. A.* **110,** 15644–9 (2013).

282. Esvelt, K. M., Mali, P., Braff, J. L., Moosburner, M., Yaung, S. J. & Church, G. M. Orthogonal Cas9 proteins for RNA-guided gene regulation and editing. *Nat. Methods* **10,** 1116–21 (2013).

283. Burma, S., Chen, B. P. C. & Chen, D. J. Role of non-homologous end joining (NHEJ) in maintaining genomic integrity. *DNA Repair* **5,** 1042–1048 (2006).

284. Dudás, A. & Chovanec, M. DNA double-strand break repair by homologous recombination. *Mutat. Res.* **566,** 131–167 (2004).

285. Mali, P., Yang, L., Esvelt, K. M., Aach, J., Guell, M., DiCarlo, J. E., Norville, J. E. & Church, G. M. RNA-Guided Human Genome Engineering via Cas9_Sup. *Science (80-.).* **339,** 823–6 (2013).

286. Nikolsky, Y., Sviridov, E., Yao, J., Dosymbekov, D., Ustyansky, V., Kaznacheev, V., Dezso, Z., Mulvey, L., Macconaill, L. E., Winckler, W., Serebryiskaya, T., Nikolskaya, T. & Polyak, K. Genome-wide functional synergy between amplified and mutated genes in human breast cancer. *Cancer Res* **68,** 9532–9540 (2008).

287. Pereira, B., Chin, S. F., Rueda, O. M., Vollan, H. K., Provenzano, E., Bardwell, H. A., Pugh, M., Jones, L., Russell, R., Sammut, S. J., Tsui, D. W., Liu, B., Dawson, S. J., Abraham, J., Northen, H., Peden, J. F., Mukherjee, A., Turashvili, G., Green, A. R., McKinney, S., Oloumi, A., Shah, S., Rosenfeld, N., Murphy, L., Bentley, D. R., Ellis, I. O., Purushotham, A., Pinder, S. E., Borresen-Dale, A. L., Earl, H. M., Pharoah, P. D., Ross, M. T., Aparicio, S. & Caldas, C. The somatic mutation profiles of 2,433 breast cancers refines their genomic and transcriptomic landscapes. *Nat Commun* **7,** 11479 (2016).

288. Cancer Genome Atlas, N. Comprehensive molecular portraits of human breast tumours. *Nature* **490,** 61–70 (2012).

289. Gao, J., Aksoy, B. A., Dogrusoz, U., Dresdner, G., Gross, B., Sumer, S. O., Sun, Y., Jacobsen, A., Sinha, R., Larsson, E., Cerami, E., Sander, C. & Schultz, N. Integrative analysis of complex cancer genomics and clinical profiles using the cBioPortal. *Sci. Signal.* **6,** pl1 (2013).

290. Cerami, E., Gao, J., Dogrusoz, U., Gross, B. E., Sumer, S. O., Aksoy, B. A.,

Jacobsen, A., Byrne, C. J., Heuer, M. L., Larsson, E., Antipin, Y., Reva, B., Goldberg, A. P., Sander, C. & Schultz, N. The cBio cancer genomics portal: an open platform for exploring multidimensional cancer genomics data. *Cancer Discov* **2,** 401–404 (2012).

291. Diermeier, S., Horvath, G., Knuechel-Clarke, R., Hofstaedter, F., Szollosi, J. & Brockhoff, G. Epidermal growth factor receptor coexpression modulates susceptibility to Herceptin in HER2/neu overexpressing breast cancer cells via specific erbB-receptor interaction and activation. *Exp Cell Res* **304,** 604–619 (2005).

292. Barretina, J., Caponigro, G., Stransky, N., Venkatesan, K., Margolin, A. A., Kim, S., Wilson, C. J., Garraway, L. A., *et al.* The Cancer Cell Line Encyclopedia enables predictive modelling of anticancer drug sensitivity. *Nature* **483,** 603–7 (2012).

293. Popp, M. W. & Maquat, L. E. Leveraging rules of nonsense-mediated mRNA decay for genome engineering and personalized medicine. *Cell* **165,** 1319–1332 (2016).

294. Duda, K., Lonowski, L. A., Kofoed-Nielsen, M., Ibarra, A., Delay, C. M., Kang, Q., Yang, Z., Pruett-Miller, S. M., Bennett, E. P., Wandall, H. H., Davis, G. D., Hansen, S. H. & Frödin, M. High-efficiency genome editing via 2A-coupled co-expression of fluorescent proteins and zinc finger nucleases or CRISPR/Cas9 nickase pairs. *Nucleic Acids Res.* **42,** (2014).

295. Engelman, J. A., Zhang, X., Galbiati, F., Volonte, D., Sotgia, F., Pestell, R. G., Minetti, C., Scherer, P. E., Okamoto, T. & Lisanti, M. P. Molecular genetics of the caveolin gene family: implications for human cancers, diabetes, Alzheimer disease, and muscular dystrophy. *Am J Hum Genet* **63,** 1578–1587 (1998).

296. Giuliano, M., Trivedi, M. V. & Schiff, R. Bidirectional crosstalk between the estrogen receptor and human epidermal growth factor receptor 2 signaling pathways in breast cancer: Molecular basis and clinical implications. *Breast Care* **8,** 256–262 (2013).

297. Sukhatme, V. P., Cao, X., Chang, L. C., Tsai-Morris, C. H., Stamenkovich, D., Ferreira, P. C. P., Cohen, D. R., Edwards, S. A., Shows, T. B., Curran, T., Le Beau, M. M. & Adamson, E. D. A zinc finger-encoding gene coregulated with c-fos during growth and differentiation, and after cellular depolarization. *Cell* **53,** 37–43 (1988).

298. Ping-Pui., W., F., M., K.V., C., C., B., H.C., H., A.G., S., Wong, P.-P., Miranda, F., Chan, K. V, Berlato, C., Hurst, H. C. & Scibetta, A. G. Histone demethylase KDM5B collaborates with TFAP2C and Myc to repress the cell cycle inhibitor p21(cip) (CDKN1A). *Mol. Cell. Biol.* **32,** 1633–44 (2012).

299. Bahrami, S. & Drabløs, F. Gene regulation in the immediate-early response process. *Advances in Biological Regulation* **62,** 37–49 (2016).

300. Yang, H., Yang, X., Lang, J. C. & Chaum, E. Tissue culture methods can strongly induce immediate early gene expression in retinal pigment epithelial cells. *J. Cell. Biochem.* **98,** 1560–1569 (2006).

301. Takegawa, N., Nonagase, Y., Yonesaka, K., Sakai, K., Maenishi, O., Ogitani, Y., Tamura, T., Nishio, K., Nakagawa, K. & Tsurutani, J. DS-8201a, a new HER2-targeting antibody–drug conjugate incorporating a novel DNA topoisomerase I inhibitor, overcomes HER2-positive gastric cancer T-DM1 resistance. *Int. J. Cancer* **141,** 1682–1689 (2017).

302. Matkar, S., Sharma, P., Gao, S., Gurung, B., Katona, B. W., Liao, J., Muhammad, A. B., Kong, X. C., Wang, L., Jin, G., Dang, C. V. & Hua, X. An

Epigenetic Pathway Regulates Sensitivity of Breast Cancer Cells to HER2 Inhibition via FOXO/c-Myc Axis. *Cancer Cell* **28,** 472–485 (2015).

303. Berns, K., Sonnenblick, A., Gennissen, A., Brohée, S., Hijmans, E. M., Evers, B., Fumagalli, D., Desmedt, C., Loibl, S., Denkert, C., Neven, P., Guo, W., Zhang, F., Knijnenburg, T. A., Bosse, T., Van Der Heijden, M. S., Hindriksen, S., Nijkamp, W., Wessels, L. F. A., Joensuu, H., Mills, G. B., Beijersbergen, R. L., Sotiriou, C. & Bernards, R. Loss of ARID1A activates ANXA1, which serves as a predictive biomarker for trastuzumab resistance. *Clin. Cancer Res.* **22,** 5238–5248 (2016).

304. Wei, L.-L., Wu, X.-J., Gong, C.-C. & Pei, D.-S. Egr-1 suppresses breast cancer cells proliferation by arresting cell cycle progression via down-regulating CyclinDs. *Int J Clin Exp Pathol* **10,** 10212–10222 (2017).

305. Huang, R. P., Fan, Y., de Belle, I., Niemeyer, C., Gottardis, M. M., Mercola, D. & Adamson, E. D. Decreased Egr-1 expression in human, mouse and rat mammary cells and tissues correlates with tumor formation. *Int J Cancer* **72,** 102–109 (1997).

306. Coller, H. A., Grandori, C., Tamayo, P., Colbert, T., Lander, E. S., Eisenman, R. N. & Golub, T. R. Expression analysis with oligonucleotide microarrays reveals that MYC regulates genes involved in growth, cell cycle, signaling, and adhesion. *Proc. Natl. Acad. Sci. U. S. A.* **97,** 3260–5 (2000).

307. Liao, D. J. & Dickson, R. B. c-Myc in breast cancer. *Endocrine-Related Cancer* **7,** 143–164 (2000).

308. Kozono, D., Li, J., Nitta, M., Sampetrean, O., Gonda, D., Kushwaha, D. S., Merzon, D., Ramakrishnan, V., Zhu, S., Zhu, K., Matsui, H., Harismendy, O., Hua, W., Mao, Y., Kwon, C.-H., Saya, H., Nakano, I., Pizzo, D. P., VandenBerg, S. R. & Chen, C. C. Dynamic epigenetic regulation of glioblastoma tumorigenicity through LSD1 modulation of MYC expression. *Proc. Natl. Acad. Sci.* **112,** E4055–E4064 (2015).

309. Zhang, S., Chen, Y., Guo, W., Yuan, L., Zhang, D., Xu, Y., Nemeth, E., Ganz, T. & Liu, S. Disordered hepcidin-ferroportin signaling promotes breast cancer growth. *Cell. Signal.* **26,** 2539–2550 (2014).

310. Pinnix, Z. K., Miller, L. D., Wang, W., D'Agostino, R., Kute, T., Willingham, M. C., Hatcher, H., Tesfay, L., Sui, G., Di, X., Torti, S. V & Torti, F. M. Ferroportin and iron regulation in breast cancer progression and prognosis. *Sci. Transl. Med.* **2,** 43ra56 (2010).

311. Wang, Y. C., Morrison, G., Gillihan, R., Guo, J., Ward, R. M., Fu, X., Botero, M. F., Healy, N. A., Hilsenbeck, S. G., Phillips, G. L., Chamness, G. C., Rimawi, M. F., Osborne, C. K. & Schiff, R. Different mechanisms for resistance to trastuzumab versus lapatinib in HER2-positive breast cancers--role of estrogen receptor and HER2 reactivation. *Breast Cancer Res* **13,** R121 (2011).

312. Diermeier-Daucher, S., Breindl, S., Buchholz, S., Ortmann, O. & Brockhoff, G. Modular anti-EGFR and anti-Her2 targeting of SK-BR-3 and BT474 breast cancer cell lines in the presence of ErbB receptor-specific growth factors. *Cytom. Part A* **79 A,** 684–693 (2011).

313. Li, W.-X., He, K., Tang, L., Dai, S.-X., Li, G.-H., Lv, W.-W., Guo, Y.-C., An, S.-Q., Wu, G.-Y., Liu, D. & Huang, J.-F. Comprehensive tissue-specific gene set enrichment analysis and transcription factor analysis of breast cancer by integrating 14 gene expression datasets. *Oncotarget* **8,** 6775–6786 (2017).

314. Nwosu, Z. C., Ebert, M. P., Dooley, S. & Meyer, C. Caveolin-1 in the regulation of cell metabolism: a cancer perspective. *Mol. Cancer* **15,** 71 (2016).

315. Van Den Eynden, G. G., Van Laere, S. J., Van Der Auwera, I., Merajver, S. D., Van Marck, E. A., Van Dam, P., Vermeulen, P. B., Dirix, L. Y. & Van Golen, K. L. Overexpression of caveolin-1 and -2 in cell lines and in human samples of inflammatory breast cancer. *Breast Cancer Res. Treat.* **95,** 219–228 (2006).

316. Patani, N., Lambros, M. B., Natrajan, R., Dedes, K. J., Geyer, F. C., Ward, E., Martin, L. A., Dowsett, M. & Reis-Filho, J. S. Non-existence of caveolin-1 gene mutations in human breast cancer. *Breast Cancer Res. Treat.* **131,** 307–310 (2012).

317. Lee, H., Park, D. S., Razani, B., Russell, R. G., Pestell, R. G. & Lisanti, M. P. Caveolin-1 mutations (P132L and null) and the pathogenesis of breast cancer: Caveolin-1 (P132L) behaves in a dominant-negative manner and caveolin-1 (-/-) null mice show mammary epithelial cell hyperplasia. *Am. J. Pathol.* **161,** 1357–1369 (2002).

318. Ferraldeschi, R., Latif, A., Clarke, R. B., Spence, K., Ashton, G., O'Sullivan, J., Evans, D. G., Howell, A. & Newman, W. G. Lack of caveolin-1 (P132L) somatic mutations in breast cancer. *Breast Cancer Research and Treatment* **132,** 1185–1186 (2012).

319. Secombe, J., Li, L., Carlos, L. & Eisenman, R. N. The Trithorax group protein Lid is a trimethyl histone H3K4 demethylase required for dMyc-induced cell growth. *Genes Dev.* **21,** 537–551 (2007).

320. Rahmatpanah, F., Jia, Z., Chen, X., Jones, F. E., McClelland, M. & Mercola, D. Expression of HER2 in Breast Cancer Promotes a Massive Reorganization of Gene Activity and Suggests a Role for Epigenetic Regulation. (2012). doi:10.4172/2153-0602.1000e102

321. Kumandan, S., Mahadevan, N. R., Chiu, K., DeLaney, A. & Zanetti, M. Activation of the unfolded protein response bypasses trastuzumab-mediated inhibition of the PI-3K pathway. *Cancer Lett.* **329,** 236–242 (2013).